

**UNCLASSIFIED**

**AD NUMBER**

**AD864056**

**LIMITATION CHANGES**

**TO:**

**Approved for public release; distribution is unlimited.**

**FROM:**

**Distribution authorized to DoD only;  
Administrative/Operational Use; NOV 1969. Other  
requests shall be referred to Army Electronic  
Command, Fort Monmouth, NJ 07703-5601.**

**AUTHORITY**

**ECOM D/A ltr, 18 Jun 1976**

**THIS PAGE IS UNCLASSIFIED**

THIS REPORT HAS BEEN DELIMITED  
AND CLEARED FOR PUBLIC RELEASE  
UNDER DOD DIRECTIVE 5200.20 AND  
NO RESTRICTIONS ARE IMPOSED UPON  
ITS USE AND DISCLOSURE.

DISTRIBUTION STATEMENT A

APPROVED FOR PUBLIC RELEASE;  
DISTRIBUTION UNLIMITED,

AD 883333  
AD 864056



AD

**TECHNICAL REPORT ECOM-0251-2  
CORRELATION BANDWIDTH  
MEASUREMENTS  
OVER TROPOSCATTER PATHS  
SECOND INTERIM REPORT**

**DISTRIBUTION STATEMENT**

Each transmittal of this document outside  
the United States Department of Defense  
must have prior approval of the Command-  
ing General, United States Project Office,  
The Mallard Project, Fort Monmouth, New  
Jersey.

**Richard Branham - Arnfinn Manders  
Dennis Kozakoff - Barbara Brummett**

**NOVEMBER 1969**

**ECOM**

UNITED STATES ARMY ELECTRONICS COMMAND · FORT MONMOUTH, N.J.  
**CONTRACT DAAB07-69-C-0251**  
**MARTIN MARIETTA CORPORATION**  
OR 10244-1 Orlando, Florida

#### DISCLAIMERS

Findings in this report are not to be construed as an official Department of the Army position unless so designated by other authorized documents.

The citation of trade names and names of manufacturers in this report is not to be construed as an official government enforcement or approval of commercial products or services referenced herein.

TECHNICAL REPORT ECOM 0251-2  
NOVEMBER 1969

CORRELATION BANDWIDTH MEASUREMENTS  
OVER TROPOSCATTER PATHS

SECOND INTERIM REPORT  
August 1969 to November 1969  
CONTRACT NO. DAAB07-69-C-0251

DISTRIBUTION STATEMENT

Each transmittal of this document outside  
the United States Department of Defense  
must have prior approval of the Command-  
ing General, United States Project Office,  
MALLARD Project, Ft. Monmouth, New Jersey.

Prepared by

Richard Branham  
Arnfinn Manders  
Dennis Kozakoff  
Barbara Brummett

Martin Marietta Corporation  
Orlando, Florida

For

U.S. ARMY ELECTRONICS COMMAND, FORT MONMOUTH, N.J.

## CONTENTS

I.	Program Objectives . . . . .	1
II.	Summary. . . . .	3
III.	Fade Rate-Correlation Bandwidth-Stability in the Common Volume . . . . .	5
A.	Fade Rate . . . . .	5
B.	Stability of the Air in the Common Volume . . . . .	6
C.	Correlation Function Computer Study . . . . .	7
IV.	Reduced Data . . . . .	9
A.	Cross Correlation Coefficients. . . . .	11
B.	Diurnal Effects on Correlation Bandwidth. . . . .	17
C.	Narrow Spacing Correlation Coefficient Measurements . . . .	21
D.	Typical Examples of Propagation Data. . . . .	25
E.	Anomalies in Propagation. . . . .	73
Appendix A.	. . . . .	89
Appendix B.	. . . . .	101
Appendix C.	. . . . .	115
References.	. . . . .	121

PRECEDING PAGE BLANK-NOT FILMED.

ILLUSTRATIONS

1. Two Path Model Illustrating the Origin of Time Selective Fading . . . . .	5
2. Pressure-Temperature Curve Used for Estimating the Stability of the Air in the Common Volume. . . . .	7
3. Envelope Cross Correlation Coefficients; Ontario Center, Summer; C-Band, Wide . . . . .	12
4. Envelope Cross Correlation Coefficients; Ontario Center, Summer; X-Band, Wide . . . . .	12
5. Envelope Cross Correlation Coefficients; Whitford Field, Summer; C-Band, Wide . . . . .	13
6. Envelope Cross Correlation Coefficients; Whitford Field, Summer; X-Band, Wide . . . . .	13
7. Envelope Cross Correlation Coefficients; Point Petre, September; C-Band, Wide. . . . .	14
8. Envelope Cross Correlation Coefficients; Point Petre, September; X-Band, Wide. . . . .	14
9. Envelope Cross Correlation Coefficients; Point Petre, September; C-Band, Wide. . . . .	15
10. Envelope Cross Correlation Coefficients; Point Petre, September; X-Band, Wide. . . . .	15
11. Envelope Cross Correlation Coefficients; Point Petre, September; C-Band, Wide. . . . .	16
12. Envelope Cross Correlation Coefficients; Point Petre, September; X-Band, Wide. . . . .	16
13. Fade Rate Distribution; Ontario Center, Summer; C-Band . . . . .	18
14. Fade Rate Distribution; Ontario Center, Summer; X-Band . . . . .	18
15. Distribution of Fade Duration; Ontario Center, Summer; C-Band . . . . .	19
16. Distribution of Fade Duration; Ontario Center, Summer; X-Band . . . . .	19
17. Distribution of Fade Duration; Ontario Center, Summer; C-Band . . . . .	20
18. Distribution of Fade Duration; Ontario Center, Summer; X-Band . . . . .	20

19.	Envelope Cross Correlation Coefficients; Whitford Field, Summer; X-Band, Narrow . . . . .	22
20.	Envelope Cross Correlation Coefficients; Whitford Field, Summer; C-Band, Narrow . . . . .	22
21.	Envelope Cross Correlation Coefficients; Whitford Field, Summer; X-Band, Narrow . . . . .	23
22.	Envelope Cross Correlation Coefficients; Point Petre, September; X-Band, Narrow. . . . .	23
23.	Envelope Cross Correlation Coefficients; Point Petre, September; C-Band, Narrow. . . . .	24
24.	Envelope Cross Correlation Coefficients; Ontario Center, Summer; X-Band, Wide . . . . .	26
25.	Fade Rate Distribution; Ontario Center, Summer; X-Band . . . . .	27
26.	Distribution of Fade Duration; Ontario Center, Summer; X-Band . .	27
27.	Signal Amplitude Level; Ontario Center, Summer; X-Band . . . . .	28
28.	Distribution of Depth of Fades; Ontario Center. Summer; C-Band .	28
29.	Envelope Cross Correlation Coefficients; Ontario Center, Summer; C-Band, Wide . . . . .	29
30.	Fade Rate Distribution; Ontario Center, Summer; C-Band . . . . .	29
31.	Distribution of Fade Duration; Ontario Center, Summer; C-Band. .	30
32.	Signal Amplitude Level; Ontario Center, Summer; C-Band . . . . .	30
33.	Distribution of Depth of Fades; Ontario Center, Summer; C-Band .	31
34.	Envelope Cross Correlation Coefficients; Ontario Center, Summer; X-Band, Wide . . . . .	31
35.	Fade Rate Distribution; Ontario Center, Summer; X-Band . . . . .	32
36.	Distribution of Fade Duration; Ontario Center, Summer; X-Band. .	32
37.	Signal Amplitude Level; Ontario Center, Summer; X-Band . . . . .	33
38.	Distribution of Depth of Fades; Ontario Center, Summer; X-Band .	33
39.	Envelope Cross Correlation Coefficients; Ontario Center, Summer; C-Band, Wide . . . . .	34
40.	Fade Rate Distribution; Ontario Center, Summer; C-Band . . . . .	34
41.	Distribution of Fade Duration; Ontario Center, Summer; C-Band. .	35
42.	Signal Amplitude Level; Ontario Center, Summer; C-Band . . . . .	35
43.	Distribution of Depth of Fades; Ontario Center, Summer; C-Band .	36
44.	Envelope Cross Correlation Coefficients; Ontario Center, Summer; C-Band, Wide . . . . .	36
45.	Fade Rate Distribution; Ontario Center, Summer; C-Band . . . . .	37

46.	Distribution of Fade Duration; Ontario Center, Summer; C-Band . . . . .	37
47.	Signal Amplitude Level; Ontario Center, Summer; C-Band . . . . .	38
48.	Distribution of Depth of Fades; Ontario Center, Summer; C-Band . . . . .	38
49.	Envelope Cross Correlation Coefficients; Ontario Center, Summer; X-Band, Wide . . . . .	39
50.	Fade Rate Distribution; Ontario Center, Summer; X-Band . . . . .	39
51.	Distribution of Fade Duration; Ontario Center, Summer; X-Band . . . . .	40
52.	Signal Amplitude Level; Ontario Center, Summer; X-Band . . . . .	40
53.	Distribution of Depth of Fades; Ontario Center, Summer; X-Band . . . . .	41
54.	Envelope Cross Correlation Coefficients; Whitford Field, Summer; C-Band, 500 kc and Wide Spacing. . . . .	43
55.	Envelope Cross Correlation Coefficients; Whitford Field, Summer; C-Band, Wide . . . . .	44
56.	Fade Rate Distribution; Whitford Field, Summer; C-Band . . . . .	44
57.	Signal Amplitude Level; Whitford Field, Summer; C-Band . . . . .	45
58.	Distribution of Fade Duration; Whitford Field, Summer; C-Band . . . . .	45
59.	Distribution of Depth of Fades; Whitford Field, Summer; C-Band . . . . .	46
60.	Envelope Cross Correlation Coefficients; Whitford Field, Summer; C-Band, Wide . . . . .	46
61.	Fade Rate Distribution; Whitford Field, Summer; C-Band . . . . .	47
62.	Envelope Cross Correlation Coefficients; Whitford Field, Summer; X-Band, Wide . . . . .	47
63.	Fade Rate Distribution; Whitford Field, Summer; X-Band . . . . .	48
64.	Envelope Cross Correlation Coefficients; Whitford Field, Summer; C-Band, Wide . . . . .	48
65.	Fade Rate Distribution; Whitford Field, Summer; C-Band . . . . .	49
66.	Signal Amplitude Level; Whitford Field, Summer; C-Band . . . . .	49
67.	Distribution of Depth of Fades; Whitford Field, Summer; C-Band . . . . .	50
68.	Envelope Cross Correlation Coefficients; Whitford Field, Summer; X-Band, Wide . . . . .	50
69.	Fade Rate Distribution; Whitford Field, Summer; C-Band . . . . .	51
70.	Envelope Cross Correlation Coefficients; Point Petre, September; C-Band, Wide. . . . .	53
71.	Fade Rate Distribution; Point Petre, September; C-Band . . . . .	53
72.	Distribution of Fade Duration; Point Petre, September; C-Band . . . . .	54
73.	Signal Amplitude Level; Point Petre, September; C-Band . . . . .	54
74.	Distribution of Depth of Fades; Point Petre, September; C-Band . . . . .	55

75.	Envelope Cross Correlation Coefficients; Point Petre, September; X-Band, Wide . . . . .	55
76.	Fade Rate Distribution; Point Petre, September; X-Band. . . . .	56
77.	Distribution of Fade Duration; Point Petre, September; X-Band .	56
78.	Signal Amplitude Level; Point Petre, September; X-Band. . . . .	57
79.	Distribution of Depth of Fades; Point Petre, September; X-Band.	57
80.	Envelope Cross Correlation Coefficients; Point Petre, September; C-Band, Wide . . . . .	58
81.	Fade Rate Distribution; Point Petre, September; C-Band. . . . .	58
82.	Distribution of Fade Duration; Point Petre, September; C-Band .	59
83.	Signal Amplitude Level; Point Petre, September; C-Band. . . . .	59
84.	Distribution of Depth of Fades; Point Petre, September; C-Band.	60
85.	Envelope Cross Correlation Coefficients; Point Petre September; X-Band, Wide . . . . .	60
86.	Fade Rate Distribution; Point Petre, September; X-Band. . . . .	61
87.	Distribution of Fade Duration; Point Petre, September; X-Band .	61
88.	Signal Amplitude Level; Point Petre, September; X-Band. . . . .	62
89.	Distribution of Depth of Fades; Point Petre, September; X-Band	62
90.	Envelope Cross Correlation Coefficients; Point Petre, September; C-Band, Wide . . . . .	63
91.	Fade Rate Distribution; Point Petre, September; C-Band. . . . .	63
92.	Distribution of Fade Duration; Point Petre, September; C-Band .	64
93.	Signal Amplitude Level; Point Petre, September; C-Band. . . . .	64
94.	Distribution of Depth of Fades; Point Petre, September; C-Band.	65
95.	Envelope Cross Correlation Coefficients; Point Petre, September; X-Band, Wide . . . . .	65
96.	Fade Rate Distribution; Point Petre, September; X-Band. . . . .	66
97.	Distribution of Fade Duration; Point Petre, September; X-Band .	66
98.	Signal Amplitude Level; Point Petre, September; X-Band. . . . .	67
99.	Distribution of Depth of Fades; Point Petre, September; X-Band.	67
100.	Envelope Cross Correlation Coefficients; Point Petre, September; C-Band, Wide . . . . .	68
101.	Fade Rate Distribution; Point Petre, September; C-Band. . . . .	68
102.	Distribution of Fade Duration; Point Petre, September; C-Band .	69
103.	Signal Amplitude Level; Point Petre, September; C-Band. . . . .	69

104.	Distribution of Depth of Fades; Point Petre, September; C-Band. . .	70
105.	Envelope Cross Correlation Coefficients; Point Petre September; X-Band, Wide . . . . .	70
106.	Fade Rate Distribution; Point Petre, September; X-Band. . . . .	71
107.	Distribution of Fade Duration; Point Petre, September; X-Band . . .	71
108.	Signal Amplitude Level; Point Petre, September; X-Band. . . . .	72
109.	Distribution of Depth of Fades; Point Petre, September; X-Band. . .	72
110.	Envelope Cross Correlation Coefficients; Ontario Center, Summer; X-Band, Wide, Ducting . . . . .	74
111.	Fade Rate Distribution; Ontario Center, Summer; X-Band, Ducting .	74
112.	Distribution of Fade Duration; Ontario Center, Summer; X-Band, Ducting . . . . .	75
113.	Signal Amplitude Level; Ontario Center, Summer; X-Band, Ducting . . . . .	75
114.	Envelope Cross Correlation Coefficients; Ontario Center, Summer; C-Band, Wide, Ducting . . . . .	76
115.	Fade Rate Distribution; Ontario Center, Summer; C-Band, Ducting .	76
116.	Distribution of Fade Duration; Ontario Center, Summer; C-Band, Ducting . . . . .	77
117.	Signal Amplitude Level; Ontario Center, Summer; C-Band, Ducting .	77
118.	Envelope Cross Correlation Coefficients; Point Petre, September; C-Band, Wide . . . . .	78
119.	Fade Rate Distribution; Point Petre, September; C-Band. . . . .	78
120.	Distribution of Fade Duration; Point Petre, September; C-Band . .	79
121.	Signal Amplitude Level; Point Petre, September; C-Band. . . . .	79
122.	Distribution of Depth of Fades; Point Petre, September; C-Band. .	80
123.	Envelope Cross Correlation Coefficients; Point Petre, September; X-Band, Wide . . . . .	80
124.	Fade Rate Distribution; Point Petre, September; X-Band. . . . .	81
125.	Distribution of Fade Duration; Point Petre, September; X-Band . .	81
126.	Signal Amplitude Level; Point Petre, September; X-Band. . . . .	82
127.	Distribution of Depth of Fades; Point Petre, September; X-Band. .	82
128.	Envelope Cross Correlation Coefficients; Ontario Center, Summer; X-Band, Wide; Airplane Effect 1 . . . . .	83
129.	Envelope Cross Correlation Coefficients; Ontario Center, Summer; X-Band, Wide; Airplane Effect 2 . . . . .	84

130.	Fade Rate Distribution; Ontario Center, Summer; X-Band. . . . .	84
131.	Fade Rate Distribution; Ontario Center, Summer; X-Band; Temperature Over 85°F . . . . .	85
132.	Envelope Cross Correlation Coefficients; Ontario Center, Summer; X-Band, Wide; Temperature Over 85°F . . . . .	86
133.	Envelope Cross Correlation Coefficients; Ontario Center, Summer; C-Band, Wide. . . . .	86
134.	Fade Rate Distribution; Ontario Center, Summer; C-Band. . . . .	87
135.	Fade Rate Distribution; Ontario Center, Summer; X-Band. . . . .	88
136.	Geometry Applicable to Correlation Bandwidth Computer Program . .	92
137.	Computer Flow Diagram for Correlation Bandwidth Computation . .	93

## I. PROGRAM OBJECTIVES

Project MALLARD is a program for the design and development of a digital, automatically switched communication system for the field Army with characteristics as described in the project MALLARD Quadripartite, Communications Plan, and Proposals for Research and Development. This digital system will be designed to transmit full duplex voice, teletype, facsimile, and digital data at various speeds with total traffic security. The communication links between points will use many different devices such as cable, microwave, radio, etc. as appropriate for the particular link. Troposcatter paths of 150 to 250 km nominal are to be used in areas where direct cable or simple microwave systems are not applicable.

The objective of this program is to obtain data necessary for the design of troposcatter modems for use in future MALLARD troposcatter systems. In support of this objective, propagation data are being collected over three types of troposcatter paths to empirically determine cross correlation versus frequency spacing and other fade statistics to provide a basis for the determination of the maximum bit rates that can be satisfactorily transmitted by frequency diversity methods with a stated error probability under known conditions of path length, path terrain, season, antenna size and beamwidth, radio frequency band, occupied bandwidth, radiated power, and frequency spacing. These data are also directly applicable to the prediction of space diversity maximum bit rates at stated error probabilities since the correlation bandwidth and fade statistics directly affect the error probabilities and bit rates obtainable.

The propagation data are being collected through the use of a fixed C- and X-band transmitting system located at the RADC troposcatter test site at Model City, New York. The receiving instrumentation is located in a special van that is moved to various locations to provide variations in terrain.

During the phase covered by the first interim report (Reference 1), a literature review on previously available data on correlation bandwidth was made. Later, these data will be combined with the field test data to form the basis to correlate bandwidth and other fade and propagation statistics in terms of identifiable parameters such as terrain, path length, weather, frequency, and beamwidth.

**PRECEDING PAGE BLANK-NOT FILMED.**

## II. SUMMARY

This second interim report on correlation bandwidth over troposcatter paths is concerned primarily with the data obtained during the first set of operations on each of the three paths. Some practical considerations are presented relative to the effects that are brought about by the stability of the atmosphere in the common volume. It appears that two mechanisms are contributing to the correlation bandwidth either singly or simultaneously. A computer study has been made to test the effect that the variables have on correlation bandwidth using the ray tracing technique introduced in the first interim report. Using temperature, humidity, pressure, and the distance between sites, it was found that these variables alone are not sufficient to describe the correlation bandwidth. The resulting computations appear to require only a scale factor to be correct. Work is continuing to perfect the model in so far as possible to predict correlation bandwidth with only surface measurable variables.

The field tests have been performed over the three paths in New York State plains region with the receiver instrumentation van located in Ontario Center for three weeks; Weedsport, N. Y., for three weeks; and Point Petre, Canada, for two weeks. This report is concerned primarily with the presentation of the reduced test data from the operation during this period.

The field data presented herein were inserted into the computer system on magnetic tape and were plotted by a computer controlled plotter. For this interim report the data are presented on a test by test basis so that the individual happenings on each test can be appraised and compared with other individual events. This enables the simultaneous events occurring at X and C-bands to be evaluated in all factors involving tropospheric propagation over the typical MALLARD links. The next interim report will contain the percentile plots of all variables.

The correlation bandwidth over troposcatter paths has been found to be anything but constant over these paths. It was found to vary significantly over a fifteen minute period from very wide to very narrow and vice versa. Fade rates are much more widespread over these paths than they were over the ECOM/Tobyhanna path in 1968 (Reference 2). Some of the high fade rates are due to aircraft, but most of them were due to propagation factors present in the New York/Lake Ontario area. Some ducting was noted at Ontario Center and at Point Petre. The signal levels at Whitford Field near Weedsport, N. Y., were usually very low and ducting was never noticed. An interesting finding in this program is that the use of X-band in place

of C-band resulted in very nearly the same degree of frequency diversity obtainable. At X-band, the fade rates were much higher than at C-band. As a result, adaptive frequency modems would have to be capable of coping with the fade rates which are twice that of C-band. Frequency-time modems are insensitive to fade rate and would also operate better in the high fade rate condition because the burst error occurrences would be of shorter duration.

All technical instrumentation problems were solved through the efforts of RADC, ECOM, and Martin Marietta personnel. These ranged from routine maintenance and obtaining special test equipment to the replacement of the C-band transmitter equipment. One unsolvable problem, however, was the low signal strength at Whitford Field. The nearby trees caused the path to use a higher transmitter takeoff angle than originally calculated, hence there was about 10 to 15 dB greater loss in the path than was anticipated. The cross correlation data and fade rates obtained at the Whitford site were satisfactory, but the depth of fade and fade durations were often not reported due to lack of fade margin in the instrumentation. Nevertheless, sufficient data were obtained to evaluate the site in all variables.

### III. FADE RATE-CORRELATION BANDWIDTH-STABILITY IN THE COMMON VOLUME

It was predicted in the first interim report that there would be two different propagation mechanisms in effect. When the air in the common volume is stable, layers will tend to occur. These layers will reflect the waves with relatively small multipath spread. When the air in the common volume is unstable, turbulence will occur. This results in incoherent scatter from a turbulent volume with a resulting greater multipath spread.

The experimental data confirm these conclusions. It can be shown that stability of the air in the common volume will, in addition to reducing the correlation bandwidth, also cause an increased fade rate. This conclusion is verified by the experimental data.

#### A. FADE RATE

Time selective fading (fading in the time domain) is caused by constructive and destructive interference by wavelets scattered by different scatterers as shown in Figure 1. The doppler shift imparted to a particular wavelet depends on the direction and magnitude of the velocity of the scatterer. Birkemeier (Reference 3) has shown that under certain conditions there is a relationship between the crosspath wind and fade rates. Under turbulent conditions this relationship usually does not exist since the velocity of the scatterers due to turbulence will be the dominant factor.

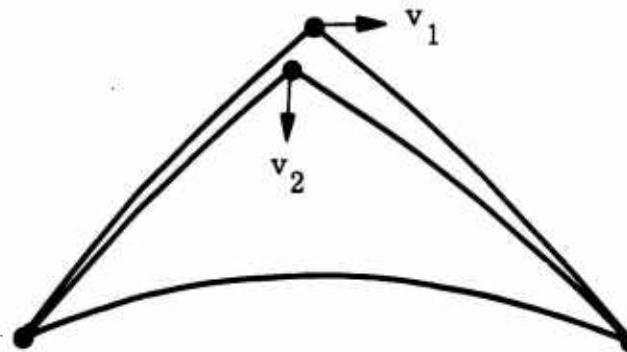


Figure 1. Two Path Model Illustrating the Origin  
of Time Selective Fading

There are thus at least two different mechanisms that lead to high fade rates. One is strong crosspath wind, another is turbulence in the common volume. Strong crosspath wind does not lead to decreased correlation bandwidth while turbulence in a common volume usually does. Therefore, care must be exercised in analyzing the data to spot the periods when the troposphere is turbulent.

#### B. STABILITY OF THE AIR IN THE COMMON VOLUME

The stability of the air within the common volume plays an important part in determining the correlation bandwidth of the troposcatter link. The correlation bandwidth under stable conditions can be evaluated as shown in Reference 1 from path parameters and gross meteorological parameters contributing to instability.

The reason for instability of the air in the common volume must be sought in the thermodynamics of the air in the layer from about 500 to 2000 meters above smooth earth level. When a small volume of air is raised it will undergo an adiabatic expansion. Work is required to make the air expand adiabatically.

As the air expands it cools off. If it were an ideal gas, this could go on indefinitely. However, since the air contains water vapor it will eventually reach a point where the temperature reaches the dew point of the mixture. Further rising of the air will cause an adiabatic expansion with condensation, a so-called pseudoadiabatic expansion. In this latter phase, energy is released. If, on balance, energy is released when a small volume of air is raised, the air is in an unstable condition.

Information to be used for estimating the stability of the atmosphere can be gained from sonde data of temperature and humidity as a function of pressure (altitude). For example, consider the pressure-temperature curve shown in Figure 2. The work required to lift a small volume of air from the 950 mb level where it will be at a temperature  $T_1$  to the 850 mb level where it will be at the temperature  $T_4$  can be estimated as follows:

Initially the air will expand adiabatically parallel to the adiabatic direction until it is saturated. This is the point  $M_2$ . From  $M_2$  to the 850 mb level the air will expand pseudoadiabatically, i.e., with condensation. Thus the air will arrive at the 850 mb level at point  $M_3$ . The area between the P-T curve and the path  $M_1 M_2 M_3 M_4$ , counting area on the right side of the curve as positive, represents the work required to move a small volume of air from the 950 mb level to the 850 mb level. If this work is positive, the atmosphere is stable; if it is negative, the atmosphere is unstable.

The method outlined in this section allows estimating the stability of the air in the common volume from detailed weather bureau reports. If one postulates a suitable thermodynamic model for the atmosphere it might be possible to obtain a fairly good estimate of the P-T curve from a sequence of ground based temperature measurements.

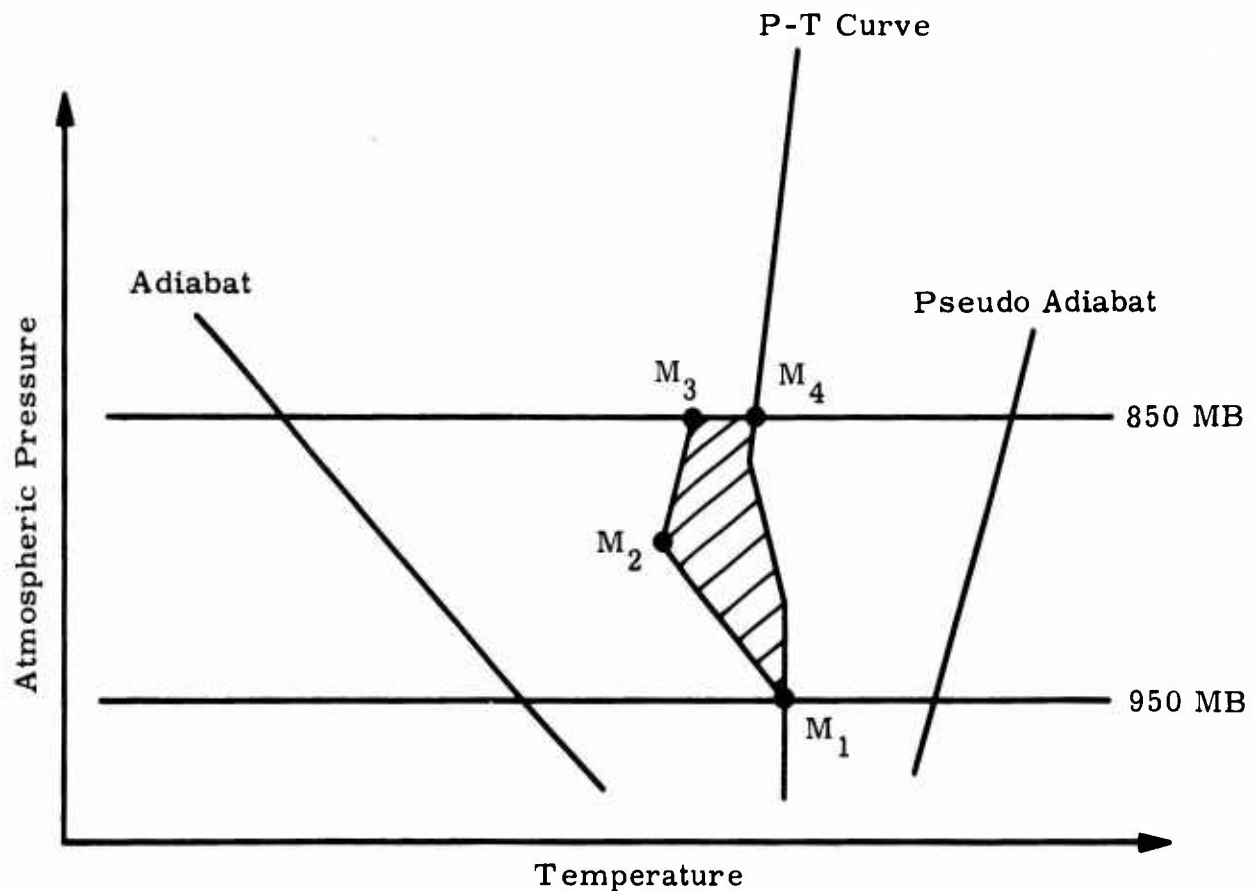


Figure 2. Pressure-Temperature Curve Used for Estimating the Stability of the Air in the Common Volume

### C. CORRELATION FUNCTION COMPUTER STUDY

The ray trace computer code presented in the first interim report was modified extensively to model the predicted correlation function for a given troposcatter link. The modified computer program presented in detail in Appendix A of this report computes the surface meteorological conditions in the vicinity of the common volume. Subsequently, ray trace solutions for the upper and lower antenna beam edges based on antenna beamwidth and link geometry permits evaluation of the multipath spread,  $\Delta$ , in microseconds. The Gaussian form of envelope correlation coefficient is then employed to numerically evaluate the function versus frequency separation in MHz.

A scale factor, SF, is employed in the correlation bandwidth model used in the computer program, and in general must be evaluated to get good agreement between the empirical and theoretical data. For instance as indicated in the first interim report, if  $SF = 1.146 \pi$ ,

good agreement between the Rice and Sunde envelope correlation function models result. Subsequently, prediction of the correlation function as based on the geometry can be obtained. While this model may particularly be good for the more isotropic scattering case, the model breaks down in that it does not account for change in the scattering mode such as due to turbulence within the common volume. Thus, since the scale factor, SF, can suitably be determined to get good curve fit between the theoretical and experimental data, it should be possible to then relate SF to other more important factors which account for large changes in the correlation bandwidth throughout the day. For instance, when the scattering mechanism is due principally to turbulence within the common volume which might occur for an unstable troposphere, it has been found that the correlation bandwidth is inversely related to fade rate. It is also known that fade rate at a given frequency increases with path length. In conclusion then, by careful correlation of the experimental data with meteorological conditions and the computer model, it should be possible to relate SF to other factors. This will be one of the objectives to be pursued during the next period and the results presented in the next interim report.

To illustrate this point the correlation bandwidth model was evaluated to compare with the Whitford C-band and X-band data taken on 29 August. The computer output for four cases selected is presented in Appendix A. For this selected example,  $N_s$  and the multipath spread as based on the geometry and weather conditions was almost identical for all, yet wide differences in the correlation bandwidths were observed. Curve fitting the theoretical curves with the experimental curves has determined that the following values of scale factor were necessary:

<u>Time</u>	<u>Data</u>	<u>Correlation Bandwidth (<math>P_e = 0.4</math>)</u>	<u>Scale Factor, SF</u>
1450	X-wide	1.3 MHz	3.34
1535	X-wide	3.0 MHz	1.45
1450	C-wide	1.2 MHz	3.61
1550	C-wide	2.7 MHz	1.61

The scale factor corresponding to the 1450 data was in both cases, in good agreement with that derived from the Sunde and Rice Models with  $SF = 1.146 \pi$ , and as such was directly related to the multipath spread. However, for the 1535 and 1550 data, the correlation bandwidth was over twice that for the 1450 data and could not be accounted for by the change in  $N_s$  as mentioned previously.

#### IV. REDUCED DATA

This report contains typical samples of the reduced data from the first round of the three paths. The transmitter is located at the RADC test site, Model City, N. Y., and the receiver sites are located at the RADC test site, Ontario Center, N. Y.; Whitford Field, Weedsport, N. Y.; and Point Petre, Ontario, Canada. The sites and path profiles are discussed at length in Reference 1.

The receiving instrumentation operated for a period of about three weeks at each site, recording signal strength versus time on magnetic tape. There were five signals for C and five signals for X band spaced so as to obtain cross correlation coefficient calculations every 1 MHz from 1 to 9 MHz. A special spacing of 200 kHz was used for the narrow spacing tests. This latter spacing was primarily used to determine the behavior of the cross correlation coefficient versus frequency at the origin. The middle channel of both types of measurements was used to calculate the fade statistics for each test.

The magnetic tapes were processed in the Martin automatic data reduction equipment (MADRE) and a CDC 6400 computer at the Martin Marietta Orlando facility. Five minutes of each C-band test and 2.5 minutes of each X-band test was reduced as a separate entity and the results plotted by a Calcomp automatic plotter. Each test was plotted for cross correlation coefficient and fade rate distribution. If available, the fade duration distributions, fade depth distributions, and signal amplitude distributions were plotted.

Generally, there were five plots made for each test, making the number of curves for the first round of testing enormous. All of these curves have not been included in this report; rather, representative plots are presented with discussions of each case.

In viewing the curves it is important that the wrong impression is not conveyed by the automatic plotter. The cross correlation coefficients are defined as unity at the origin of the curve versus frequency. As the pen moves to the next several points, a subroutine in the computer draws a smooth curve through the points. The derivative at the origin is expected to be zero, but the plotter cannot draw it as such without modifying the software. It therefore proceeds to create a non-zero derivative at the origin.

A typical test number can be interpreted as follows:

09 25 1118 06 W C

C-band

Wide frequency spacing

Sixth test of the day

Test started at 1118

The twenty fifth day of the month

The ninth month

Other suffixes are:

NC Narrow C-band

WX Wide X-band

NX Narrow X-band

Included in Appendix B is a complete listing of all the test runs at all three sites. These lists contain the tests in numerical sequence with pertinent facts such as weather in the vicinity of the transmit and receive sites and the median signal strengths measured in dB below 1 mW. Unless otherwise stated the transmitter power for Ontario Center and Point Petre at X band is 1000 watts peak with a duty cycle of 0.20 per channel and at C band the power is 500 watts peak with the same duty cycle. At Whitford Field the X-band power is boosted to 1500 watts and the C-band power remained at 500 watts. The narrow spacing tests used FM with a modulation index of 1.841. The FM system therefore provides five significant lines of CW spectra separated by 200 kHz. The central line is 5 dB below the two adjacent lines, and the next two lines moving out from center is the same amplitude as the central line. The total power at C band is 500 and at X band is 1000 watts CW.

The signal generator calibration on the wide band tests uses a peak power in dBm with the signal generator pulsed at a 0.20 duty cycle. For the narrow band tests the calibration is by CW.

Appendix C contains a listing of the August-September weather for Rochester.

#### A. CROSS CORRELATION COEFFICIENTS

Correlation bandwidth data taken simultaneously on the X- and C-band frequencies have been observed to be less frequency dependent than was predicted in an earlier MALLARD troposcatter test program (Reference 2, page 103). The correlation bandwidths measured simultaneously on 13 August 1969 at Ontario Center result in very nearly the same curves test by test for both X and C bands (Figures 3 and 4). This observation appears to be representative of the most probable situation throughout the summer data. The data from the Whitford Field (Figures 5 and 6) also show this same trend. However, the overwater path to Point Petre does not exhibit the same correlation bandwidths for X and C bands to the same degree as the Ontario Center and the Whitford data. In Figures 7 and 8, test 1 shows X and C band to be the same, while in the other two tests, the C-band data are greater than the X-band data, which is contrary to the expected result. The tests on 17 September (Figures 9 and 10) show the X band as greater than the C band. The seven runs made on 23 September however show almost identical bandwidths for both frequencies (Figures 11 and 12). The Point Petre correlation bandwidths can be summed up for the summer data as: Usually the X band has a somewhat greater bandwidth than the C band. The percentile plots which are scheduled for the next report will present the more exact relationships, but for now it can be said that the correlation bandwidths are approximately equal a sufficient percentage of the time to assume that frequency diversity is essentially equally available at X band as it is at C band. One can conclude that the multipath spread is approximately the same for either frequency and hence the wider antenna beamwidth of C band does not result in additional scatter volume.

The most important implication of this finding is that frequency diversity at X band is equally available as it is at C band when using 10 foot antennas. In fact, the C-band 10 foot antennas have a beamwidth that evidently illuminates considerably more than the maximum effective scatter volume for these paths which are typical of the MALLARD troposcatter link. Another conclusion which is evident regarding C band is that the beamwidth can be reduced by increasing the antenna diameter without losing frequency diversity. Just how far we can go in this direction can be worked out from RAKE data, but for now we know that we could increase the C-band gain to at least the same as the present X-band gain.

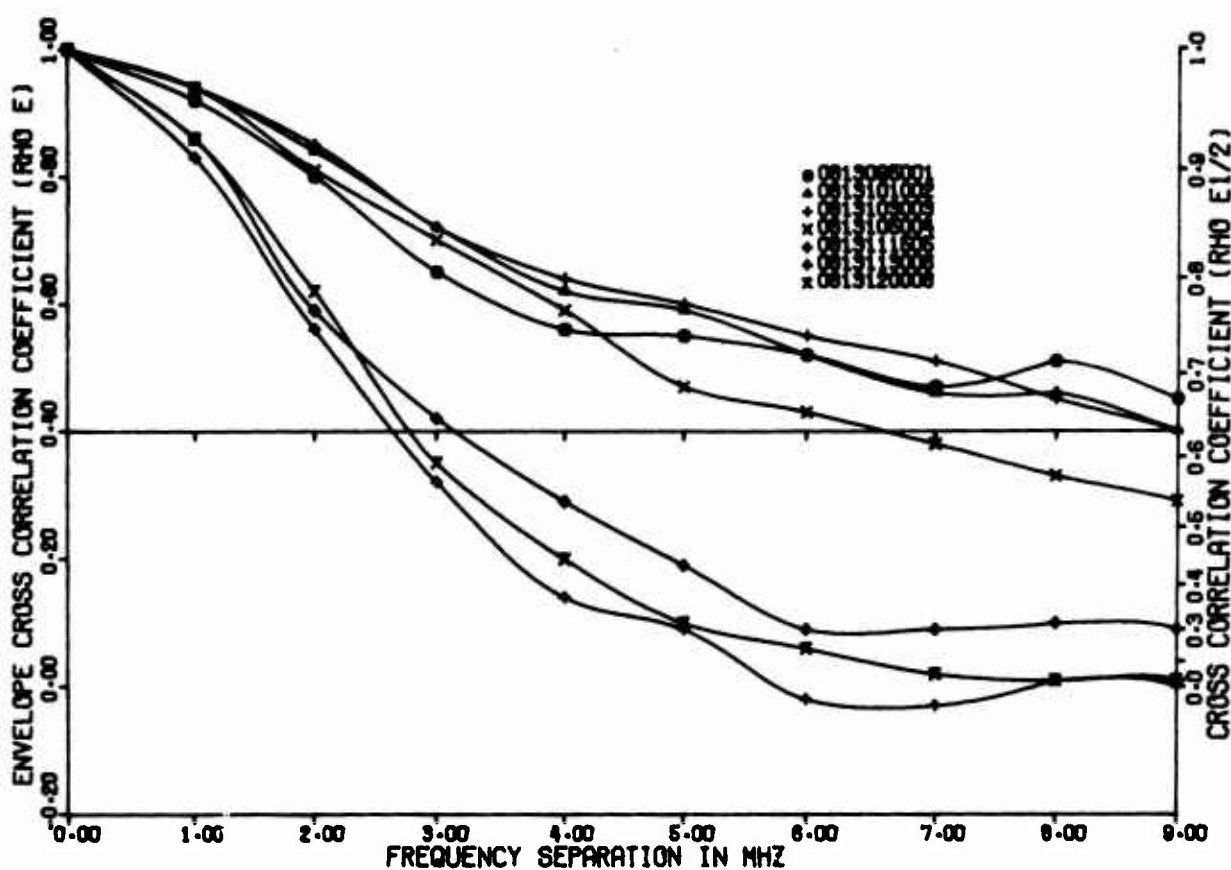


Figure 3. Envelope Cross Correlation Coefficients  
Ontario Center, Summer, C-Band, Wide

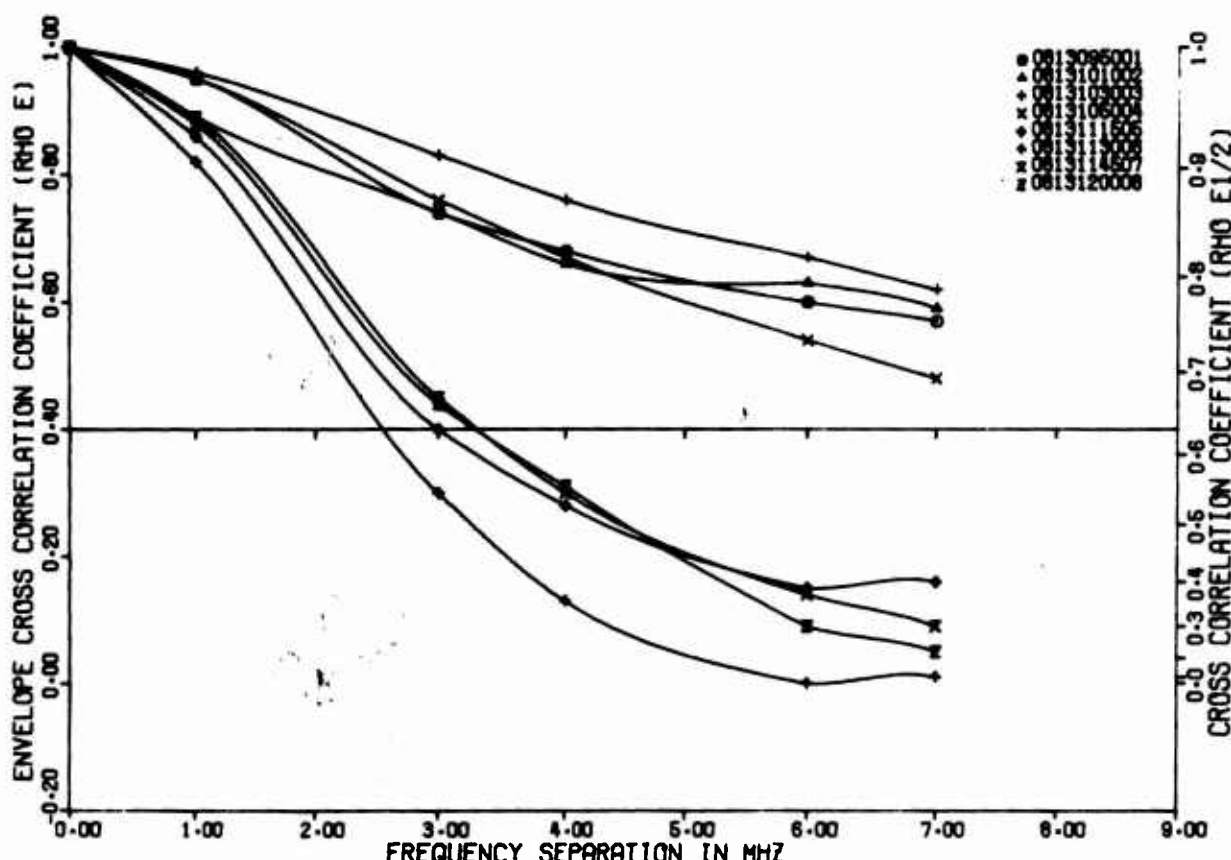


Figure 4. Envelope Cross Correlation Coefficients  
Ontario Center, Summer, X-Band, Wide

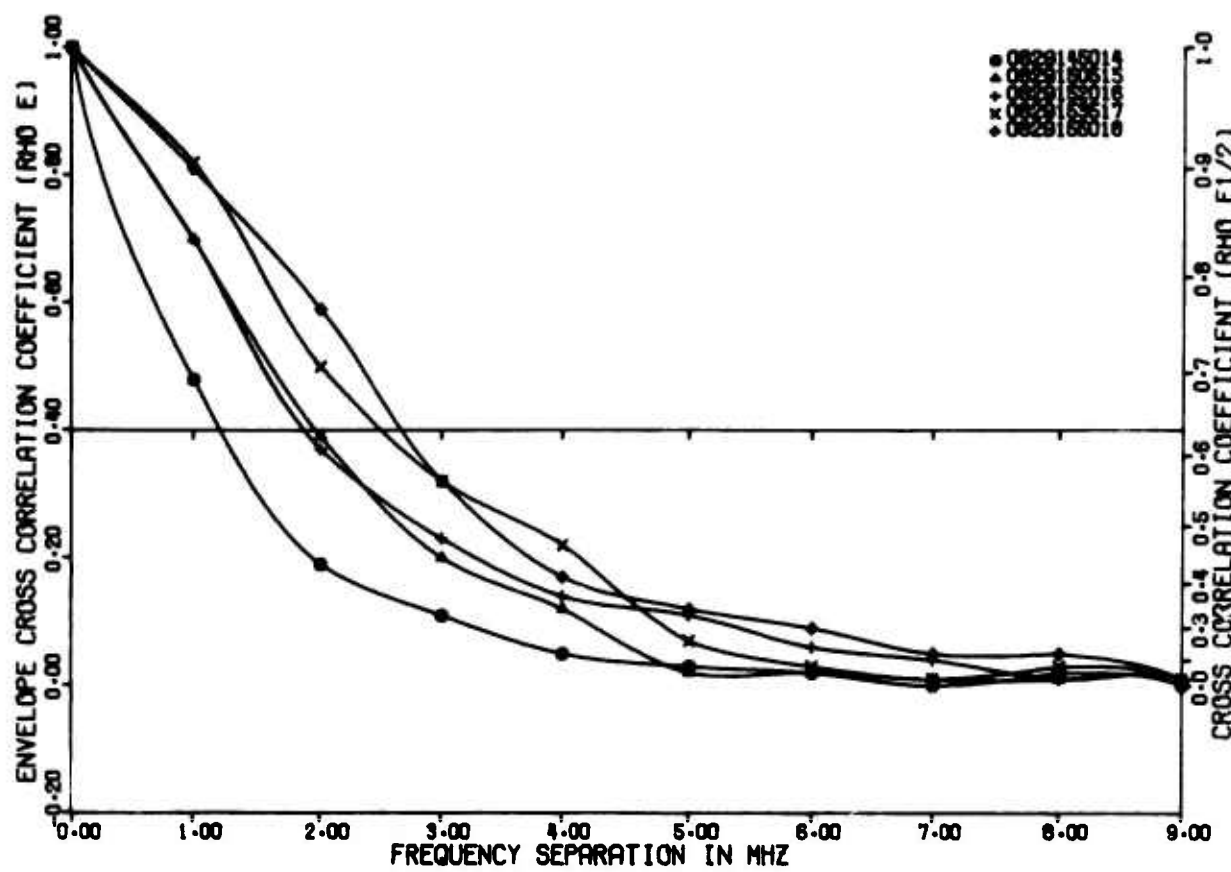


Figure 5. Envelope Cross Correlation Coefficients  
Whitford Field, Summer; C-Band, Wide

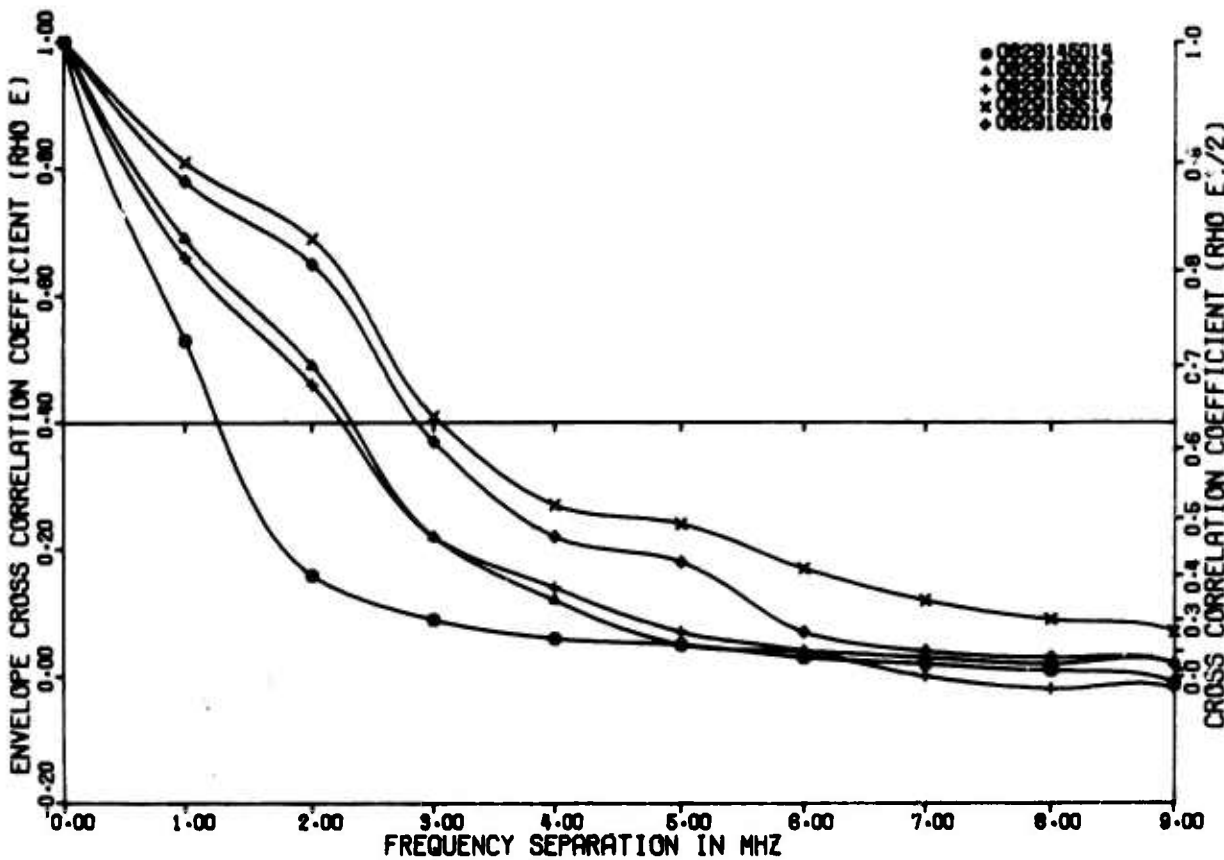


Figure 6. Envelope Cross Correlation Coefficients  
Whitford Field, Summer; X-Band, Wide

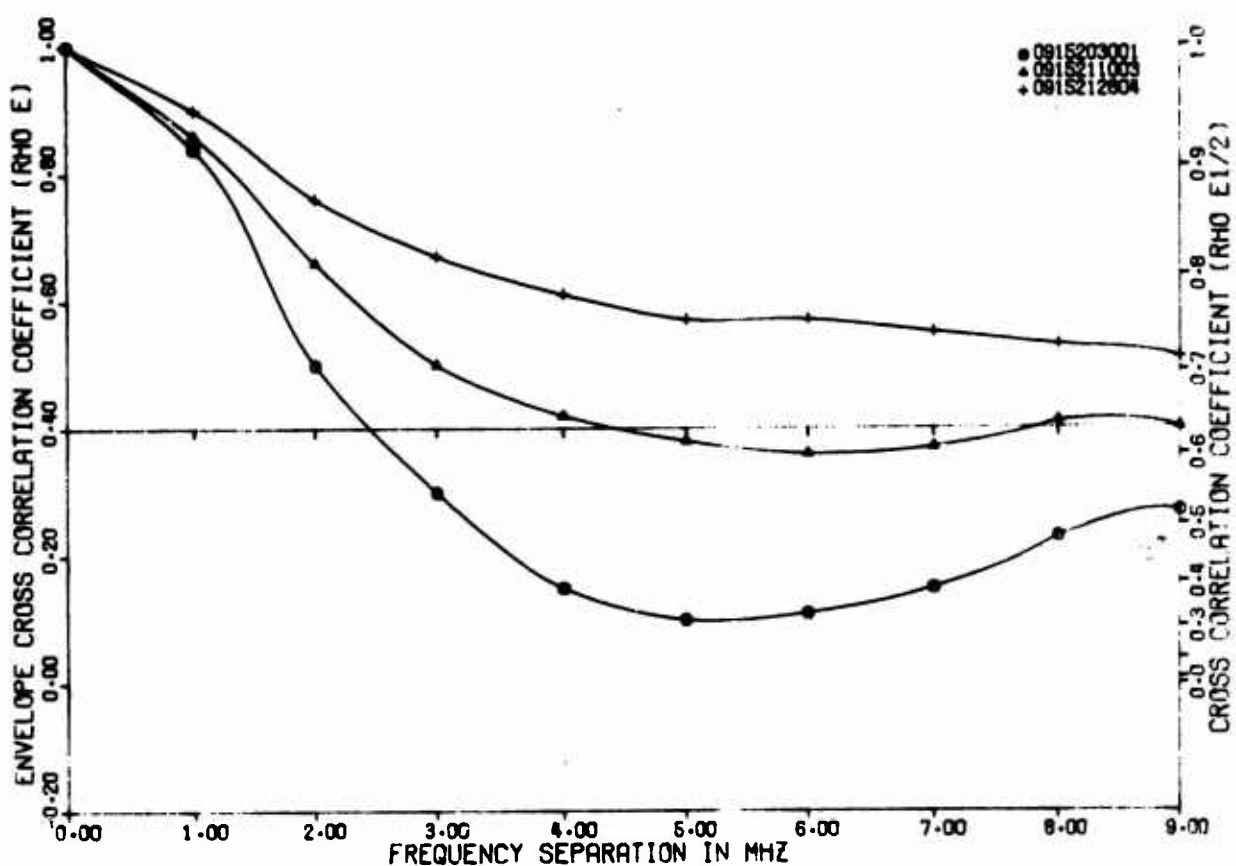


Figure 7. Envelope Cross Correlation Coefficients  
Point Petre, September; C-Band, Wide

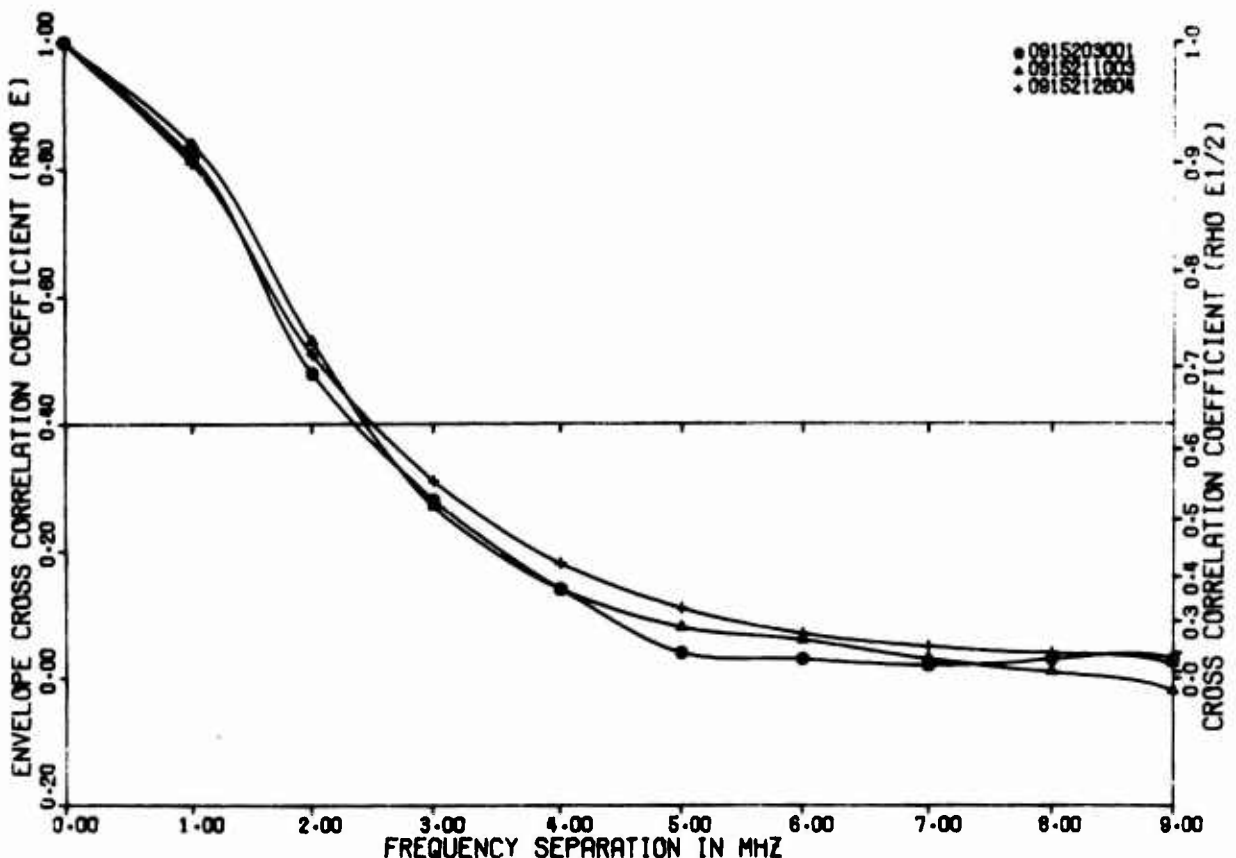


Figure 8. Envelope Cross Correlation Coefficients  
Point Petre, September; X-Band, Wide

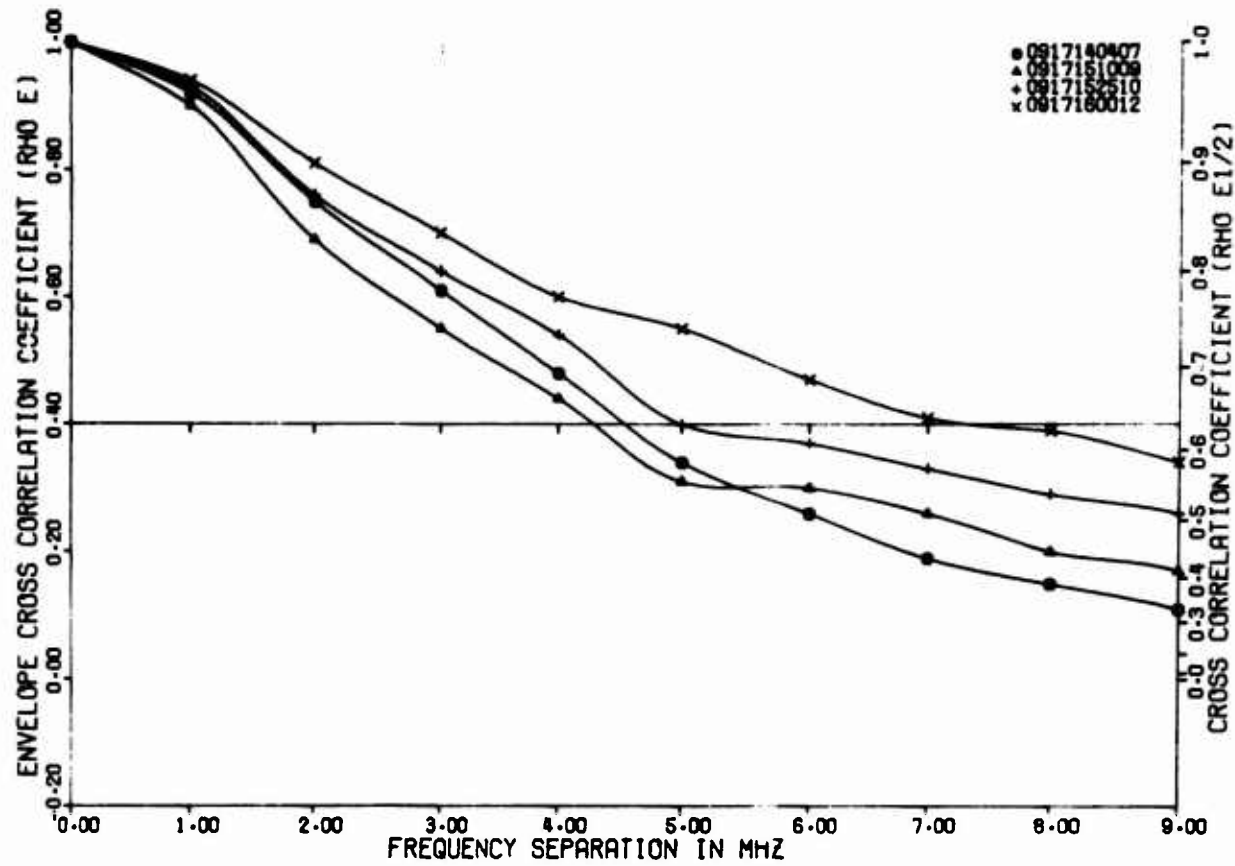


Figure 9. Envelope Cross Correlation Coefficients  
Point Petre, September; C-Band, Wide

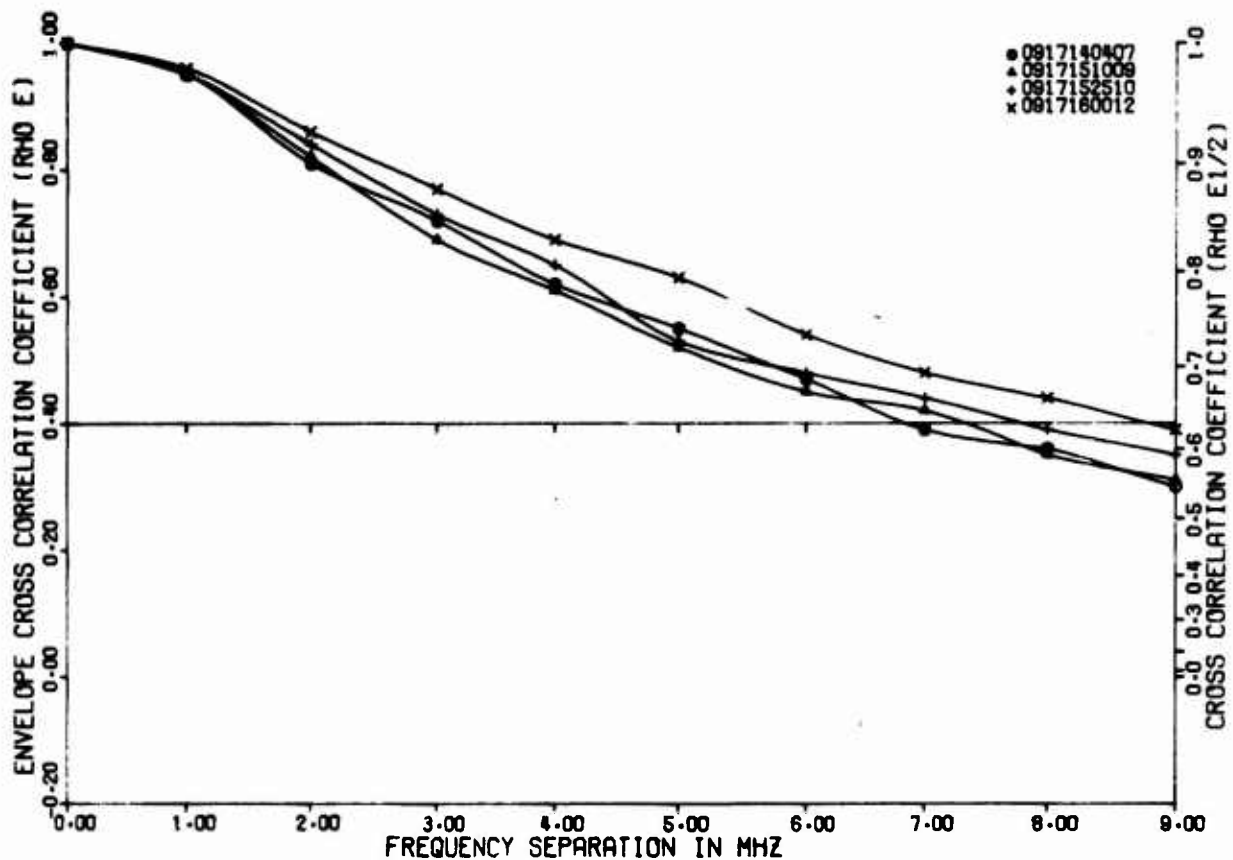


Figure 10. Envelope Cross Correlation Coefficients  
Point Petre, September; X-Band, Wide

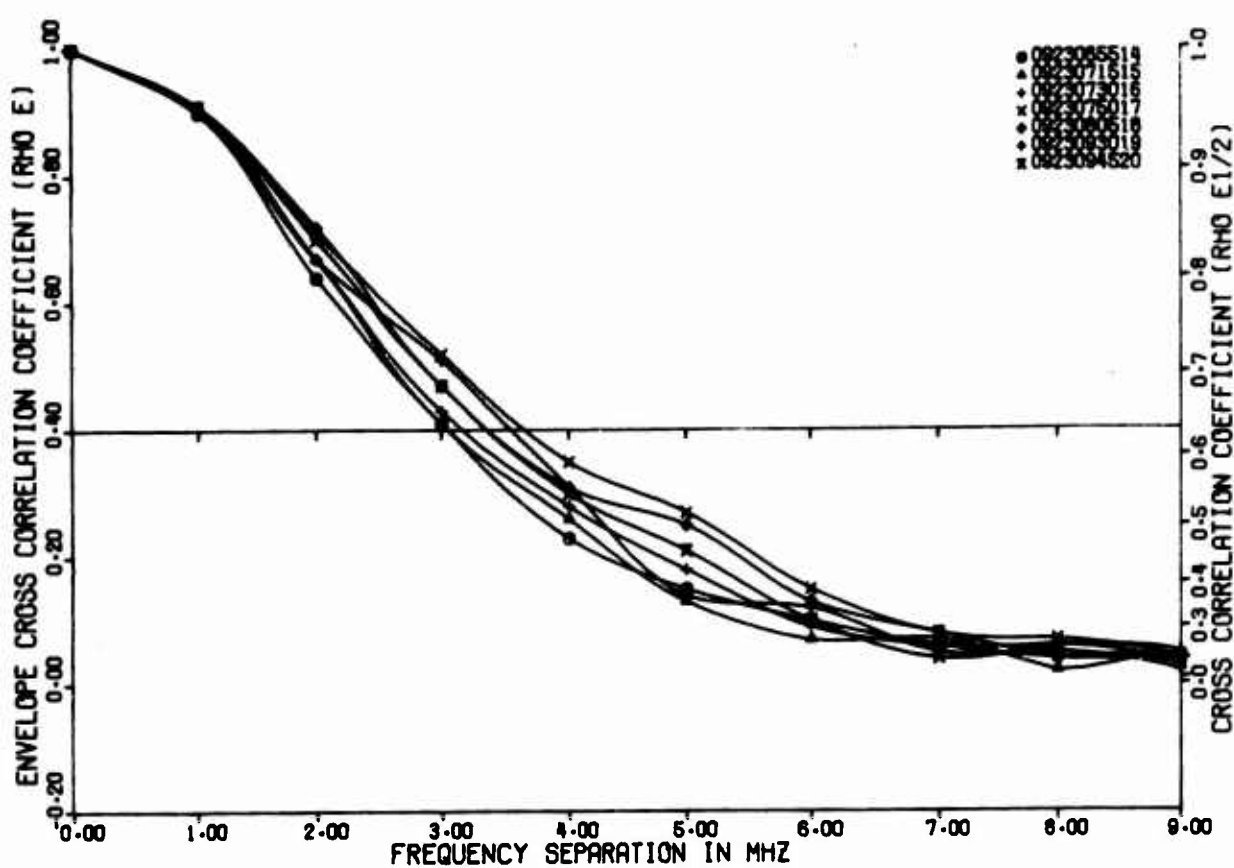


Figure 11. Envelope Cross Correlation Coefficients  
Point Petre, September; C-Band, Wide

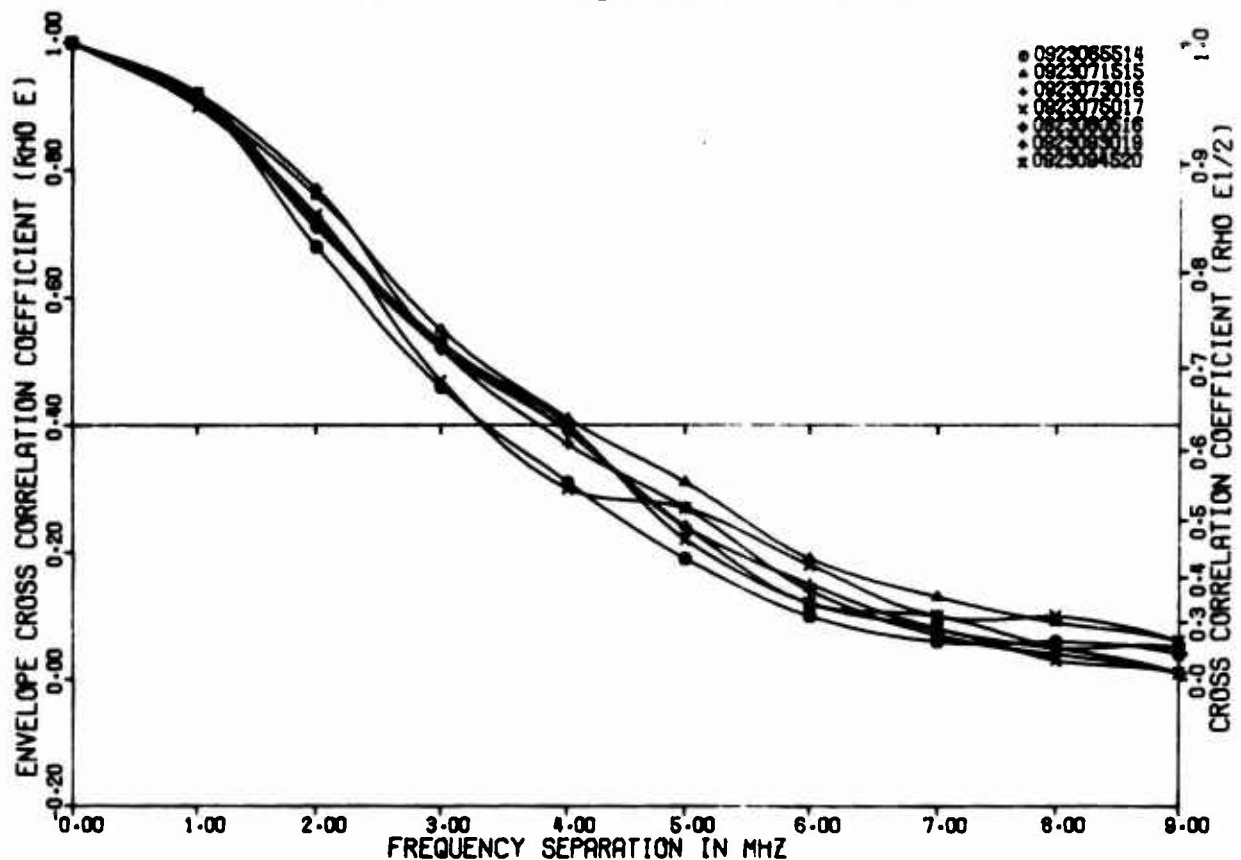


Figure 12. Envelope Cross Correlation Coefficients  
Point Petre, September; X-Band, Wide

#### B. DIURNAL EFFECTS ON CORRELATION BANDWIDTH

The diurnal effects shown in Figures 3 and 4 are of great interest because of the marked discontinuity between the fourth and fifth test on 13 August at Ontario Center. The same discontinuity is observed for both C- and X-band testing. Examination of the Rochester, N. Y. weather records for that day do not indicate any marked change in the weather observed on the ground, but quite evidently significant changes had taken place in the common volume.

A study of the fade rate distributions will show that the fade rates were in general dropping throughout the day (Figures 13 and 14), except during the discontinuity in correlation bandwidth at which time the fade rates increased. This suggests that two competing processes were in effect at the time of the discontinuity. Similarly, the distribution of fade durations (Figures 15 through 18) of the first four wideband tests show no particular variation between the first four tests which resulted in the wide correlation bandwidth and the remaining tests which resulted in the narrower bandwidth group.

While one cannot be conclusive about the weather aloft, one can hypothesize that the scattering mechanism changed from a stable phenomenon such as layers to a more turbulent phenomenon in which the atmosphere is unstable. A model for predicting this unstable behavior is currently under study and is scheduled for inclusion in the next interim report.

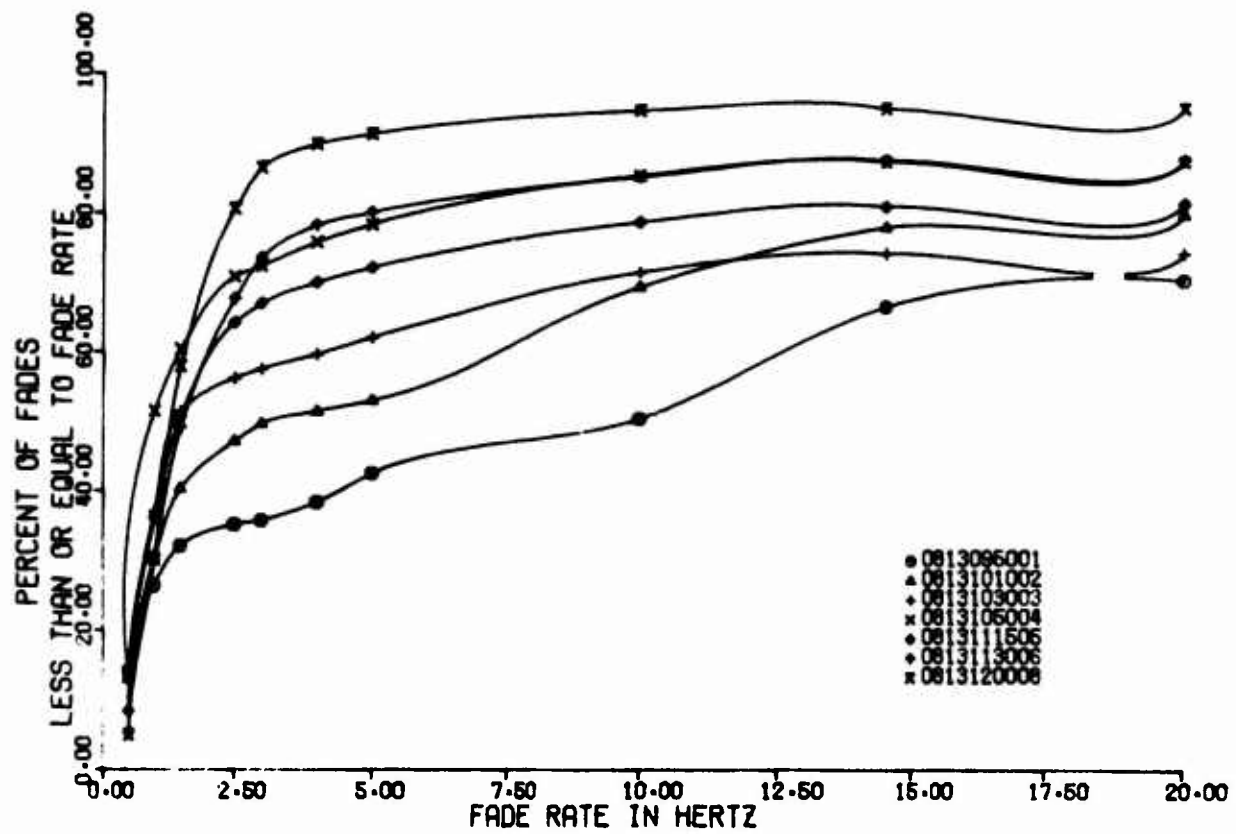


Figure 13. Fade Rate Distribution; Ontario Center, Summer; C-Band

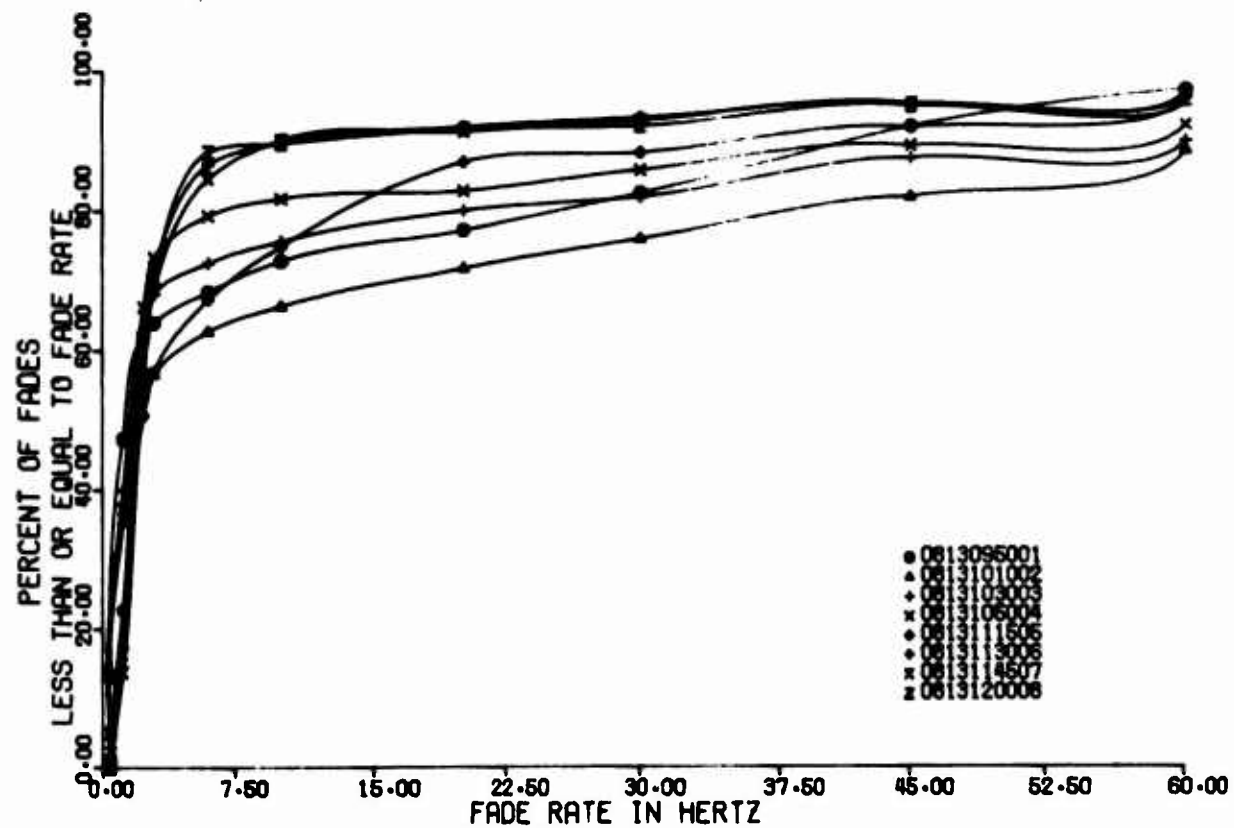


Figure 14. Fade Rate Distribution; Ontario Center, Summer; X-Band

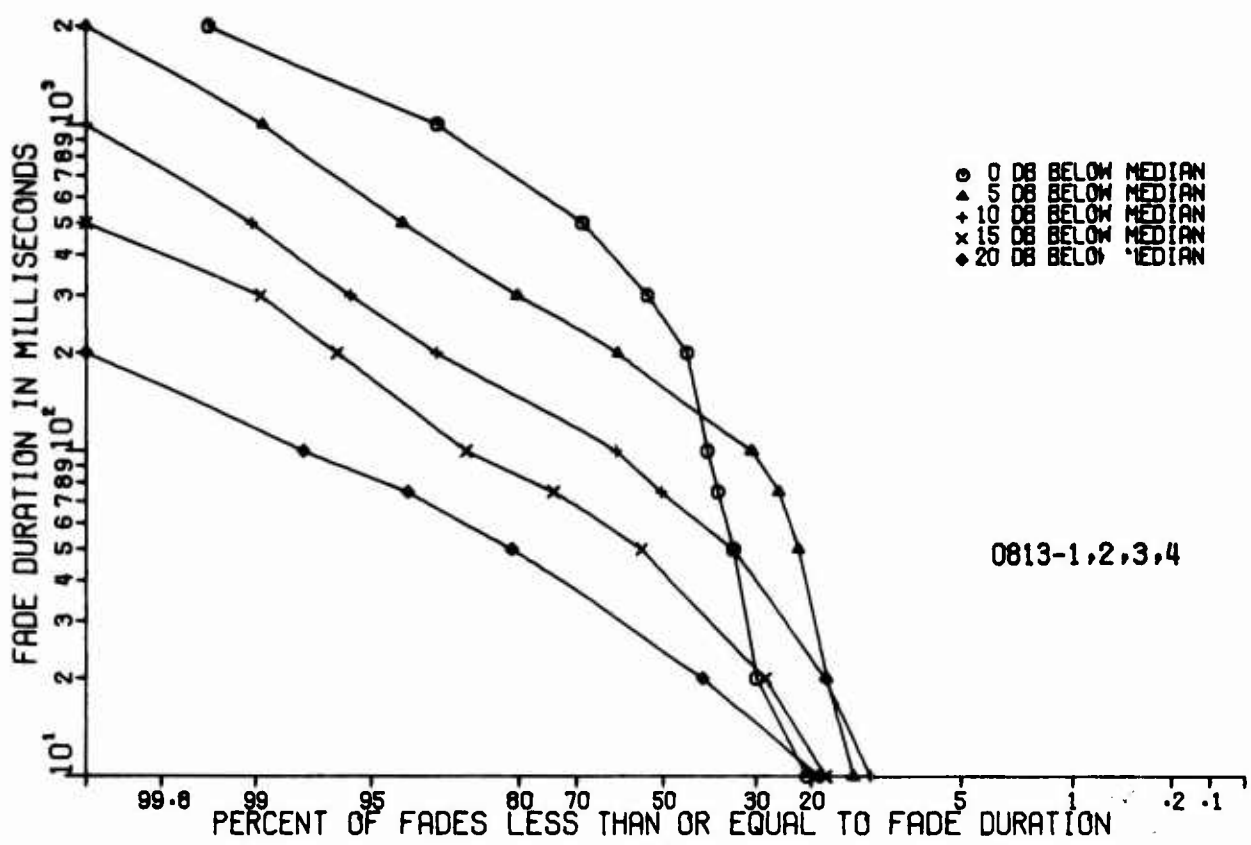


Figure 15. Distribution of Fade Duration; Ontario Center, Summer; C-Band

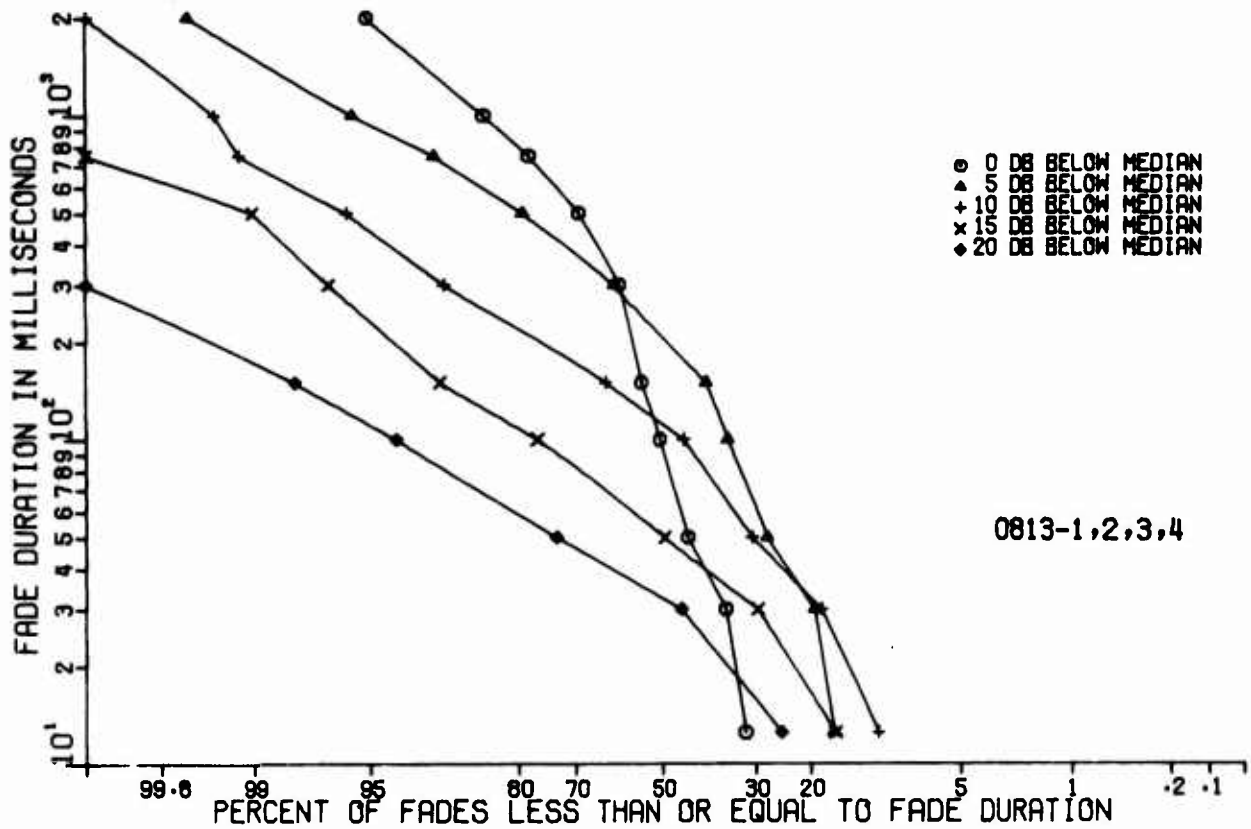


Figure 16. Distribution of Fade Duration; Ontario Center, Summer; X-Band

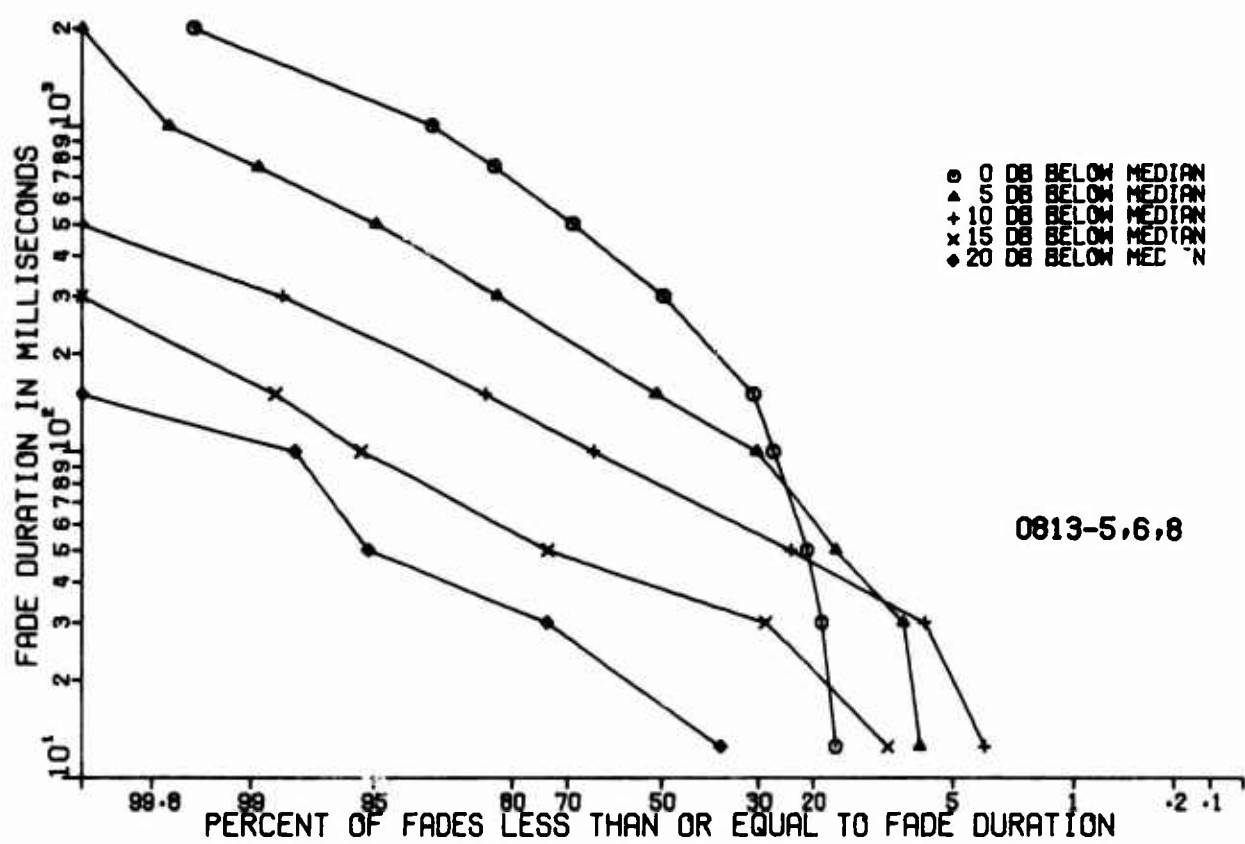


Figure 17. Distribution of Fade Duration  
Ontario Center, Summer; C-Band

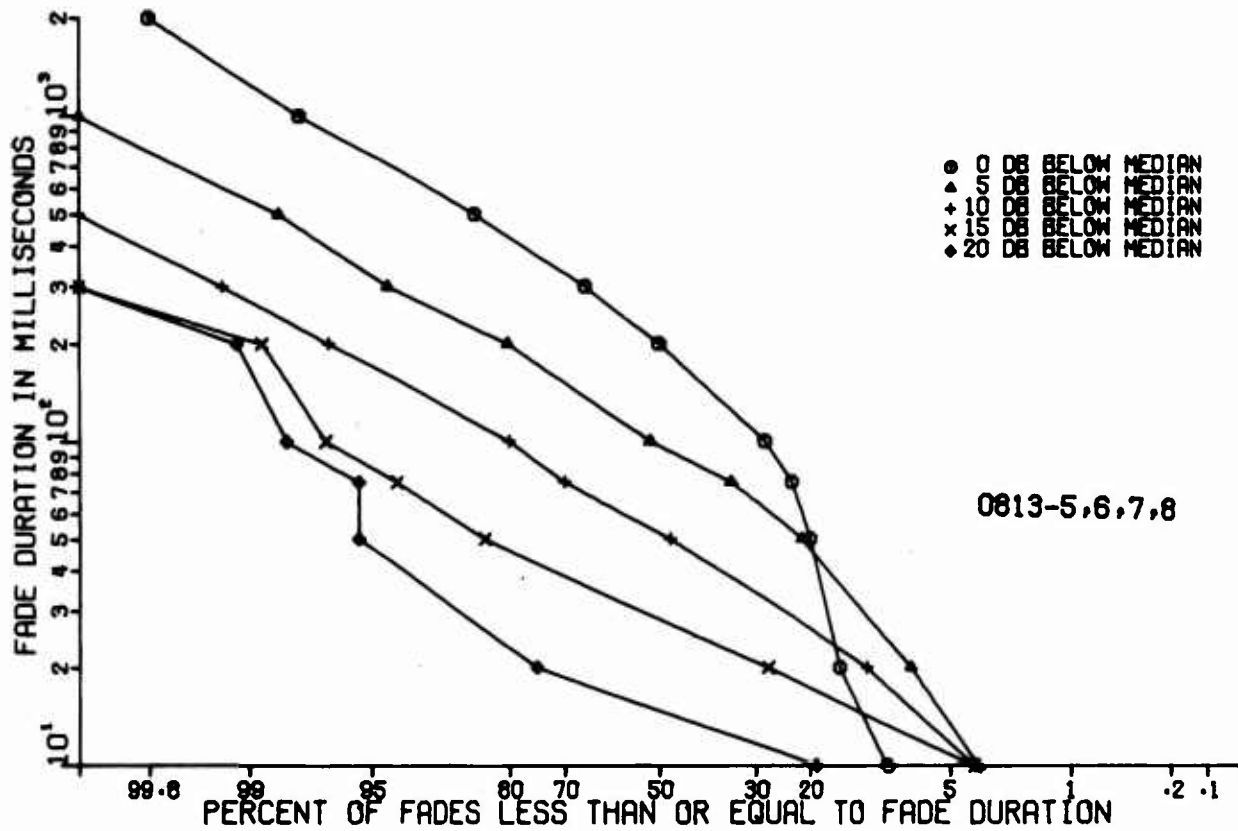


Figure 18. Distribution of Fade Duration  
Ontario Center, Summer; X-Band

### C. NARROW SPACING CORRELATION COEFFICIENT MEASUREMENTS

The narrow spacing tests indicate that the derivative of the cross correlation coefficient with respect to frequency at the origin is small and likely to be zero for both C and X band. This conclusion is supported by the plots for Ontario Center, Whitford and Point Petre (Figures 19 through 23). The data do not show conclusively that it is zero, however.

This derivative has importance in the prediction of nonreducible error rates for certain digital modems that use frequency-time matrices in their coding structure. A simple exponential function for correlation predicts a nonreducible error rate of about  $10^{-7}$  BER while a gaussian function whose derivative is zero at the origin predicts a nonreducible BER of  $10^{-11}$  (see Reference 2).

In the next period some narrow band tests will be considered using a spacing of 50 kHz to make a final test of the derivative of the cross correlation coefficient at the origin. The test should be run to study the function closer to the origin, for the curves presented to be capable of being fitted to a simple exponential. The present instrumentation cannot operate much closer than this spacing due to frequency instabilities and the required bandwidth of each channel in the receiving system. The results will be presented in the next interim report.

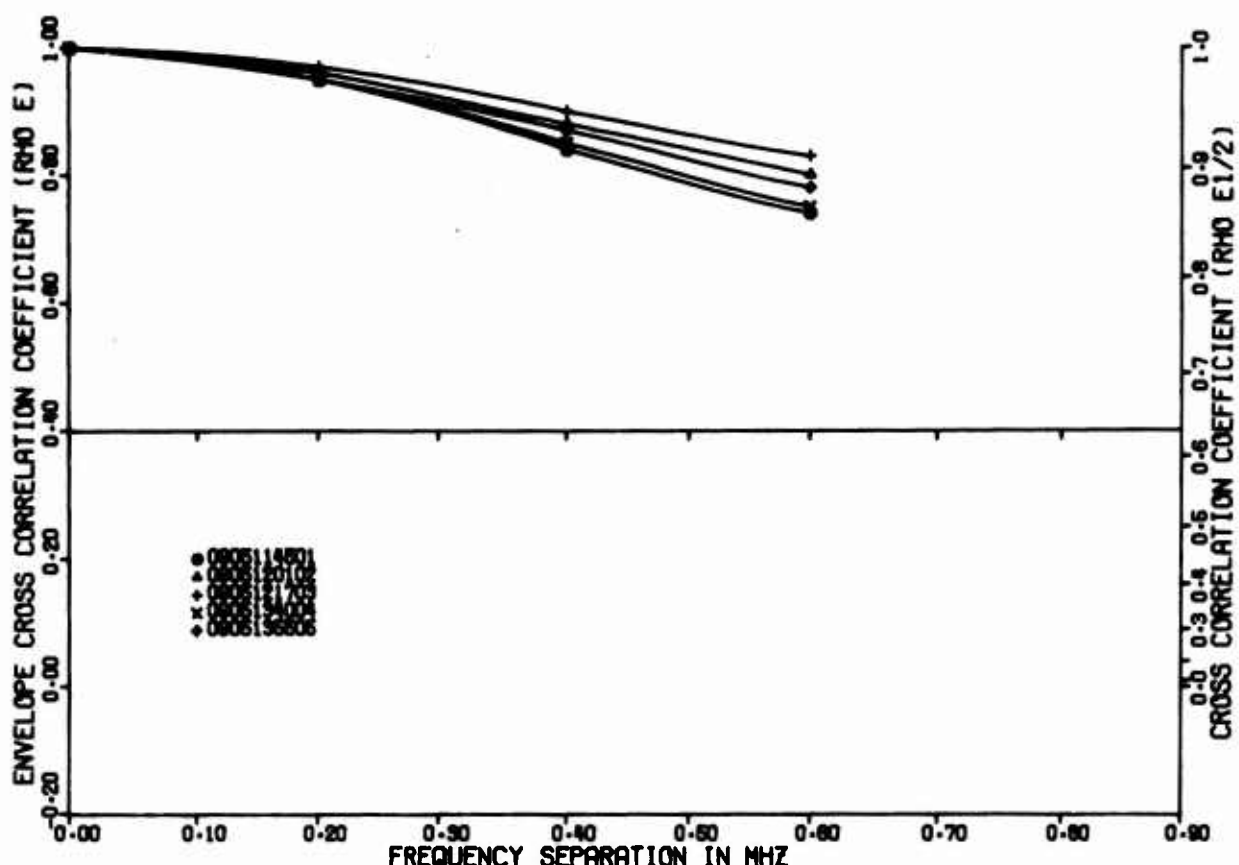


Figure 19. Envelope Cross Correlation Coefficients  
Whitford Field, Summer; X-Band, Narrow

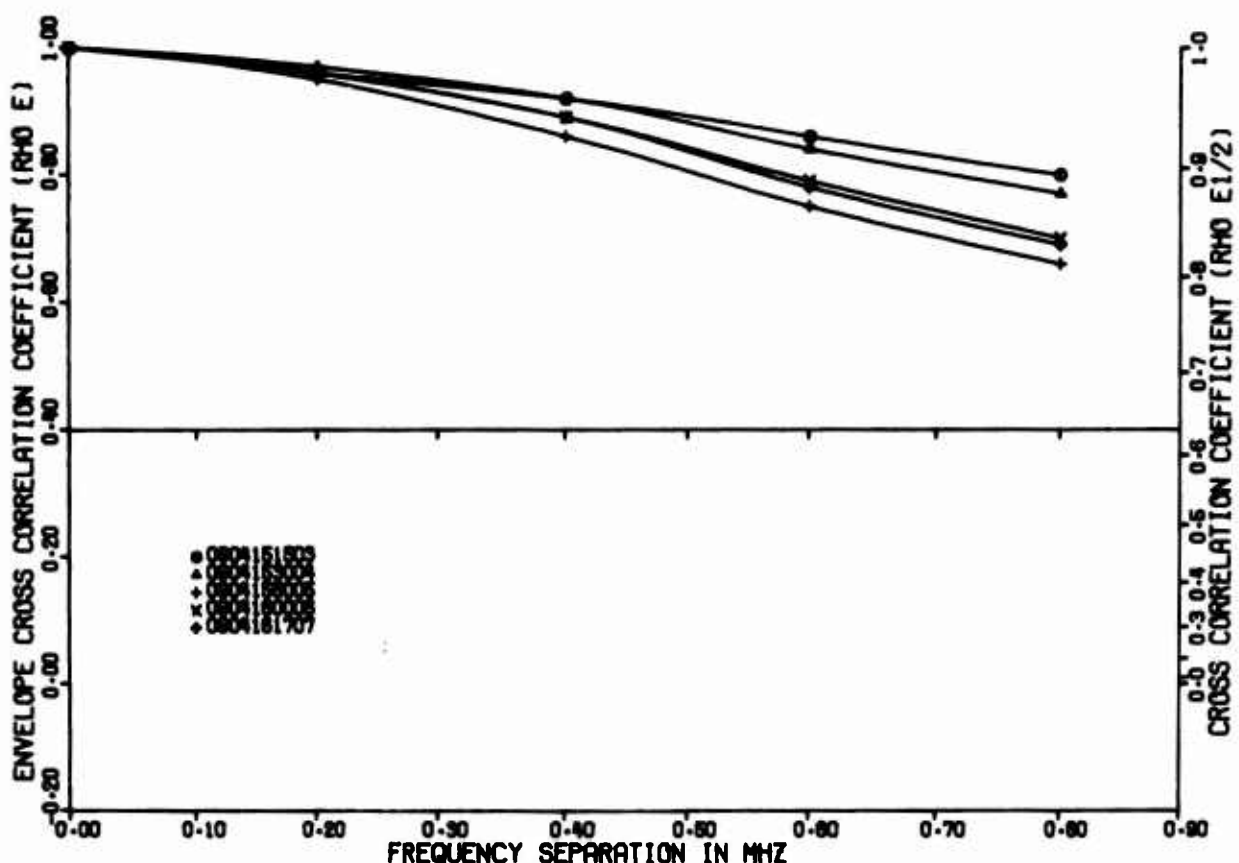


Figure 20. Envelope Cross Correlation Coefficients  
Whitford Field, Summer; C-Band, Narrow

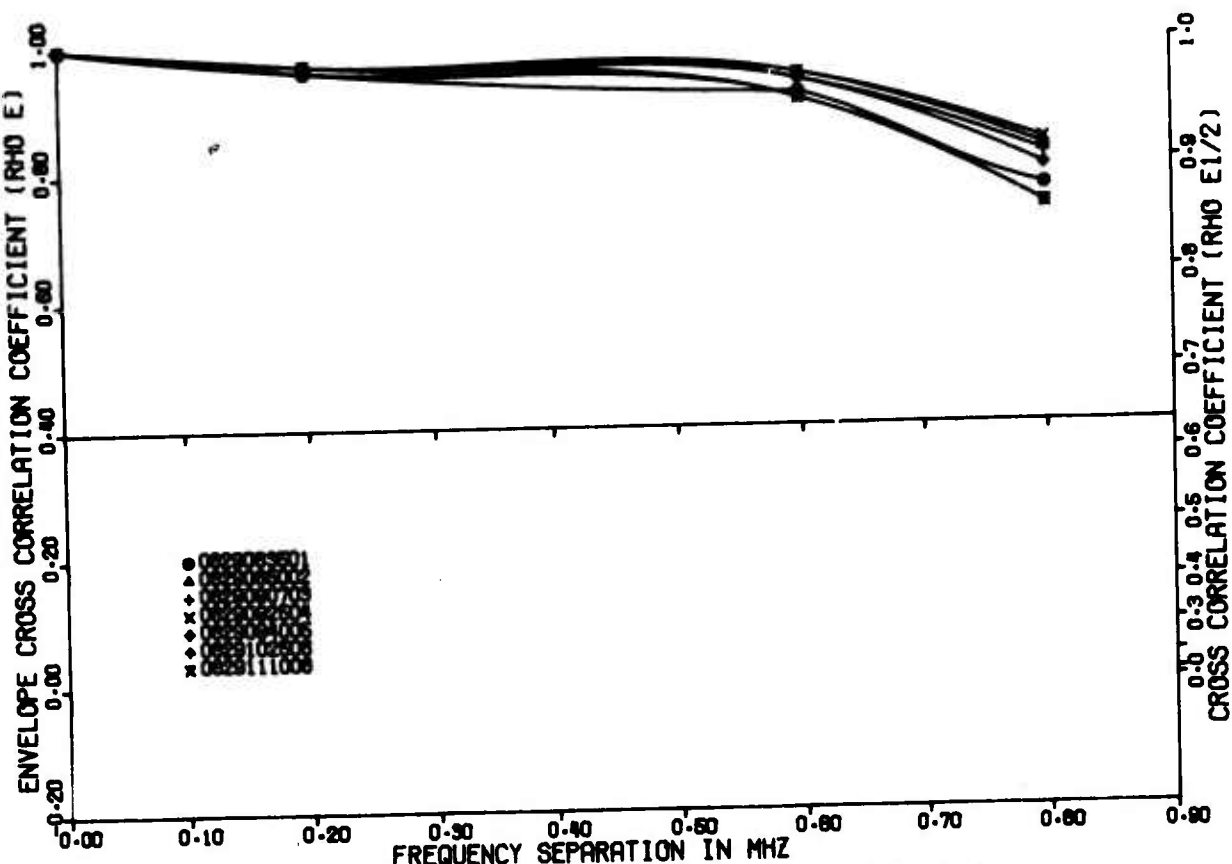


Figure 21. Envelope Cross Correlation Coefficients  
Whitford Field, Summer; X-Band, Narrow

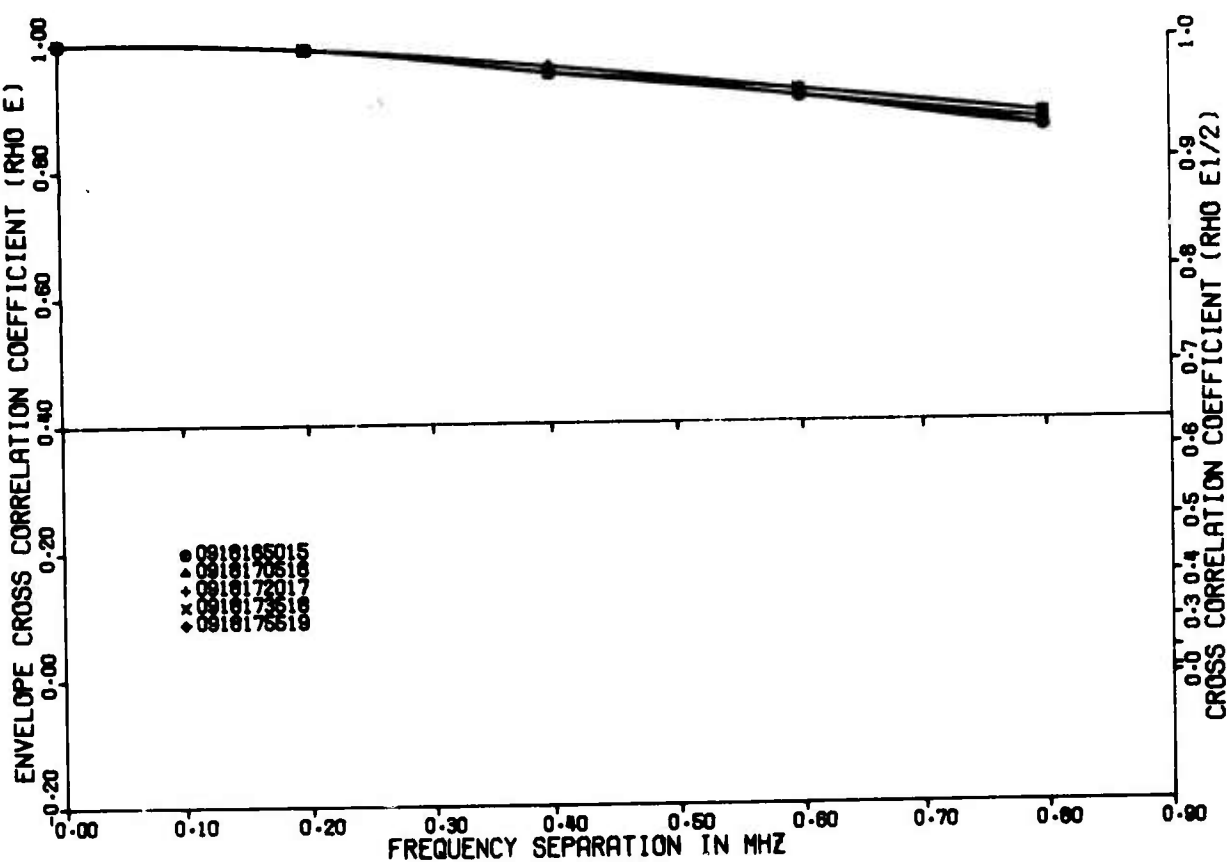


Figure 22. Envelope Cross Correlation Coefficients  
Point Petre, September; X-Band, Narrow

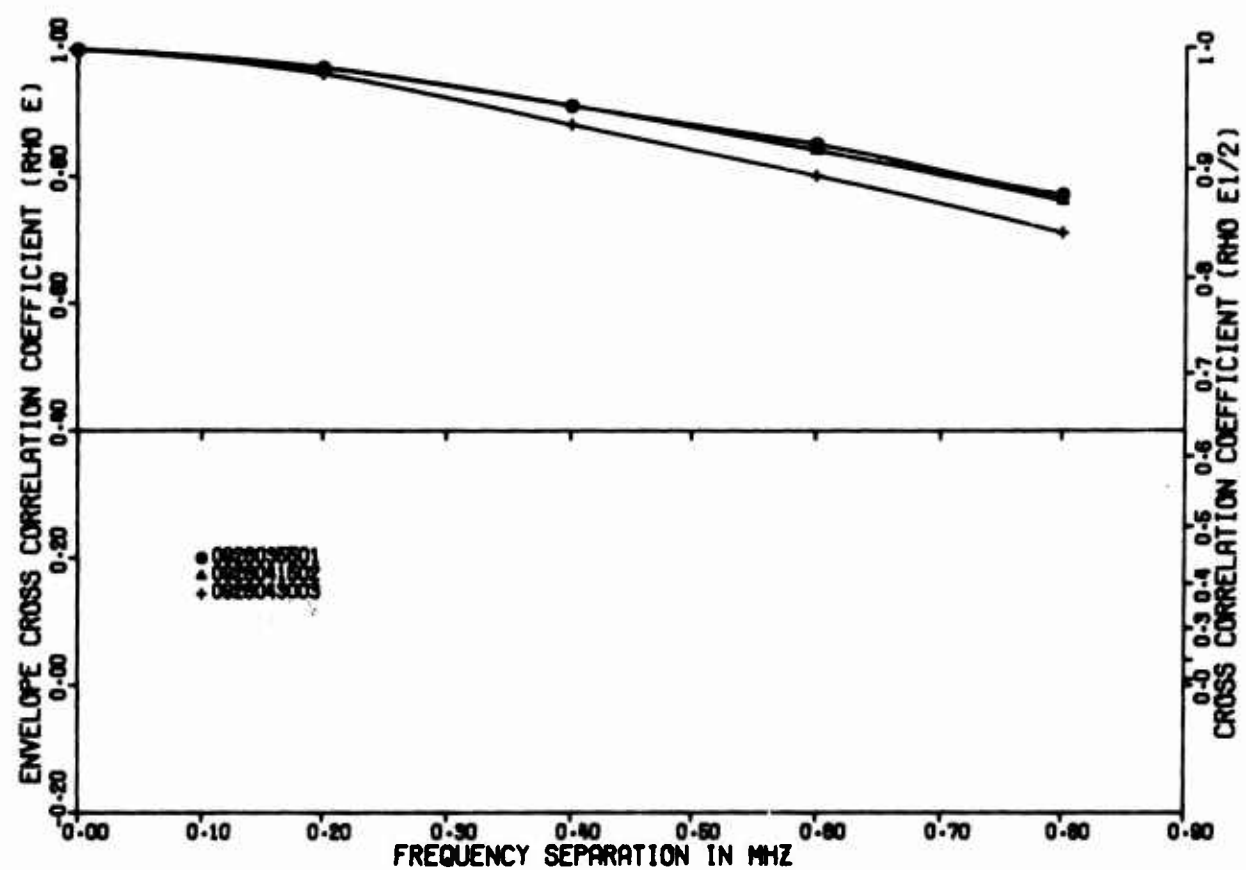


Figure 23. Envelope Cross Correlation Coefficients  
Point Petre, September; C-Band, Narrow

#### D. TYPICAL EXAMPLES OF PROPAGATION DATA

The following are representative sets of correlation bandwidth and fade statistics for the three paths during the summer of 1969. Plots of correlation bandwidth, fade rates, fade durations, signal amplitude distributions, and depth of fade distributions are presented in sets of X and C band over the same test numbers where available. In some cases the fade margins during the tests were not sufficient to plot more than correlation bandwidths and fade rates. This was especially true of the data taken at the Whitford field site due to low median signal strengths.

The curves are presented on a test by test basis to show the rapidly changing situation that exists in the troposphere that affects propagation of troposcatter signals. These changes occur over periods of a few seconds to a few hours, but rarely are they constant for an interval longer than a fraction of an hour. The next interim report will consider the upper and lower deciles of the measured variables to enable designers to establish criteria for the design of digital modems for use on the MALLARD troposcatter links.

##### 1. Ontario Center

The Ontario Center RADC test site is the shortest range troposcatter terminal in this series. It is 140 km from the transmitter at the RADC test site in Model City, N. Y. This short range would naturally predict the widest correlation bandwidth according to the curve used in the first interim report. The set of curves in Figures 24 through 28 represent the widest X-band cross correlation coefficients obtained during the summer testing period. There are no C-band data available to compare with this set of data since the C-band transmitter was inoperative at the time. Figures 29 through 33 are typical of the C-band data and show the typical extremes through which the correlation bandwidths vary during the day. Note that there is an almost one for one correspondence of the companion X-band data (Figures 34 through 38). Figures 39 through 43 show typical data obtained during the summer for C band. The data of 19 August 1969 for C band are typical of the narrowest bandwidths obtained on this path. Figures 44 through 48 and 49 through 53 are simultaneous pairs of C- and X-band tests with the exception of two tests. Here a tendency for the fade rates to run unpredictably high is very noticeable. The high fade rates caused the cumulative distributions of fade durations to appear erratic in both the X- and C-band cases. These high fade rates occur often enough to be viewed with concern because adaptive frequency modems must have time to communicate the best operating frequency across the link. These fade rates are in excess of 60 Hz and put the best frequency commands in a dangerous time shortage.

One can conclude that the correlation bandwidths on the short path are probably the widest to be expected on MALLARD troposcatter links. While this might cause some slight loss in frequency diversity, it should be noted that this disadvantage is overcome by the abundance of fade margin which was always available over this short path (see Appendix B for signal strengths). Of course, the previous conclusion that the correlation bandwidths are about the same for C or X band are noticeable in these data as well as the data presented in section III.

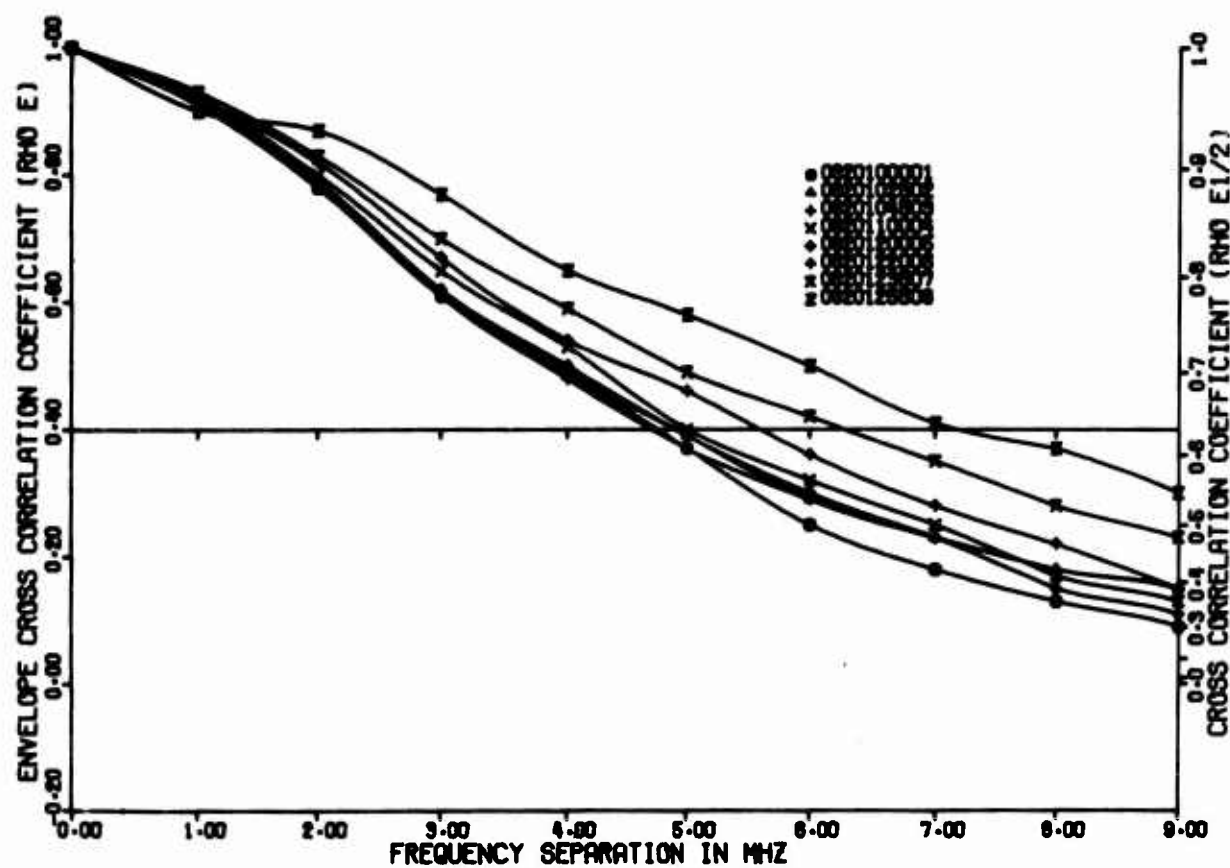


Figure 24. Envelope Cross Correlation Coefficients  
Ontario Center, Summer; X-Band, Wide

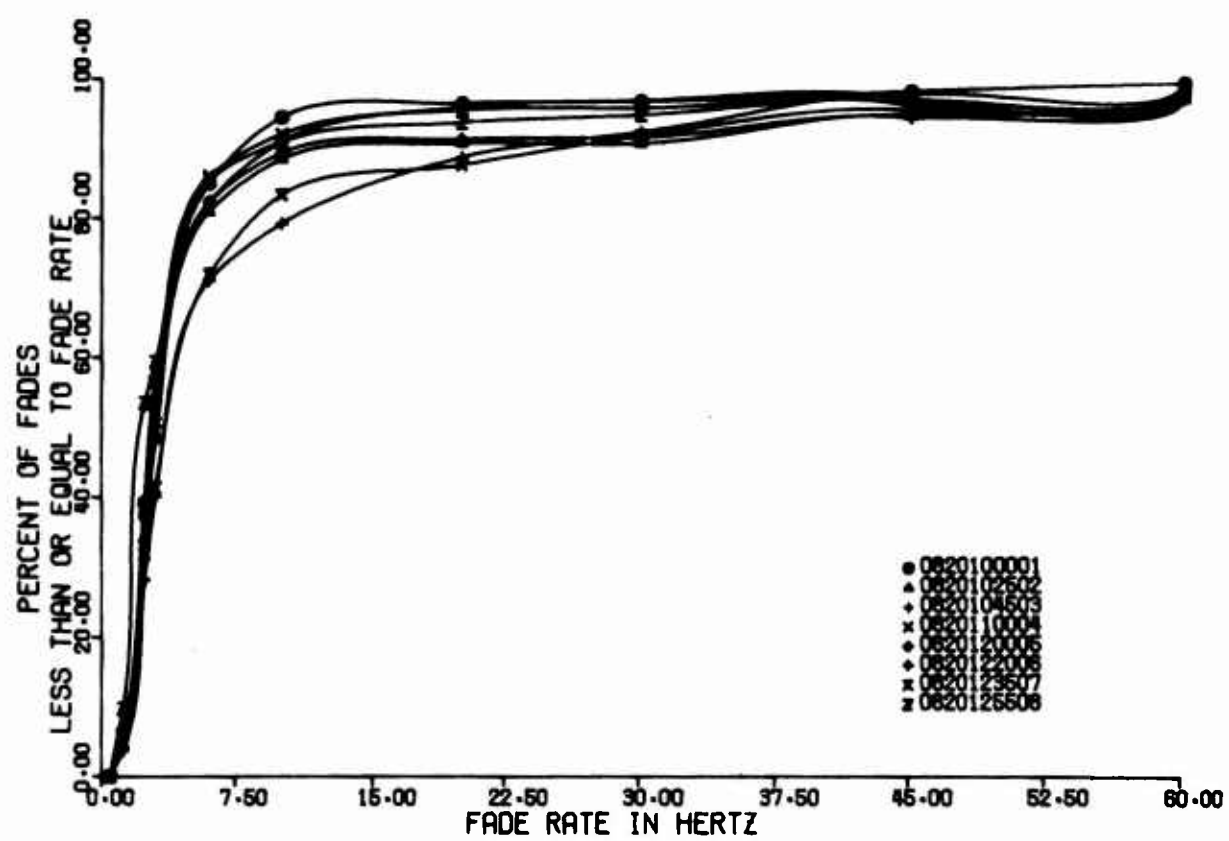


Figure 25. Fade Rate Distribution  
Ontario Center, Summer; X-Band

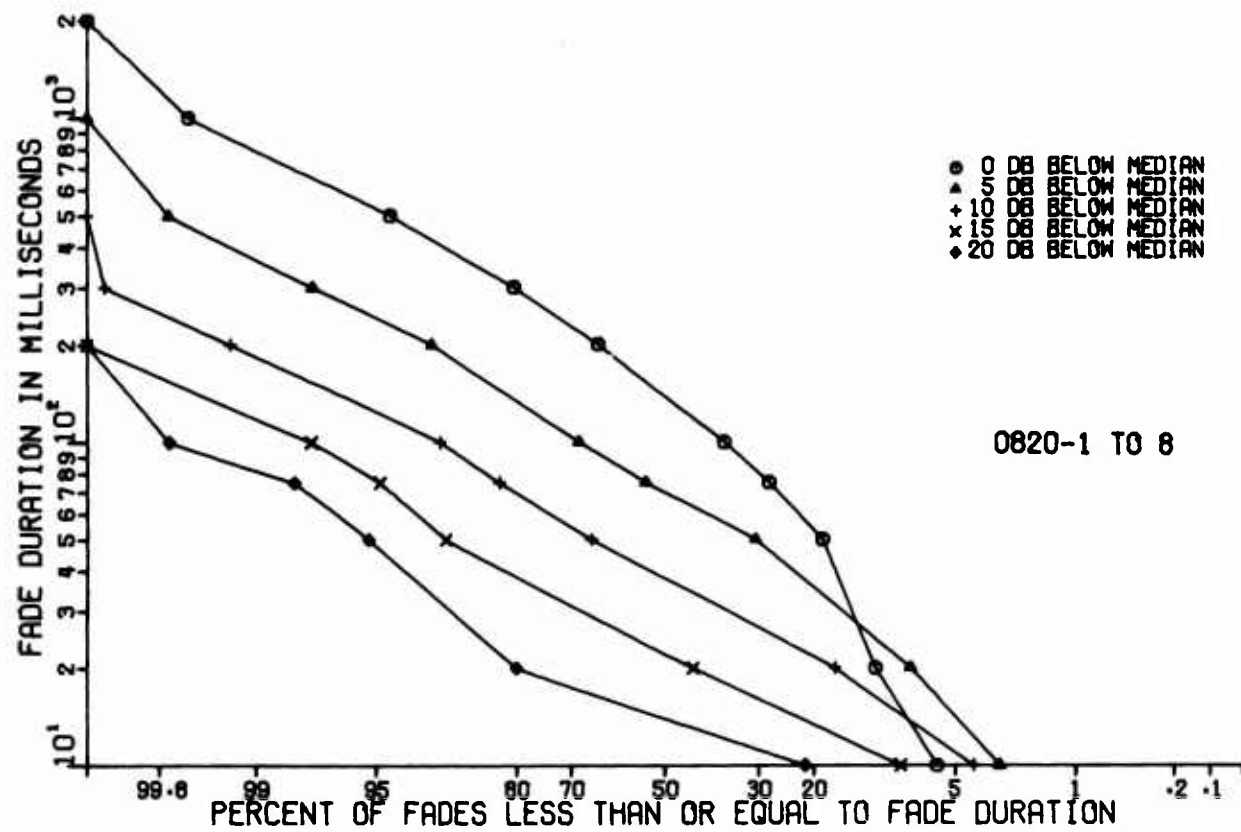


Figure 26. Distribution of Fade Duration  
Ontario Center, Summer; X-Band

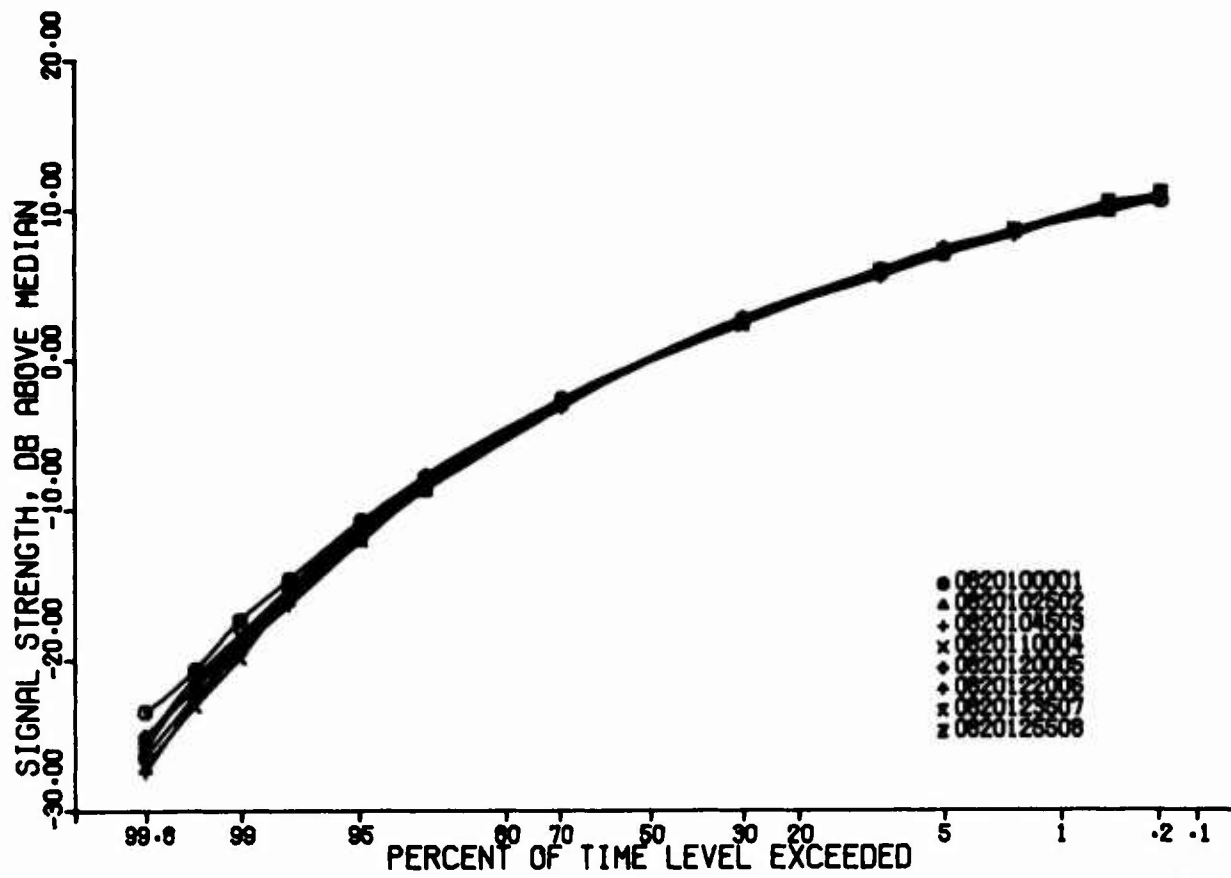


Figure 27. Signal Amplitude Level  
Ontario Center, Summer; X-Band

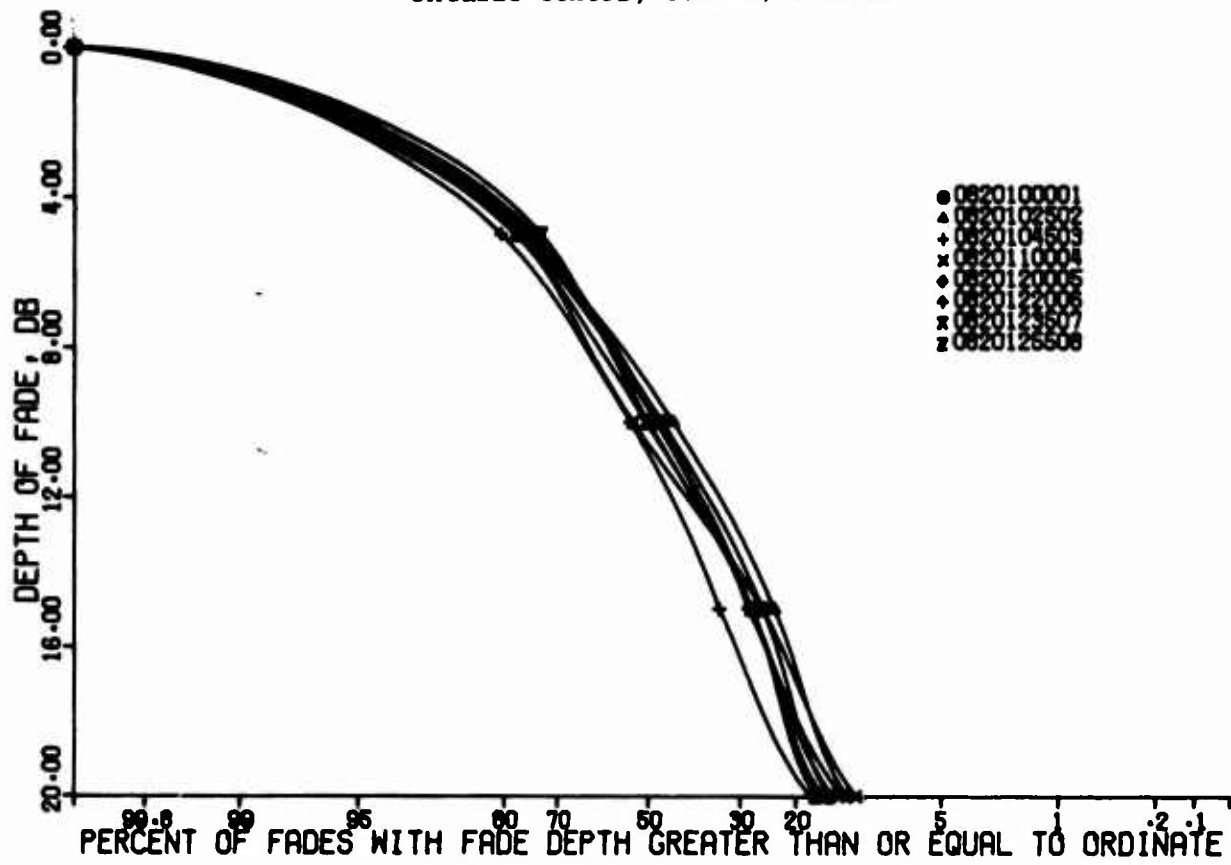


Figure 28. Distribution of Depth of Fades  
Ontario Center, Summer; C-Band

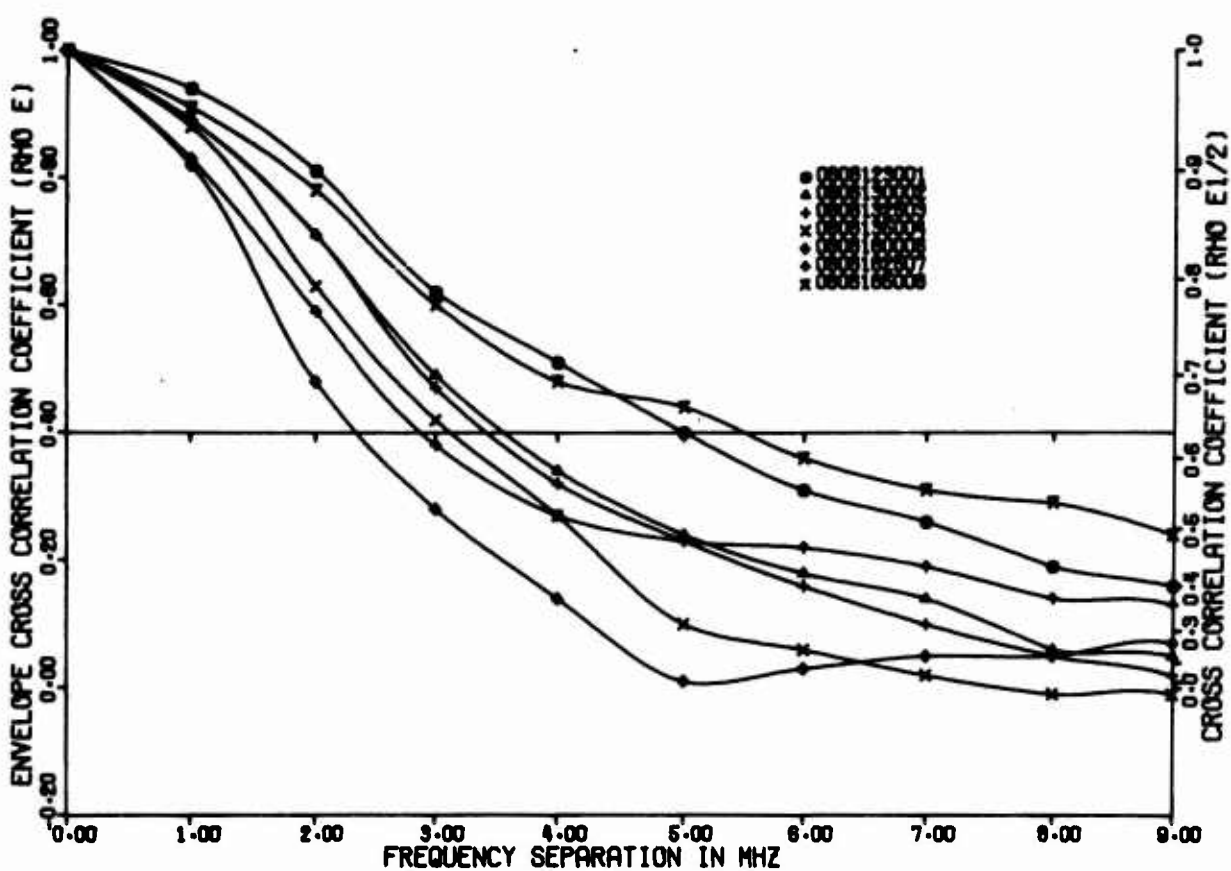


Figure 29. Envelope Cross Correlation Coefficients  
Ontario Center, Summer; C-Band, Wide

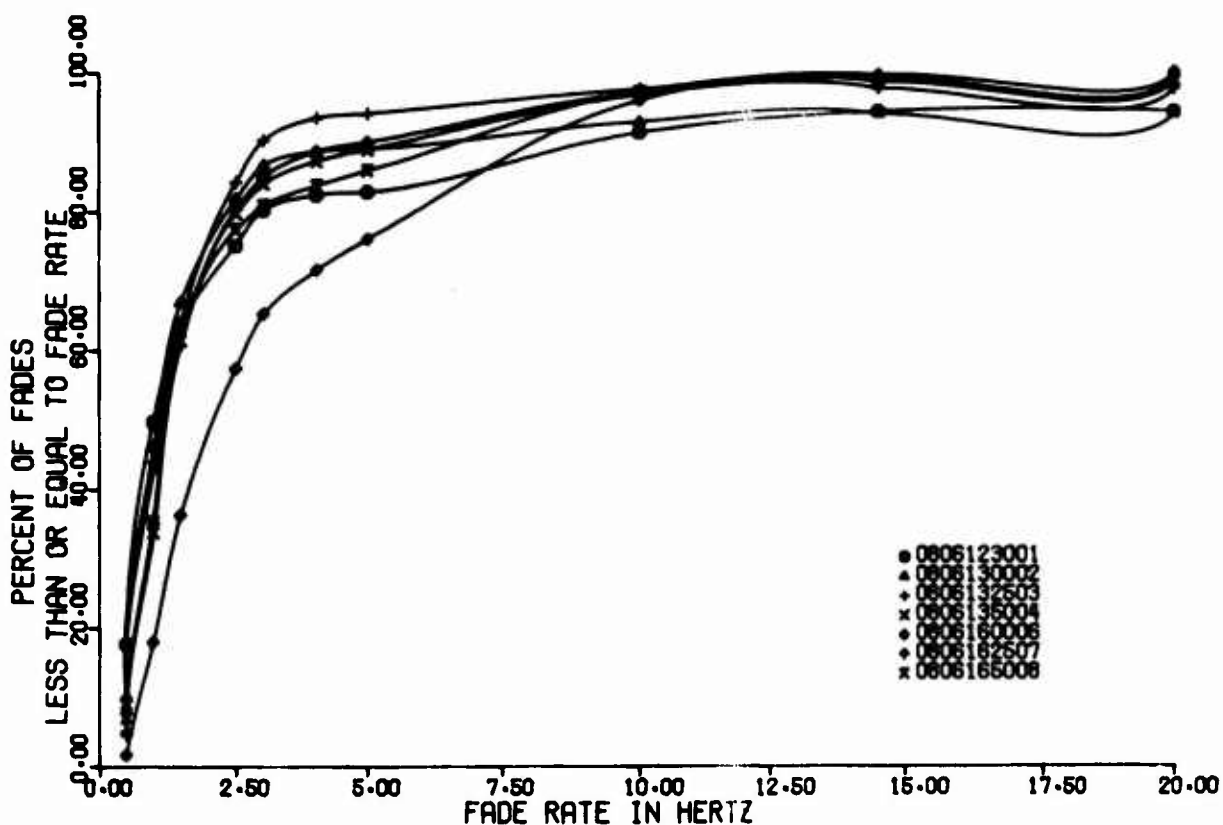


Figure 30. Fade Rate Distribution  
Ontario Center, Summer; C-Band

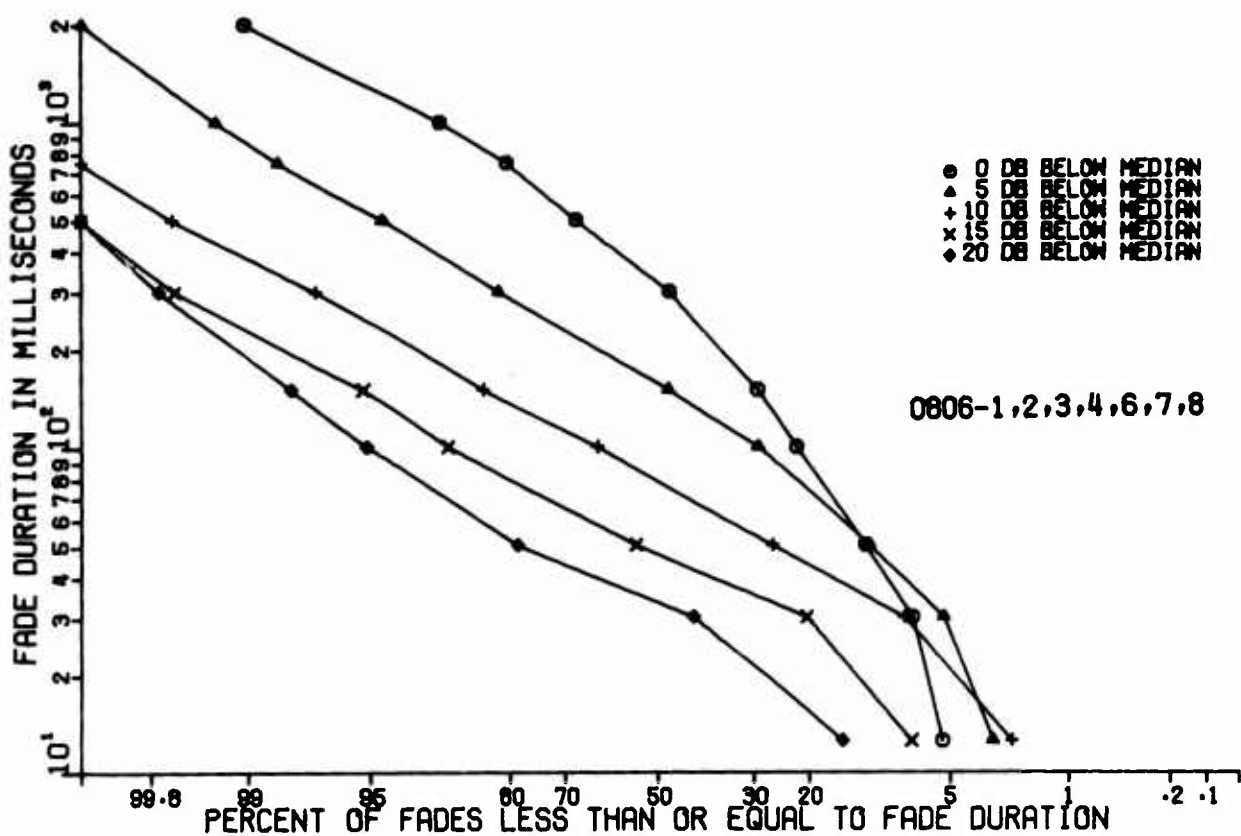


Figure 31. Distribution of Fade Duration  
Ontario Center, Summer; C-Band

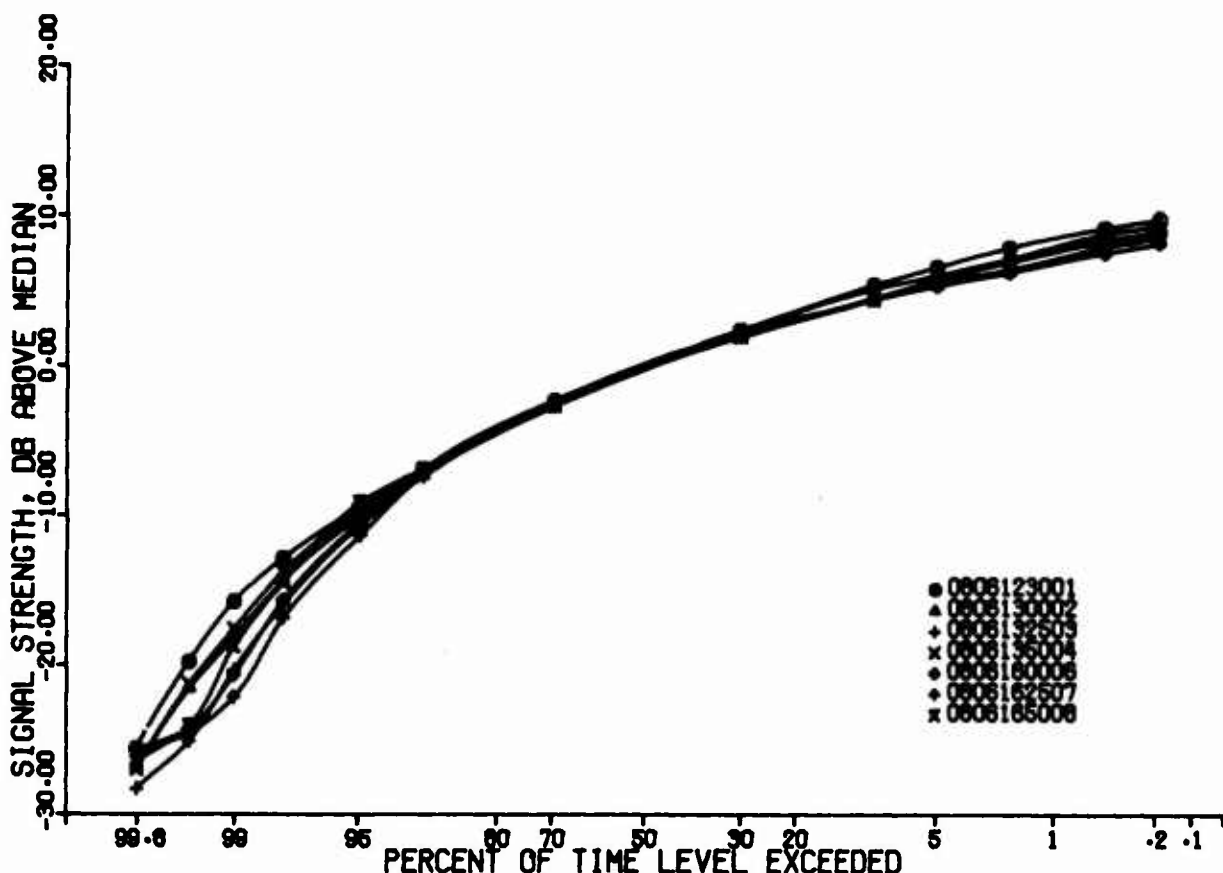
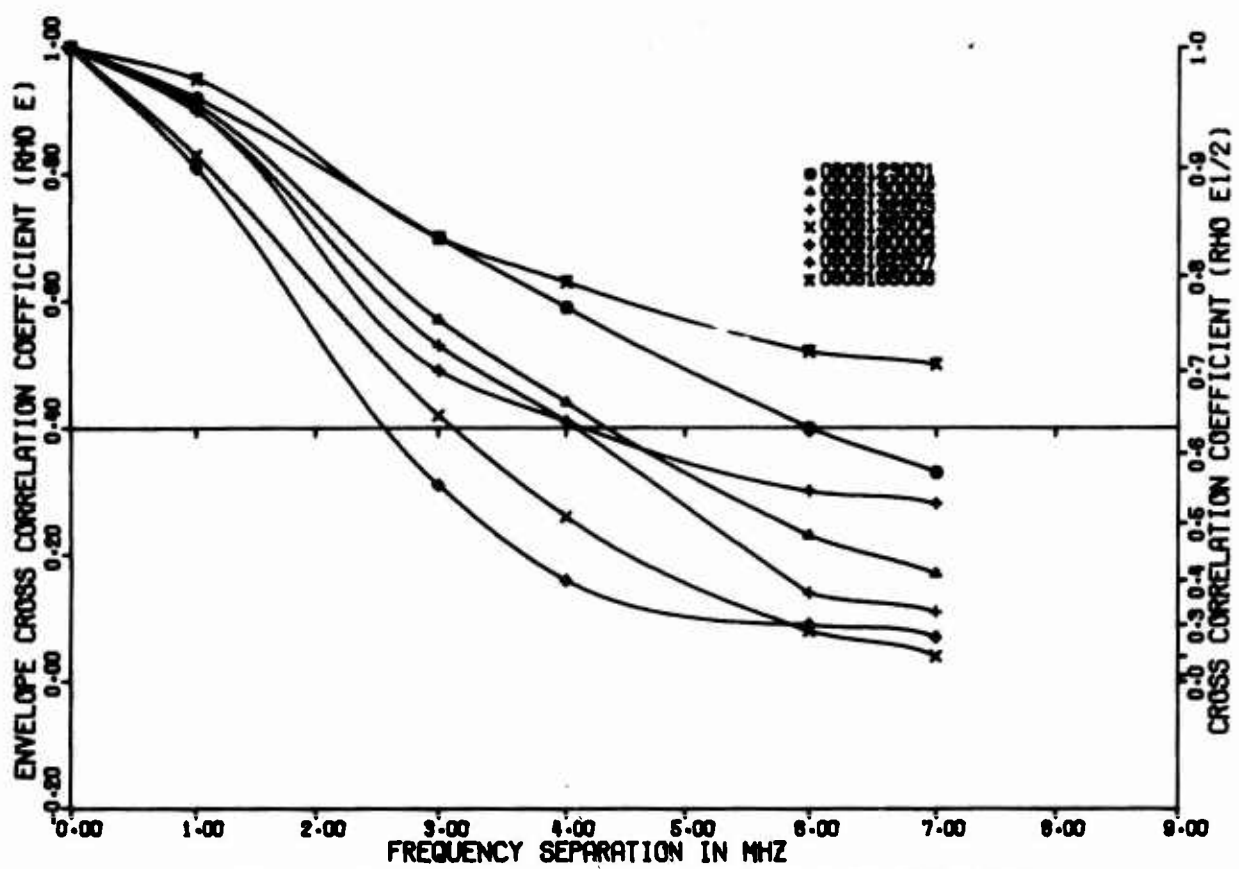
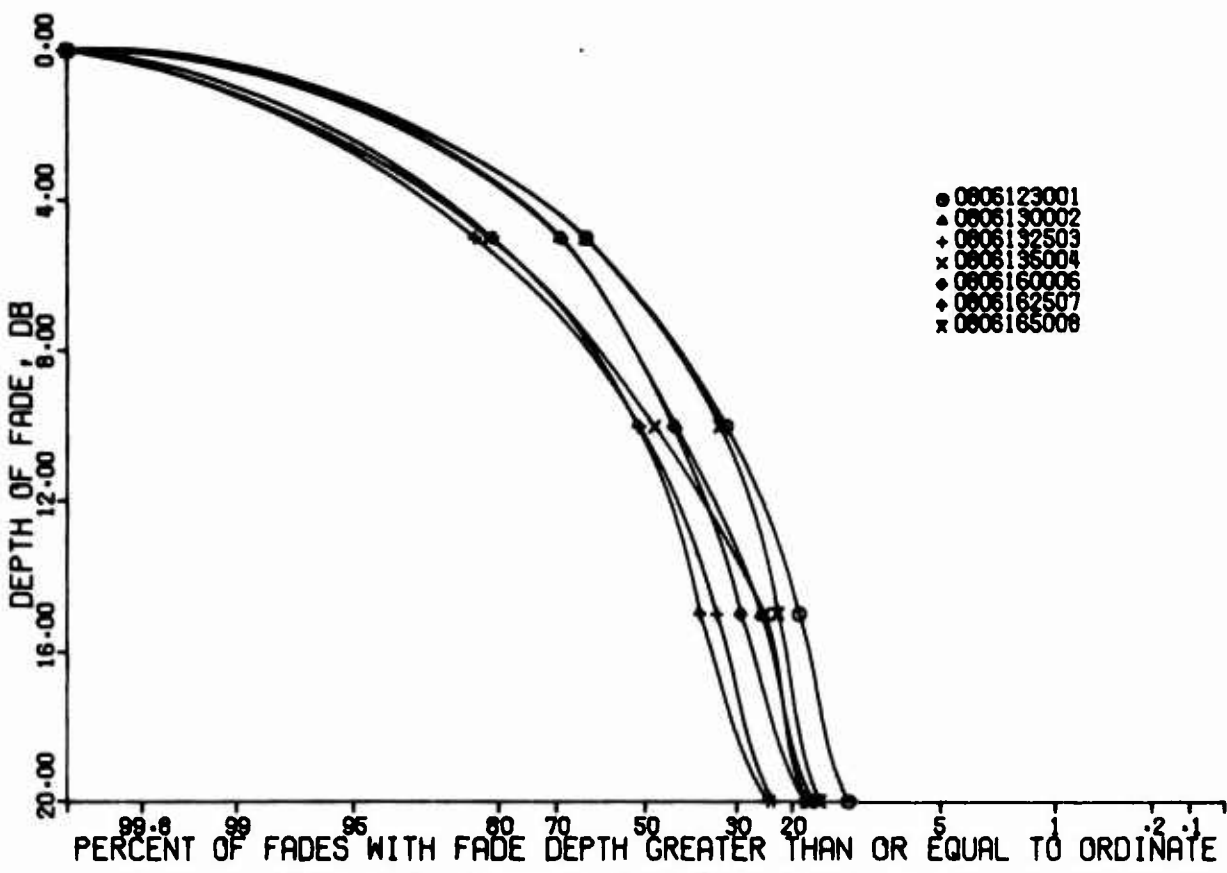


Figure 32. Signal Amplitude Level  
Ontario Center, Summer; C-Band



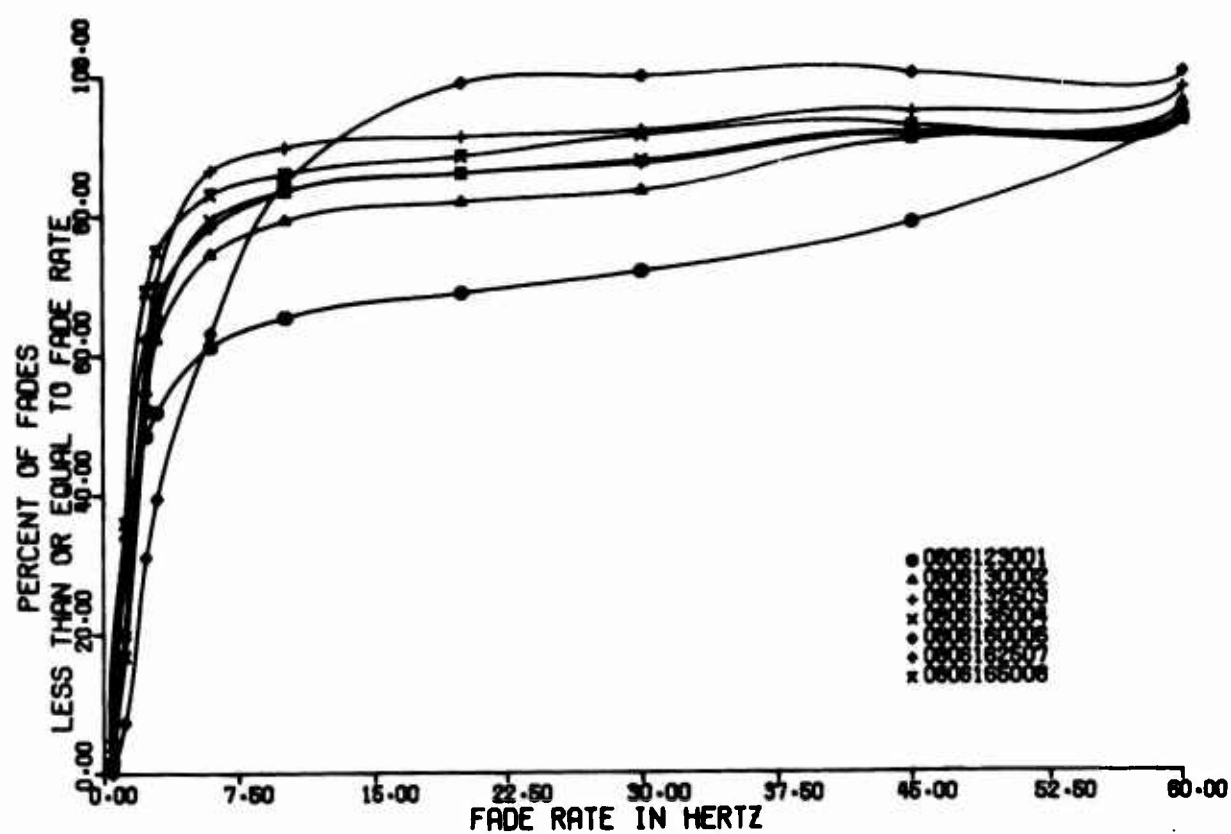


Figure 35. Fade Rate Distribution  
Ontario Center, Summer; X-Band

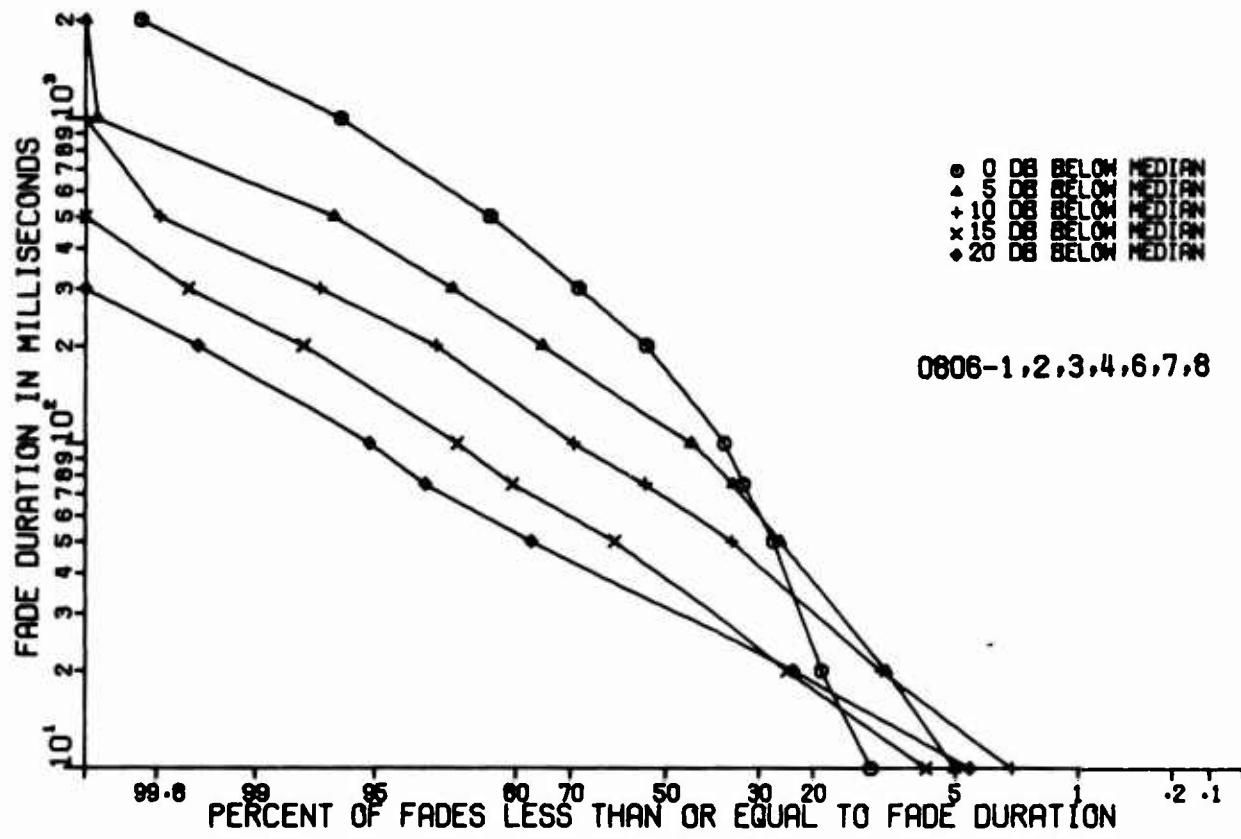


Figure 36. Distribution of Fade Duration  
Ontario Center, Summer; X-Band

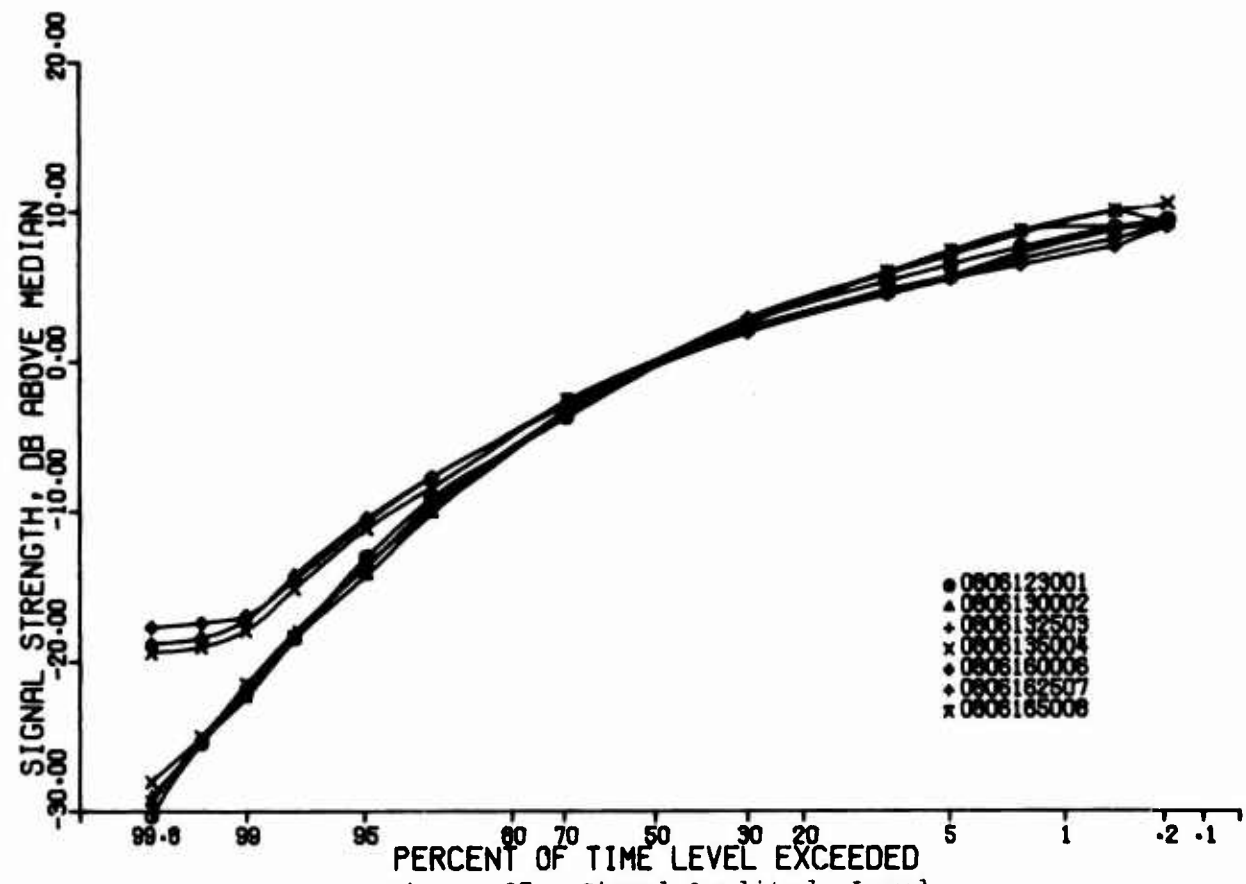


Figure 37. Signal Amplitude Level  
Ontario Center, Summer; X-Band

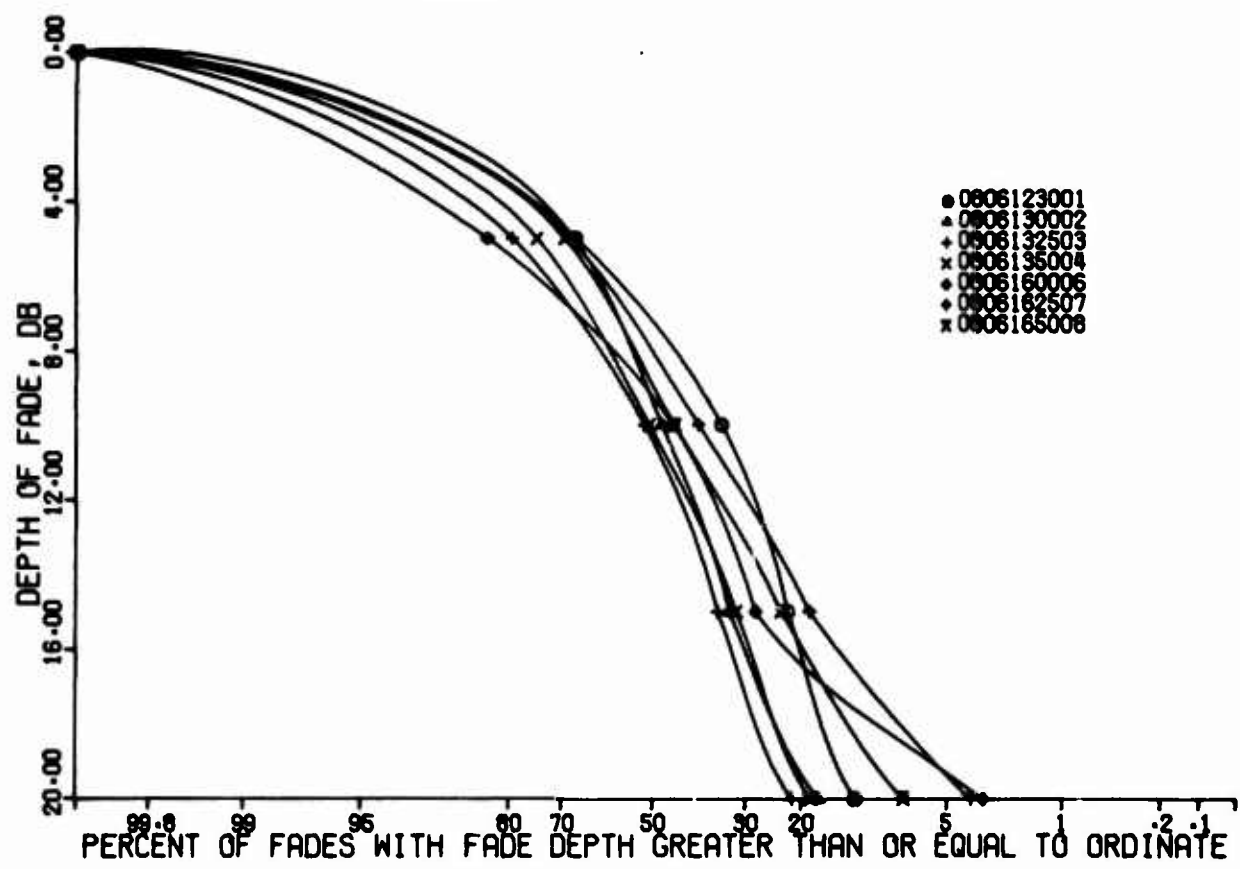


Figure 38. Distribution of Depth of Fades  
Ontario Center, Summer; X-Band

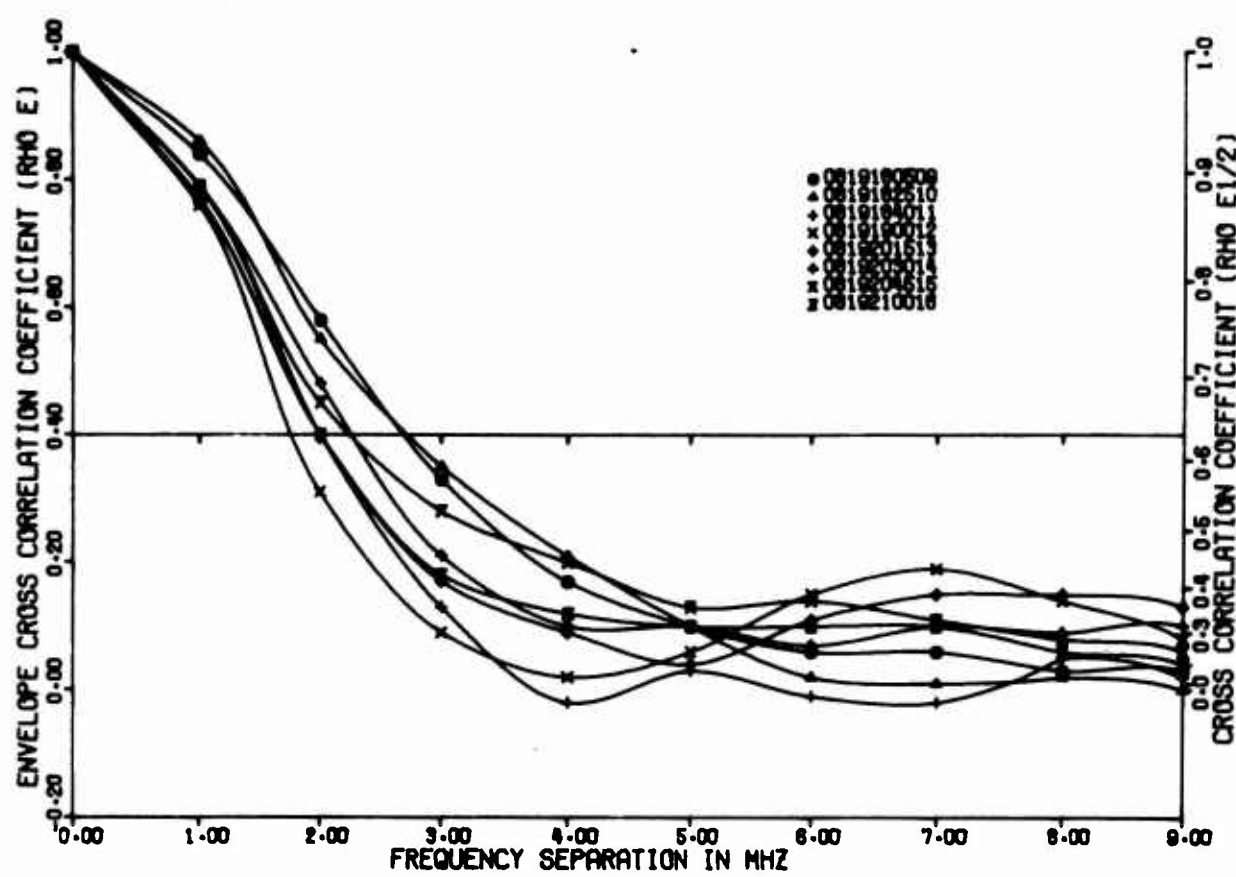


Figure 39. Envelope Cross Correlation Coefficients  
Ontario Center, Summer; C-Band, Wide

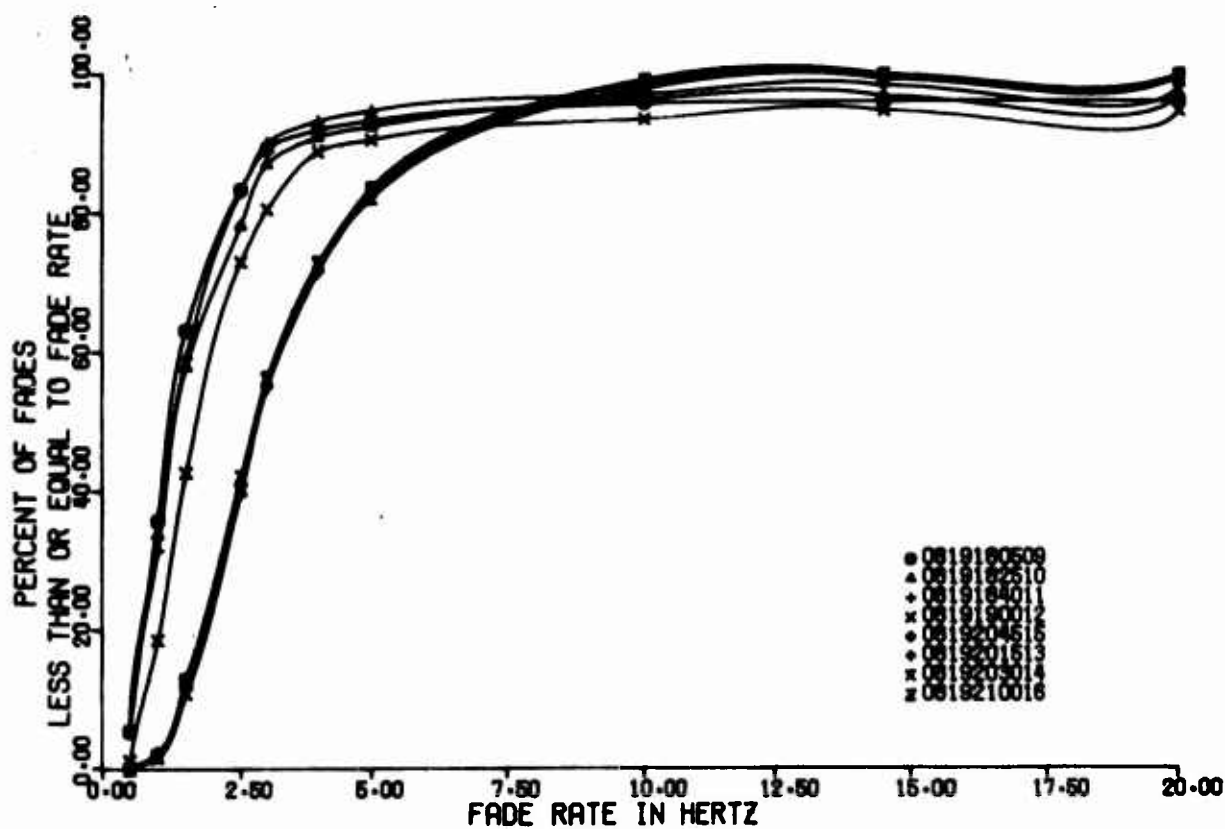


Figure 40. Fade Rate Distribution  
Ontario Center, Summer; C-Band

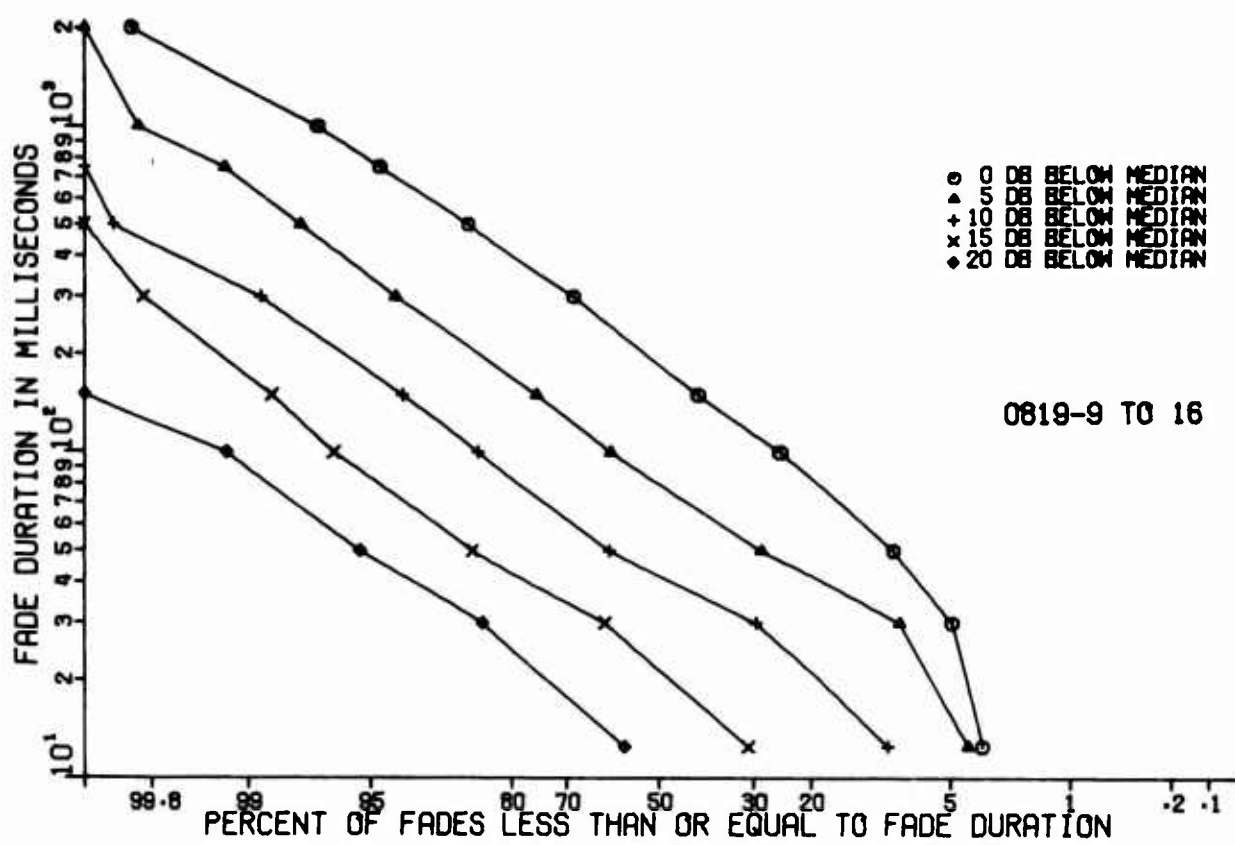


Figure 41. Distribution of Fade Duration  
Ontario Center, Summer; C-Band

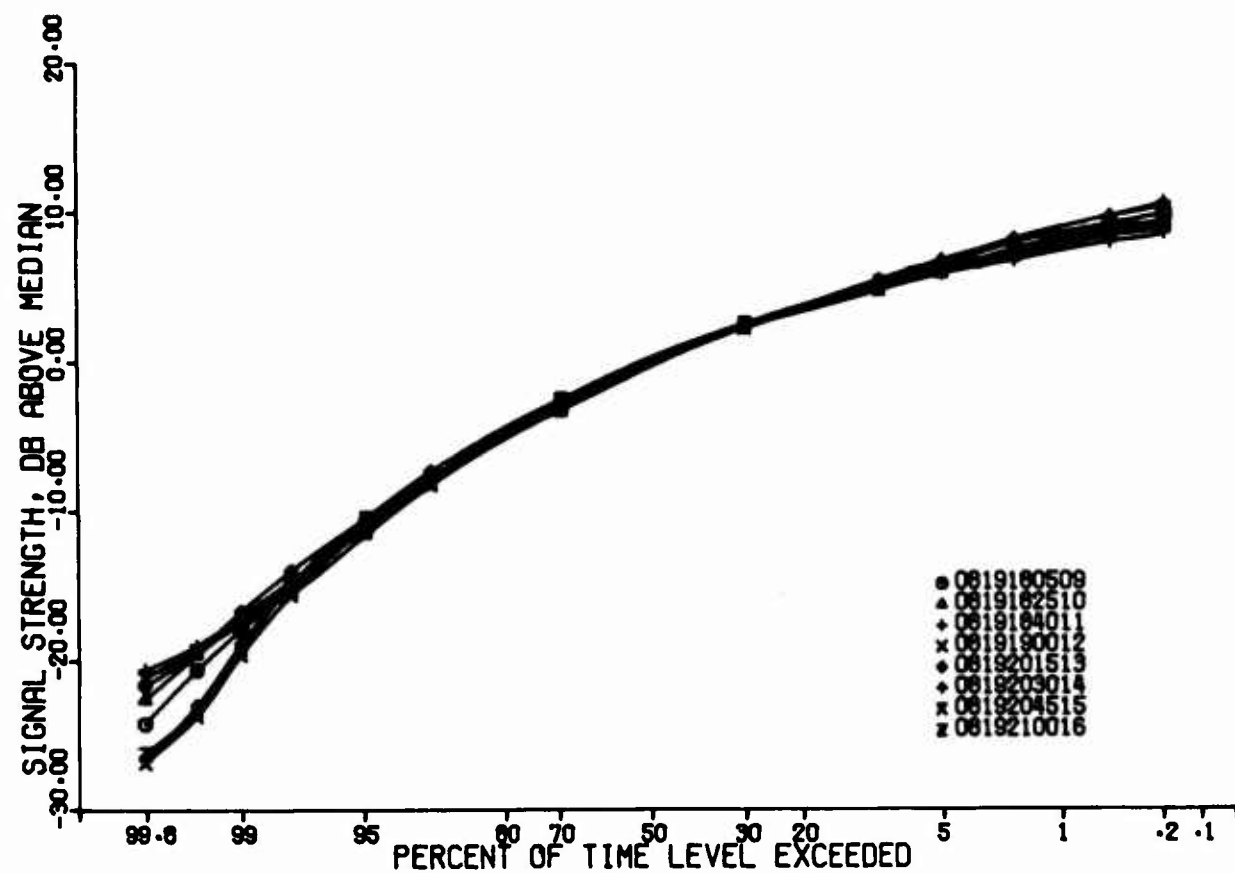


Figure 42. Signal Amplitude Level  
Ontario Center, Summer; C-Band

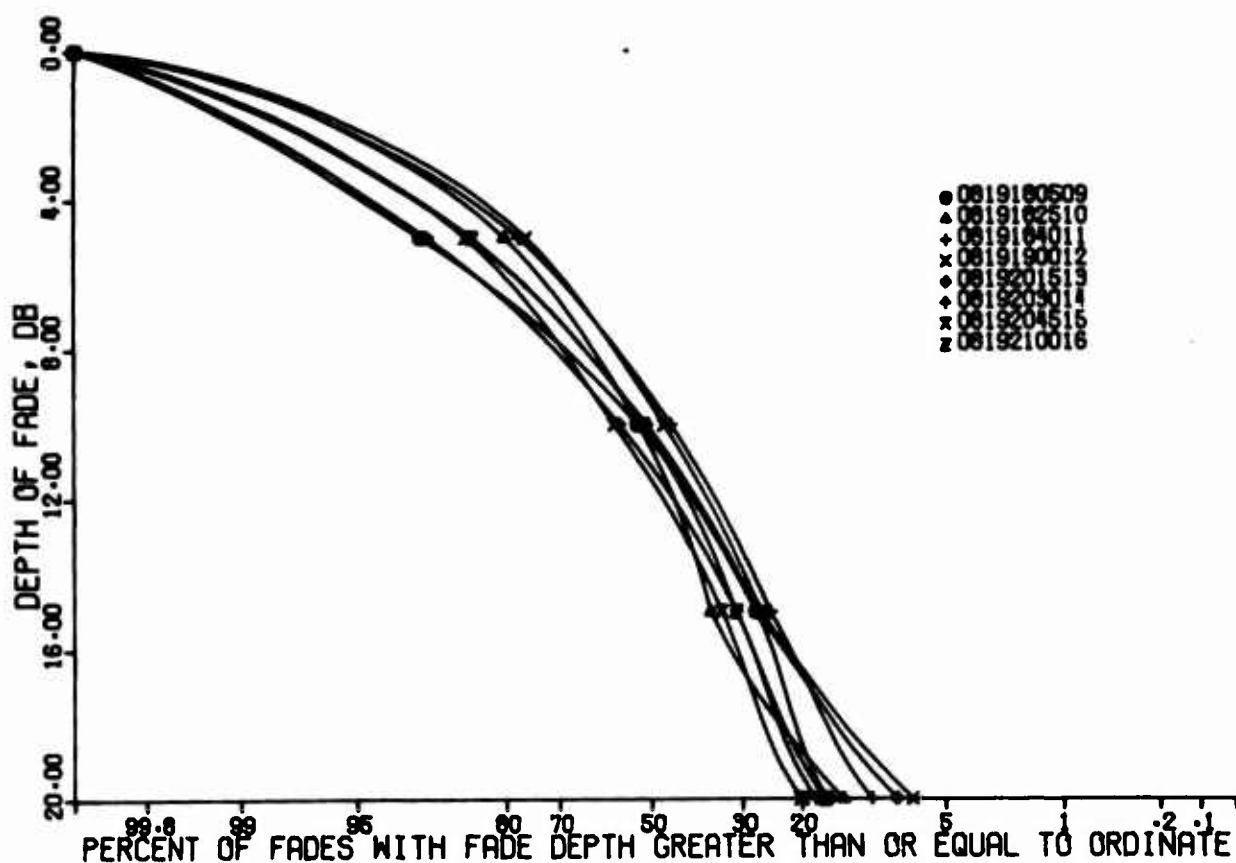


Figure 43. Distribution of Depth of Fades  
Ontario Center, Summer; C-Band

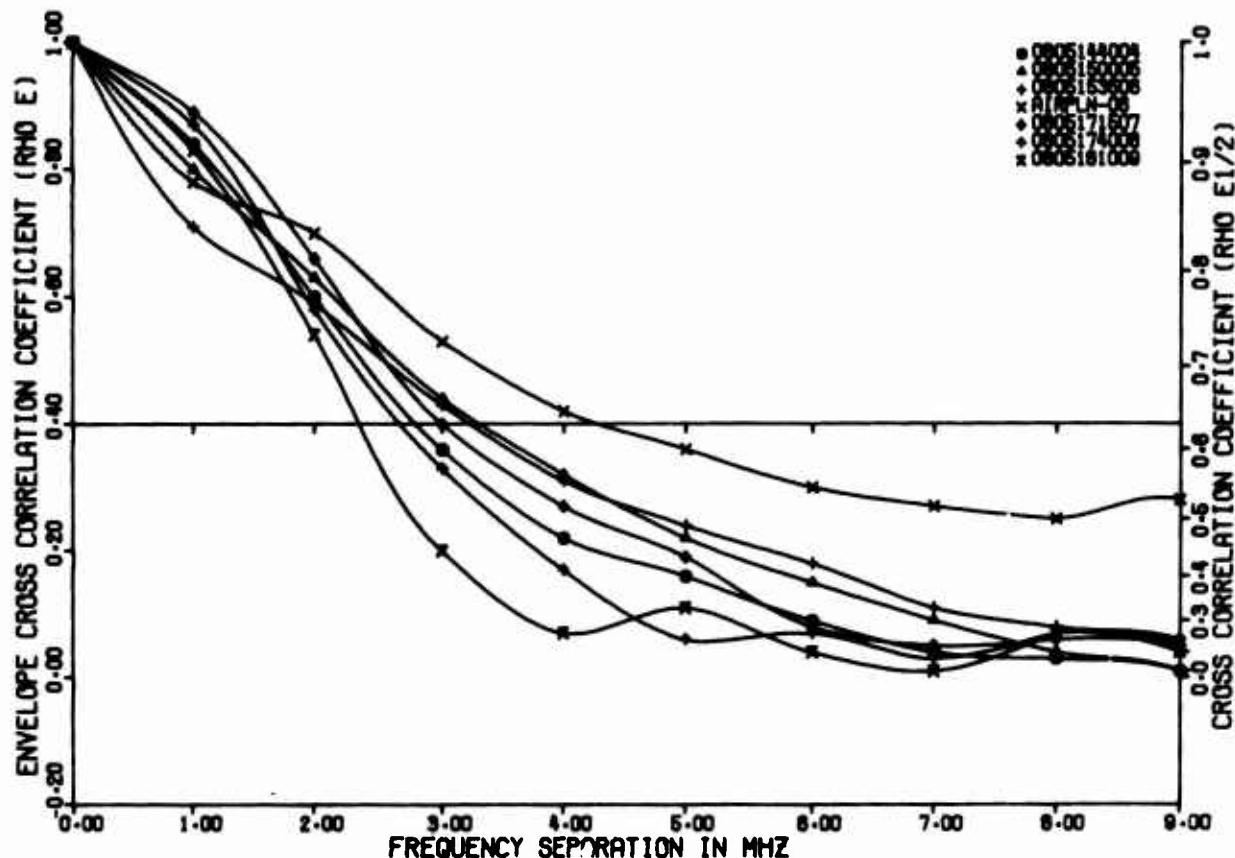


Figure 44. Envelope Cross Correlation Coefficients  
Ontario Center, Summer; C-Band, Wide

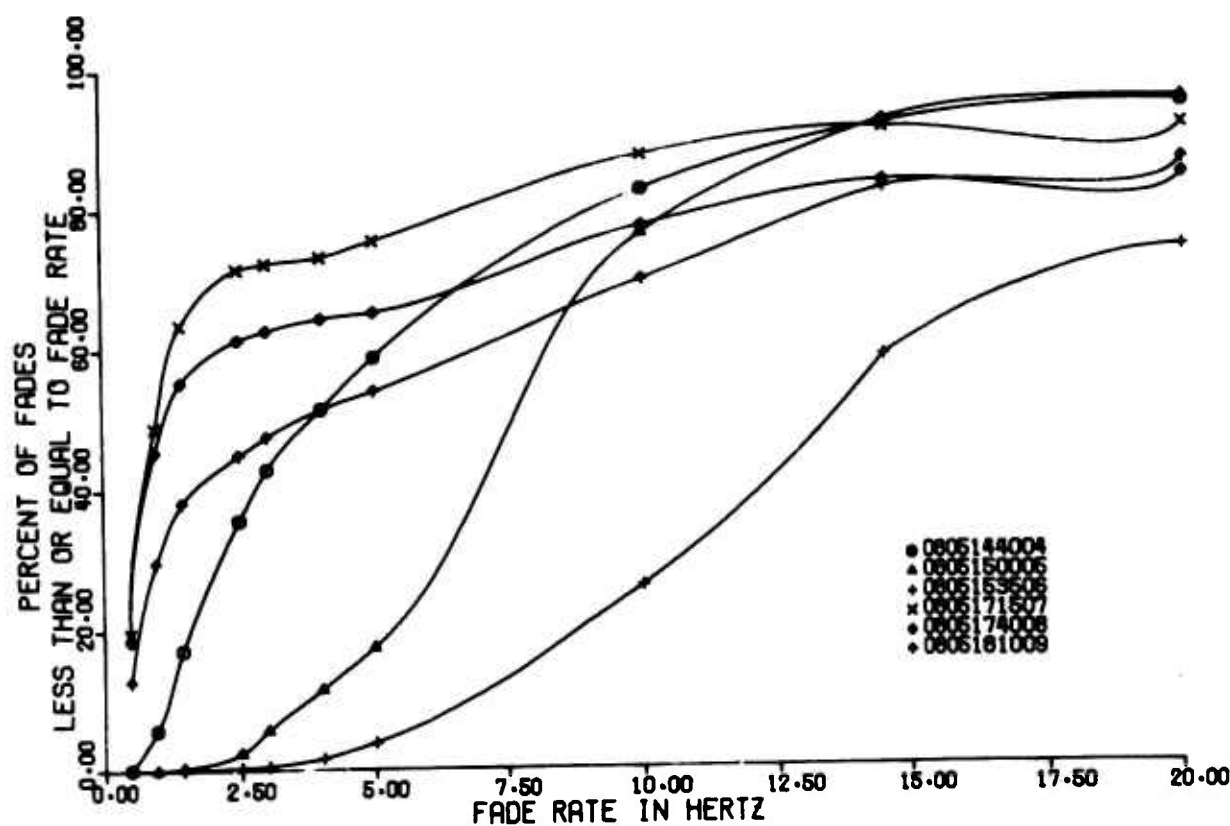


Figure 45. Fade Rate Distribution  
Ontario Center, Summer; C-Band

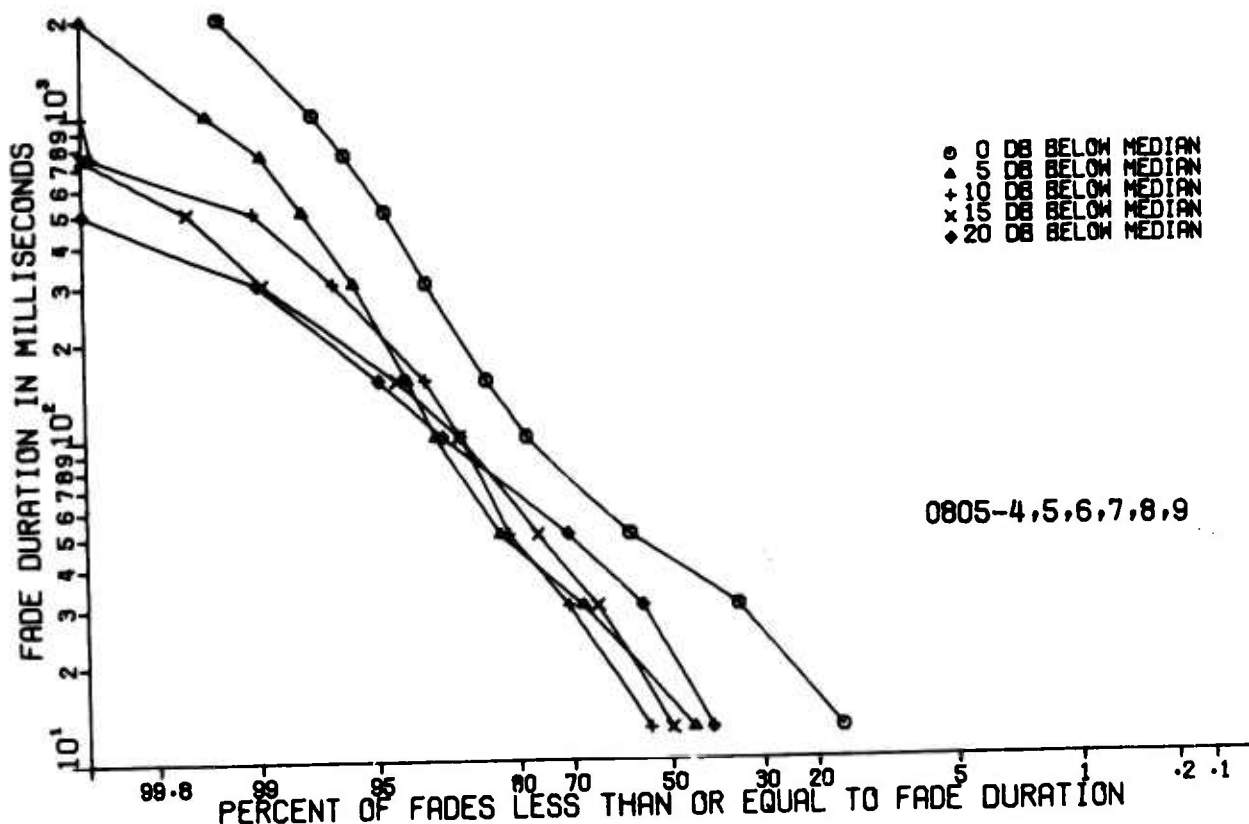


Figure 46. Distribution of Fade Duration  
Ontario Center, Summer; C-Band

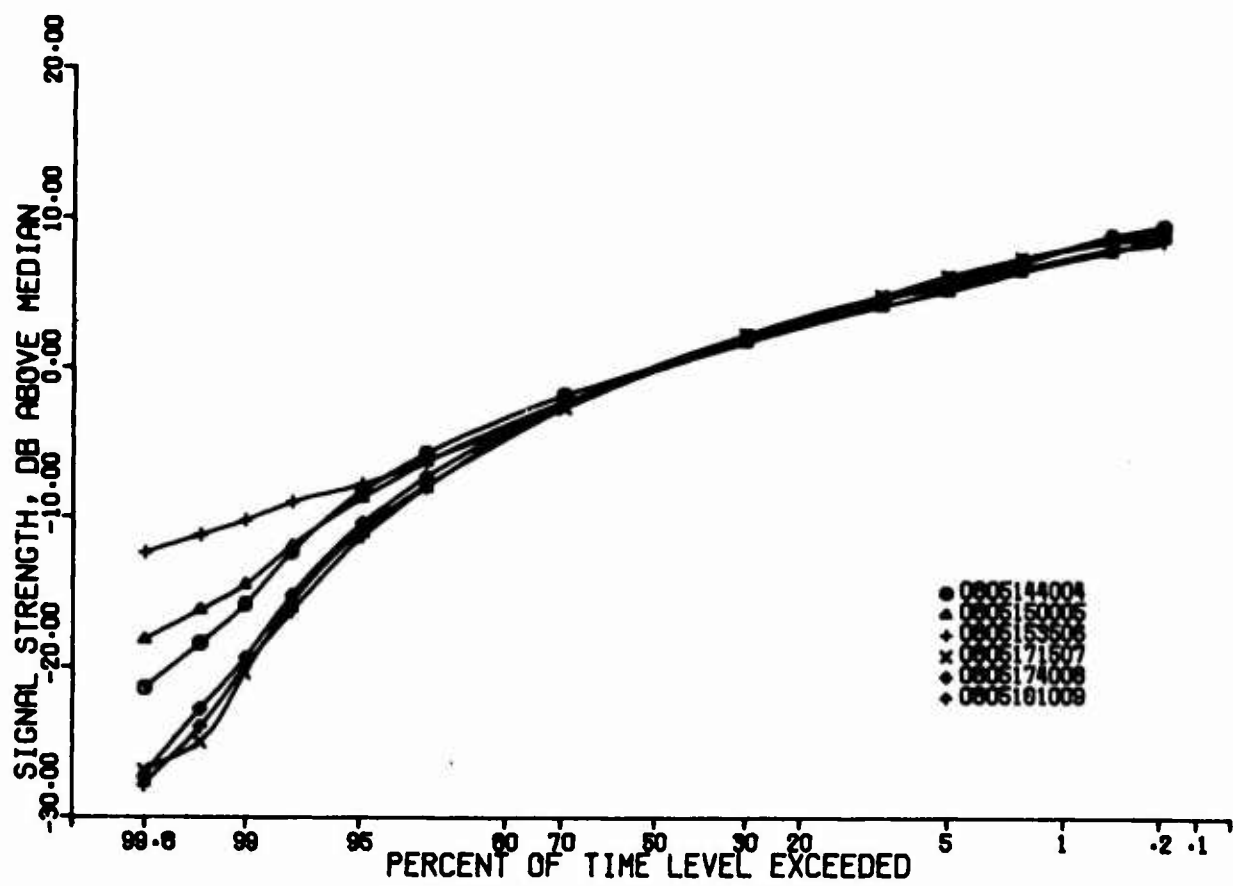


Figure 47. Signal Amplitude Level  
Ontario Center, Summer; C-Band

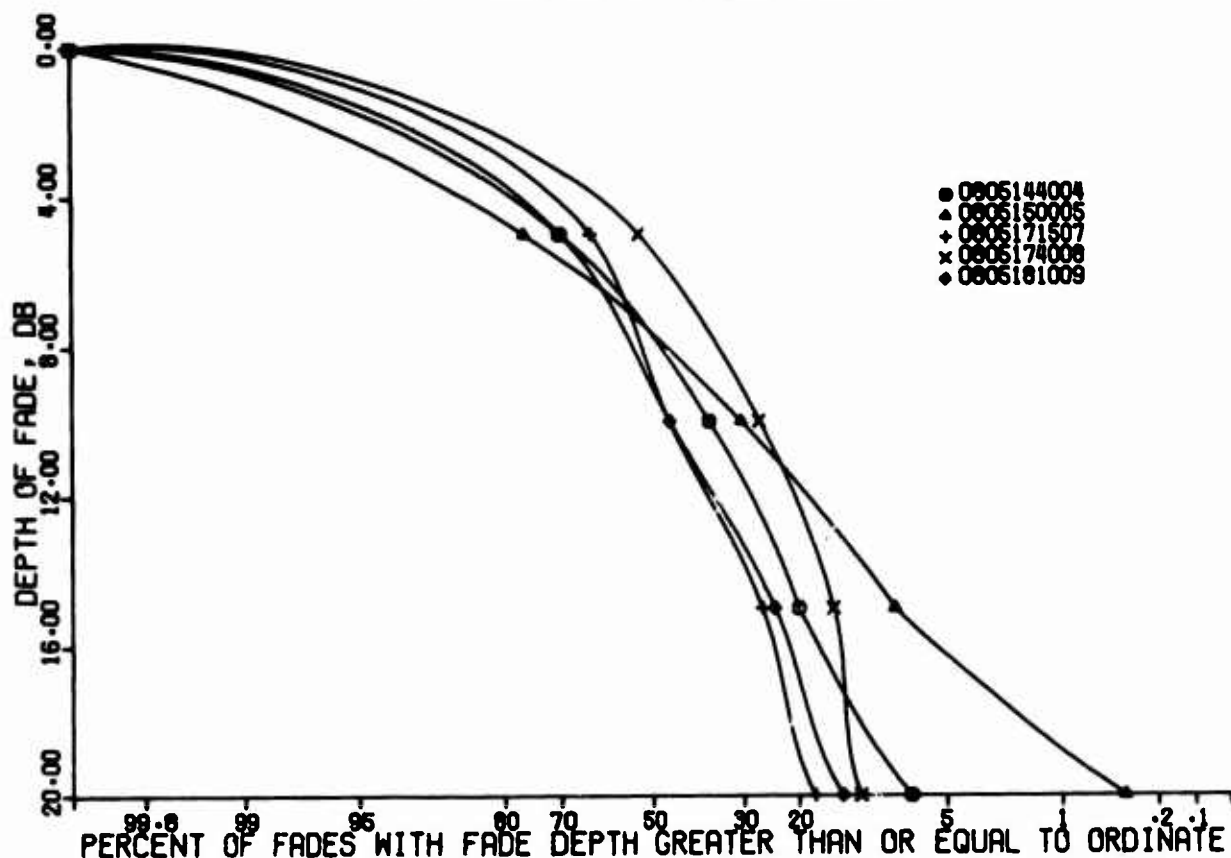


Figure 48. Distribution of Depth of Fades  
Ontario Center, Summer; C-Band

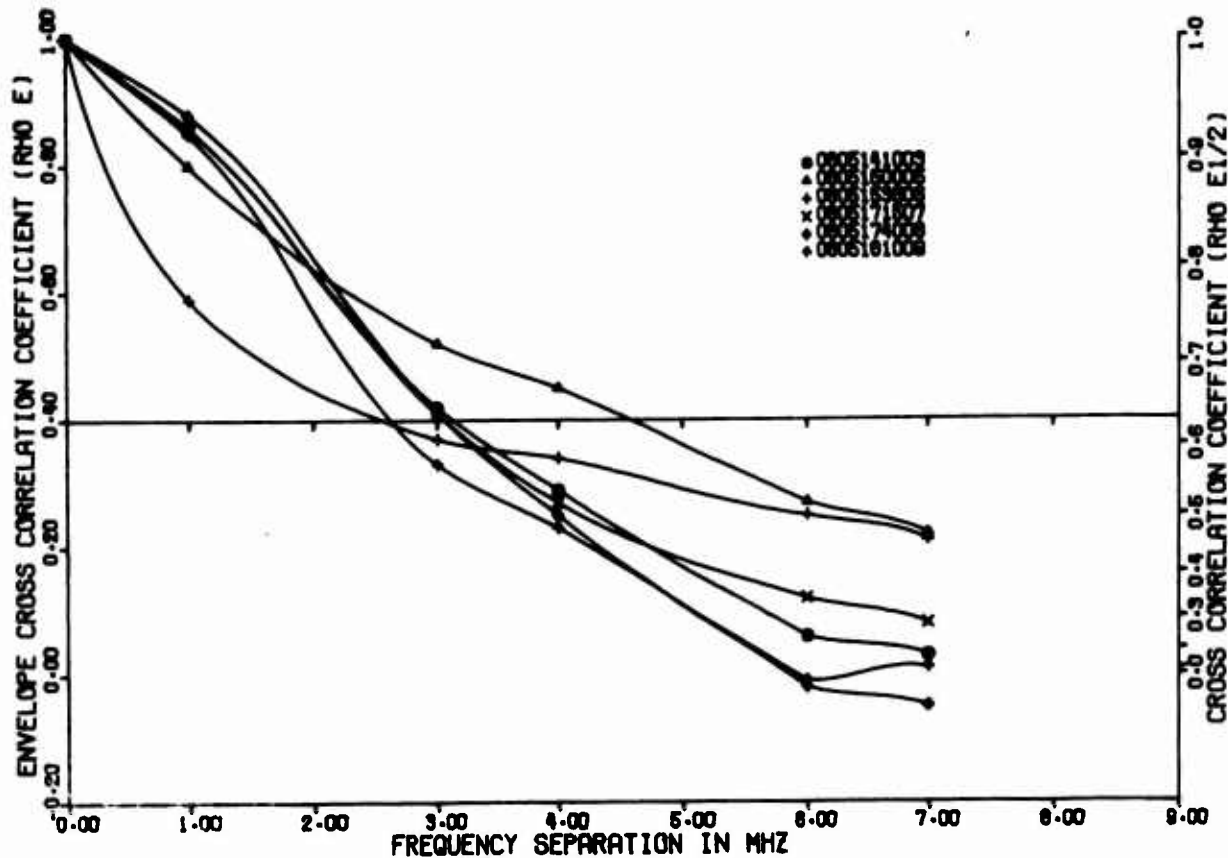


Figure 49. Envelope Cross Correlation Coefficients  
Ontario Center, Summer; X-Band, Wide

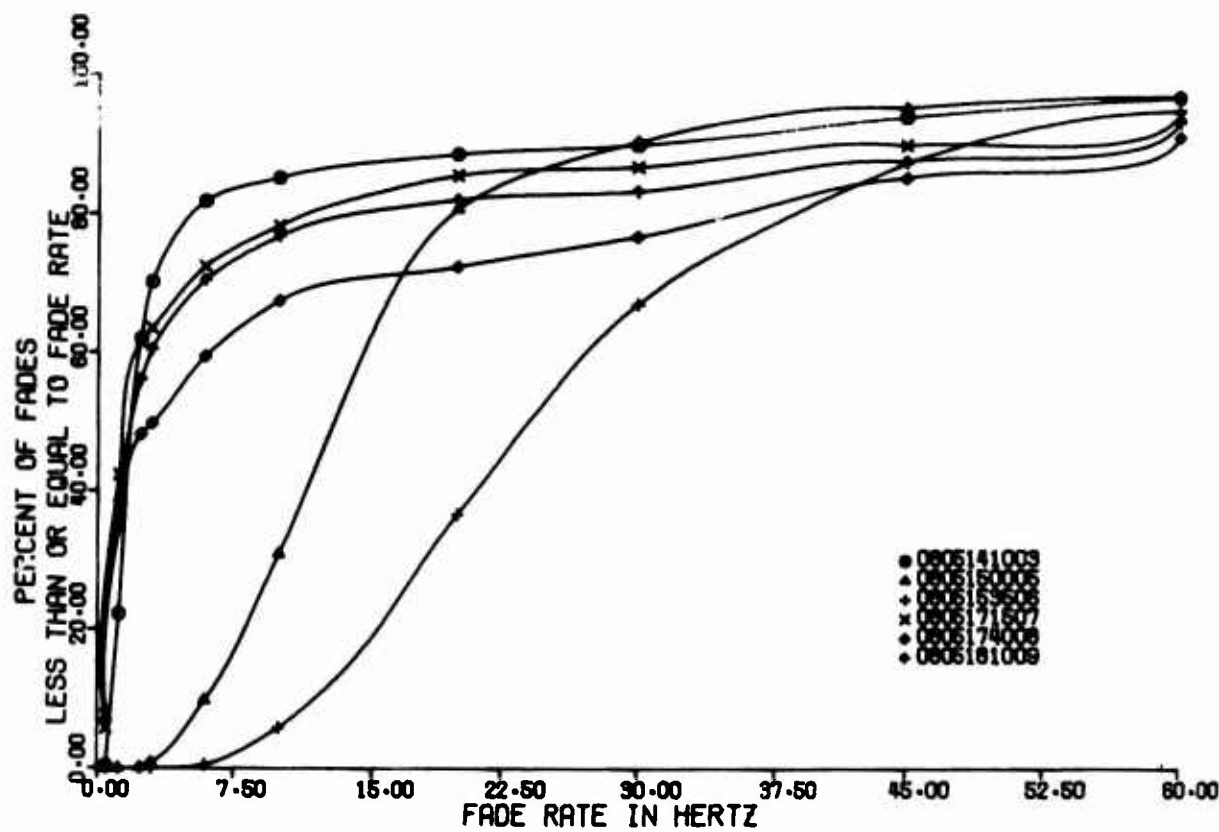


Figure 50. Fade Rate Distribution  
Ontario Center, Summer; X-Band

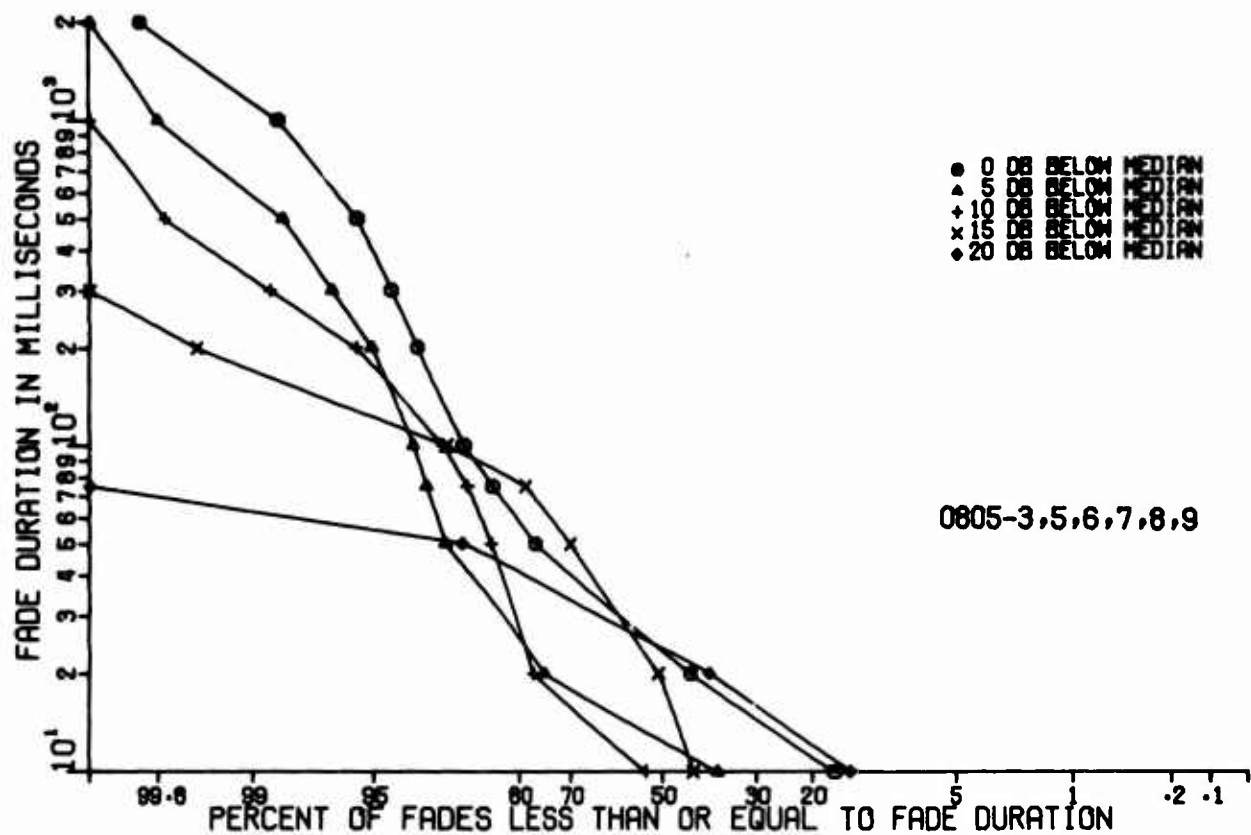


Figure 51. Distribution of Fade Duration  
Ontario Center, Summer; X-Band

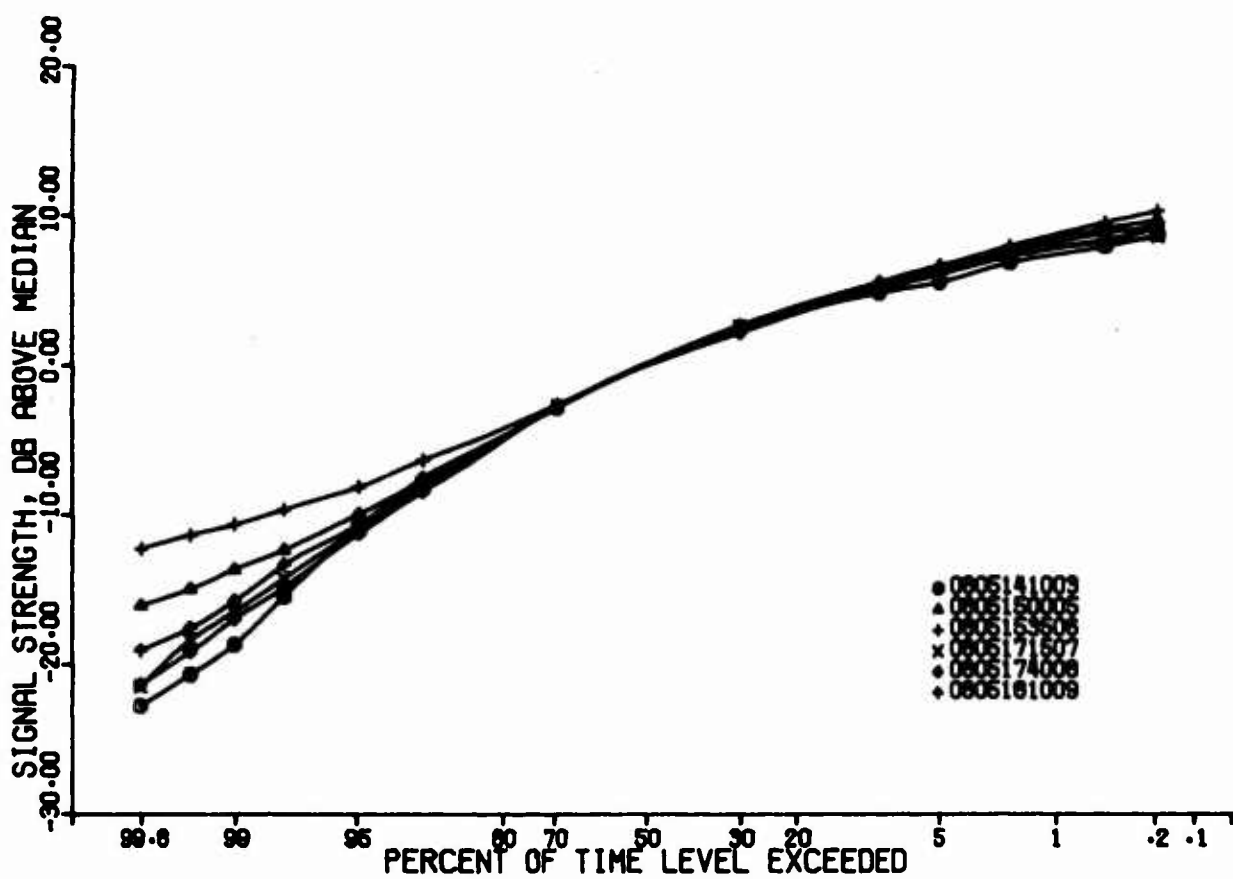


Figure 52. Signal Amplitude Level  
Ontario Center, Summer; X-Band

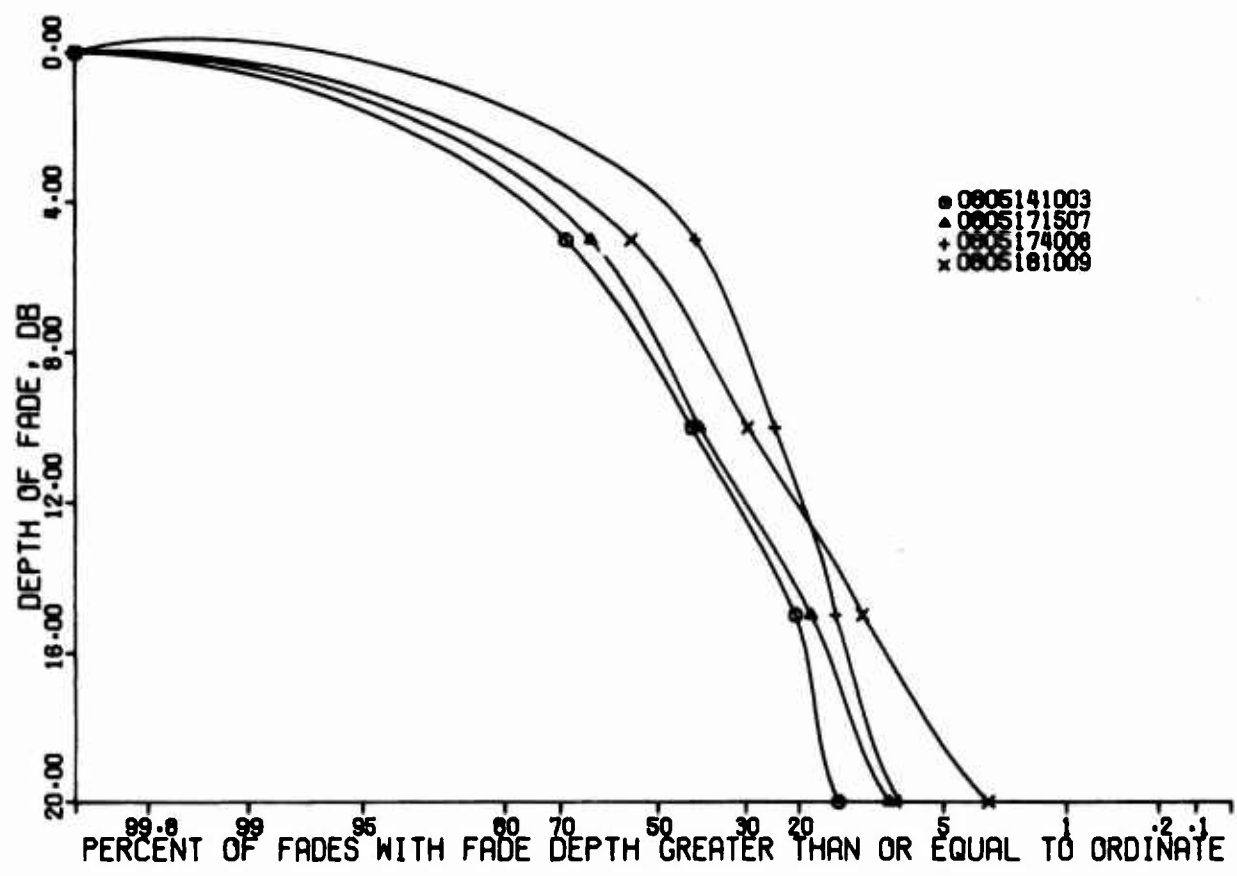


Figure 53. Distribution of Depth of Fades  
Ontario Center, Summer; X-Band

## 2. Whitford Field, Weedsport, N. Y.

The summer data at Whitford Field can be characterized by the narrowness of the correlation bandwidth as compared to the short Ontario Center path. This is to be expected on the longest path (200 km). The widest bandwidths where the envelope cross correlation coefficient goes from 1.0 to 0.4 is about 3.5 MHz for both C and X bands. The fade rates are usually slower than the Ontario Center path, but some of the tests showed high rates with median values of 10 Hz at C band and about the same at X band. The narrowest correlation bandwidths were about 1 MHz for both frequencies.

There was some concern over the low signal strengths available at this site and the effect it might have on the measured values of the cross correlation coefficients. A special test was made using receivers with a noise threshold of 135 dBm and a channel spacing of 500 kHz by FM at a modulation index of 1.84 at the transmitter. The cross correlation coefficients were measured by this method and by the regular wide band method. The results plotted in Figure 54 indicate that the signal strength and lack of fade margin do not affect the correlation bandwidth calculated, for the 200 kHz spaced curves nearly coincide with the 1 MHz spaced curves.

A typical set of measurements that indicate the more narrow cross correlation coefficients are shown in Figures 55 through 59 for C band. There are limited fade statistics for the durations, etc., due to the low fade margin on this path. A set of wider correlation bandwidths (Figures 60 and 61) for C band indicate that 2.5 to 3.5 MHz is typically the widest obtained during this test period.

X- and C-band results can be compared directly in the test results of 29 August tests number 14 through 16 (Figures 62 through 67). The X and C bandwidths are test by test very nearly the same. Test 14 has an X-band median fade rate of 17 Hz to the C-band 11 Hz. Test 15 has an X-band median rate of 4 Hz compared to the C-band median rate of 3 Hz. Test 16 has for X-band, 16 Hz, and 4 Hz for the C-band case. In nearly every test the X-band fade rates exceed the C-band rates while the correlation bandwidths remain about the same. This pair of observations adds evidence that the effective scatter volume in both cases is about the same, for the increase in fade rate would naturally follow a decrease in wavelength if all other things are left unchanged.

An interesting occurrence was noted in tests 3 and 5 of 28 August (Figures 68 and 69) and a similar occurrence was noted the next day in test 9 (Figure 62). This phenomenon of oscillating the cross correlation coefficient has been observed on a number of occasions. On 14 August at Ontario Center this type of phenomenon was observed to result in a function similar to  $\sin(x)/x$  for the correlation coefficient versus frequency (see section IV-E).

The phenomenon of ducting was never noticed at this site during the summer tests. This does not imply that it cannot happen on the Whitford site; it just did not occur during the time tests were being performed.

The Whitford summer data can be summed up as being of low signal strength with relatively narrow correlation bandwidths and slow fades when compared with the Ontario Center data. The correlation bandwidth reduction does result in a small improvement in frequency diversity modems, but not to any outstanding extent, for it has been determined in a previous MALLARD program (Reference 2) that the most significant diversity improvement is obtained when the correlation coefficient drops from 1.0 to about 0.7; thereafter practically no improvement is made. The fade rates are still high enough to cause problems in adaptive frequency modems, but this high rate is much rarer on this path than on the Ontario Center path.

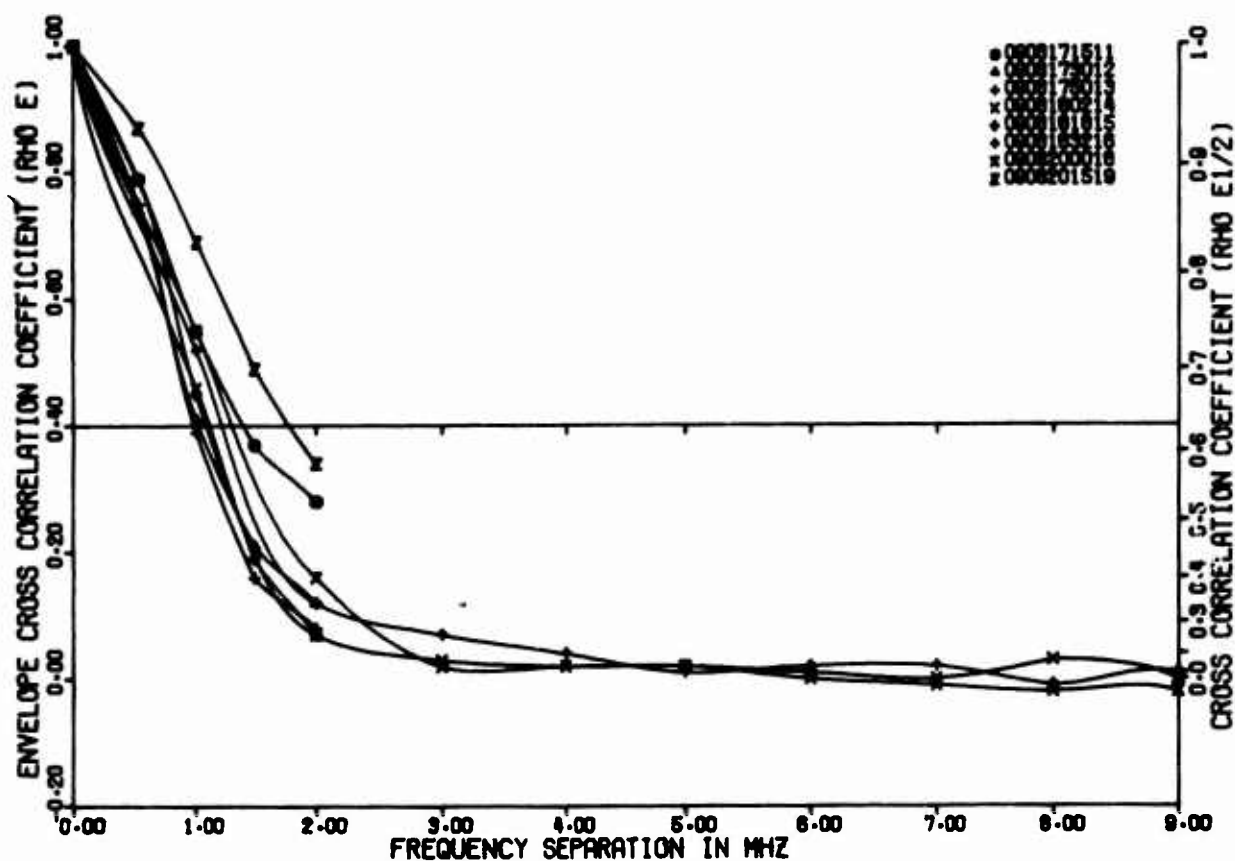


Figure 54. Envelope Cross Correlation Coefficients  
Whitford Field, Summer; C-Band, 500 kc and Wide Spacing

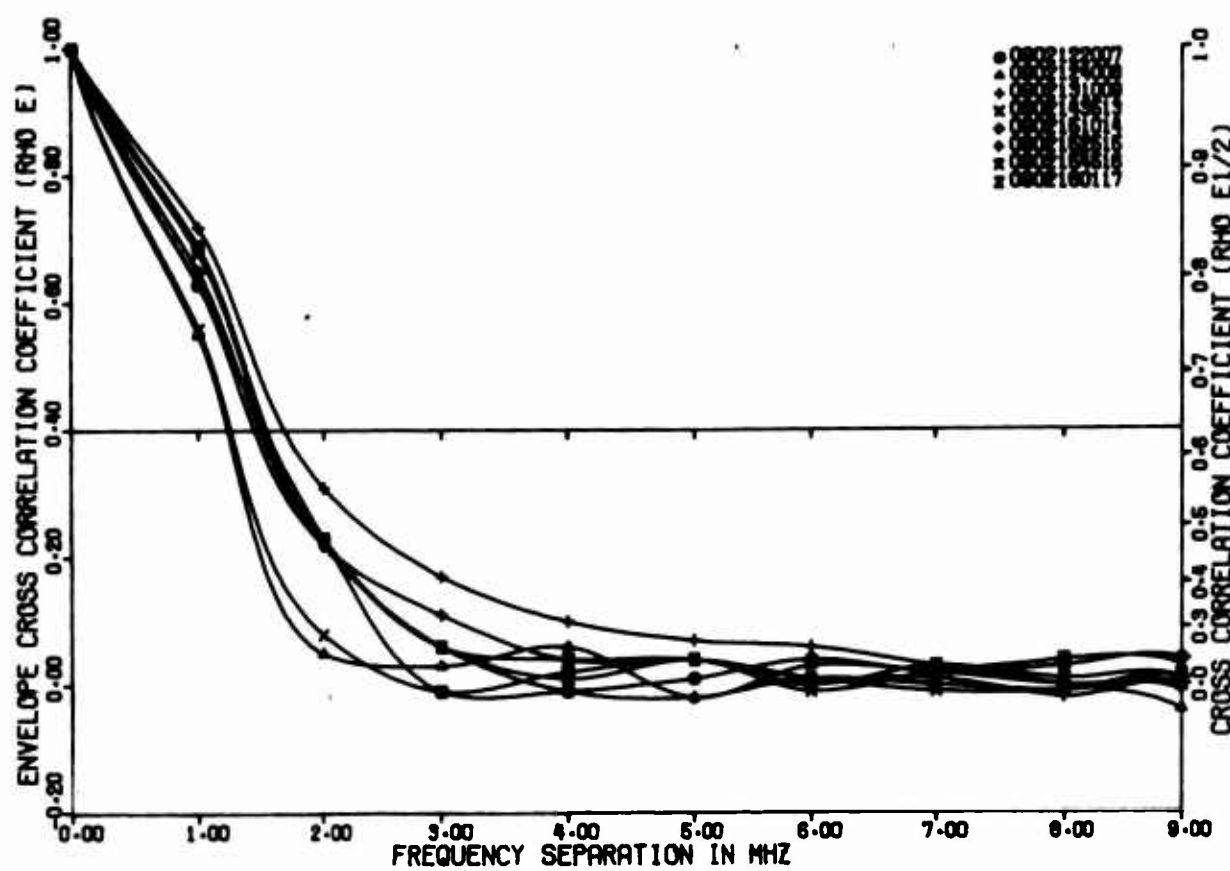


Figure 55. Envelope Cross Correlation Coefficients  
Whitford Field, Summer; C-Band, Wide

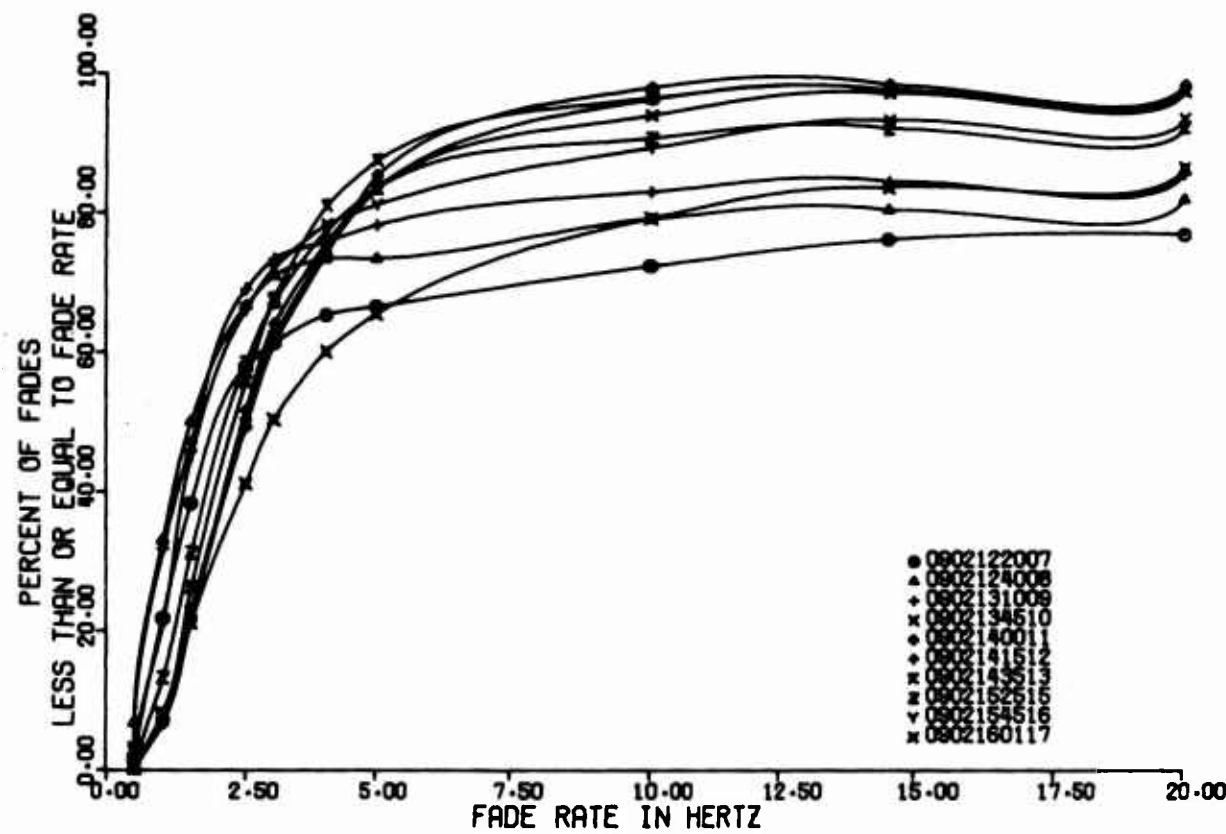


Figure 56. Fade Rate Distribution  
Whitford Field, Summer; C-Band

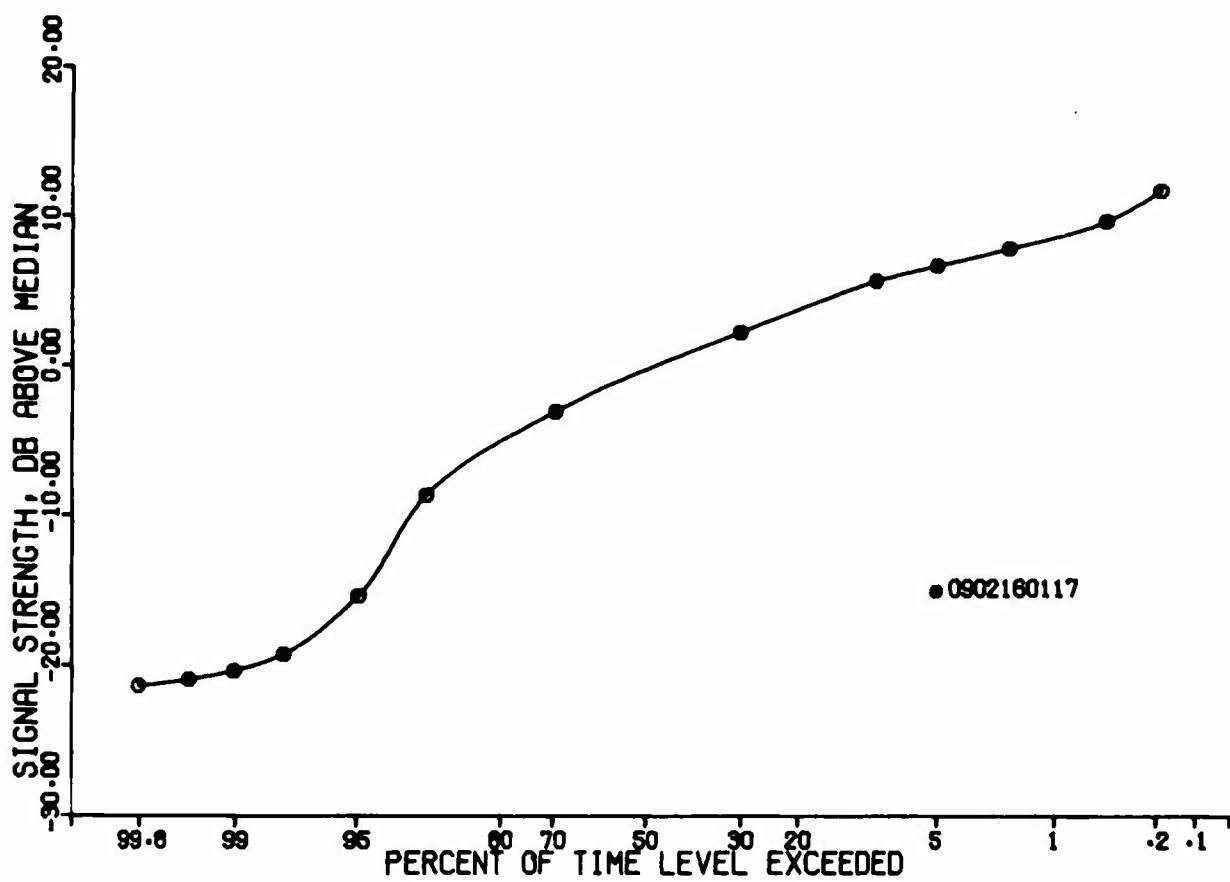


Figure 57. Signal Amplitude Level  
Whitford Field, Summer; C-Band

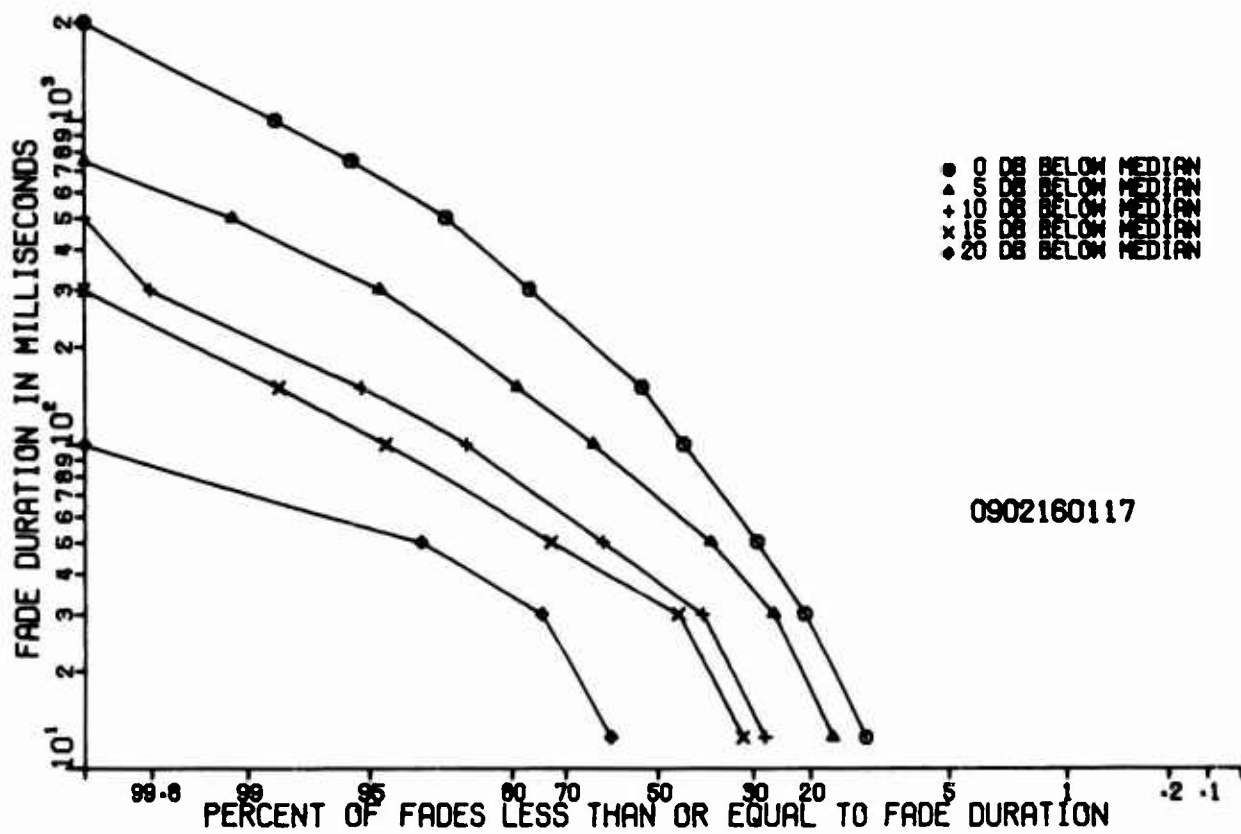


Figure 58. Distribution of Fade Duration  
Whitford Field, Summer; C-Band

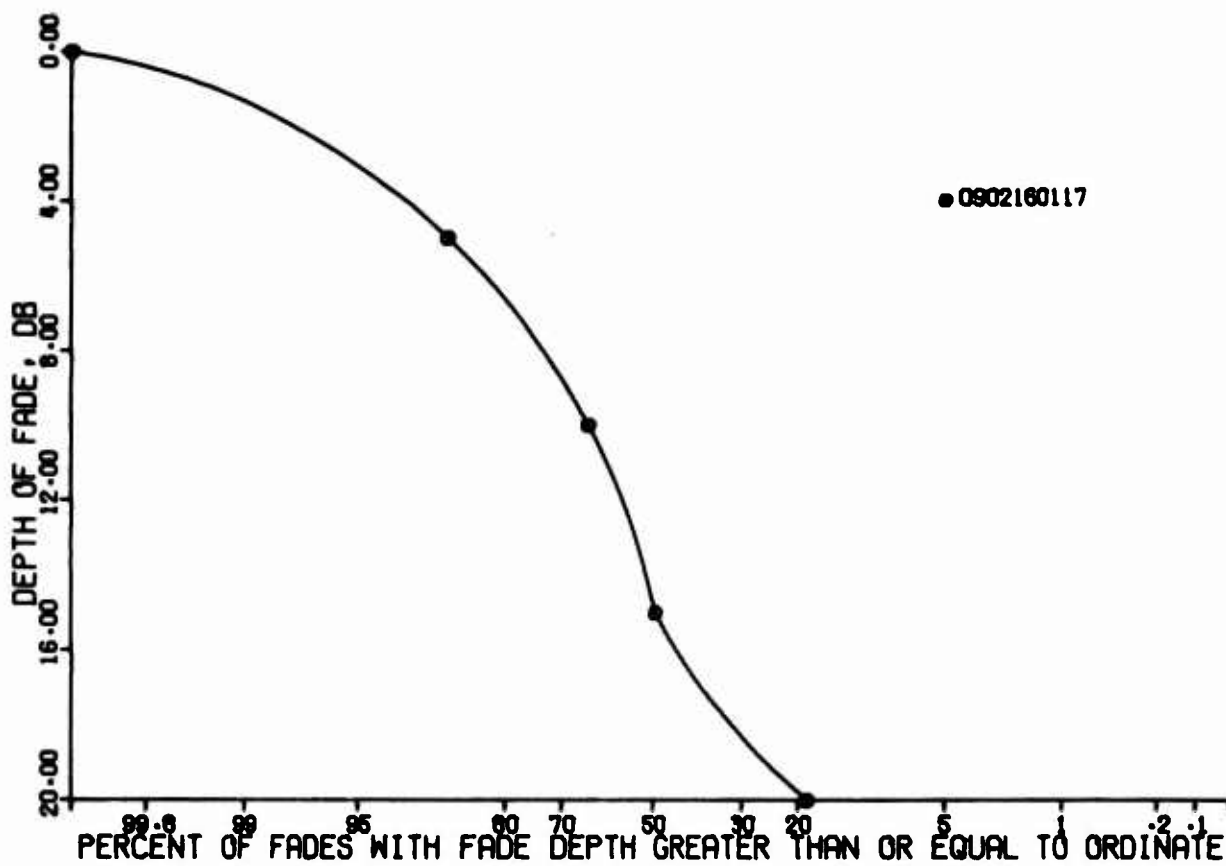


Figure 59. Distribution of Depth of Fades  
Whitford Field, Summer; C-Band

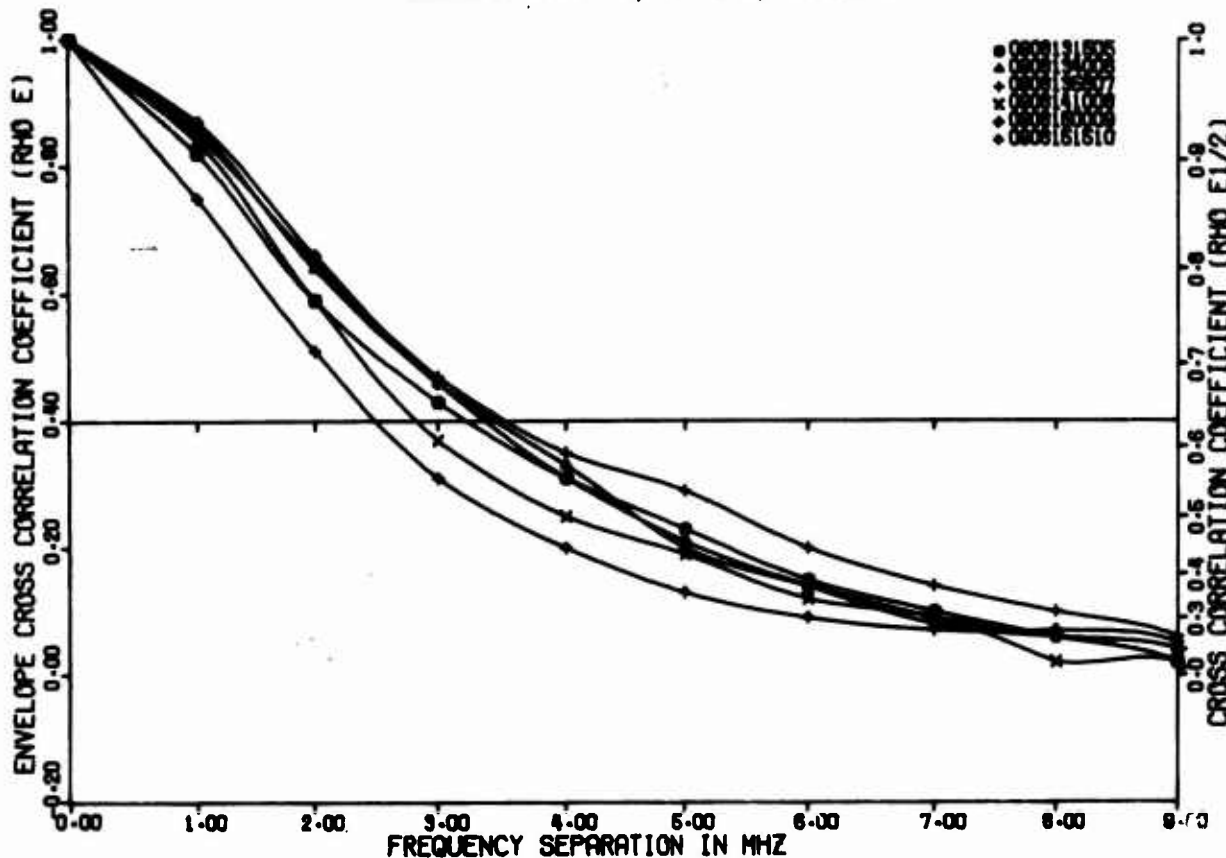


Figure 60. Envelope Cross Correlation Coefficients  
Whitford Field, Summer; C-Band, Wide

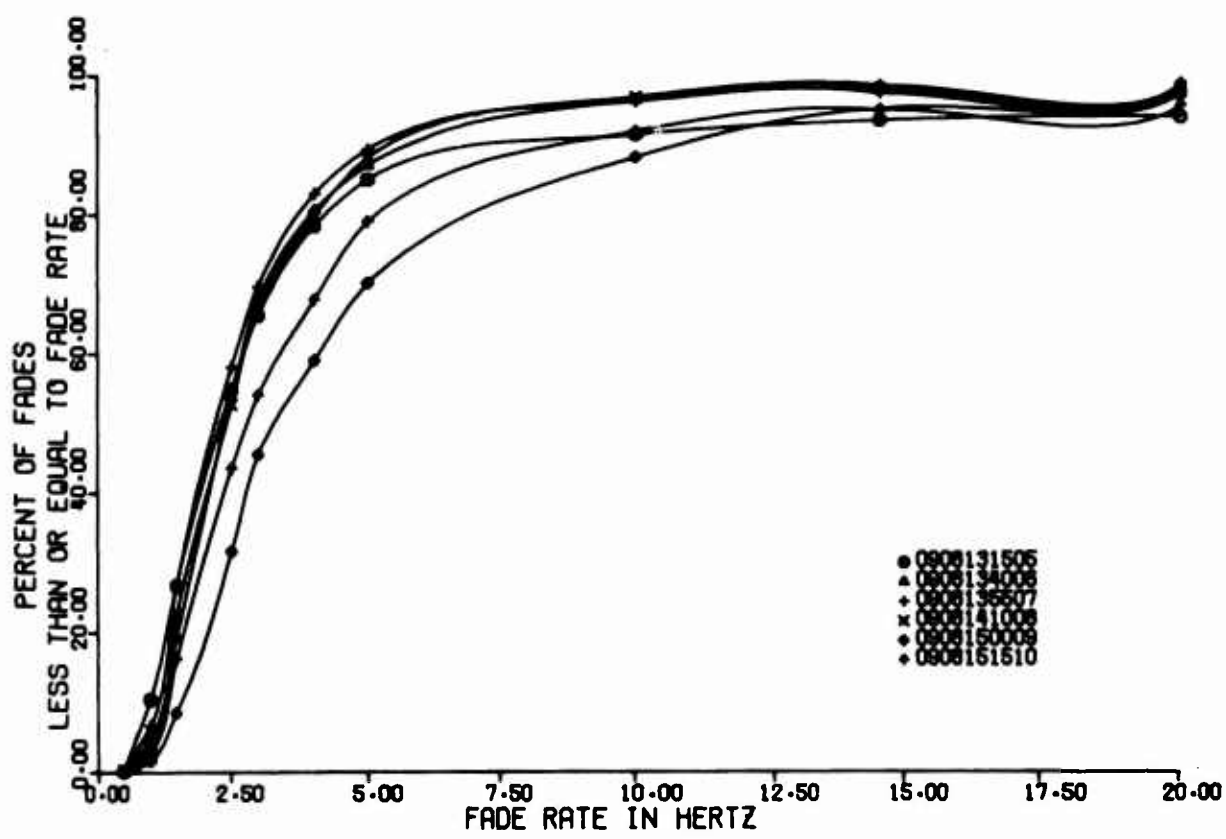


Figure 61. Fade Rate Distribution  
Whitford Field, Summer; C-Band

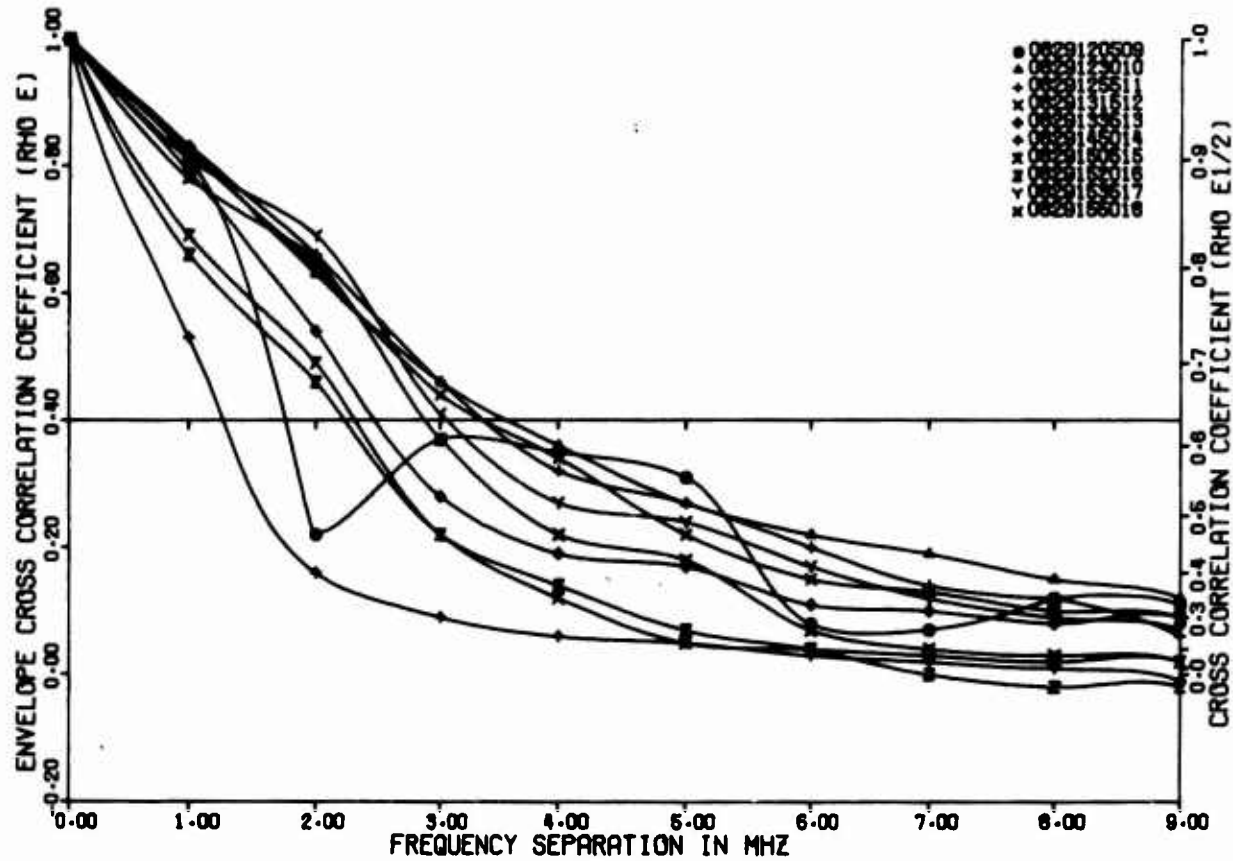


Figure 62. Envelope Cross Correlation Coefficients  
Whitford Field, Summer; X-Band, Wide

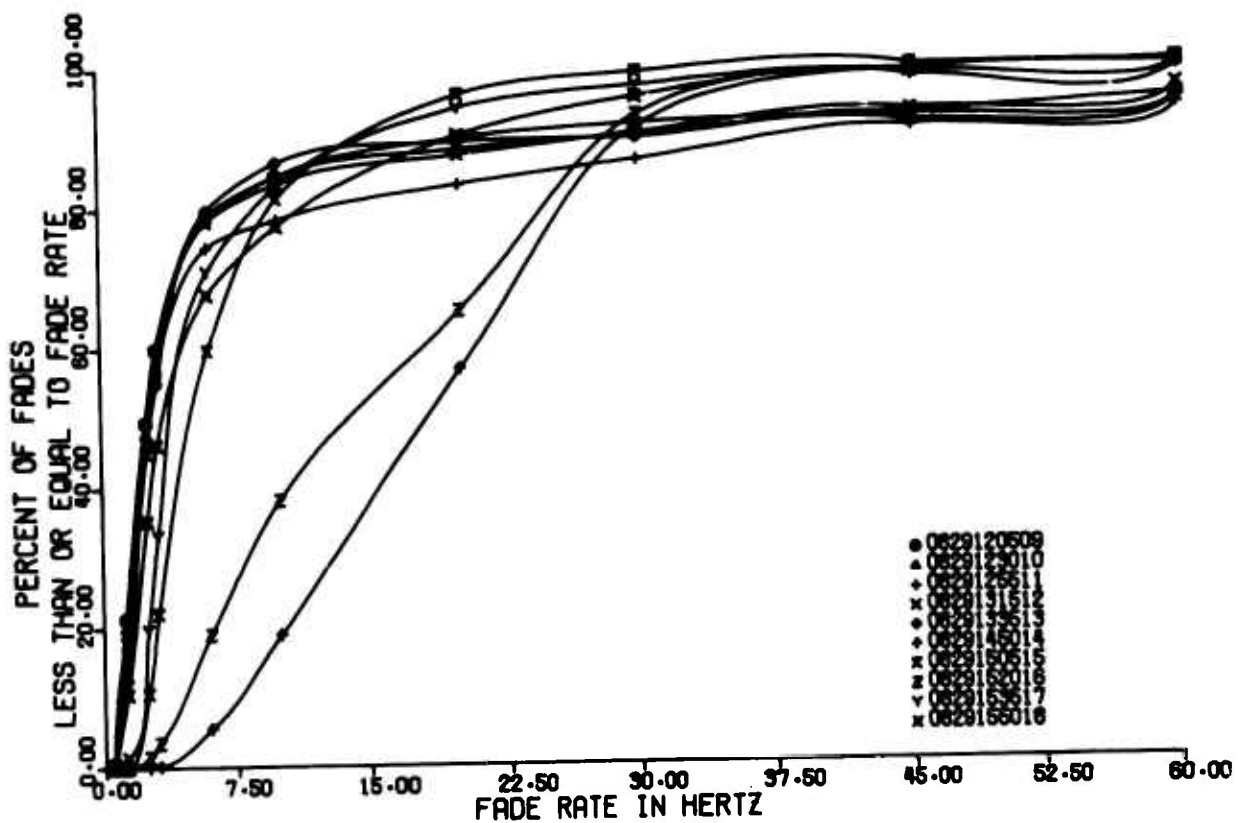


Figure 63. Fade Rate Distribution  
Whitford Field, Summer; X-Band

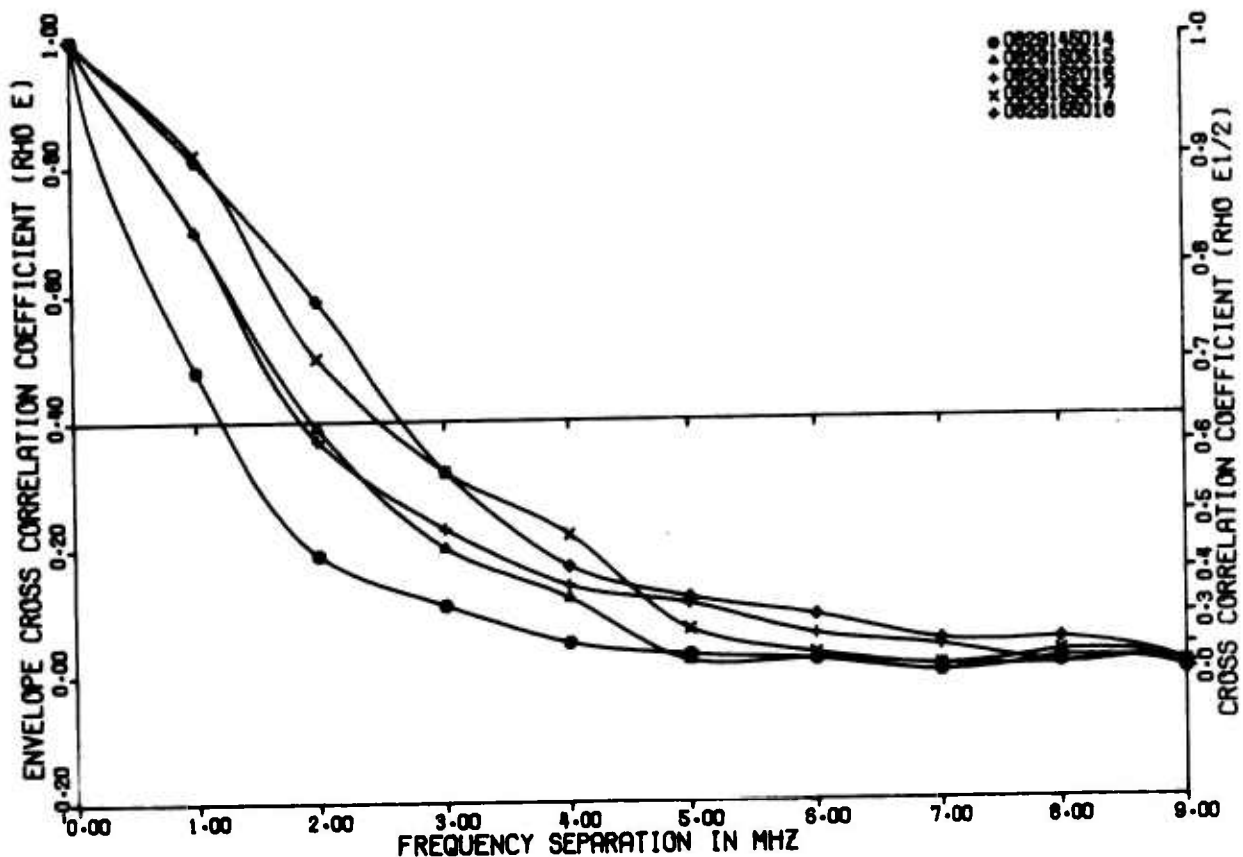


Figure 64. Envelope Cross Correlation Coefficients  
Whitford Field, Summer, C-Band, Wide

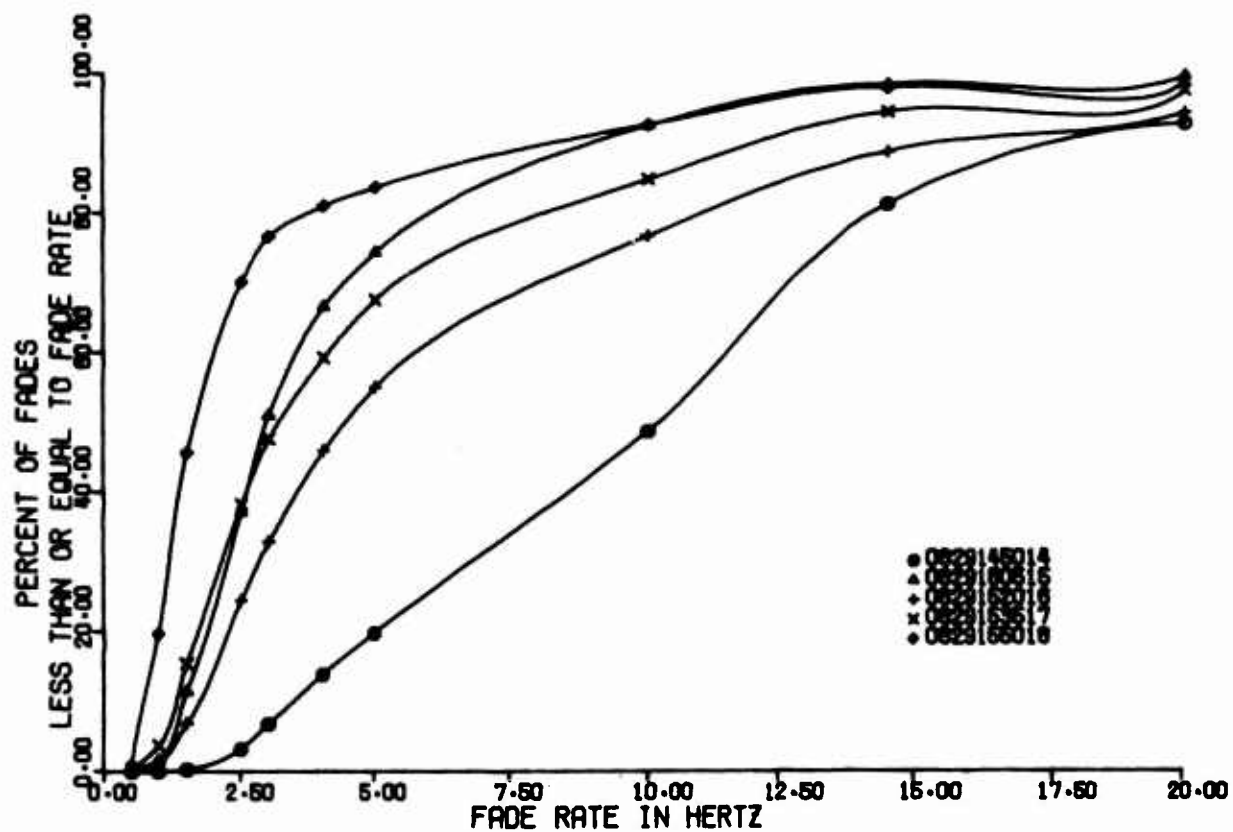


Figure 65. Fade Rate Distribution  
Whitford Field, Summer; C-Band

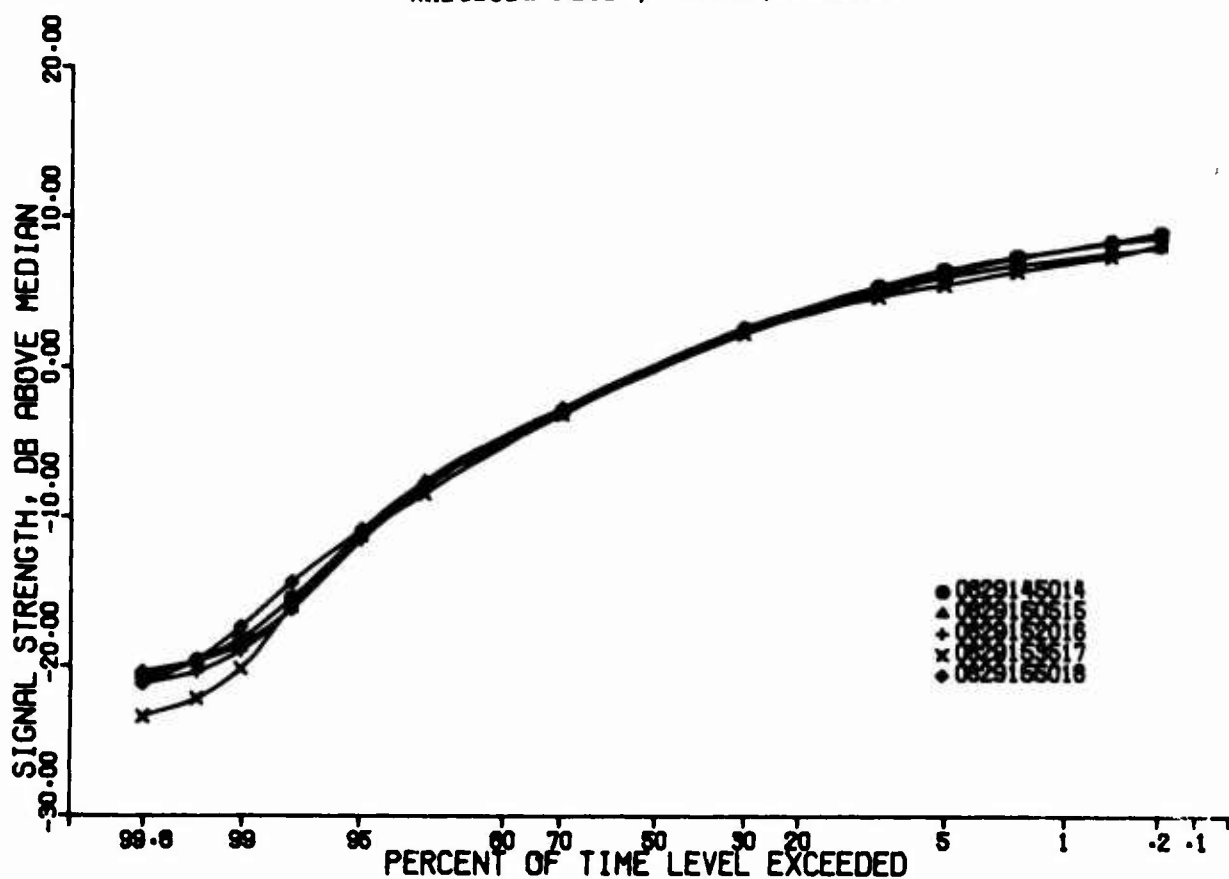


Figure 66. Signal Amplitude Level  
Whitford Field, Summer; C-Band

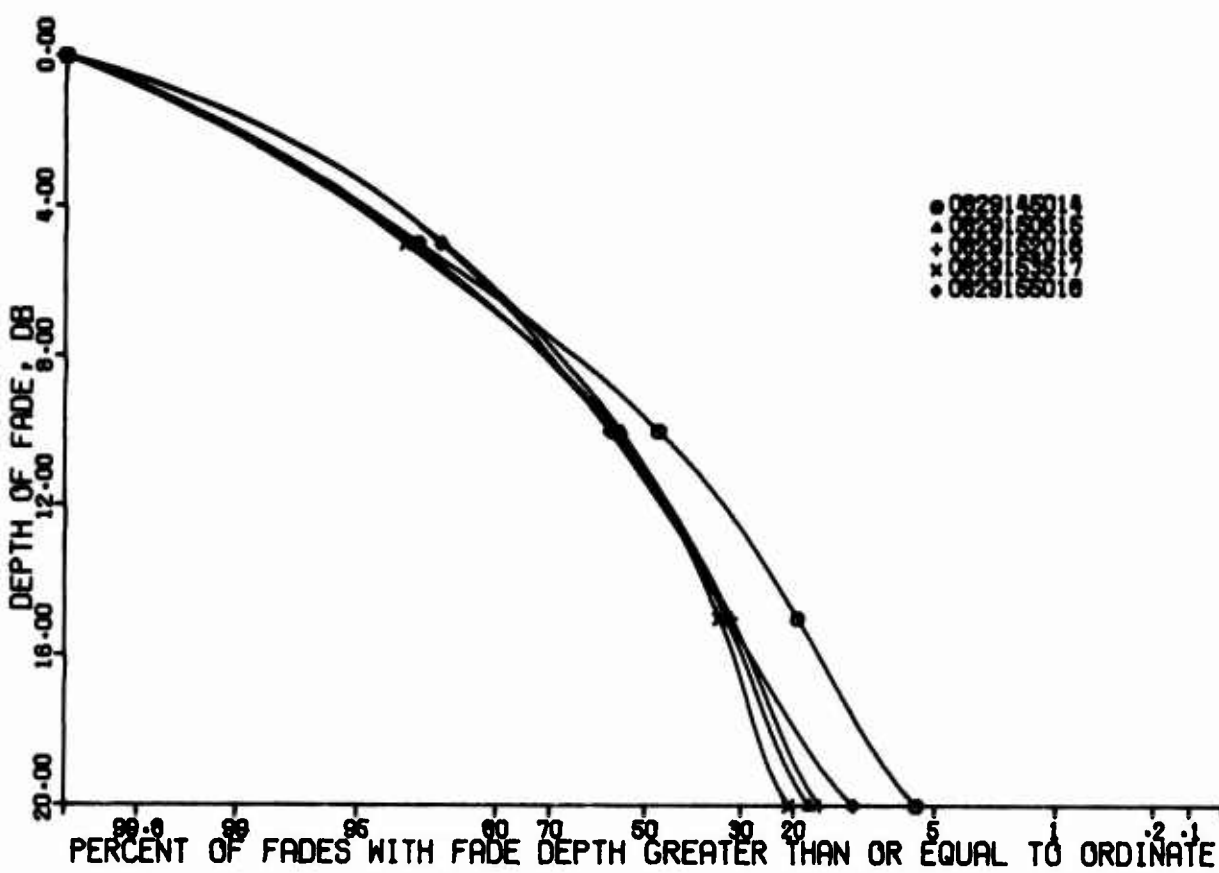


Figure 67. Distribution of Depth of Fades  
Whitford Field, Summer; C-Band

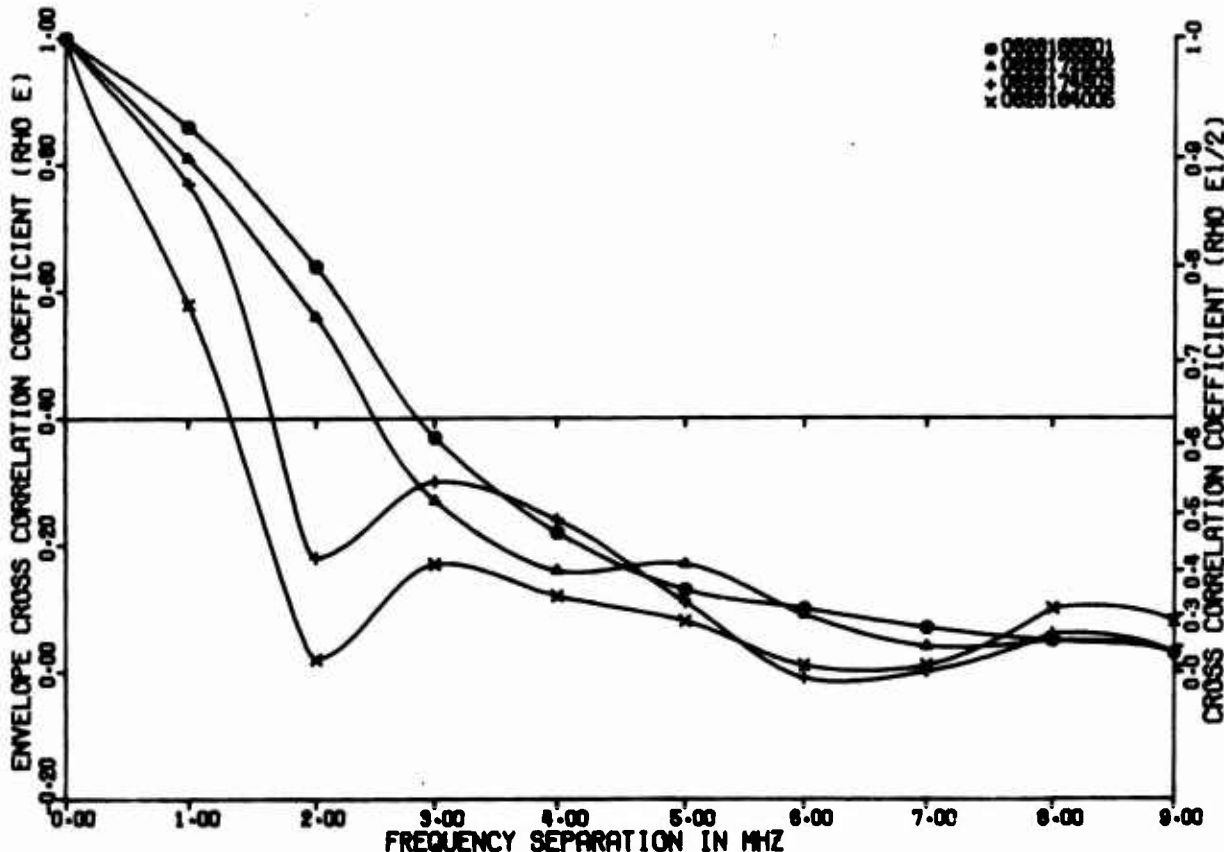


Figure 68. Envelope Cross Correlation Coefficients  
Whitford Field, Summer; X-Band, Wide

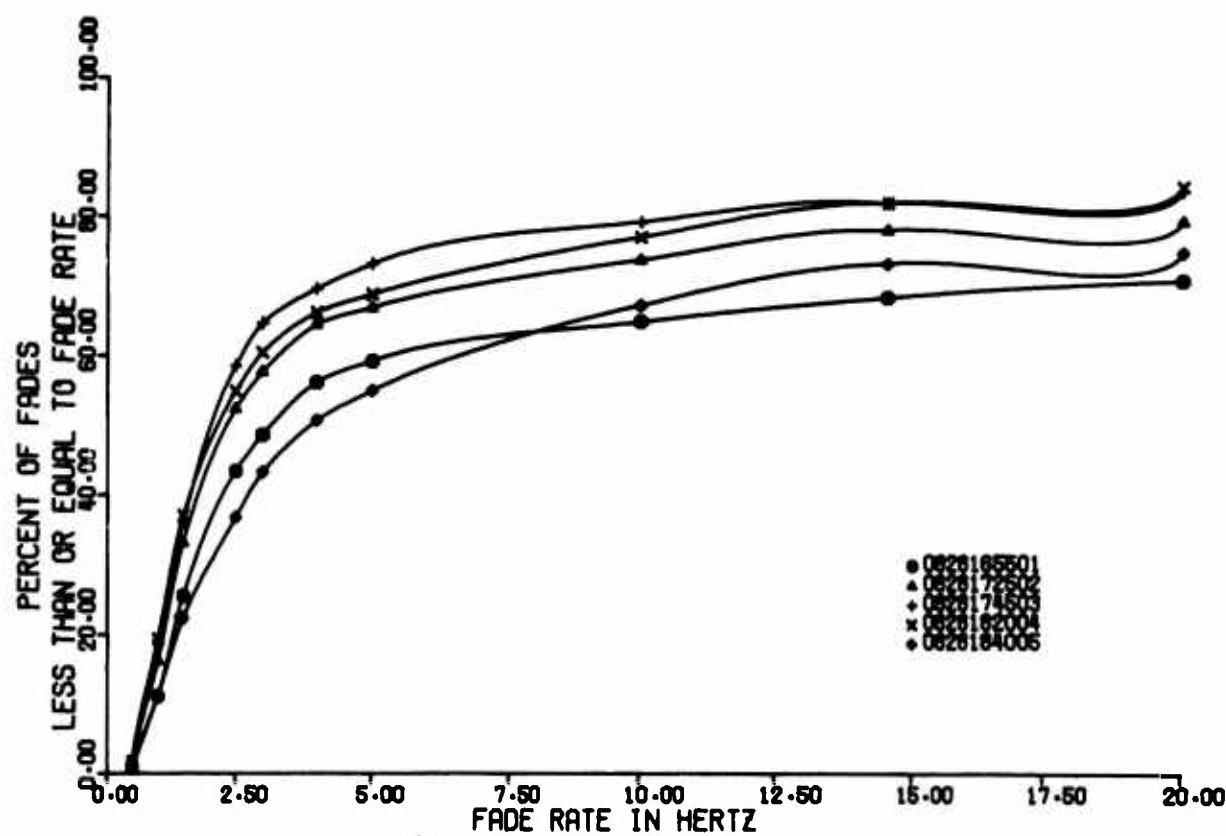


Figure 69. Fade Rate Distribution  
Whitford Field, Summer; C-Band

### 3. Point Petre

The Point Petre path is 160 km from the transmitter at Model City. For the most part, the path is over Lake Ontario. The receiver site is located on the water's edge which might have an effect on the signal characteristics. The correlation bandwidths on this path varied fr. as little as 1 to 2 MHz to as high as 7 to 9 MHz at X-band with 3 to 5 MHz as the more typical value. At C-band the minimums were about 2 MHz, but the typical maxima were in the neighborhood of 5 to 8 MHz. The typical value was around 4 to 4 MHz. This path can be characterized as one with fade rates that jump quickly to a maximum and seldom does the distribution rise slowly with frequency. The other two sites had many unusual fade rate distributions. The narrow spacing data discussed in a previous section is also more definitely gaussian in shape. Signal strength on this path was never a problem.

It is interesting to compare the following sets of curves (all X- and C-band pairs) on a test by test basis. The data presented are not exactly simultaneous, for 5 minutes of C-band are reduced per test while only 2.5 minutes of the X-band are reduced. An exact time correspondence is not possible. Figures 70 through 74 represent the widest C-band; Figures 75 through 79, the widest X-band. Figures 80 through 84 represent the narrowest C-band followed by Figures 85 through 89 for the narrowest X-band. Figures 90 through 99 represent a typical case of repetitive data while Figures 100 through 109 are typical of changing conditions that result in a wide spread of data.

In seeking reasons for the departure of the propagation factors on this path from those of the other two paths, one might consider that in the first interim report it was said that the effect of terrain on tropo-scatter is most likely due to the effect that the terrain has on the weather. Here we have a smooth overwater path which is reasonably expected to have significantly different weather in the common volume from that obtained by the overland terrain. A further factor to consider is that the path is more northeast while the other two paths were east-west. This directional difference might cause the prevailing winds to interact with the scattering mechanism in a considerably different manner.

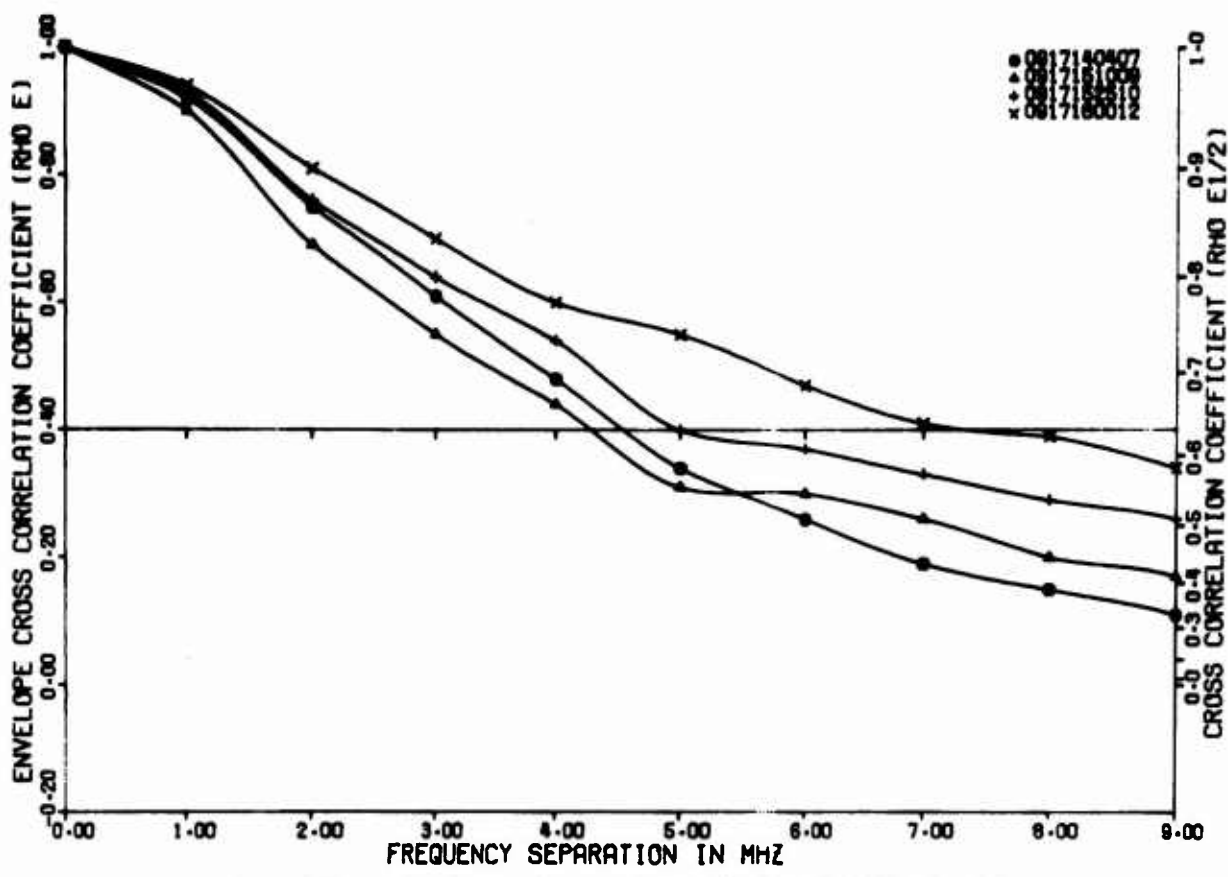


Figure 70. Envelope Cross Correlation Coefficients  
Point Petre, September; C-Band, Wide

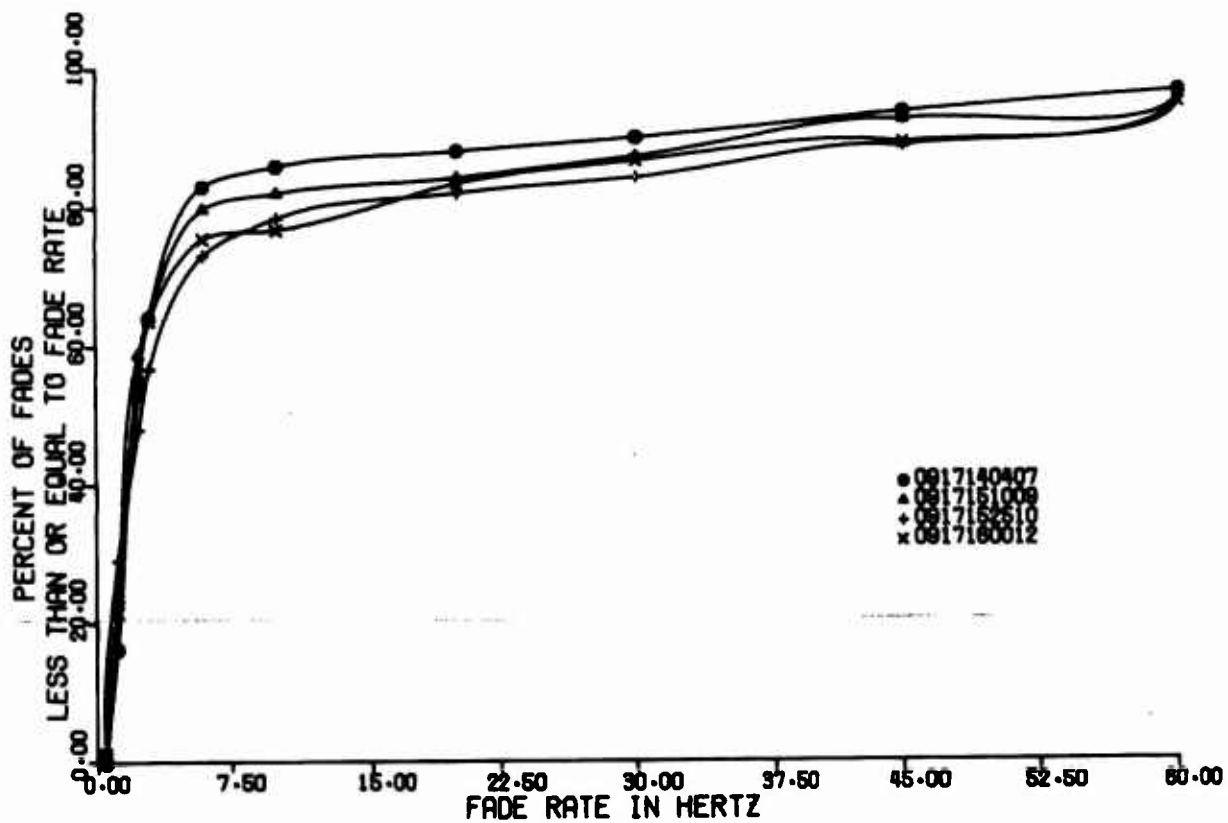


Figure 71. Fade Rate Distribution  
Point Petre, September; C-Band

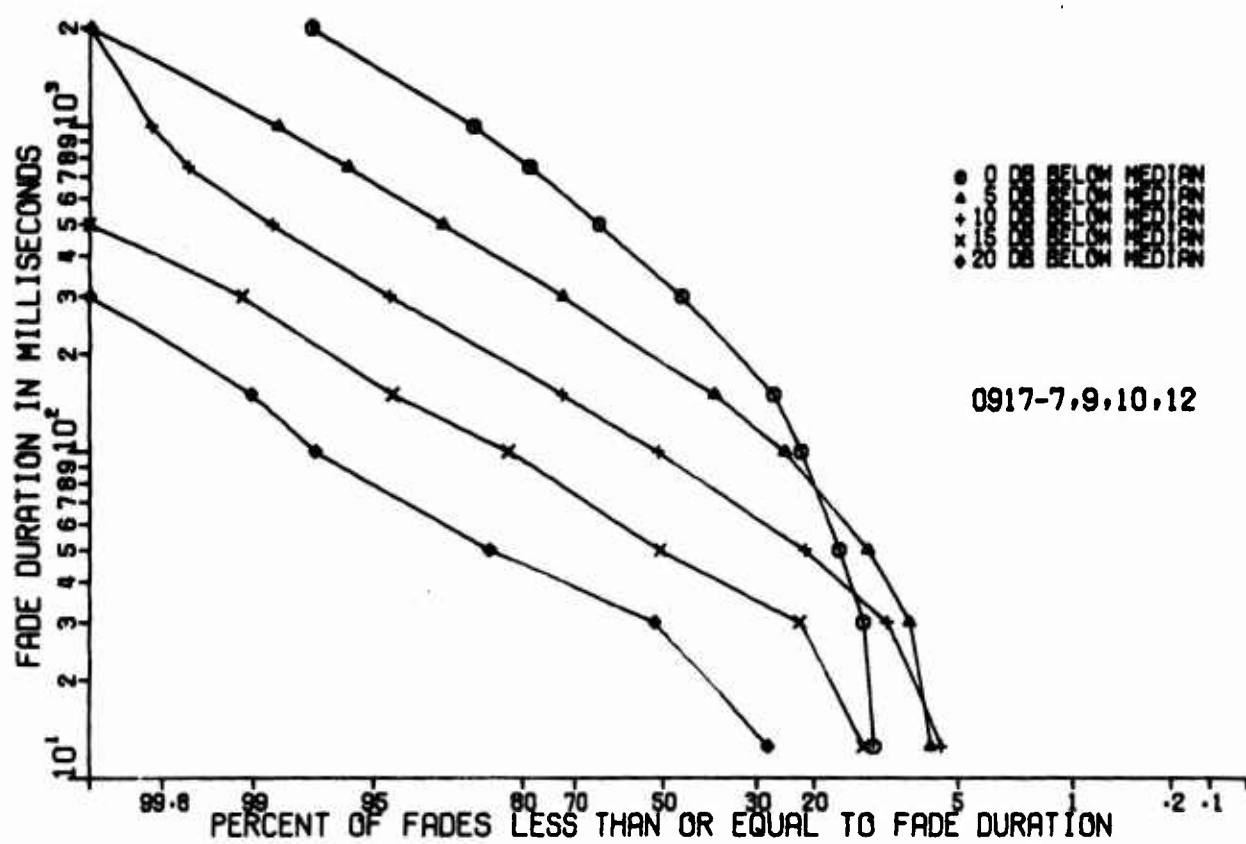


Figure 72. Distribution of Fade Duration  
Point Petre, September; C-Band

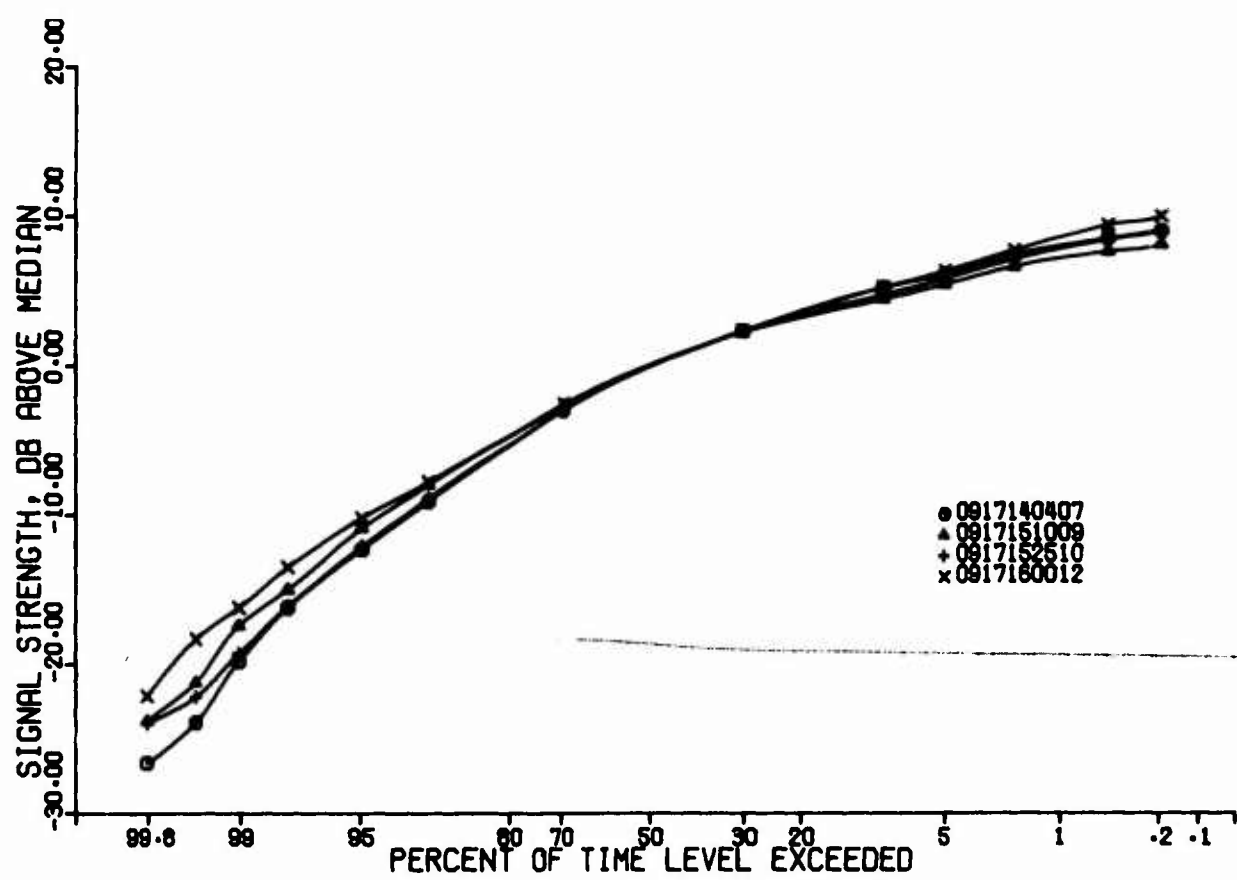


Figure 73. Signal Amplitude Level  
Point Petre, September; C-Band

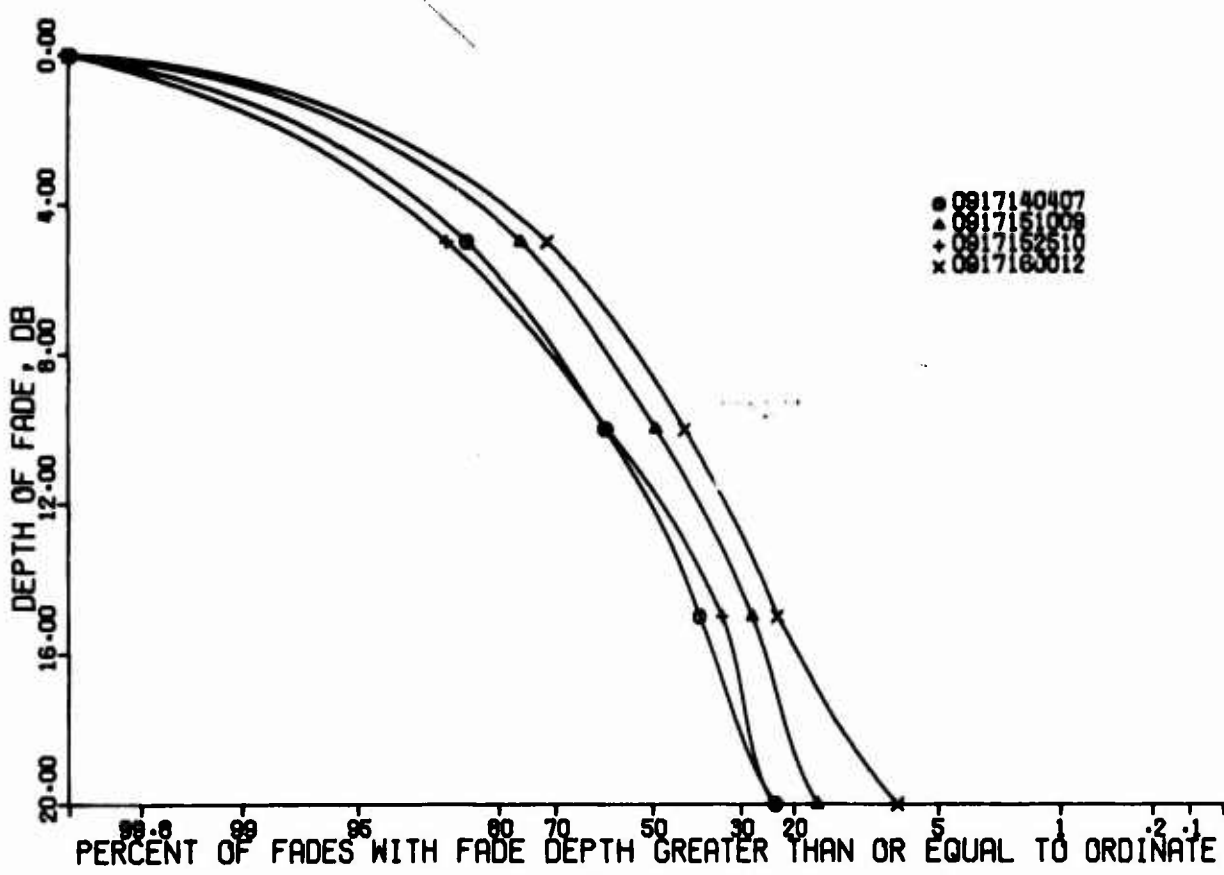


Figure 74. Distribution of Depth of Fades  
Point Petre, September; C-Band

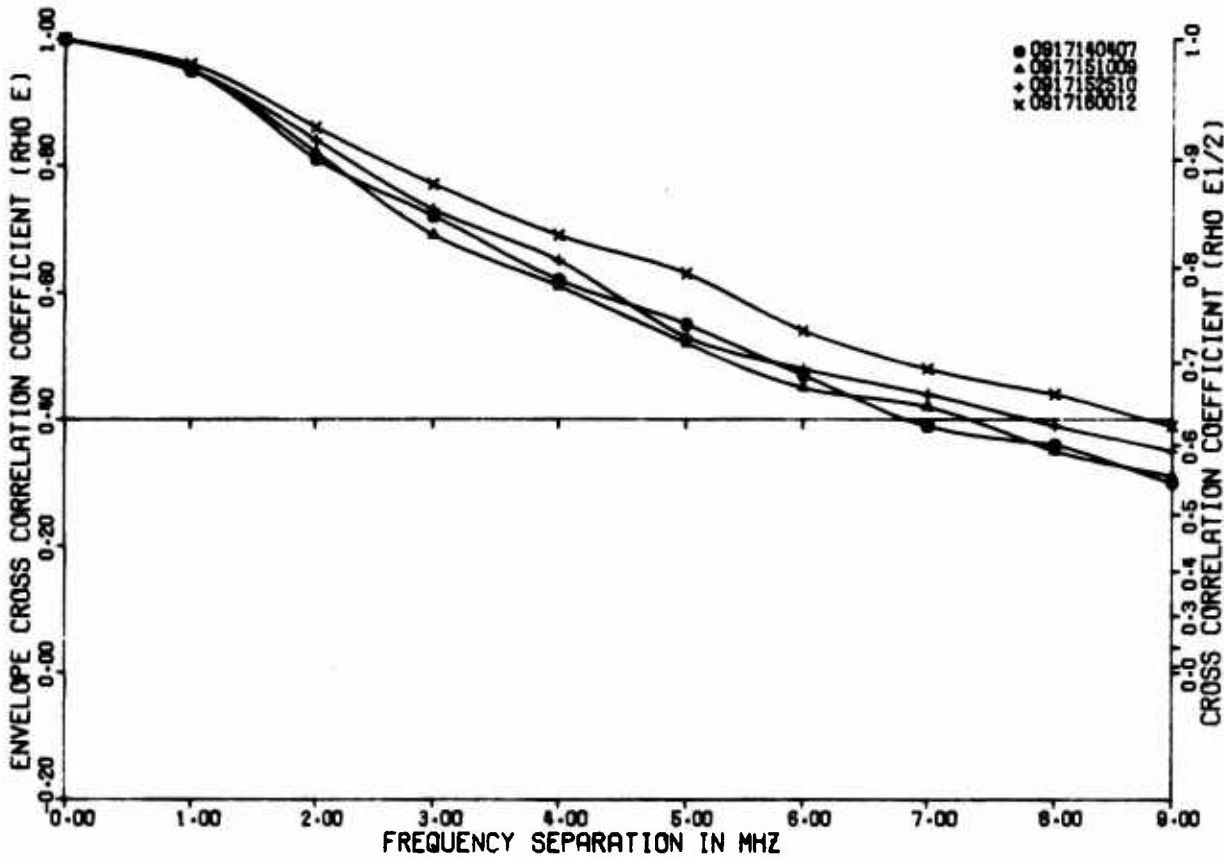


Figure 75. Envelope Cross Correlation Coefficients  
Point Petre, September; X-Band, Wide

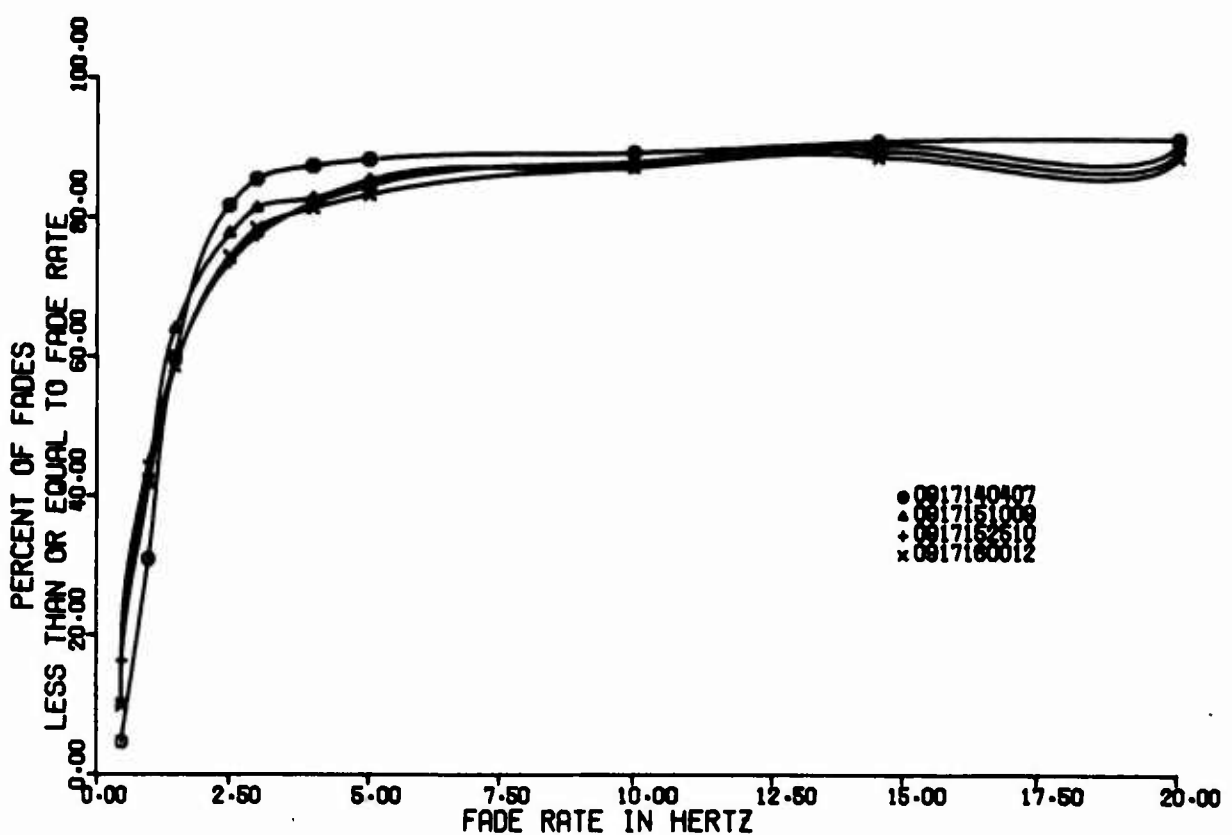


Figure 76. Fade Rate Distribution  
Point Petre, September; X-Band

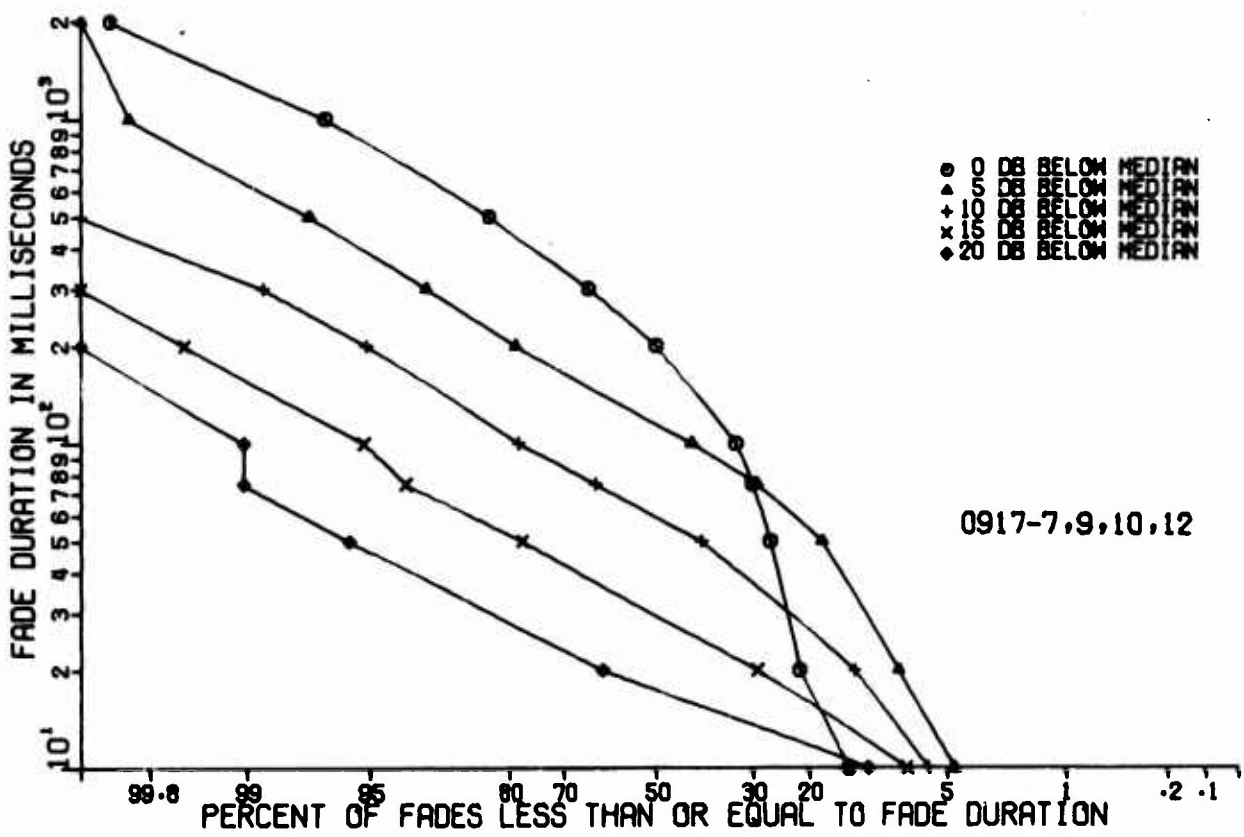


Figure 77. Distribution of Fade Duration  
Point Petre, September; X-Band

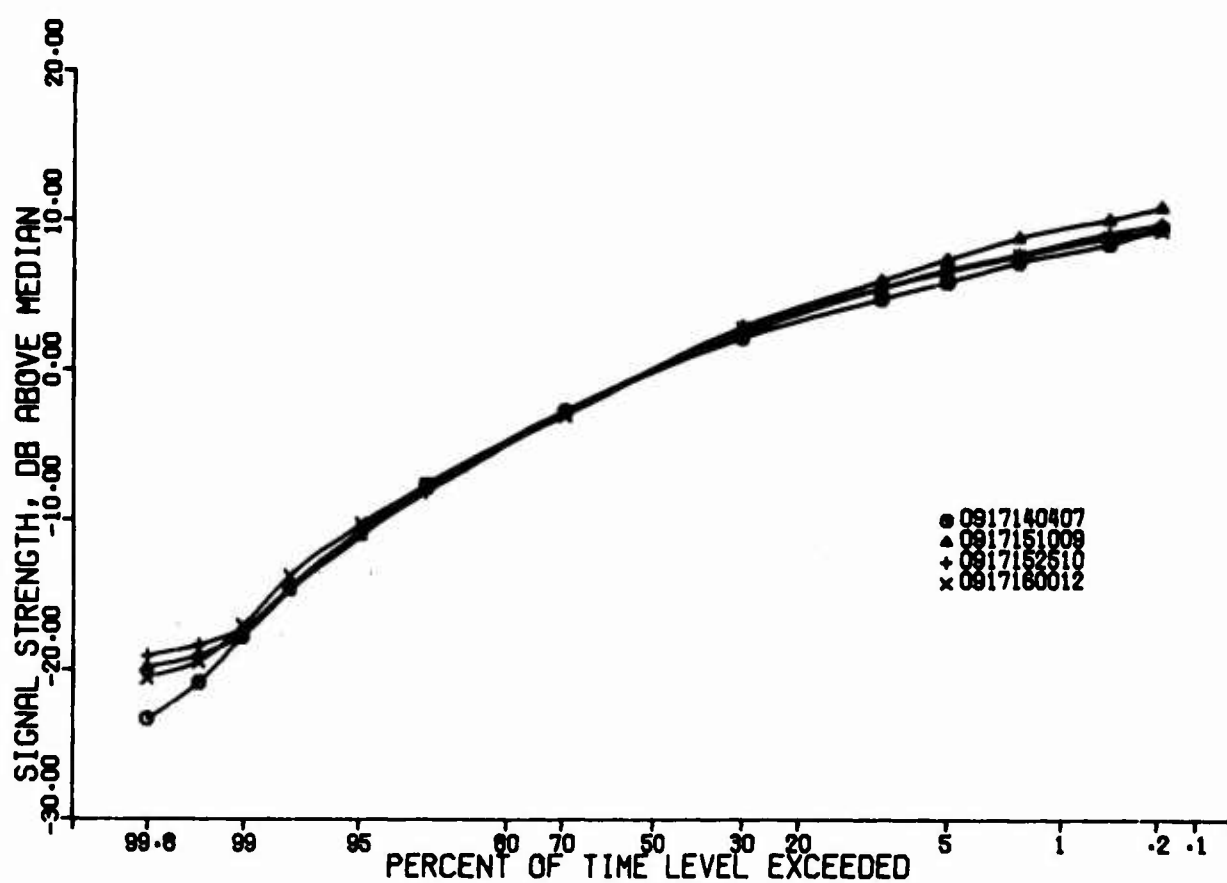


Figure 78. Signal Amplitude Level  
Point Petre, September; X-Band

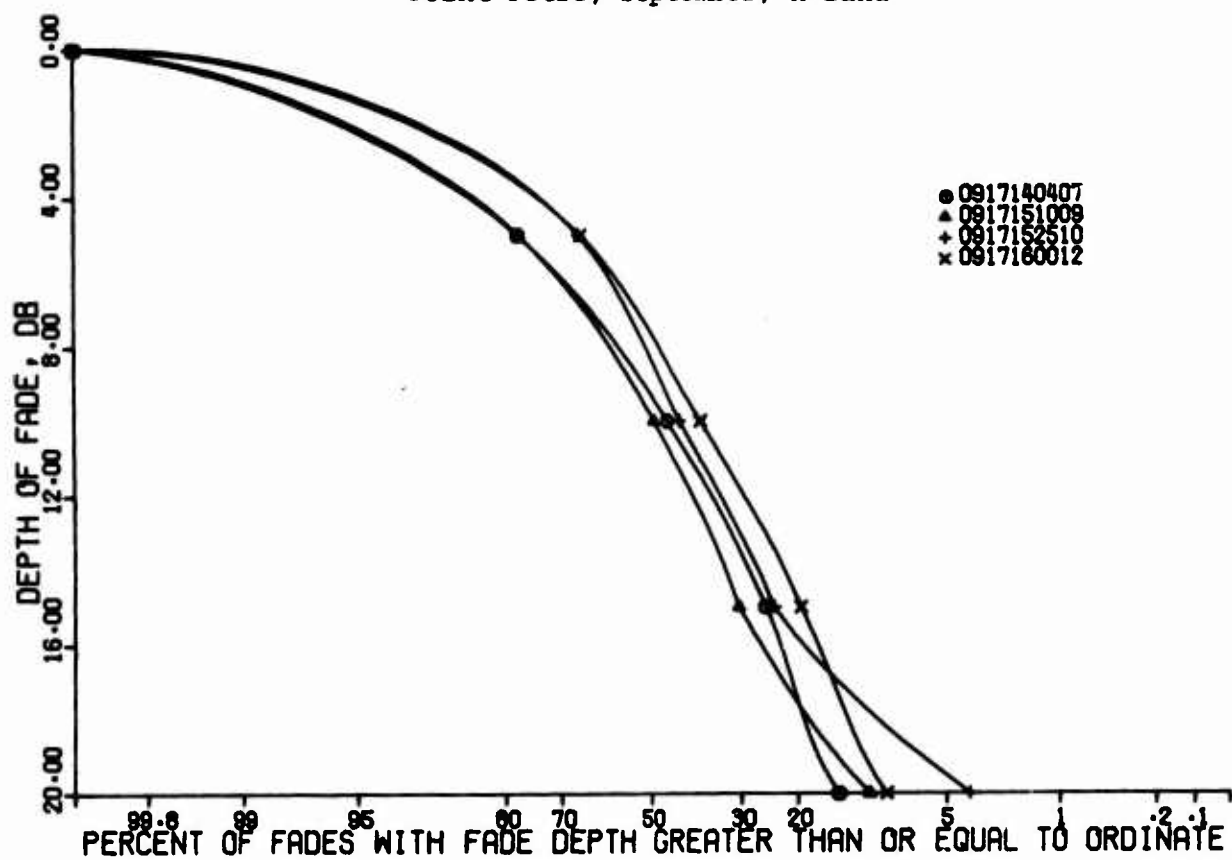


Figure 79. Distribution of Depth of Fades  
Point Petre, September; X-Band

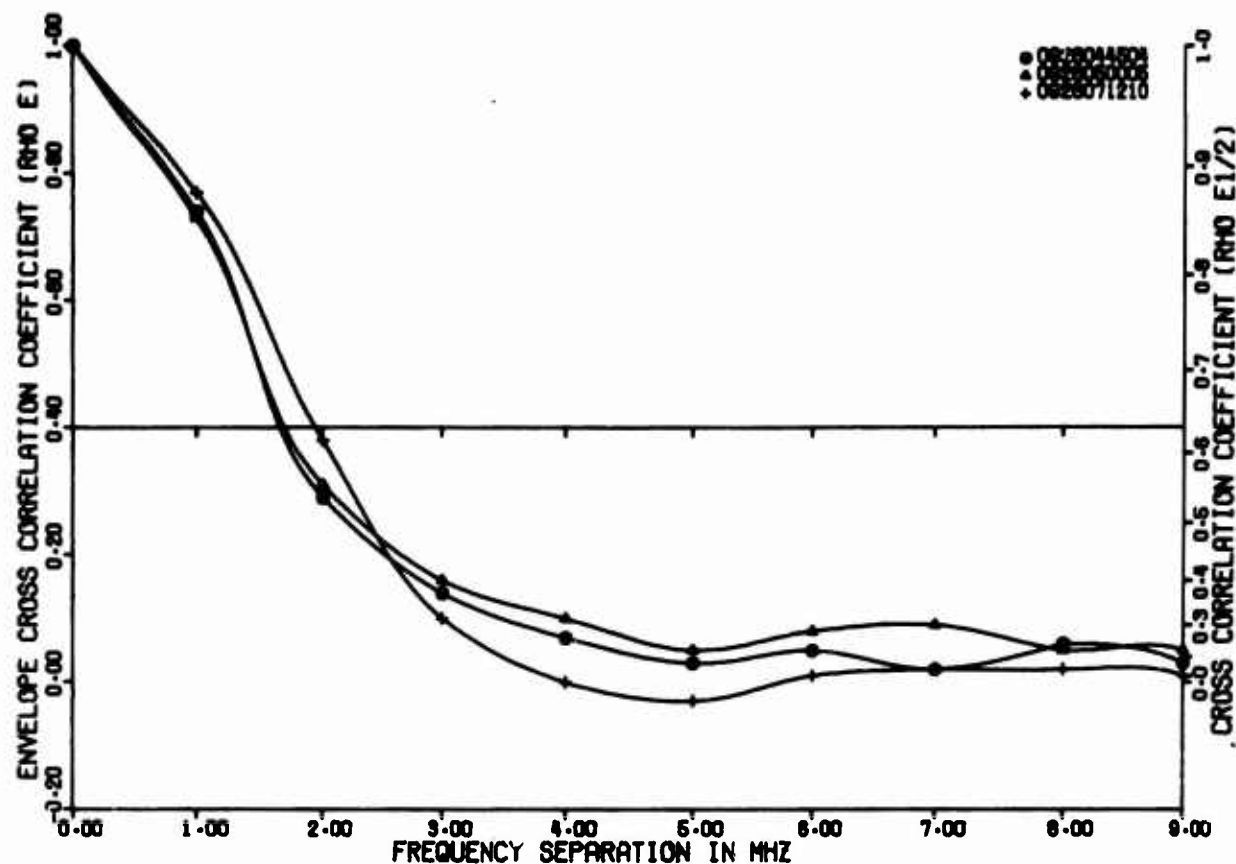


Figure 80. Envelope Cross Correlation Coefficients  
Point Petre, September; C-Band, Wide

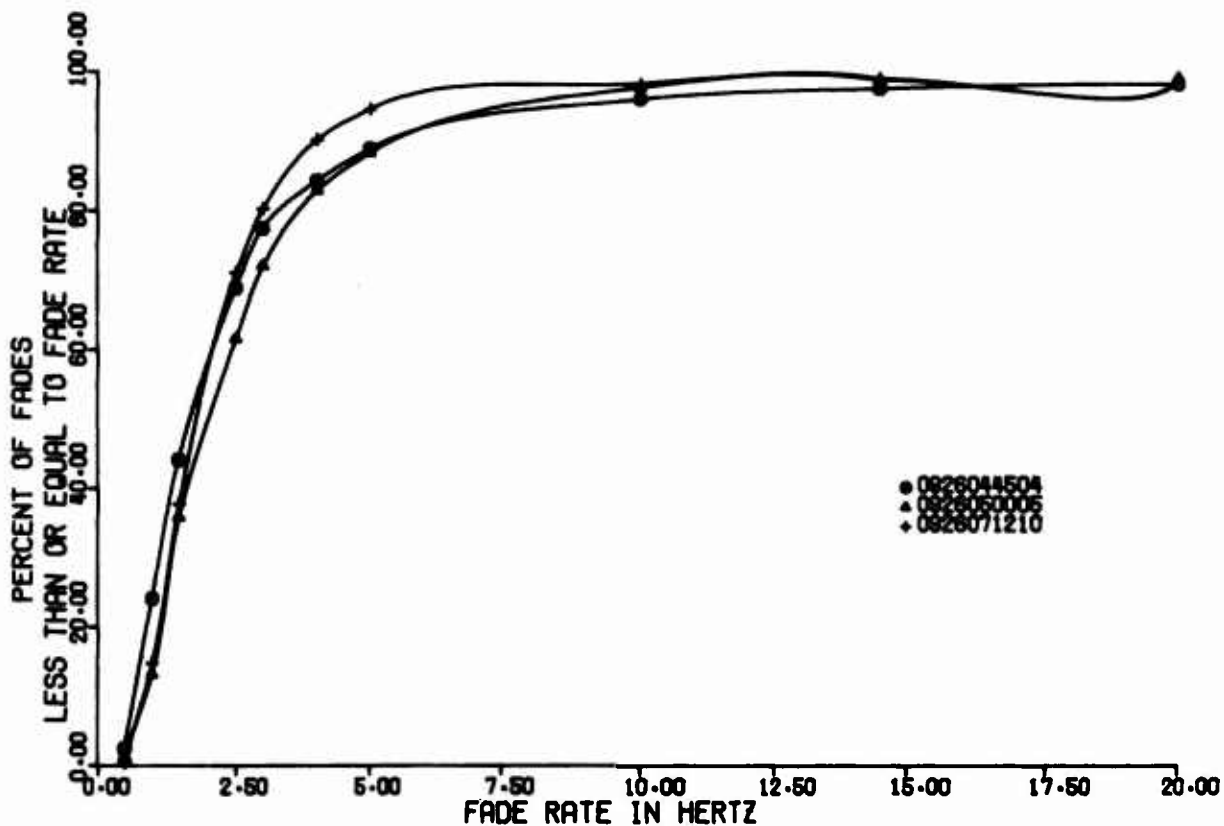


Figure 81. Fade Rate Distribution  
Point Petre, September; C-Band

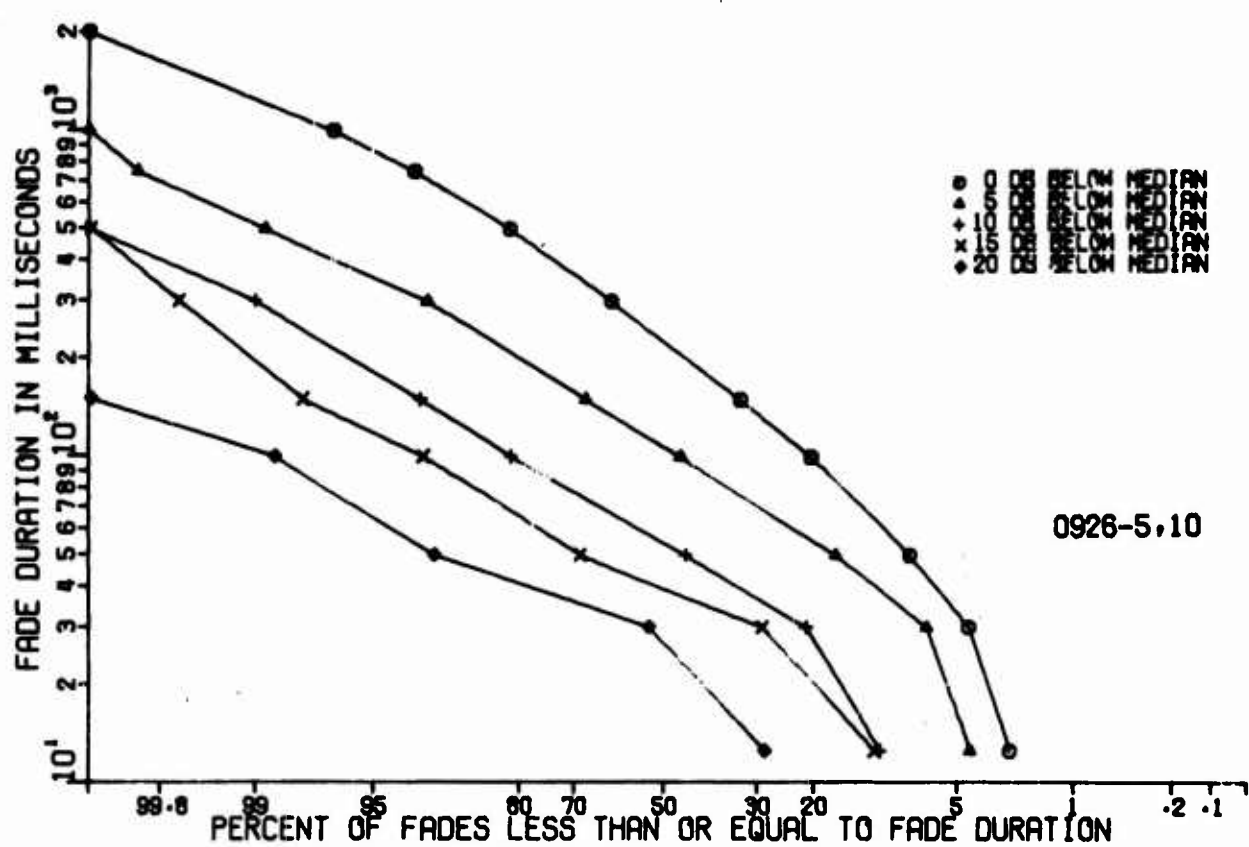


Figure 82. Distribution of Fade Duration  
Point Petre, September; C-Band

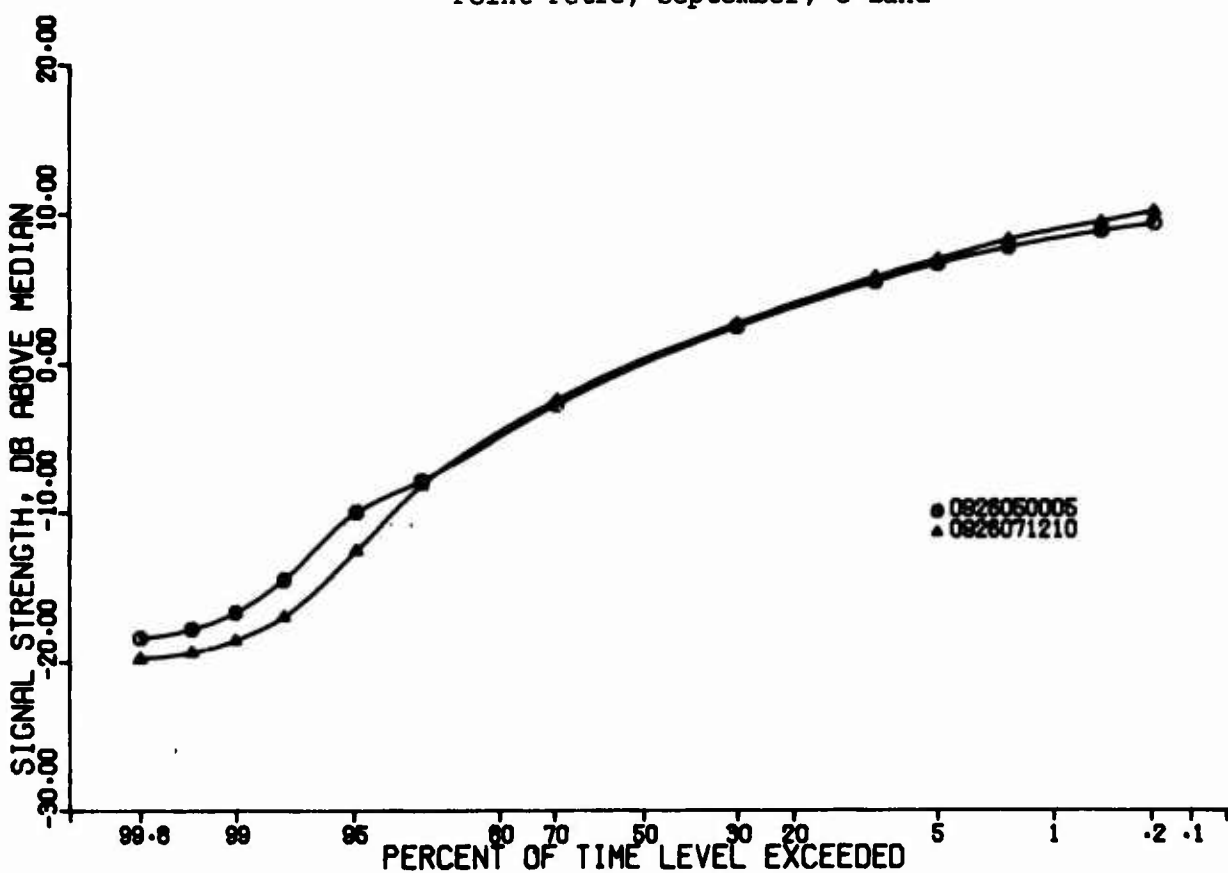


Figure 83. Signal Amplitude Level  
Point Petre, September; C-Band

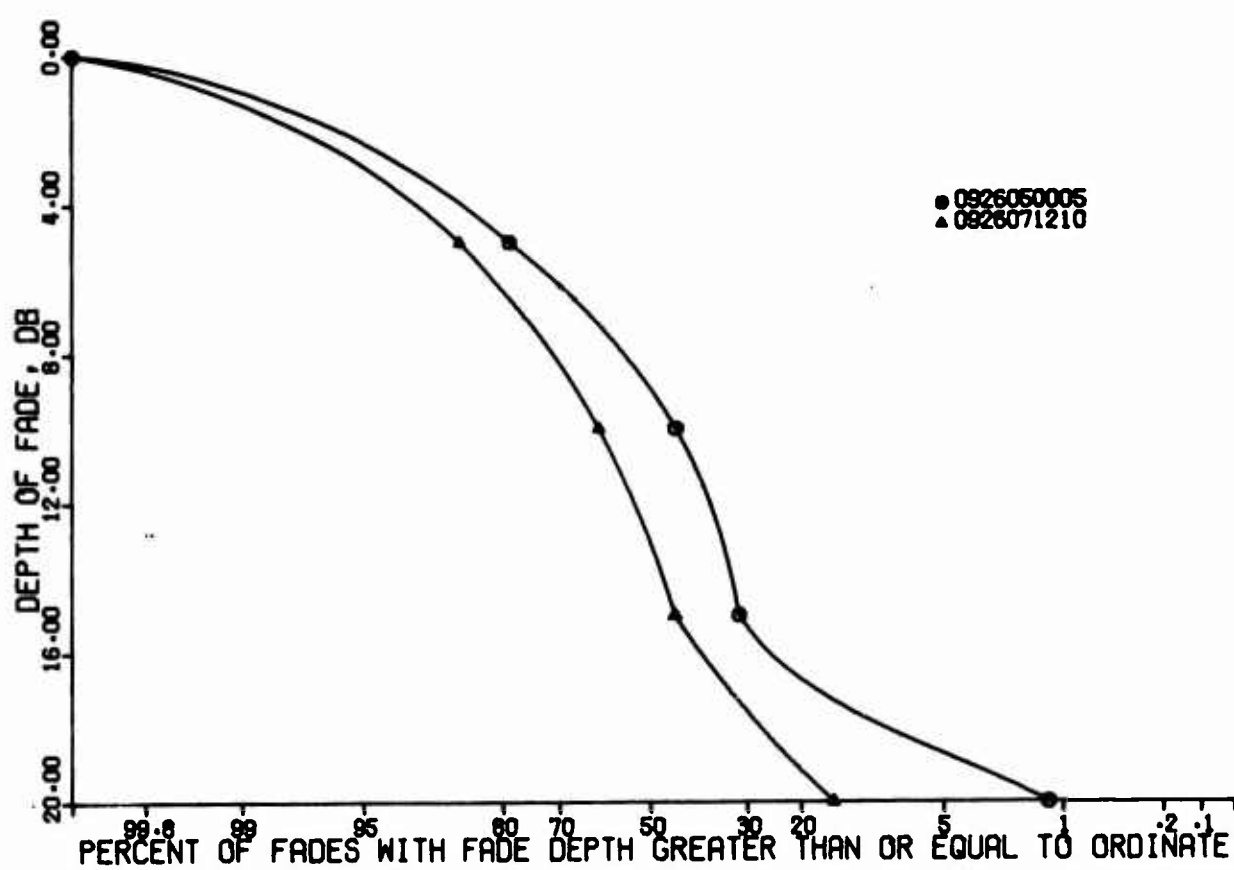


Figure 84. Distribution of Depth of Fades  
Point Petre, September; C-Band

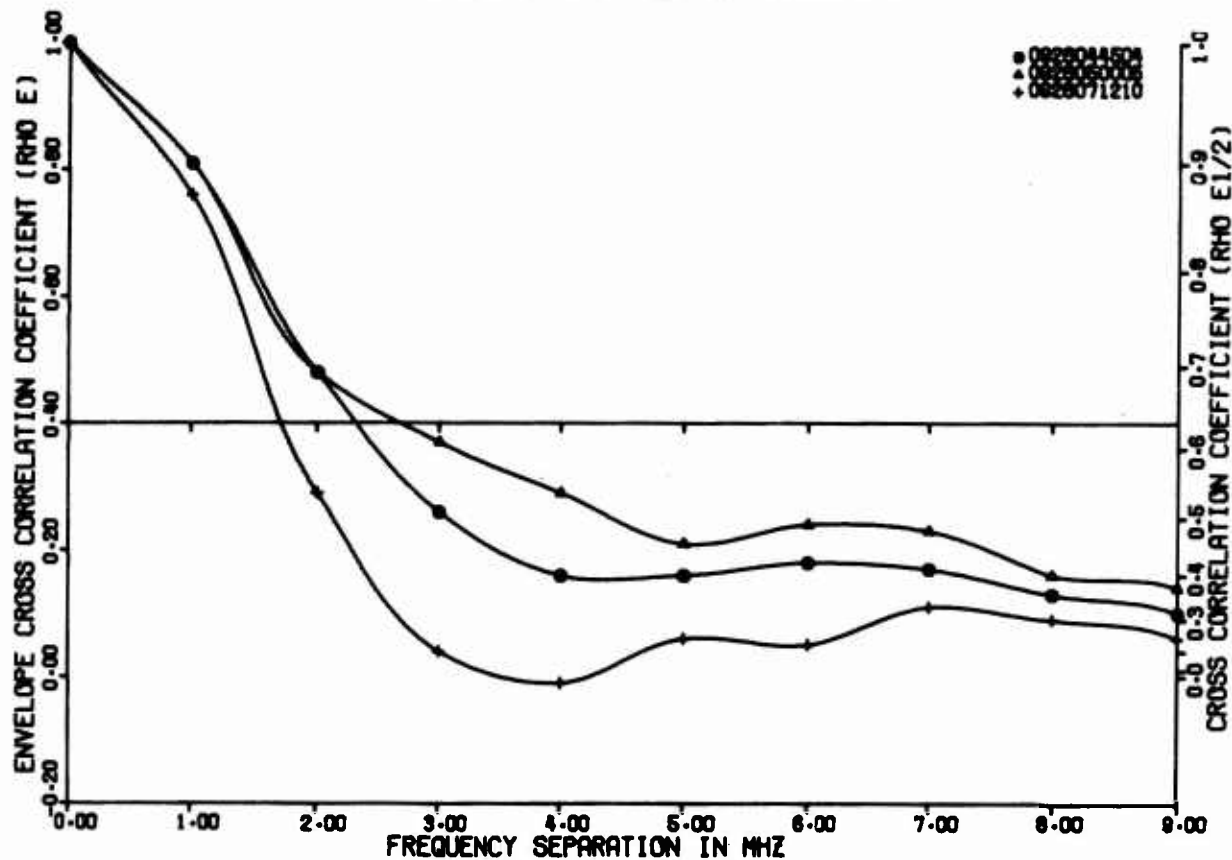


Figure 85. Envelope Cross Correlation Coefficients  
Point Petre, September; X-Band, Wide

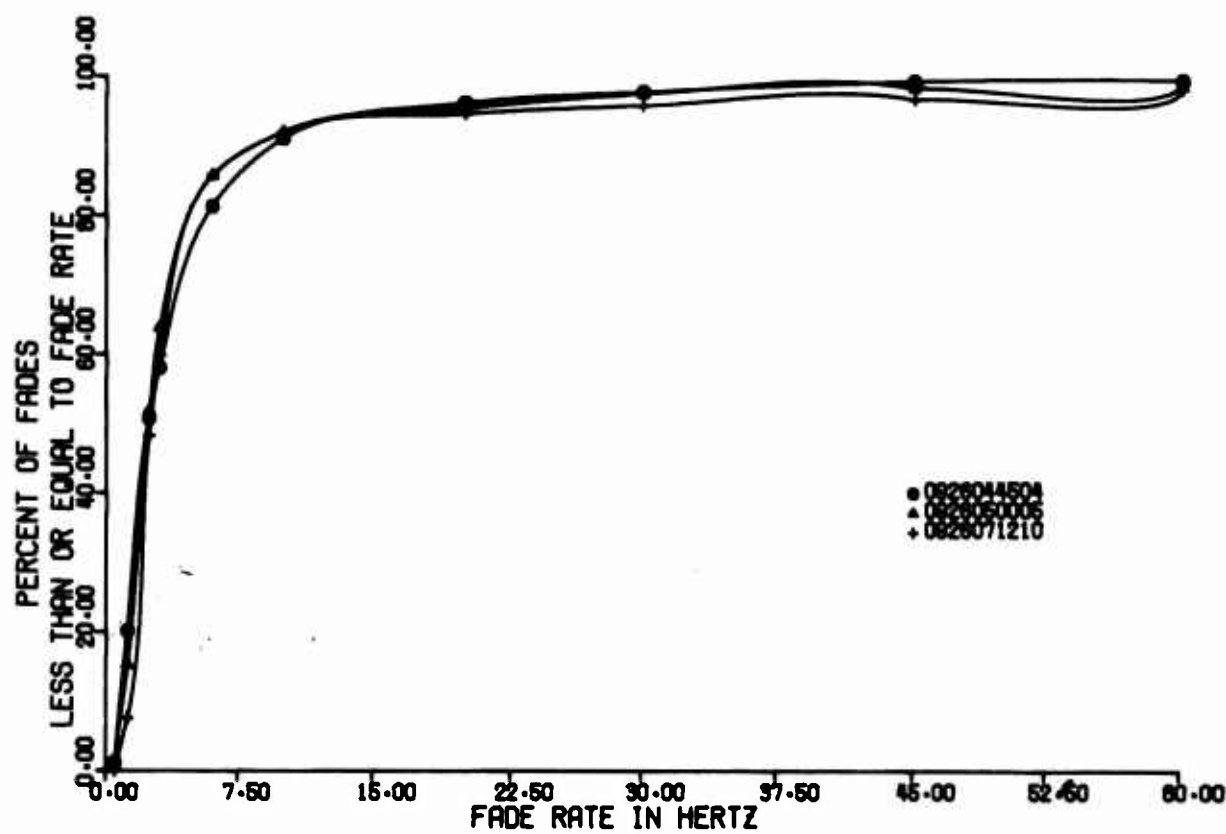


Figure 86. Fade Rate Distribution  
Point Petre, September; X-Band

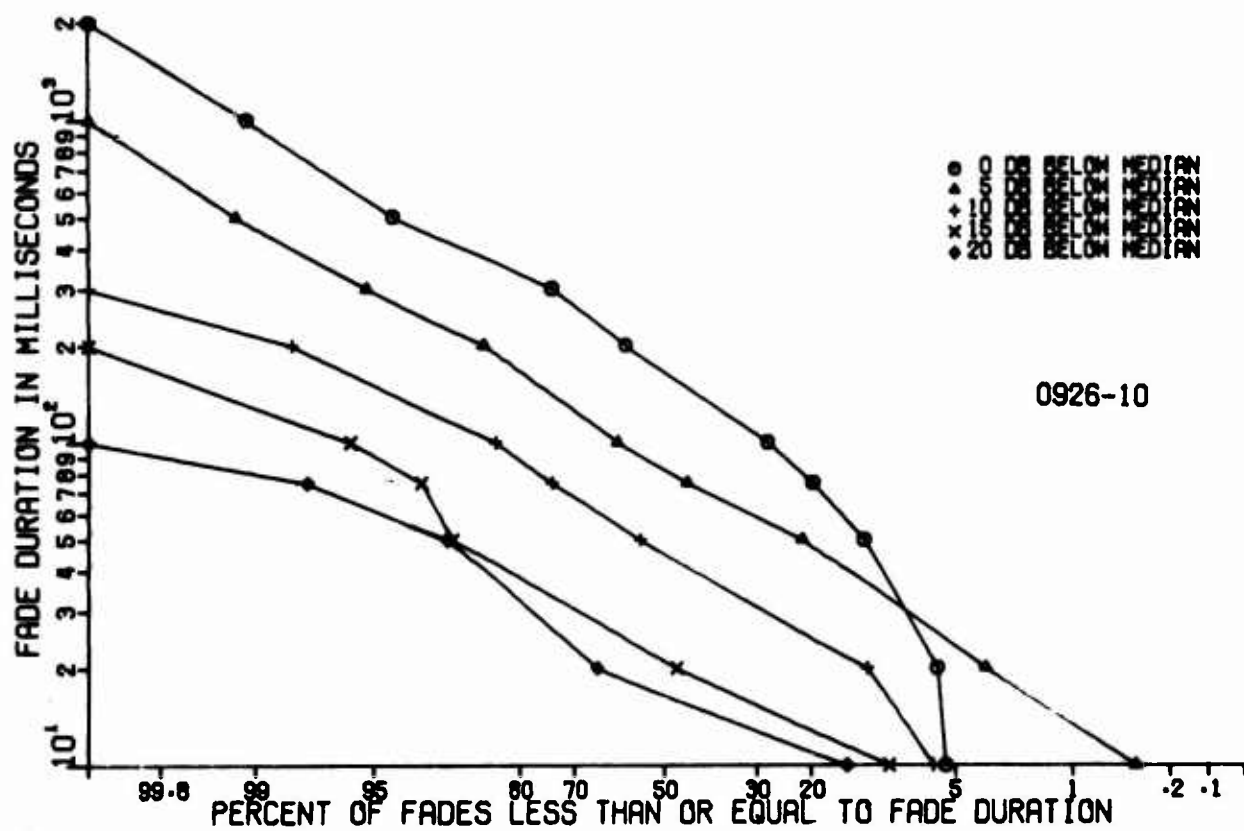


Figure 87. Distribution of Fade Duration  
Point Petre, September; X-Band

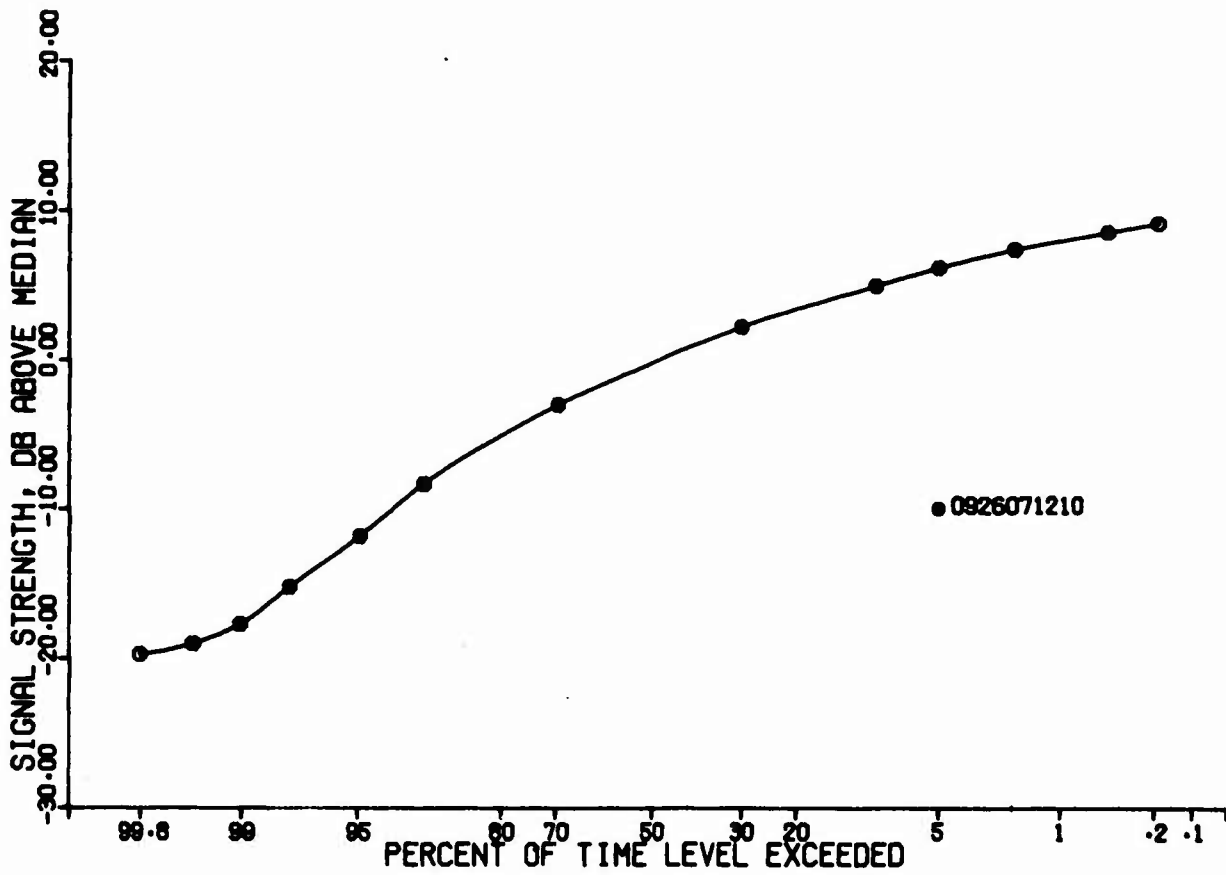


Figure 88. Signal Amplitude Level  
Point Petre, September; X-Band

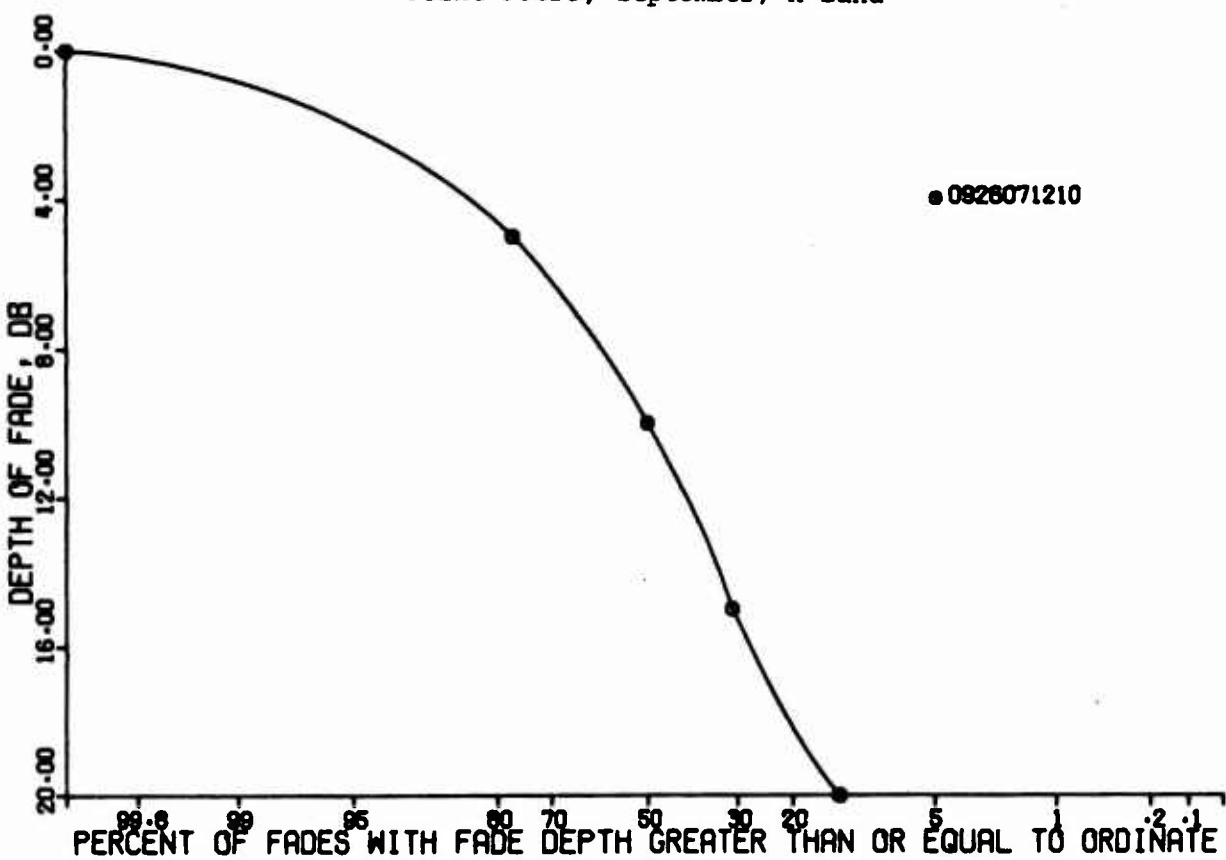


Figure 89. Distribution of Depth of Fades  
Point Petre, September; X-Band

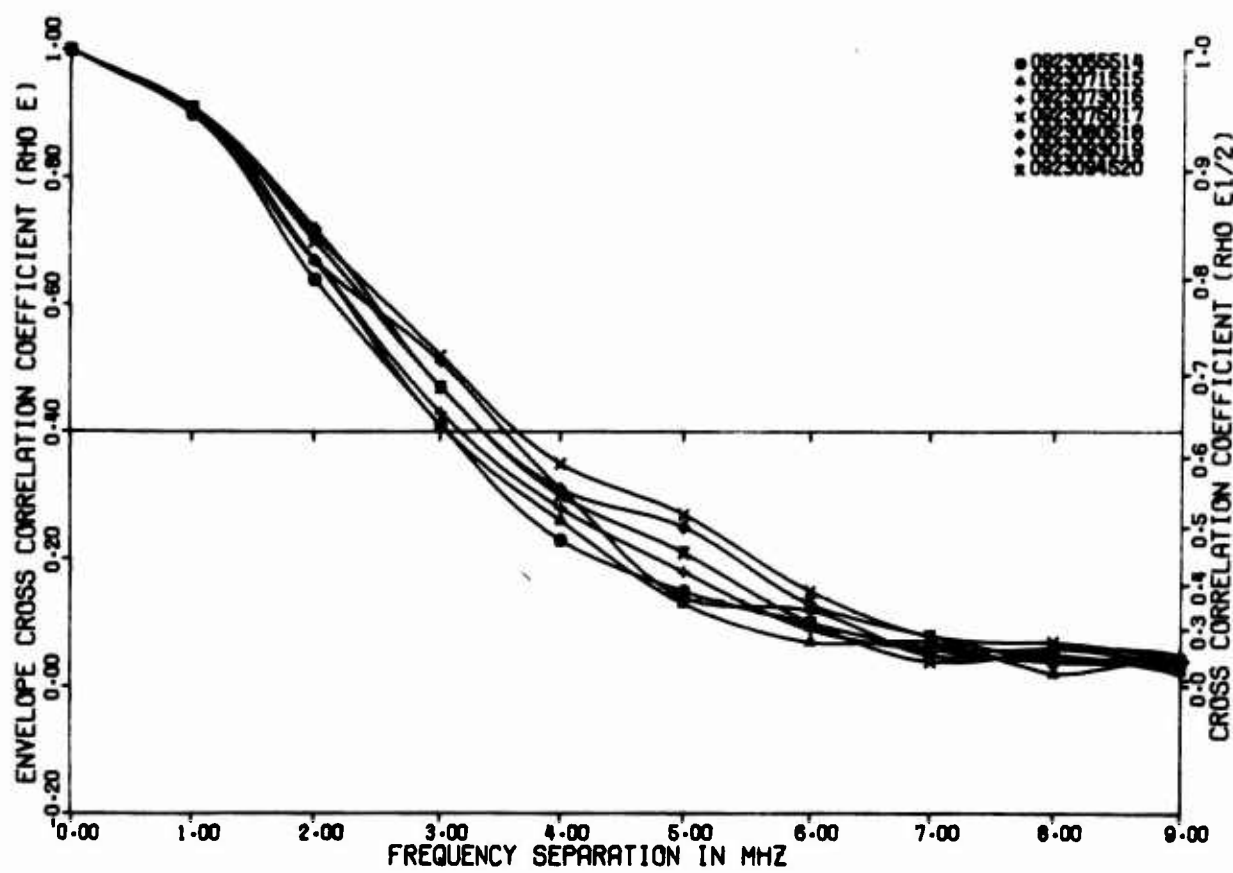


Figure 90. Envelope Cross Correlation Coefficients  
Point Petre, September; C-Band, Wide

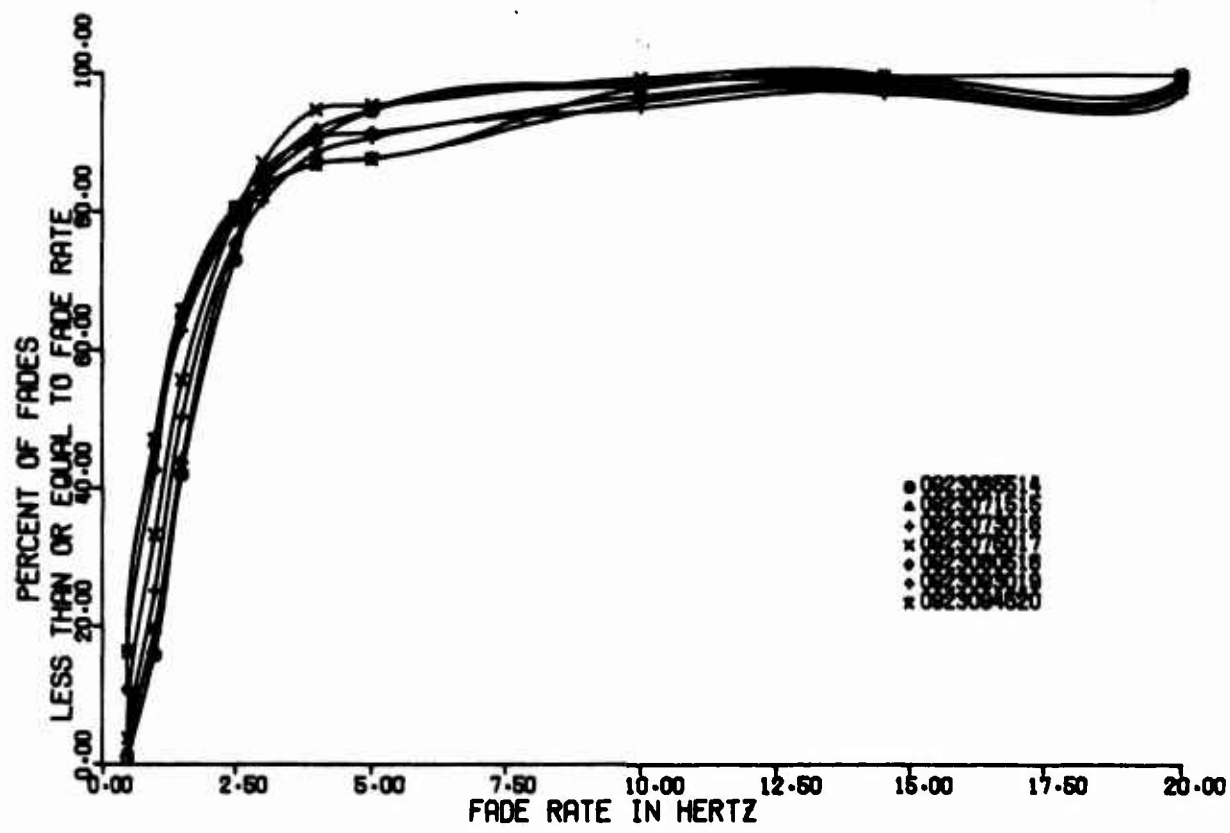


Figure 91. Fade Rate Distribution  
Point Petre, September; C-Band

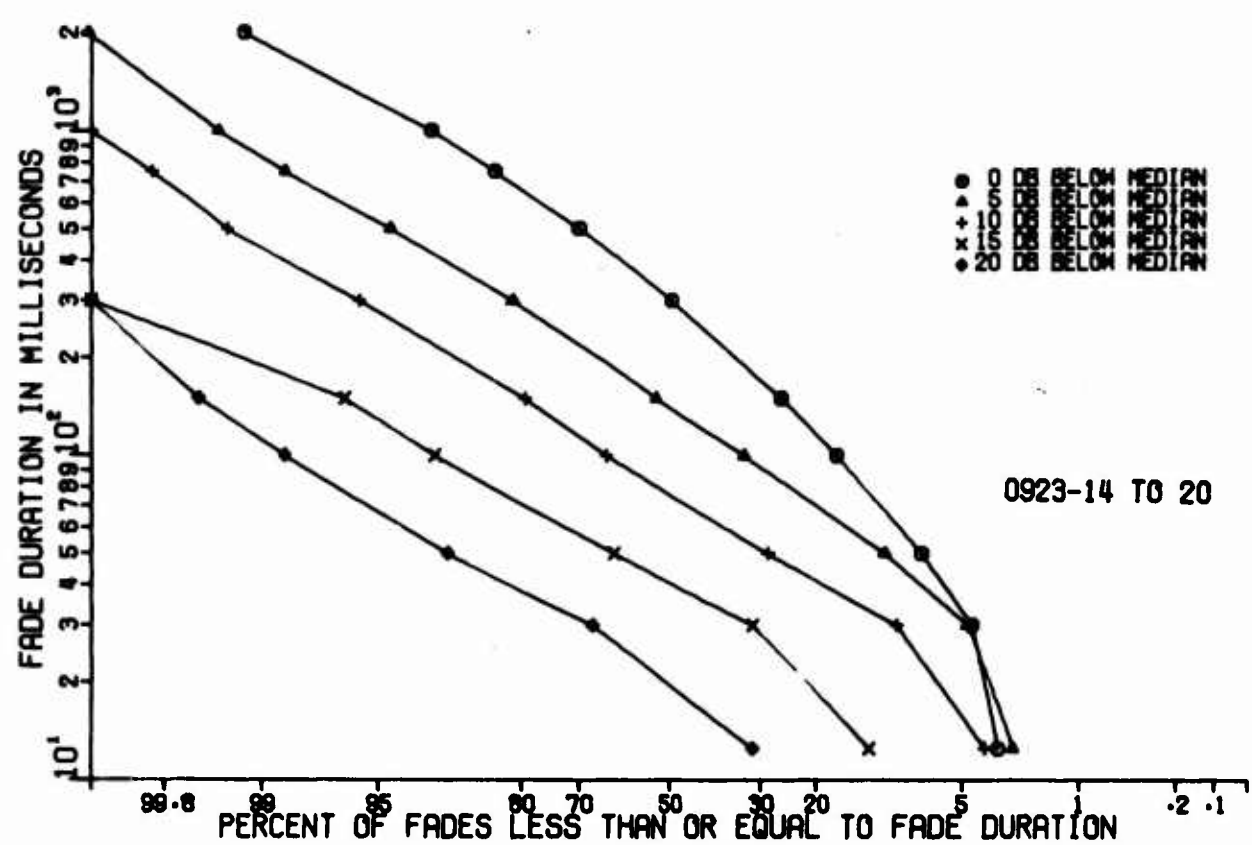


Figure 92. Distribution of Fade Duration  
Point Petre, September; C-Band

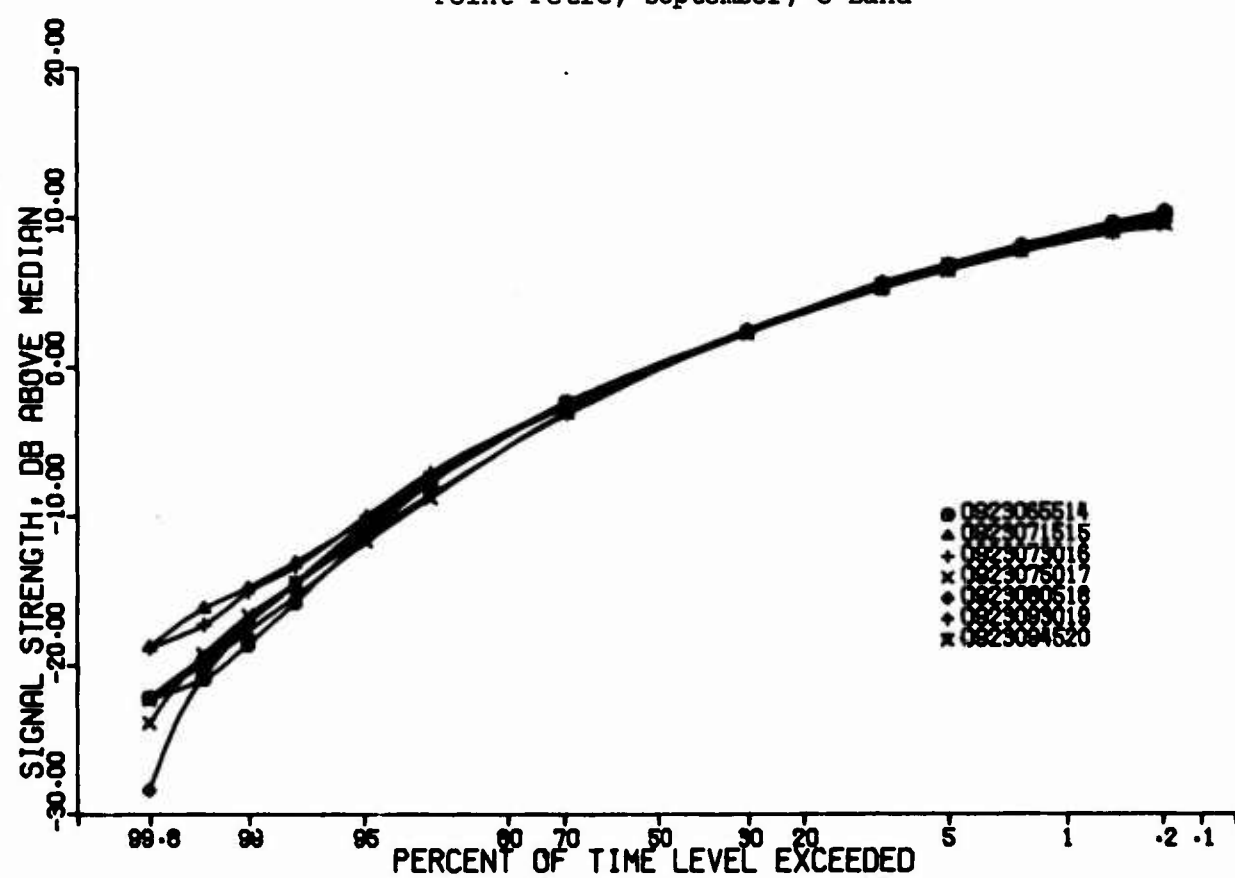


Figure 93. Signal Amplitude Level  
Point Petre, September; C-Band

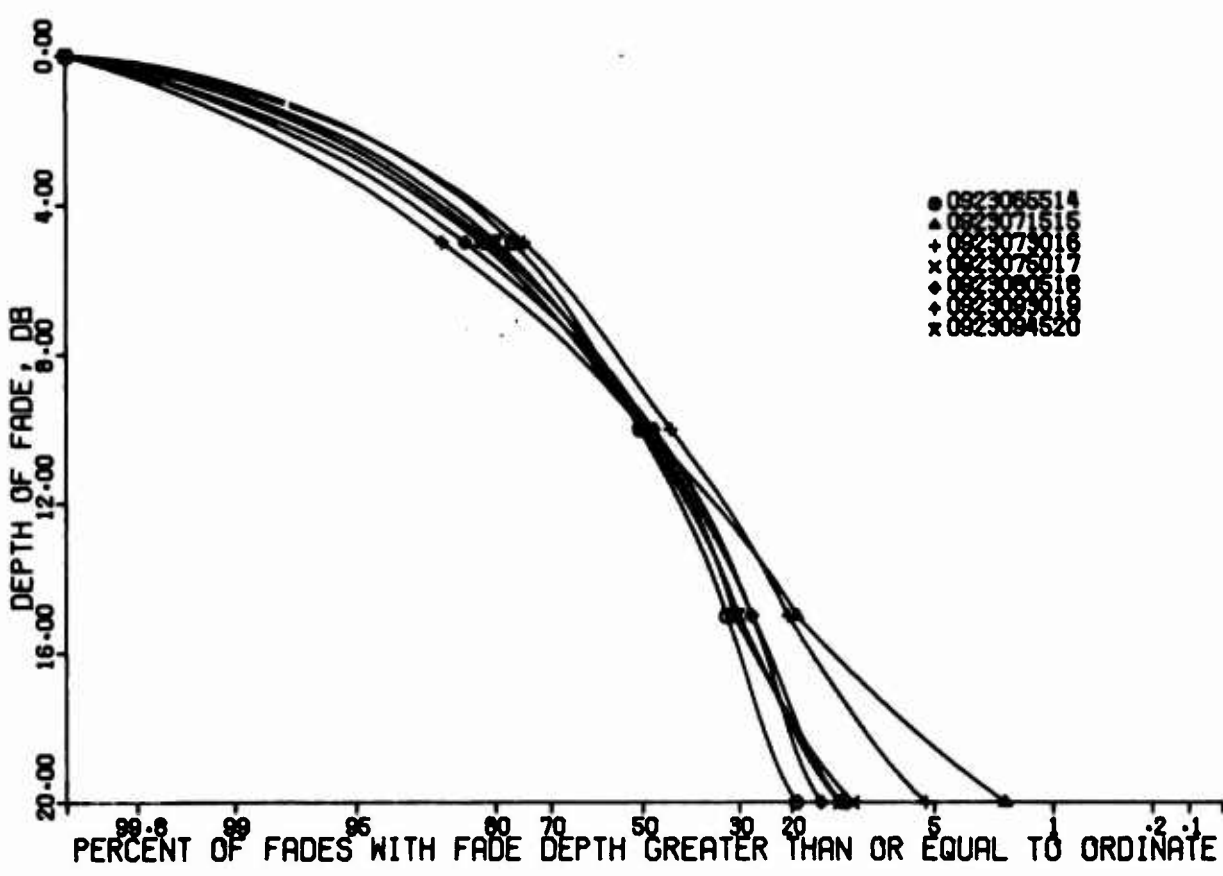


Figure 94. Distribution of Depth of Fades  
Point Petre, September; C-Band

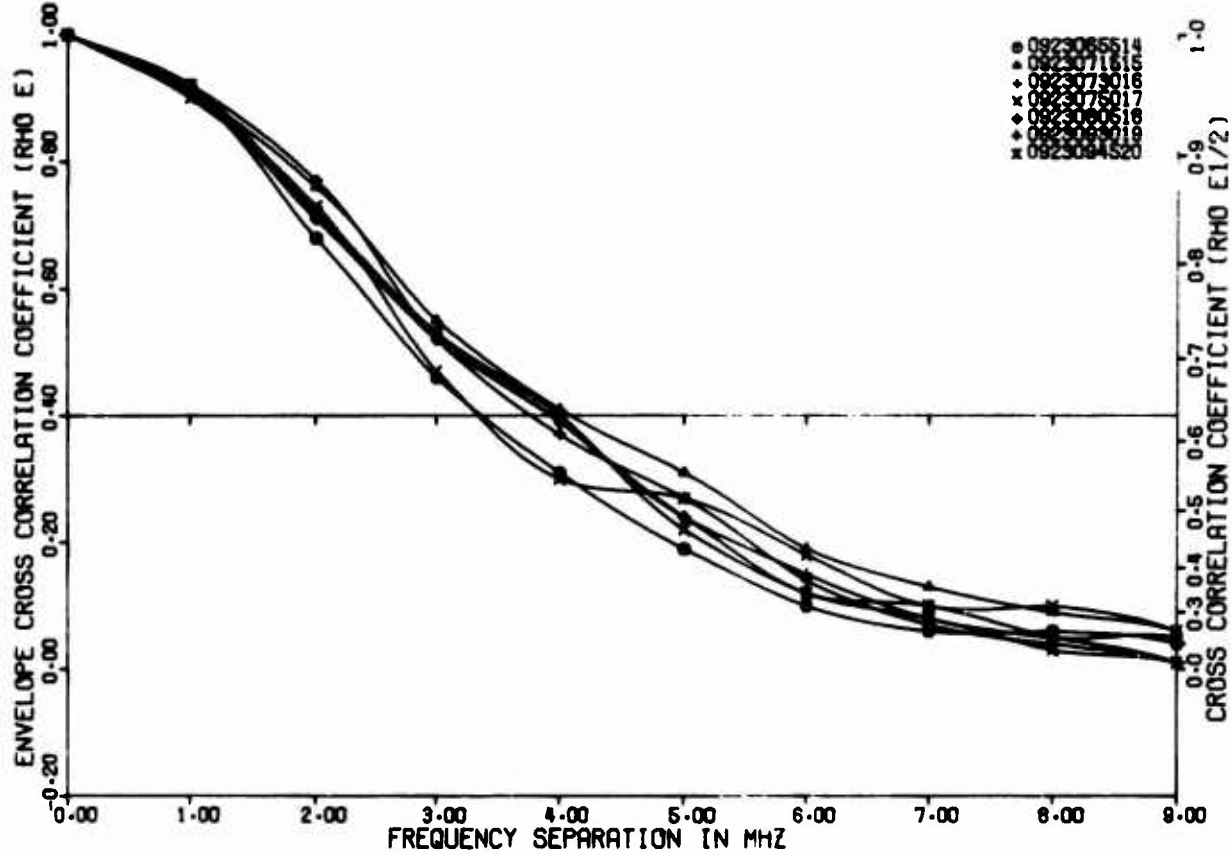


Figure 95. Envelope Cross Correlation Coefficients  
Point Petre, September, X-Band, Wide

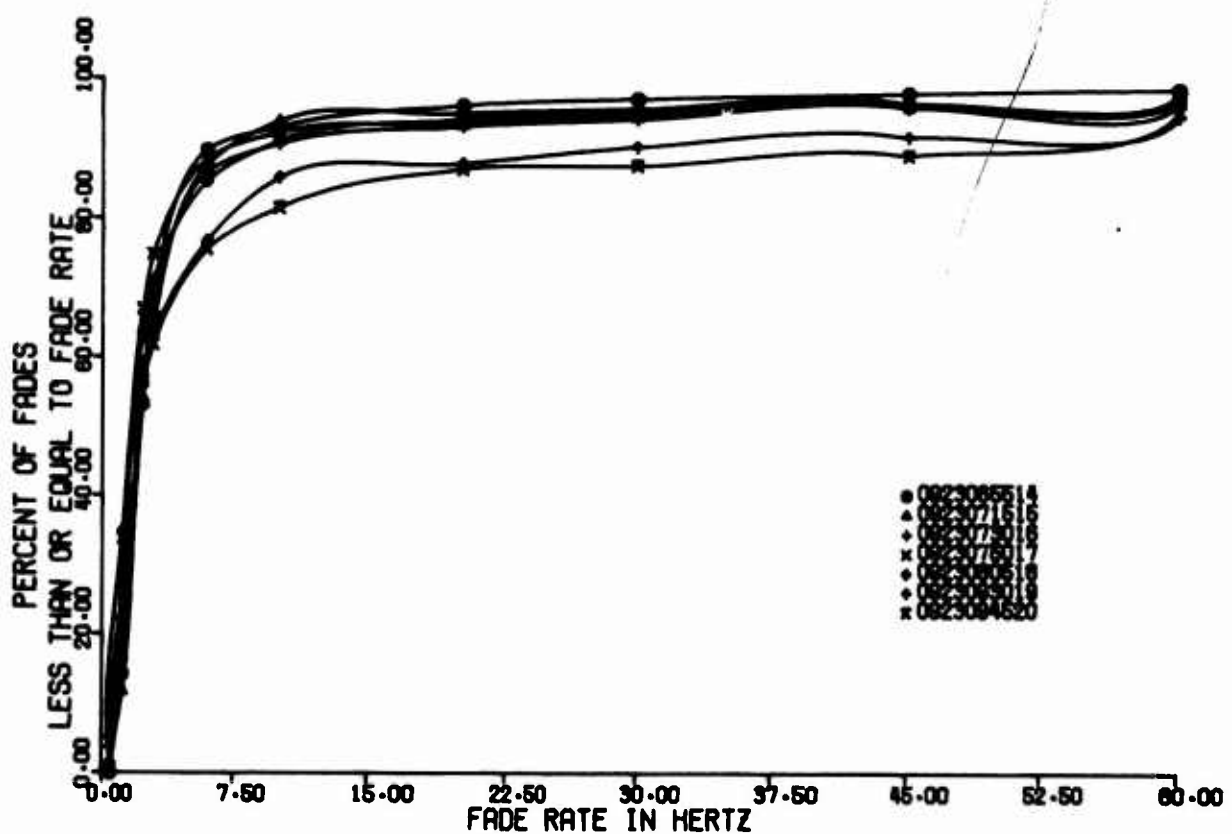


Figure 96. Fade Rate Distribution  
Point Petre, September; X-Band

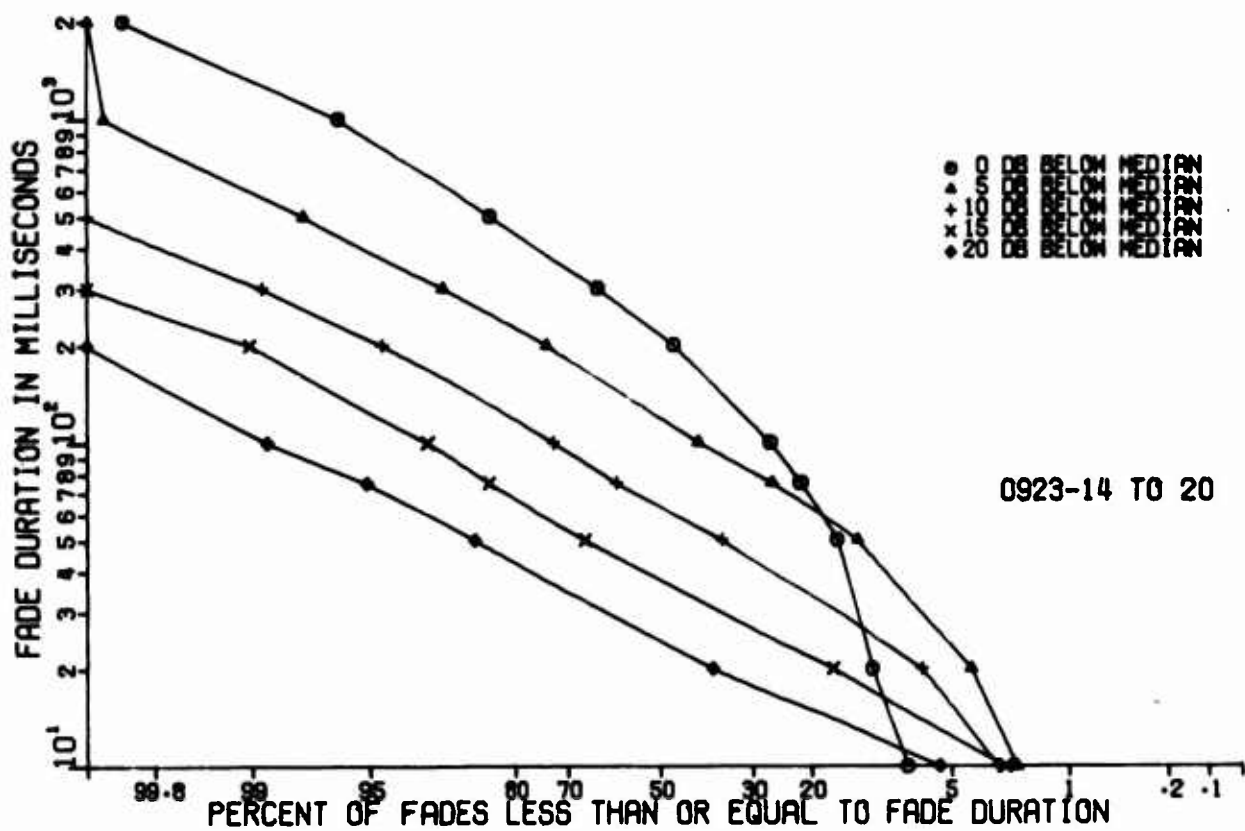


Figure 97. Distribution of Fade Duration  
Point Petre, September; X-Band

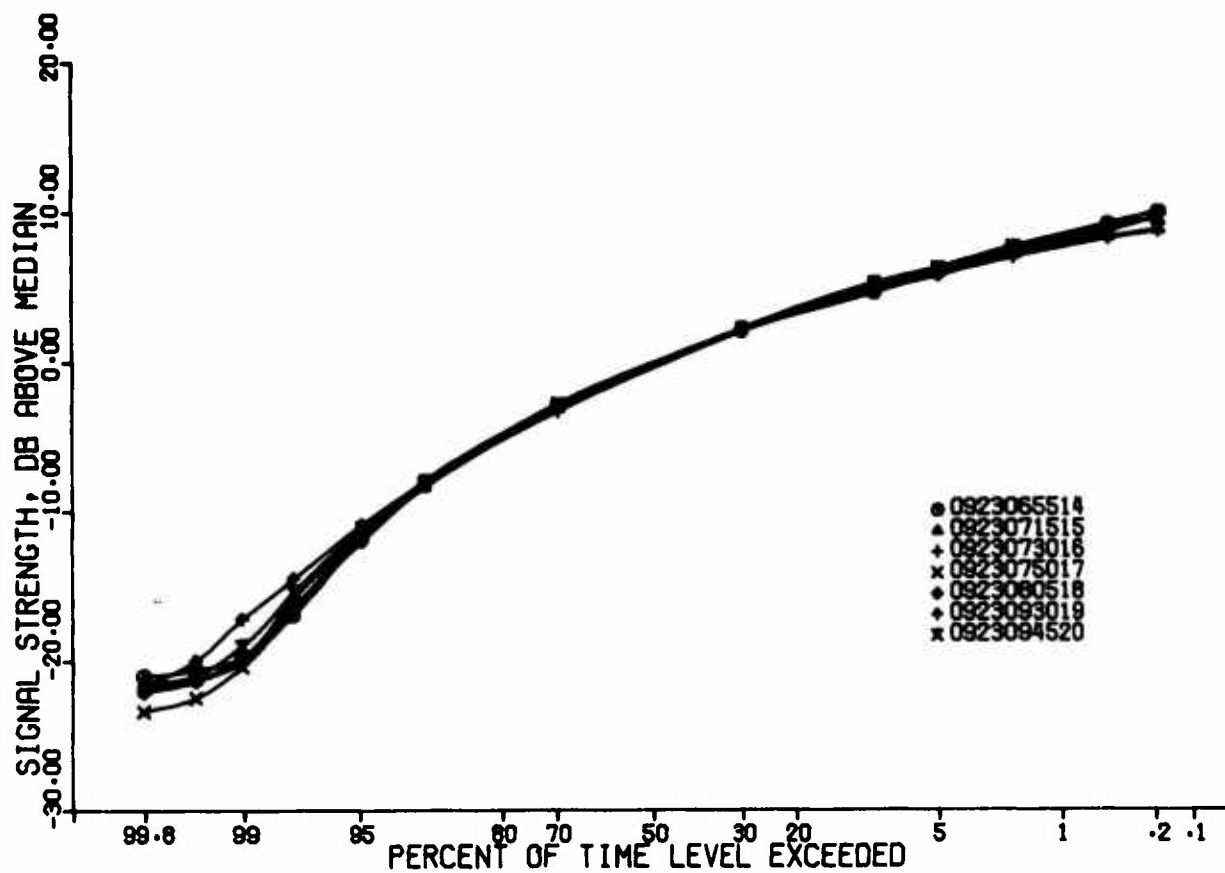


Figure 98. Signal Amplitude Level  
Point Petre, September; X-Band

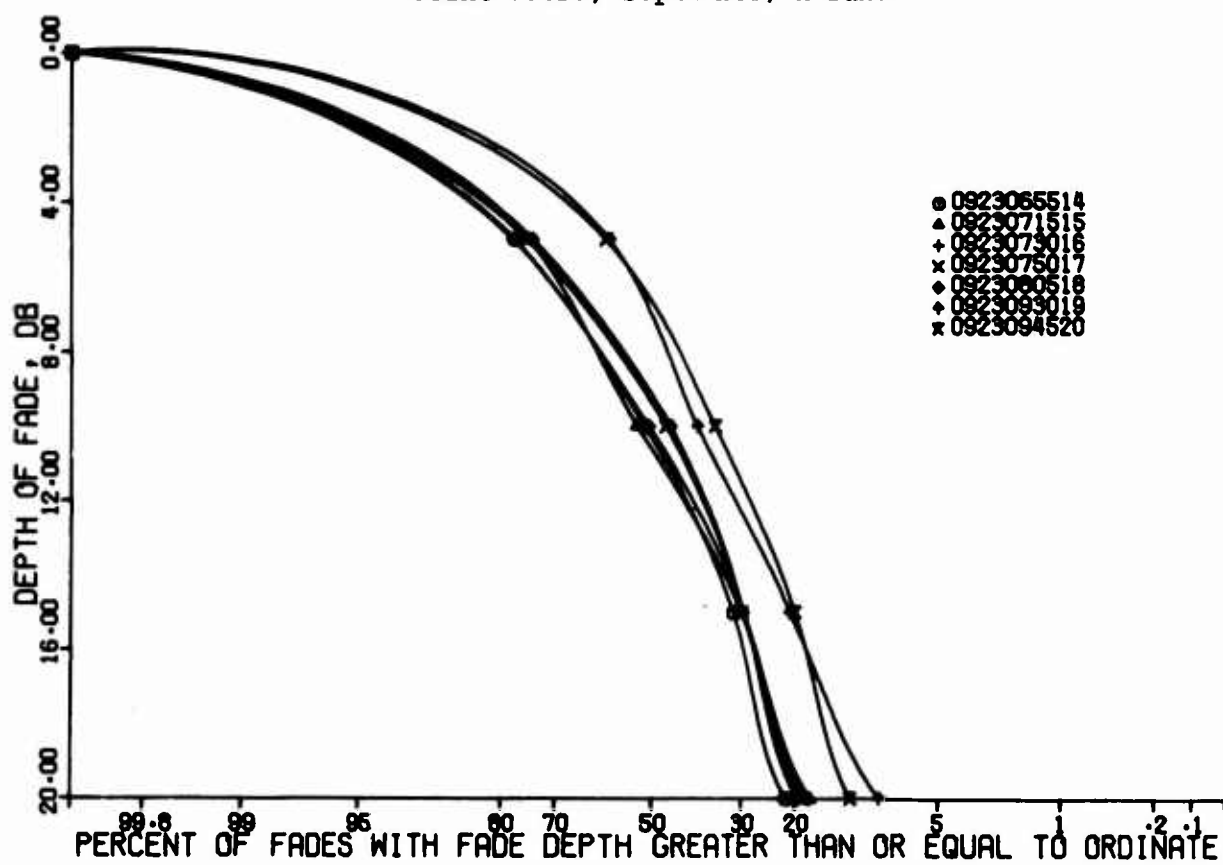


Figure 99. Distribution of Depth of Fades  
Point Petre, September; X-Band

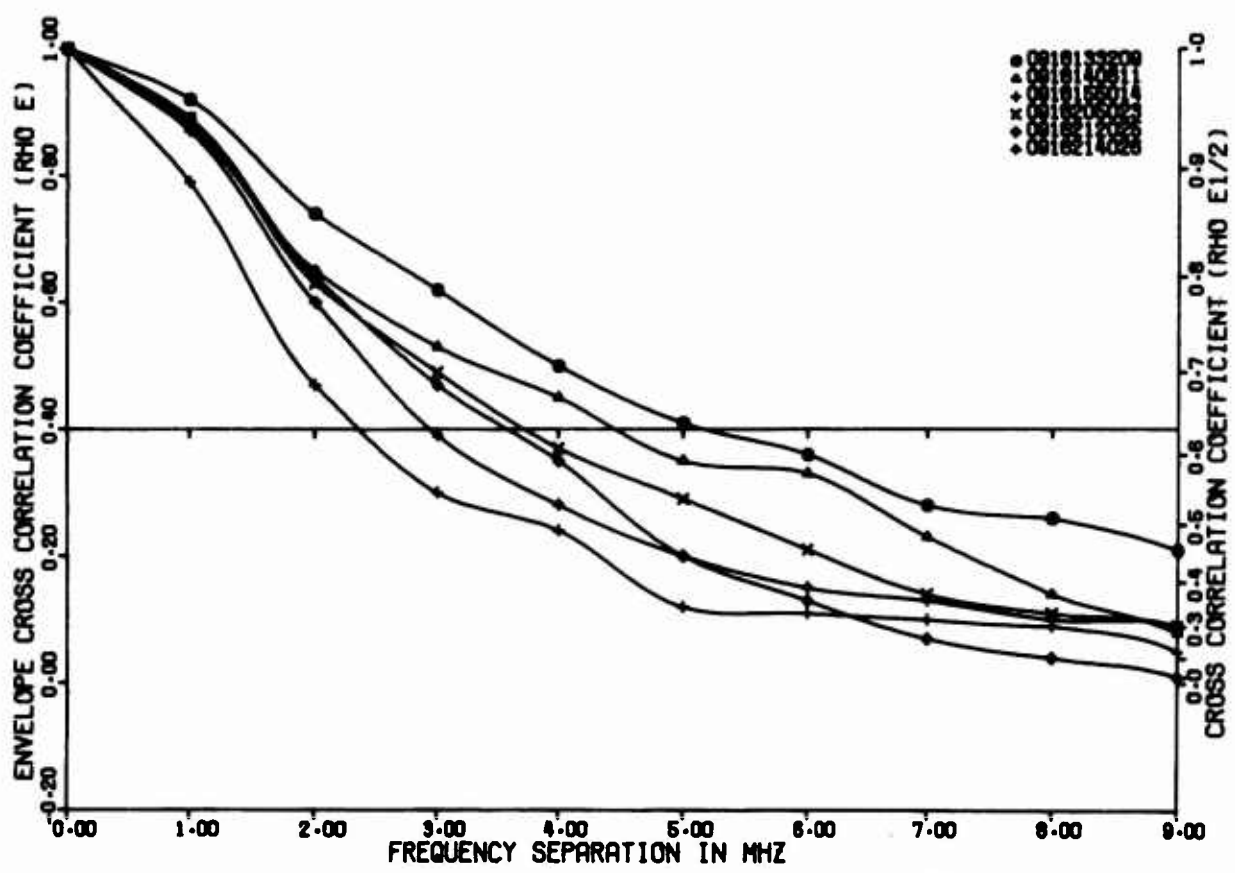


Figure 100. Envelope Cross Correlation Coefficients  
Point Petre, September; C-Band, Wide

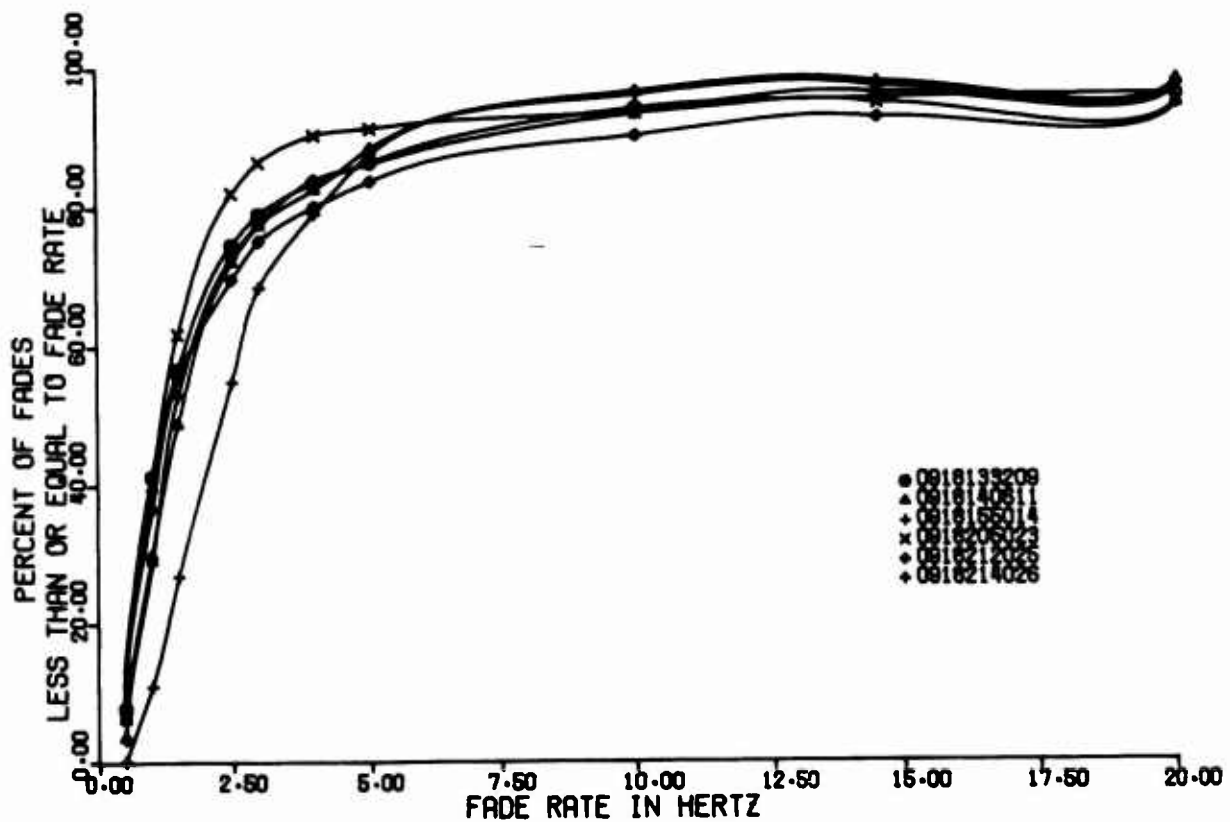


Figure 101. Fade Rate Distribution  
Point Petre, September; C-Band

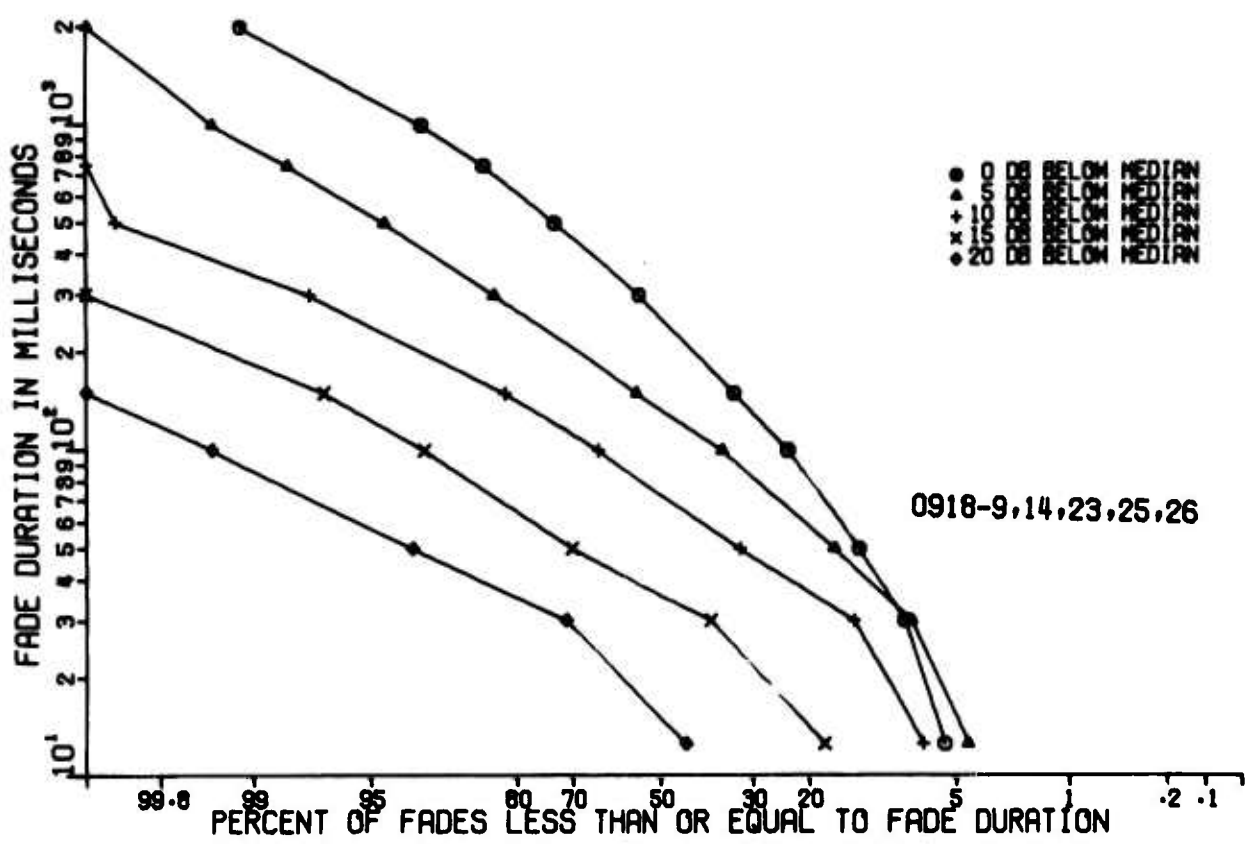


Figure 102. Distribution of Fade Duration  
Point Petre, September; C-Band

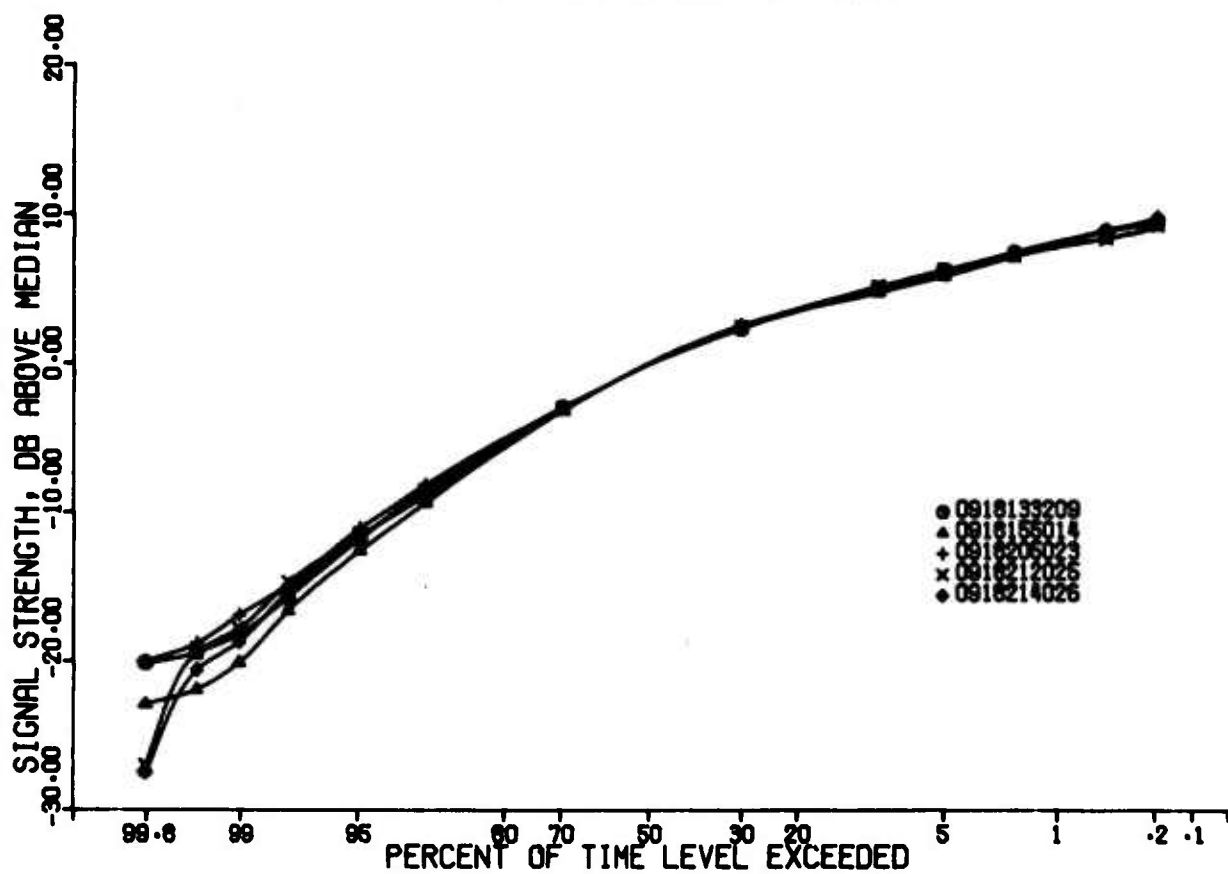


Figure 103. Signal Amplitude Level  
Point Petre, September; C-Band

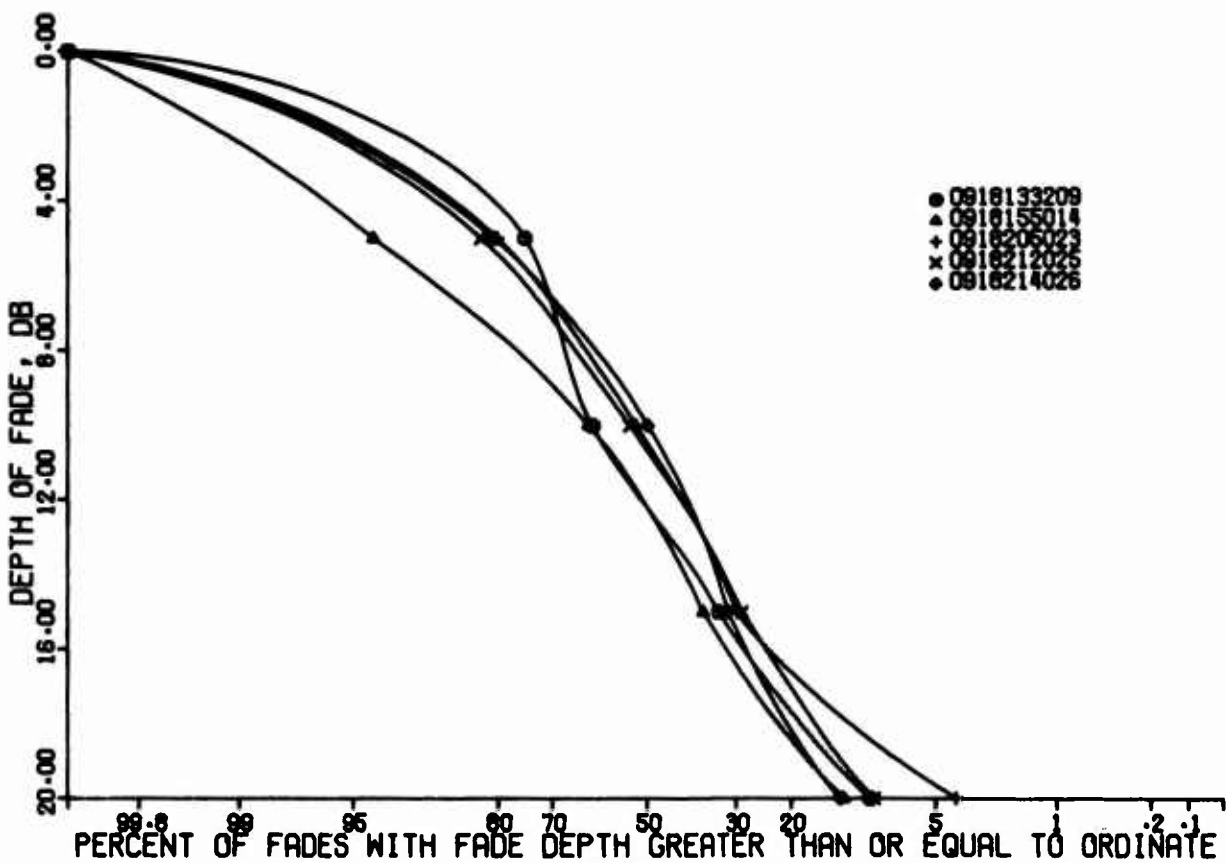


Figure 104. Distribution of Depth of Fades  
Point Petre, September; C-Band

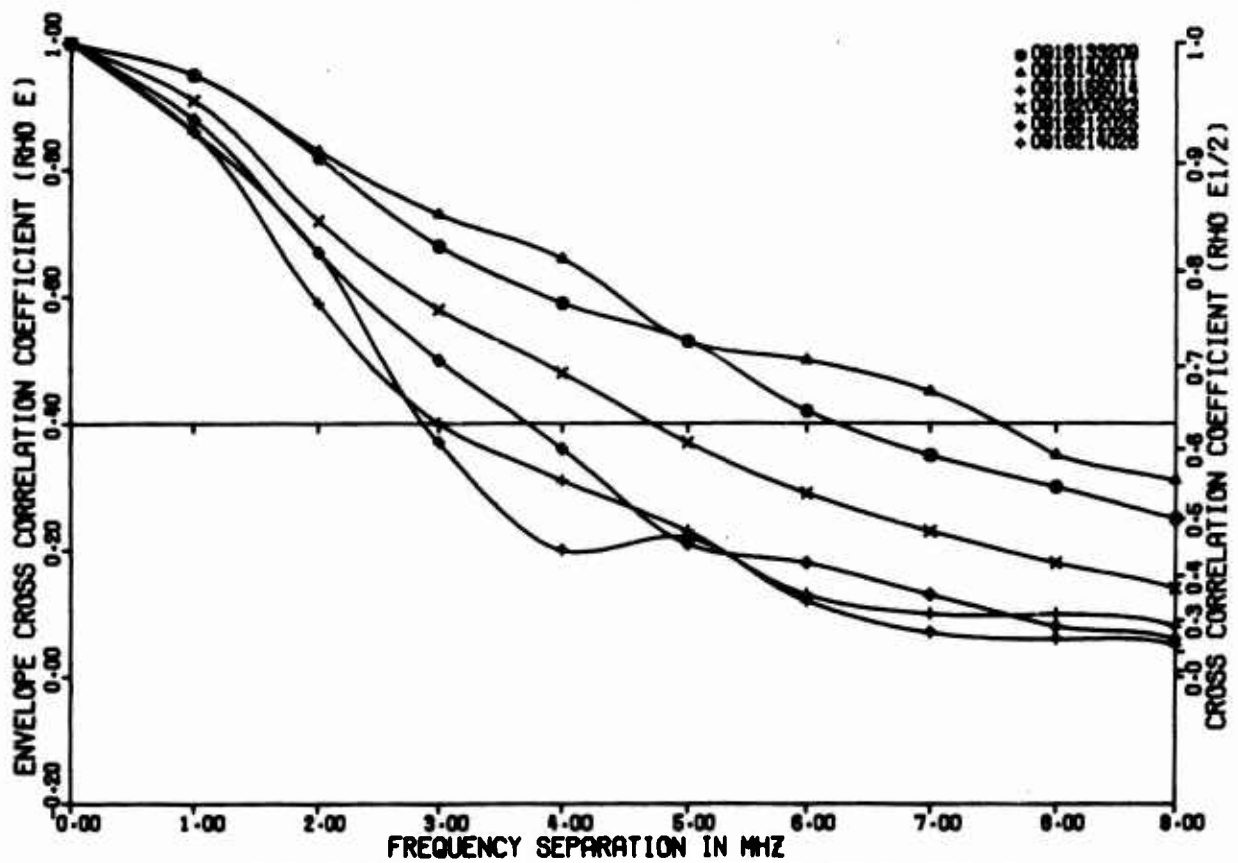


Figure 105. Envelope Cross Correlation Coefficients  
Point Petre, September; X-Band, Wide

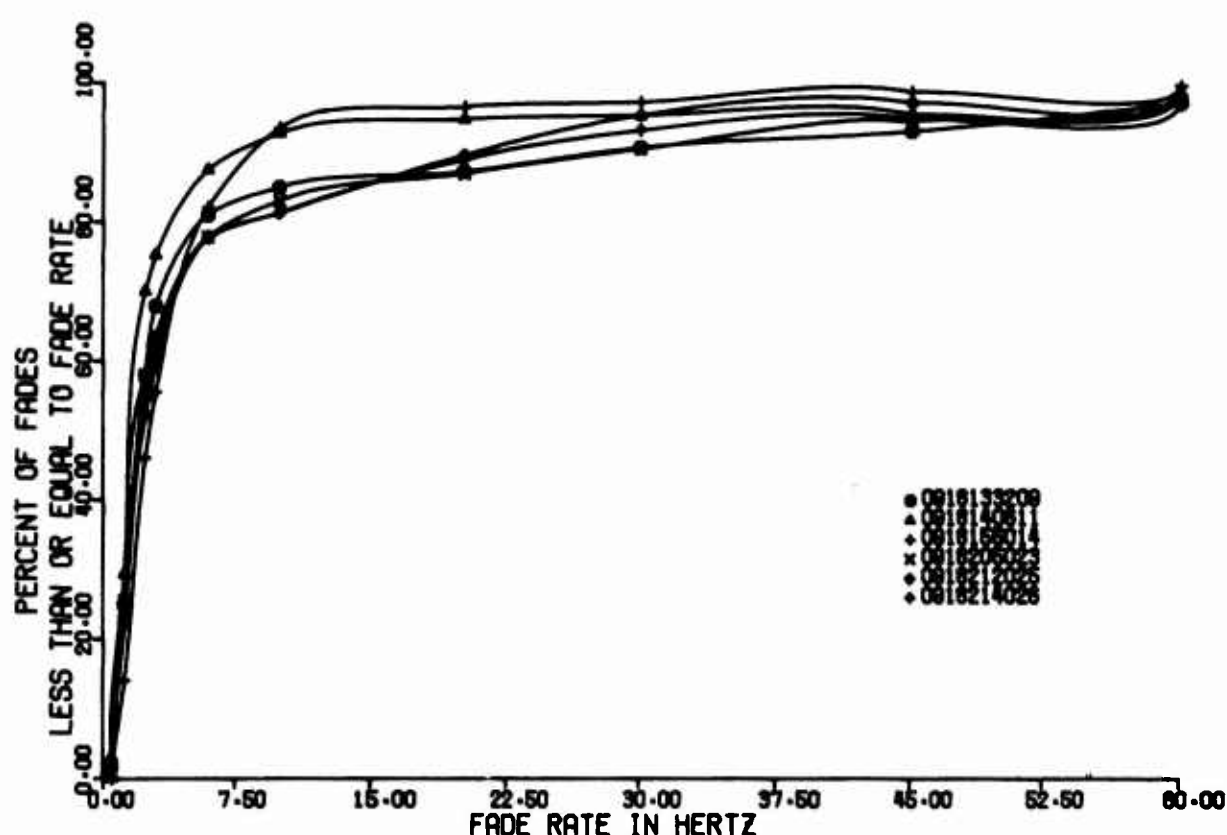


Figure 106. Fade Rate Distribution  
Point Petre, September; X-Band

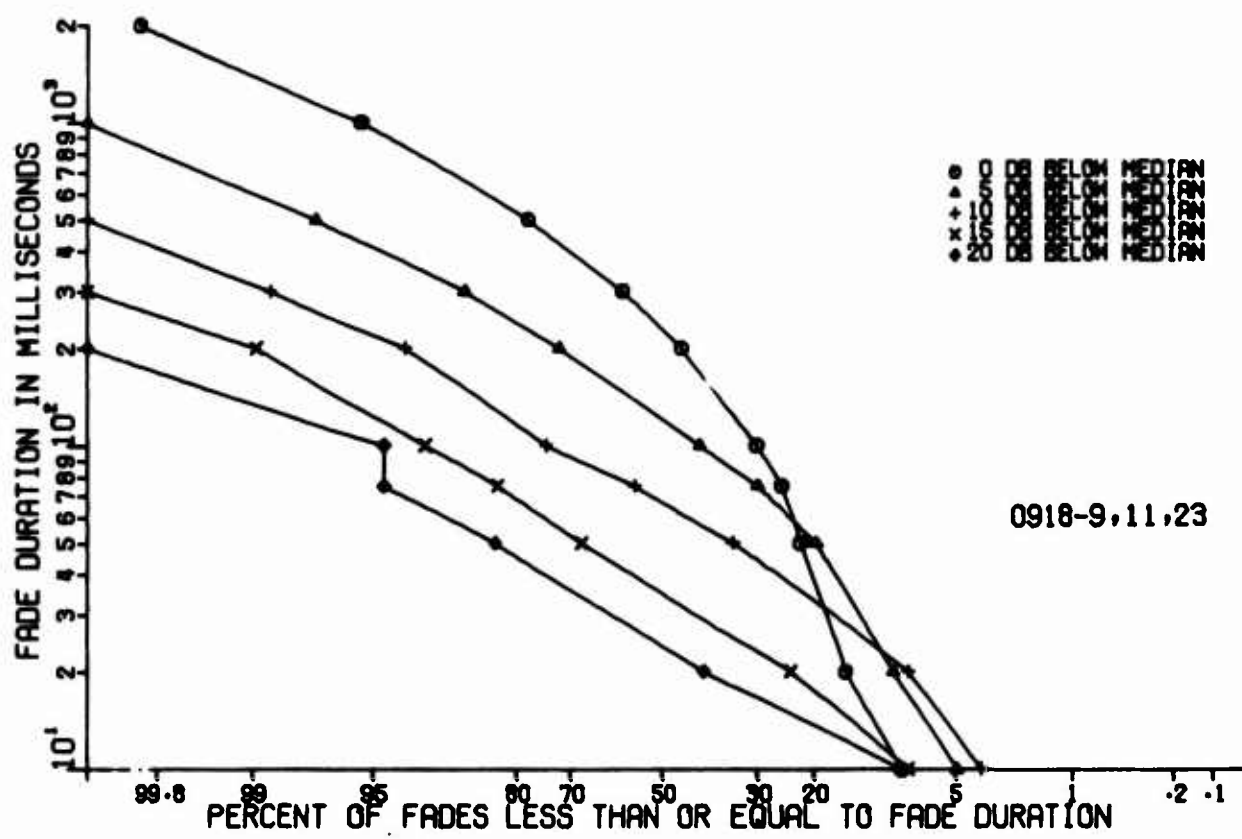


Figure 107. Distribution of Fade Duration  
Point Petre, September; X-Band

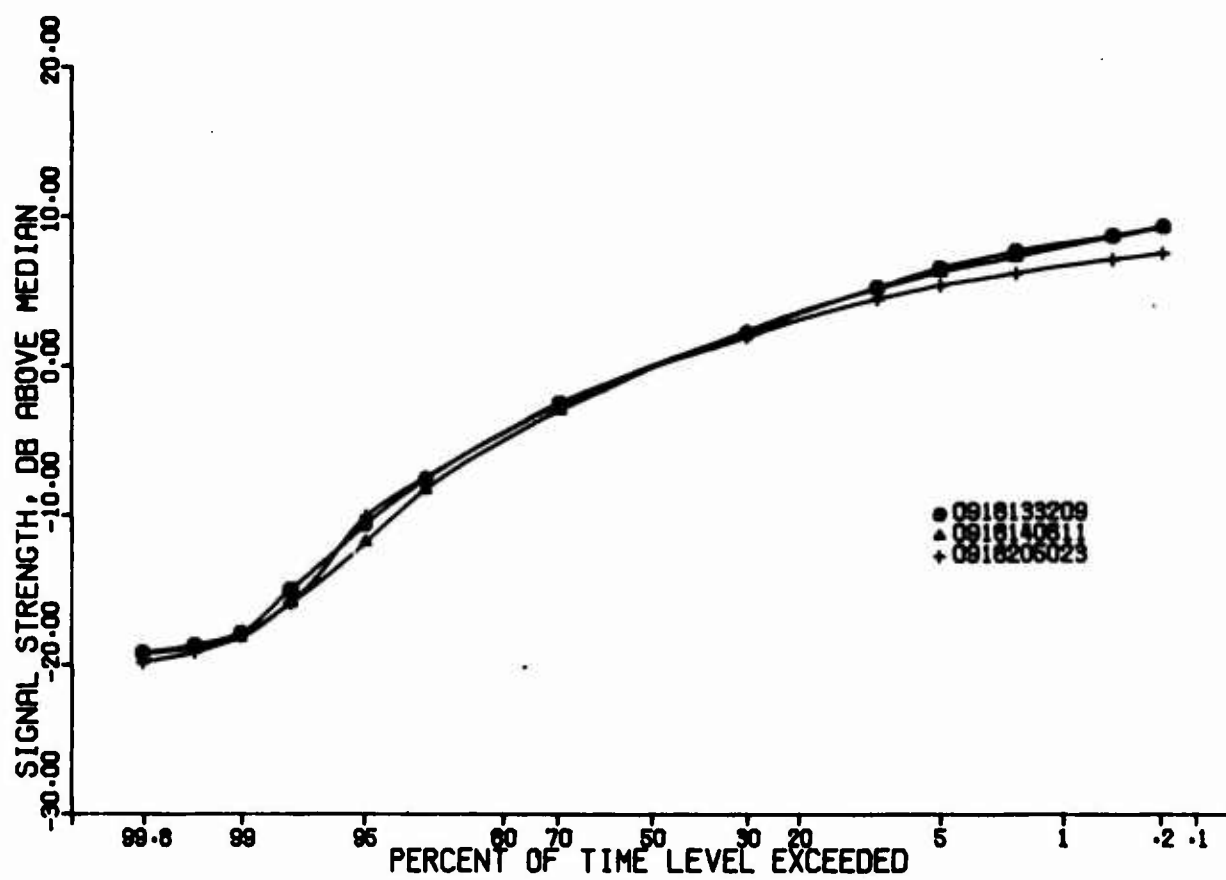


Figure 108. Signal Amplitude Level  
Point Petre, September; X-Band

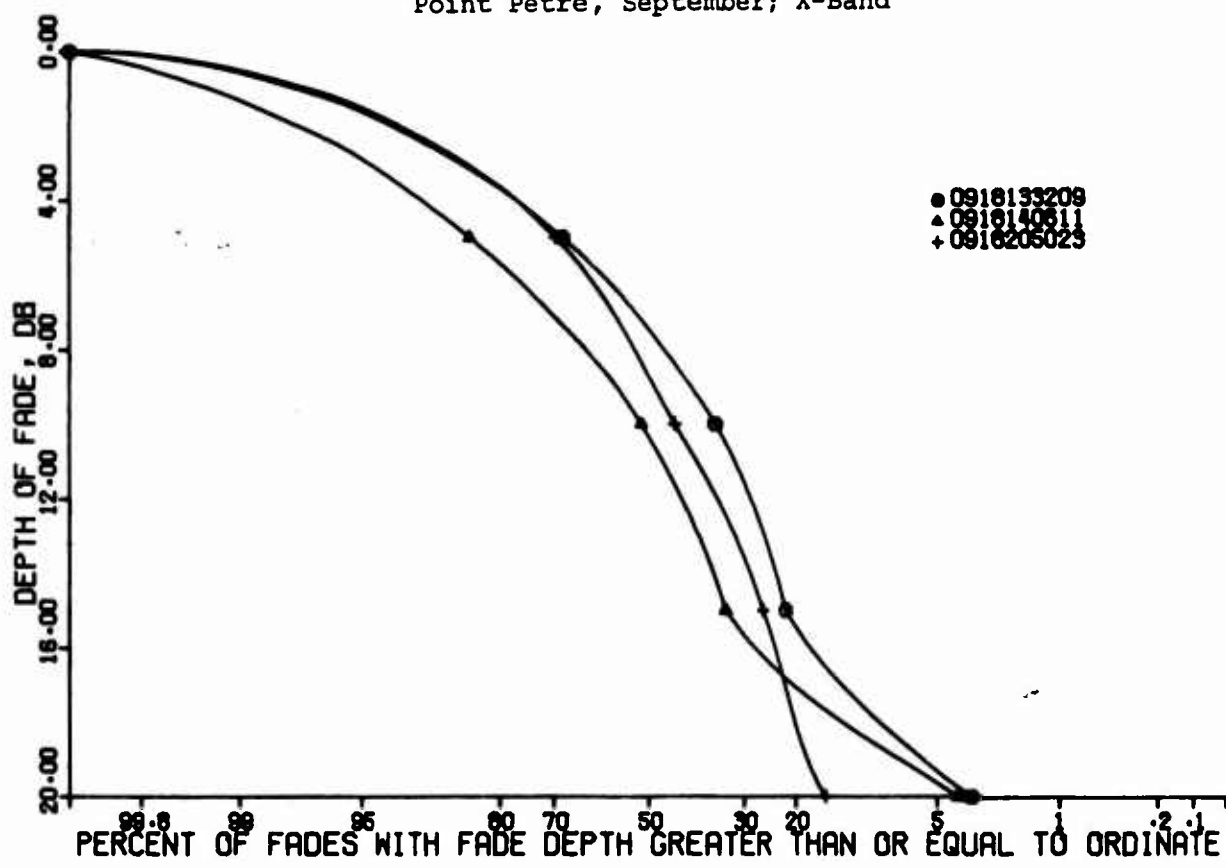


Figure 109. Distribution of Depth of Fades  
Point Petre, September; X-Band

## E. ANOMALIES IN PROPAGATION

The anomalous propagation is by its own definition due to phenomena which occur seldom and therefore merits only minor consideration in the design of modems for transmission through troposcatter. These unusual phenomena result in ducting with its usual associated high signal strength, unusually high fade rates, fluttering caused by aircraft, and unusual shapes in the correlation coefficient versus frequency curves. Some samples of each of these phenomena are included in the following paragraphs with some comments regarding the performance of frequency diversity modems during these anomalies.

### 1. Ducting

Ducting signals are identified by their relatively high signal strengths and often low depth of fades accompanied usually by a wide correlation bandwidth. However, the high signal strength is the only common denominator observed in all ducting situations identified during this test. Figures 110 through 113 show a case of X-band ducting at Ontario Center on 11 August. A cross correlation is shown to be very wide, but the fades on which the computation was made are very shallow and seldom more than 5 dB below the median. The fade rate is enormous with 10 percent of the fades greater than 60 Hz. In this situation the signal strengths were in the vicinity of -60 dBm. A short time later the C band was ducting with the results shown in Figures 114 through 117. Here the correlation bandwidth is narrow with some fades greater than 5 dB. The signal strength was about -66 dBm.

Ducting has little or no adverse effect on the frequency-time matrix type of modem that obtains diversity by the use of a number of frequencies because the diversity is not needed when the signal strength is high enough to provide sufficient fade margin to avoid digital errors. Adaptive frequency modems have no difficulty as long as their frequency commands to the receiver are properly decoded because it does not matter which frequency the modems operate on in high signal level as long as both transmitter and receiver are both on the same frequency. The occasional deep fade might cause an error in the decoding of a frequency command. The link would become broken until the time-out and start-up have been reinitiated.

Another case of ducting occurred at Point Petre where evidently the C band was experiencing a more classic case while X band was not fully ducting. Figures 118 through 122 show the C-band propagation and Figures 123 through 127 show the X band. The signal strength was -76 dBm for X band and -66 dBm for C band. The C-band ducting had the wide correlation bandwidth, very high fade rates with mostly shallow fades of which 80 percent were less than 4 dB. The unexpected phenomenon is that the X band was not strictly ducting. True, it had a wide correlation bandwidth most of the time, but the fade rates were within typical bounds and so were the signal amplitude, fade duration, and depth distributions. In this type of environment the frequency-time modem would operate with some diversity gain because the correlation coefficient dropped to about 0.8 in 2 MHz which is known to yield most of the diversity improvement (Reference 2). The adaptive frequency modem should operate in this environment reasonably well, subject of course to the occasional breaking of the link due to erroneous frequency change commands.

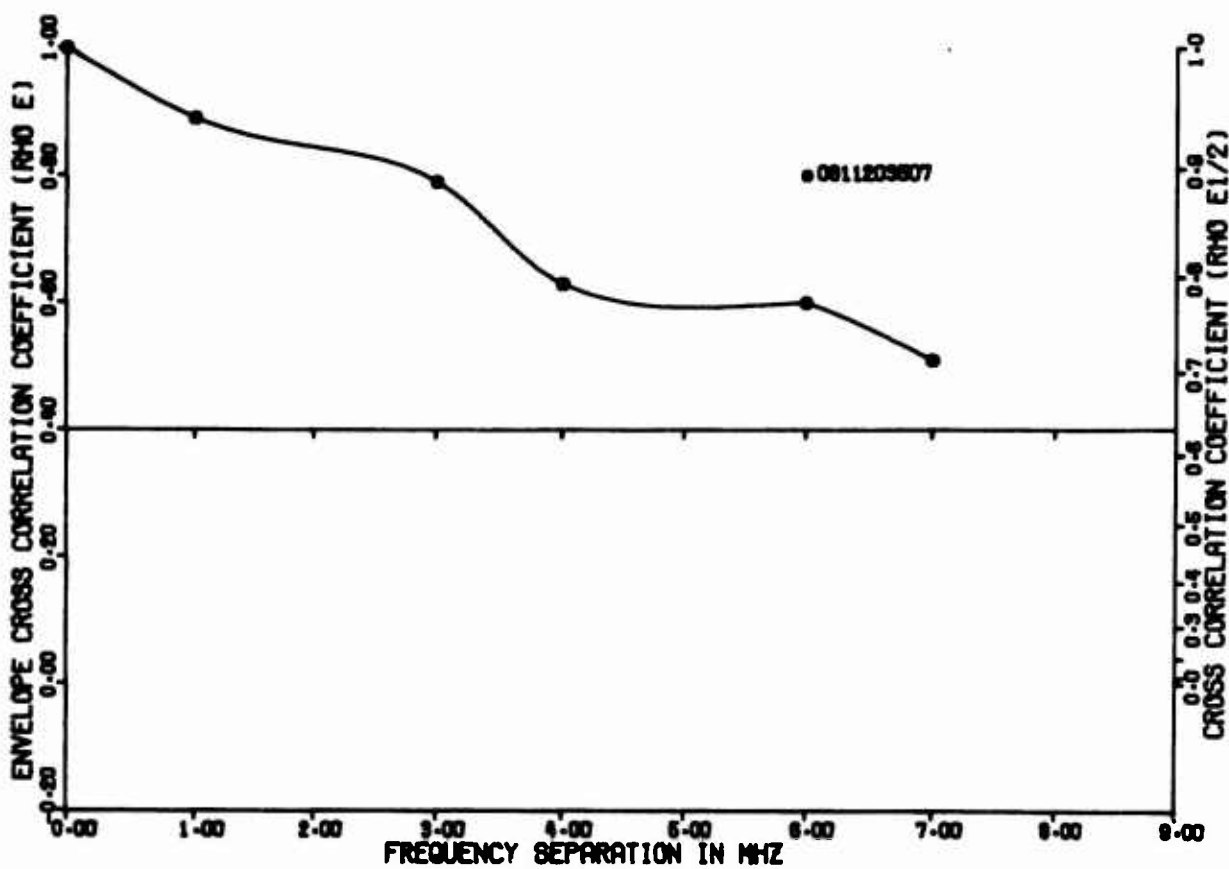


Figure 110. Envelope Cross Correlation Coefficients  
Ontario Center, Summer; X-Band, Wide, Ducting

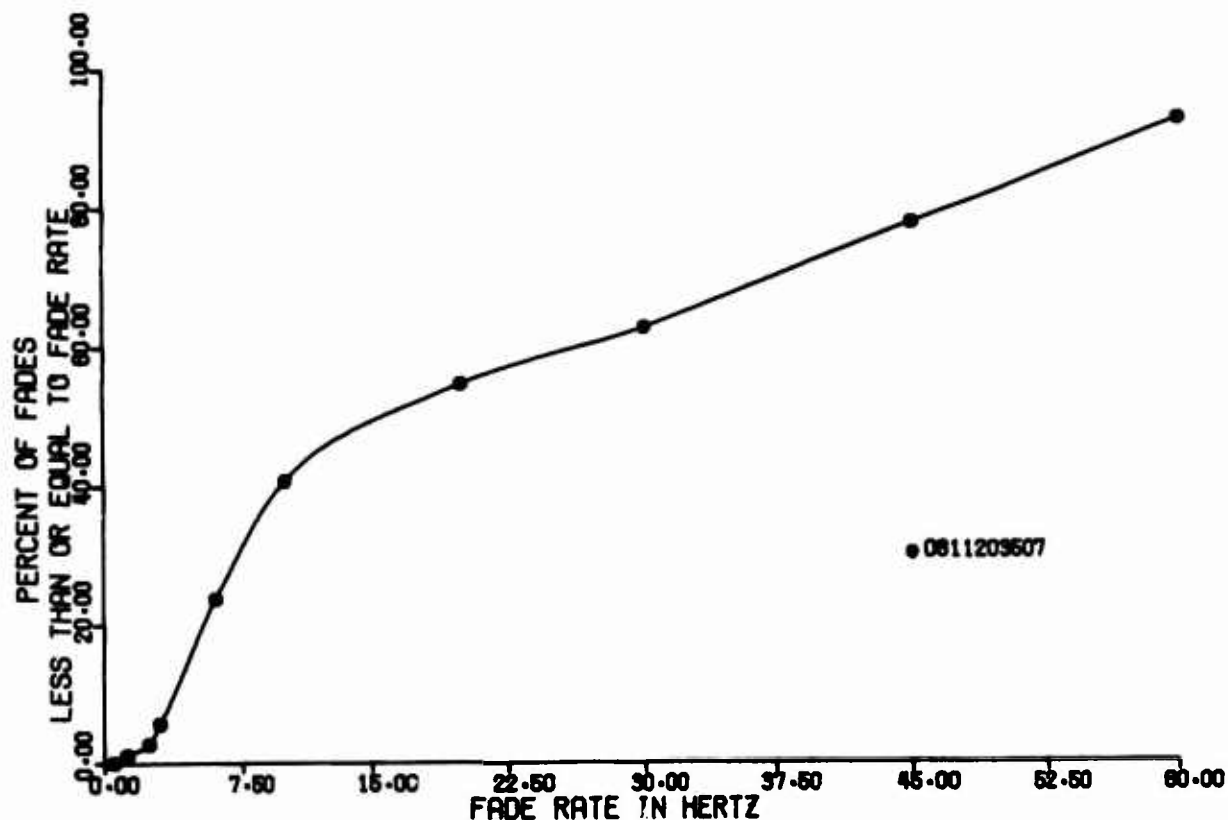


Figure 111. Fade Rate Distribution  
Ontario Center, Summer; X-band, Ducting

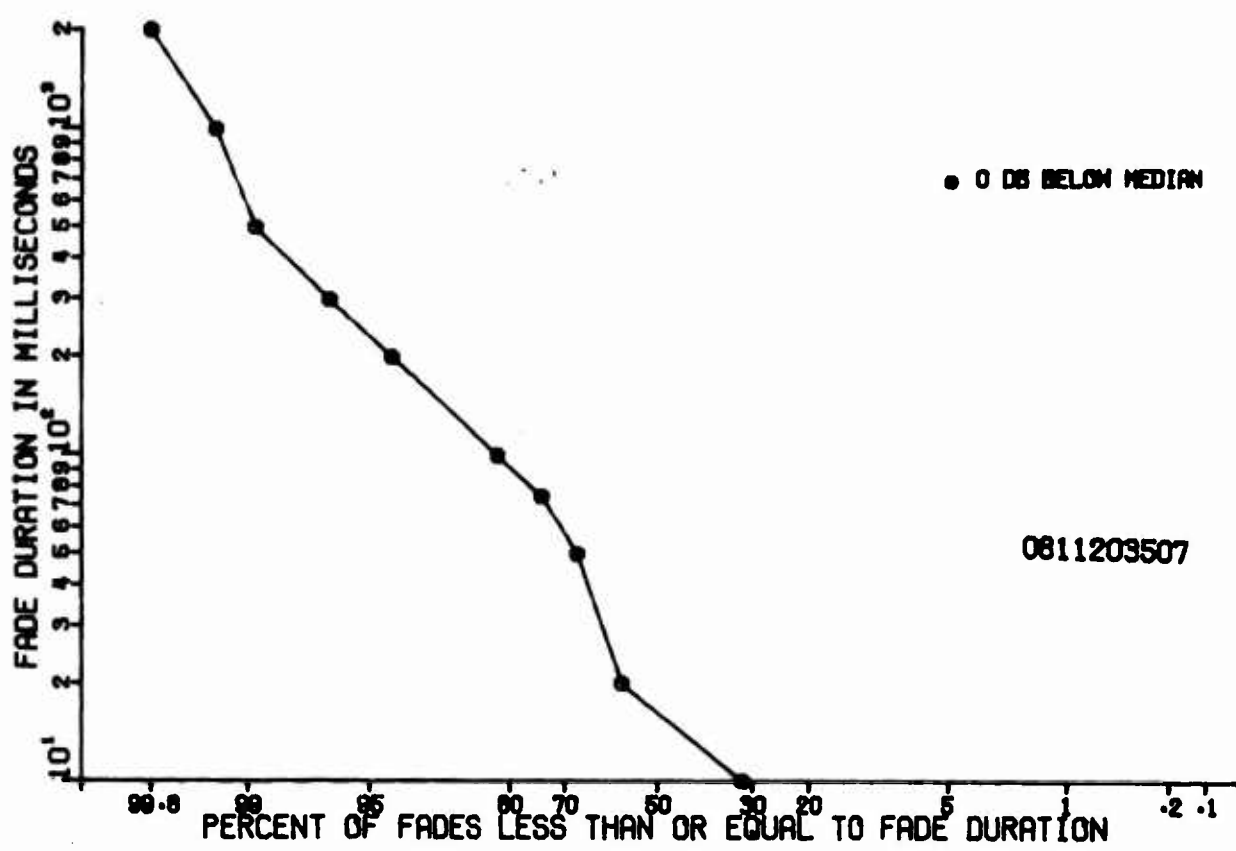


Figure 112. Distribution of Fade Duration  
Ontario Center, Summer; X-Band, Ducting

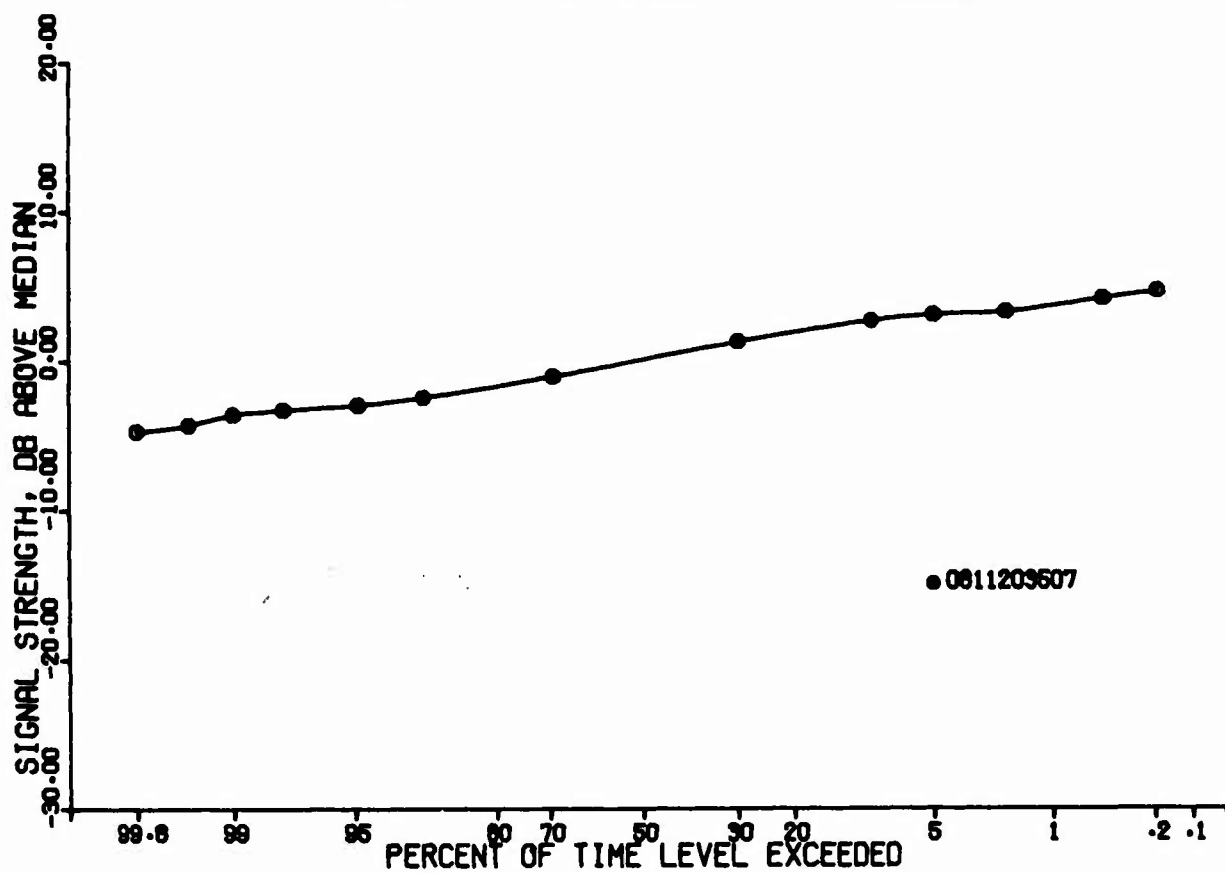


Figure 113. Signal Amplitude Level  
Ontario Center, Summer; X-Band, Ducting

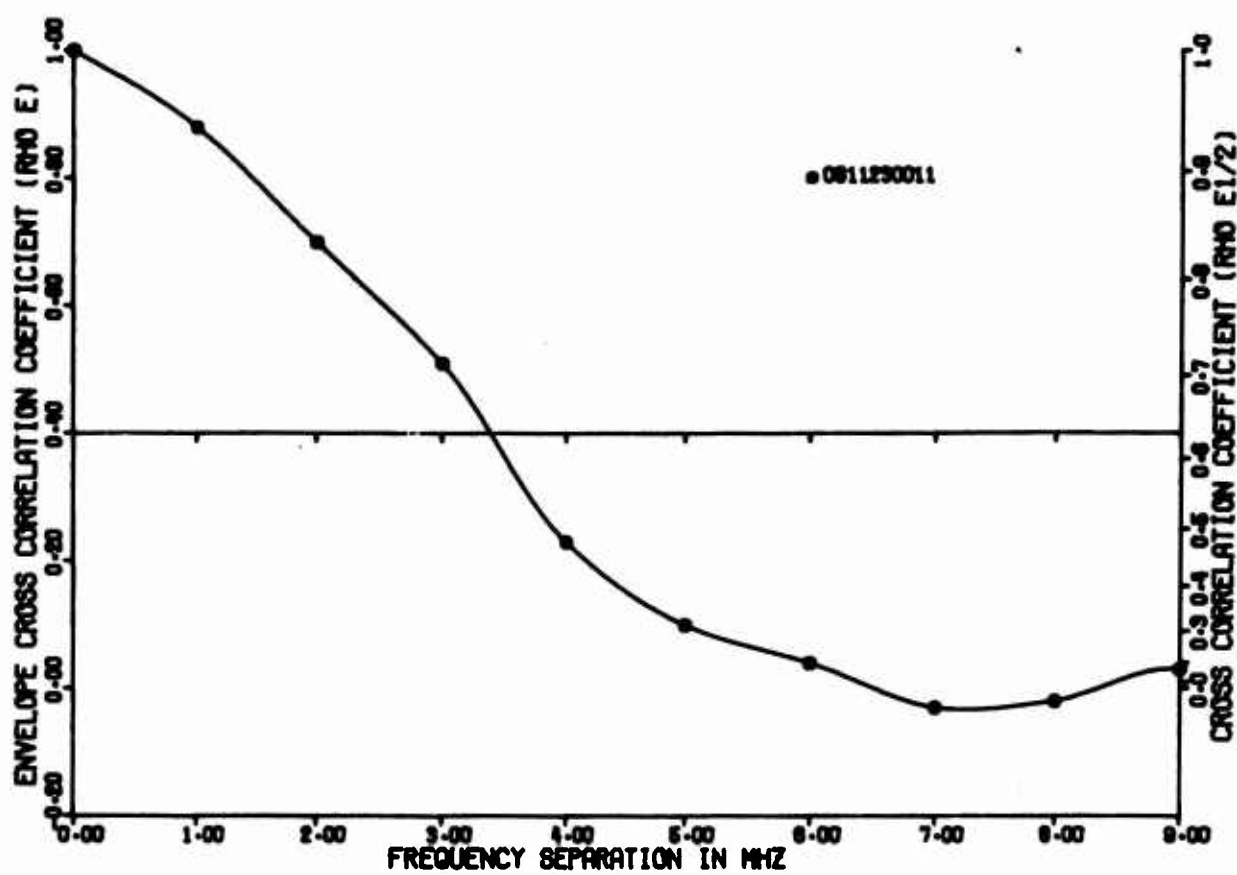


Figure 114. Envelope Cross Correlation Coefficients  
Ontario Center, Summer; C-Band, Wide, Ducting

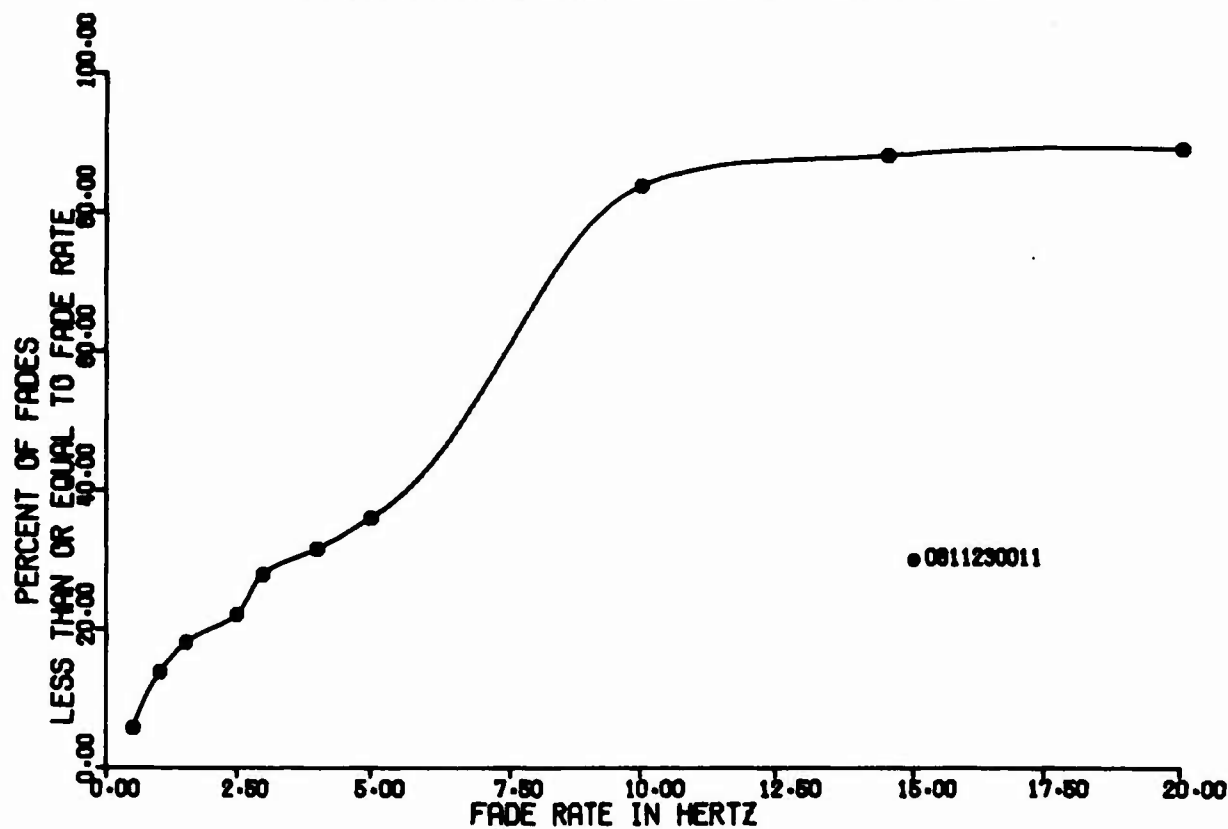


Figure 115. Fade Rate Distribution  
Ontario Center, Summer; C-Band, Ducting

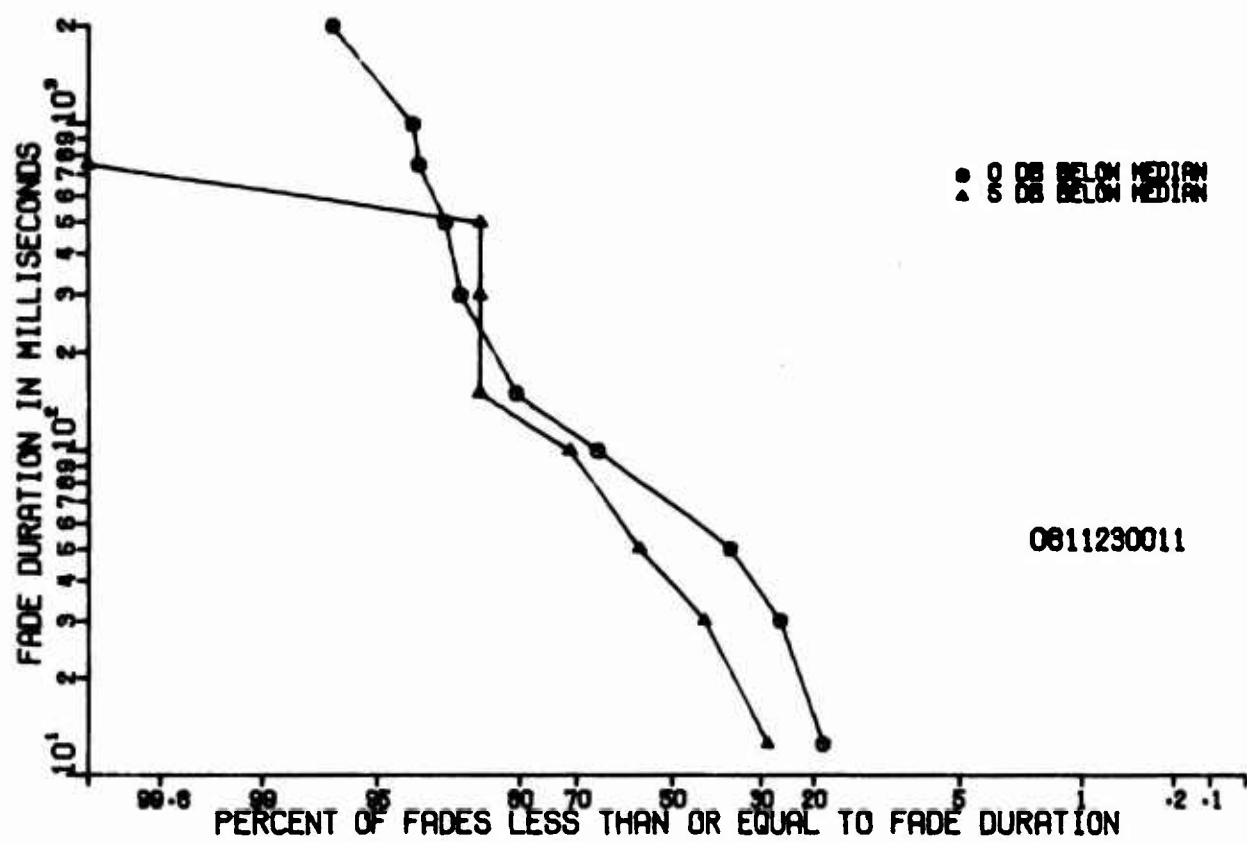


Figure 116. Distribution of Fade Duration  
Ontario Center, Summer; C-Band, Ducting

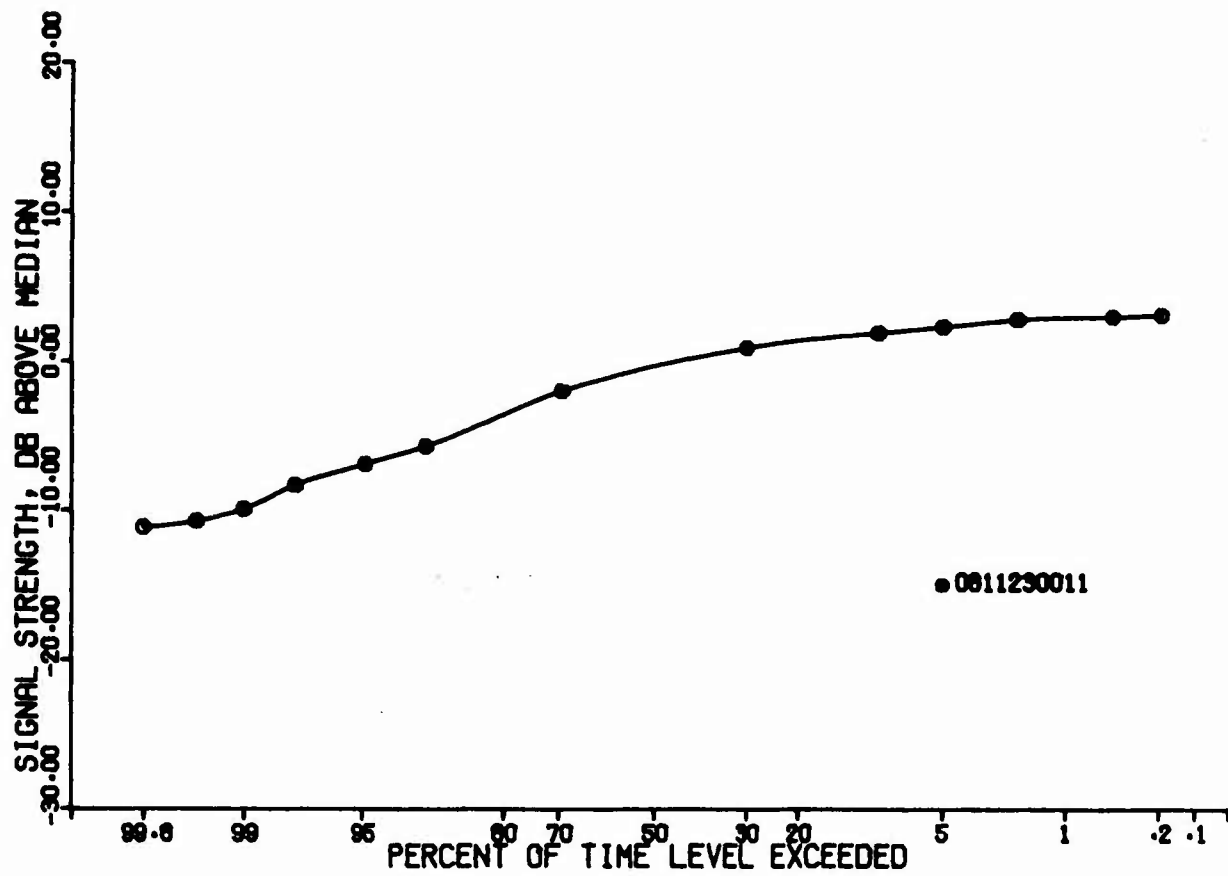


Figure 117. Signal Amplitude Level  
Ontario Center, Summer; C-Band, Ducting

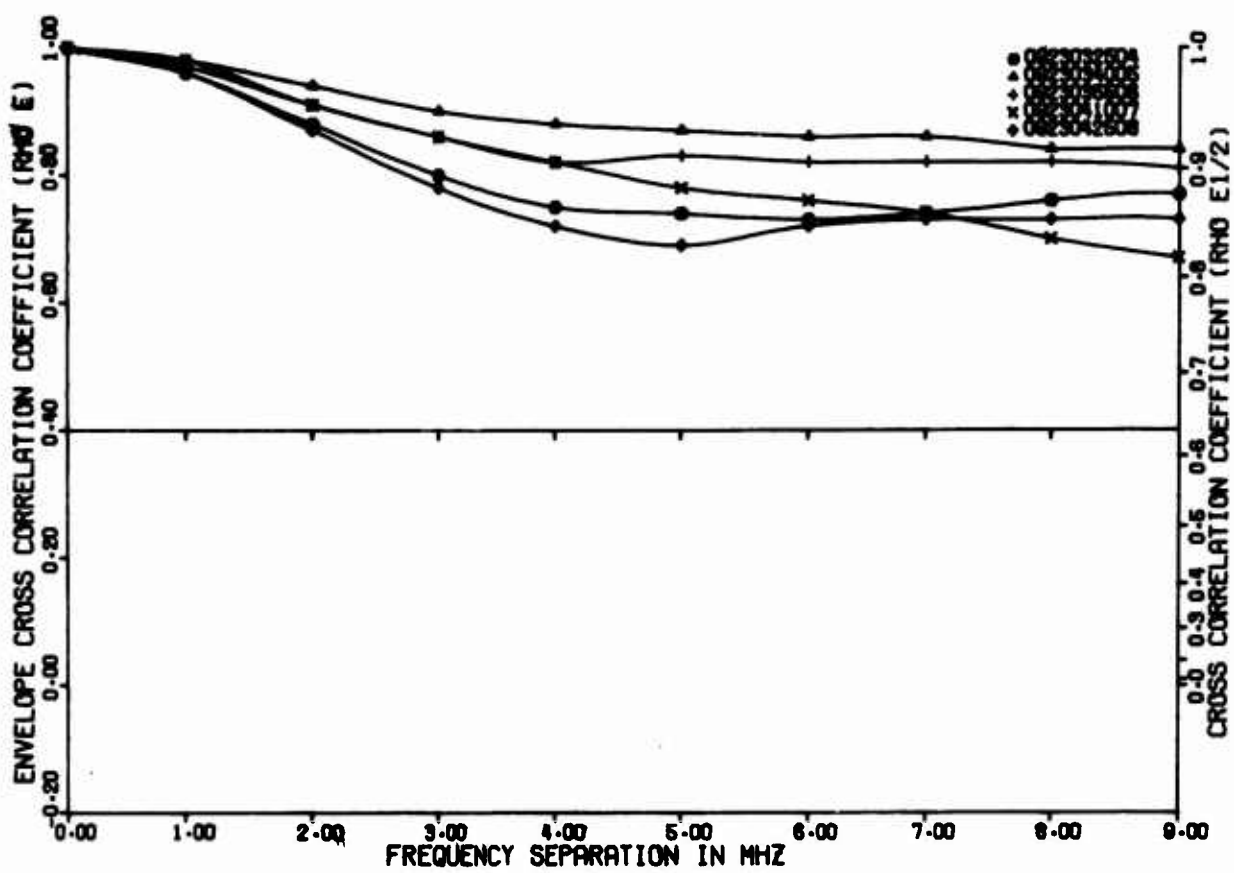


Figure 118. Envelope Cross Correlation Coefficients  
Point Petre, September; C-Band, Wide

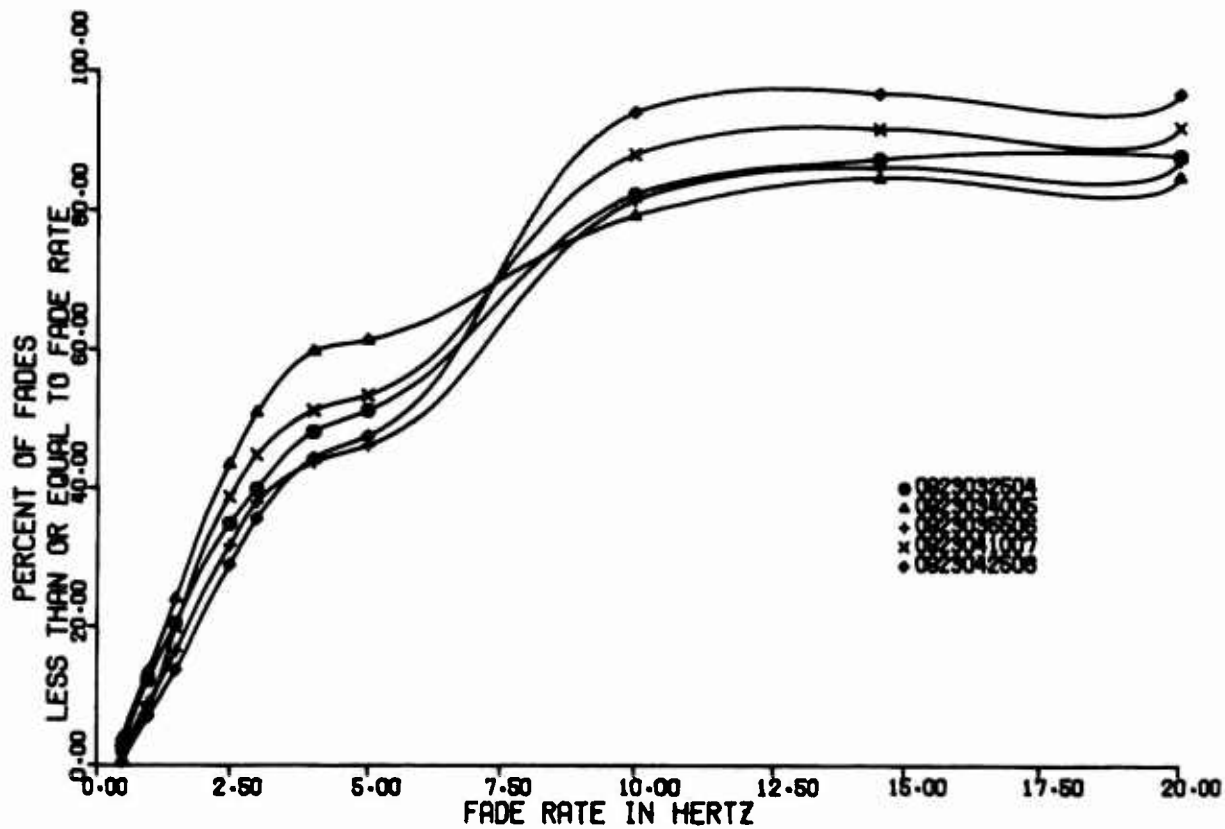


Figure 119. Fade Rate Distribution  
Point Petre, September; C-Band

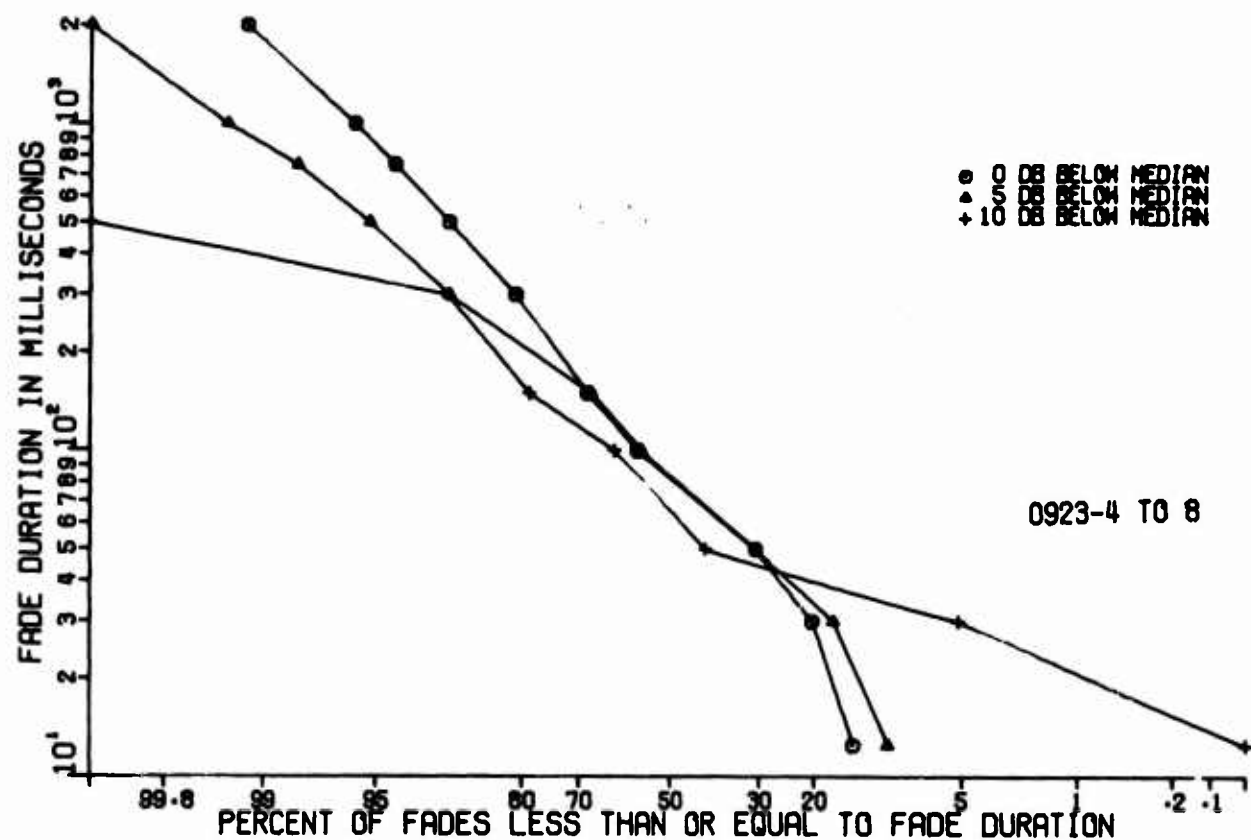


Figure 120. Distribution of Fade Duration  
Point Petre, September; C-Band

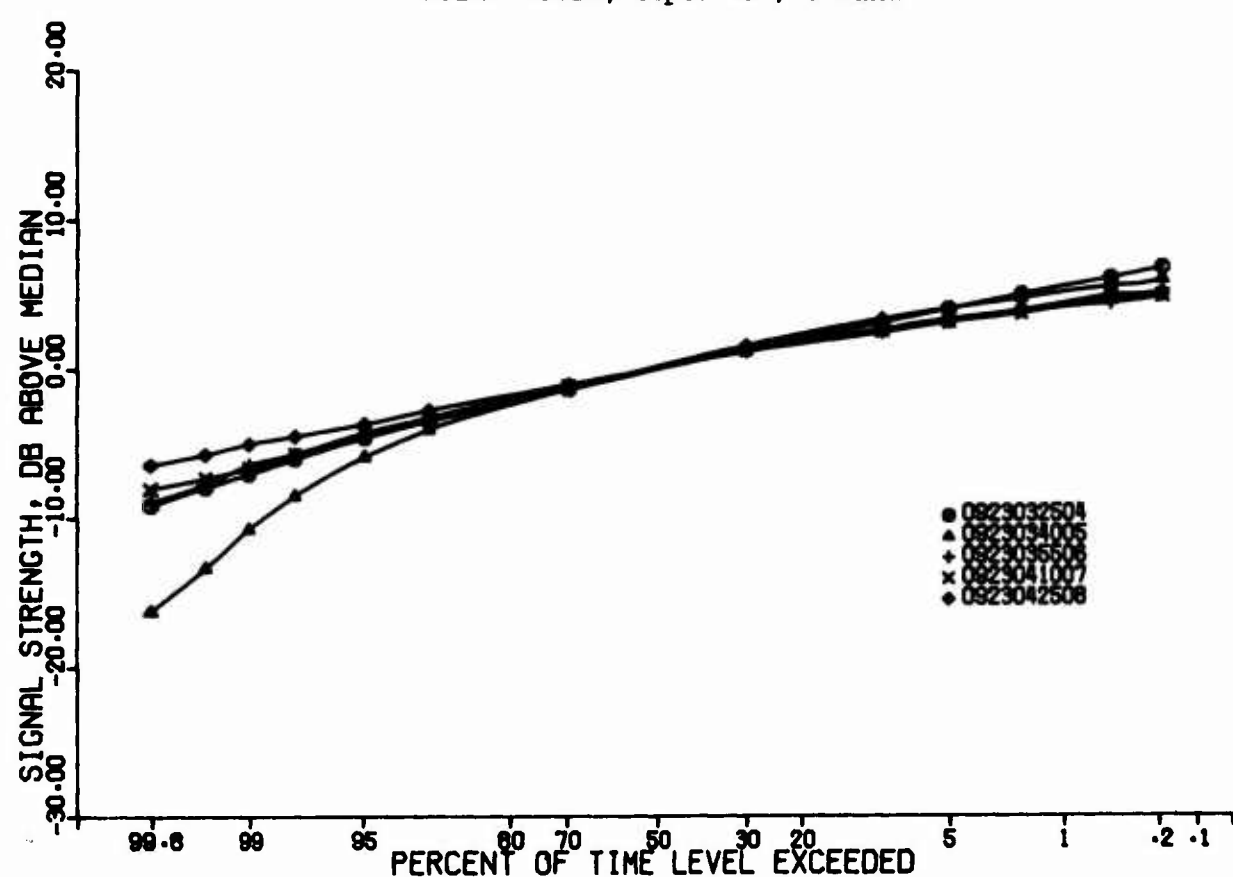


Figure 121. Signal Amplitude Level  
Point Petre, September; C-Band

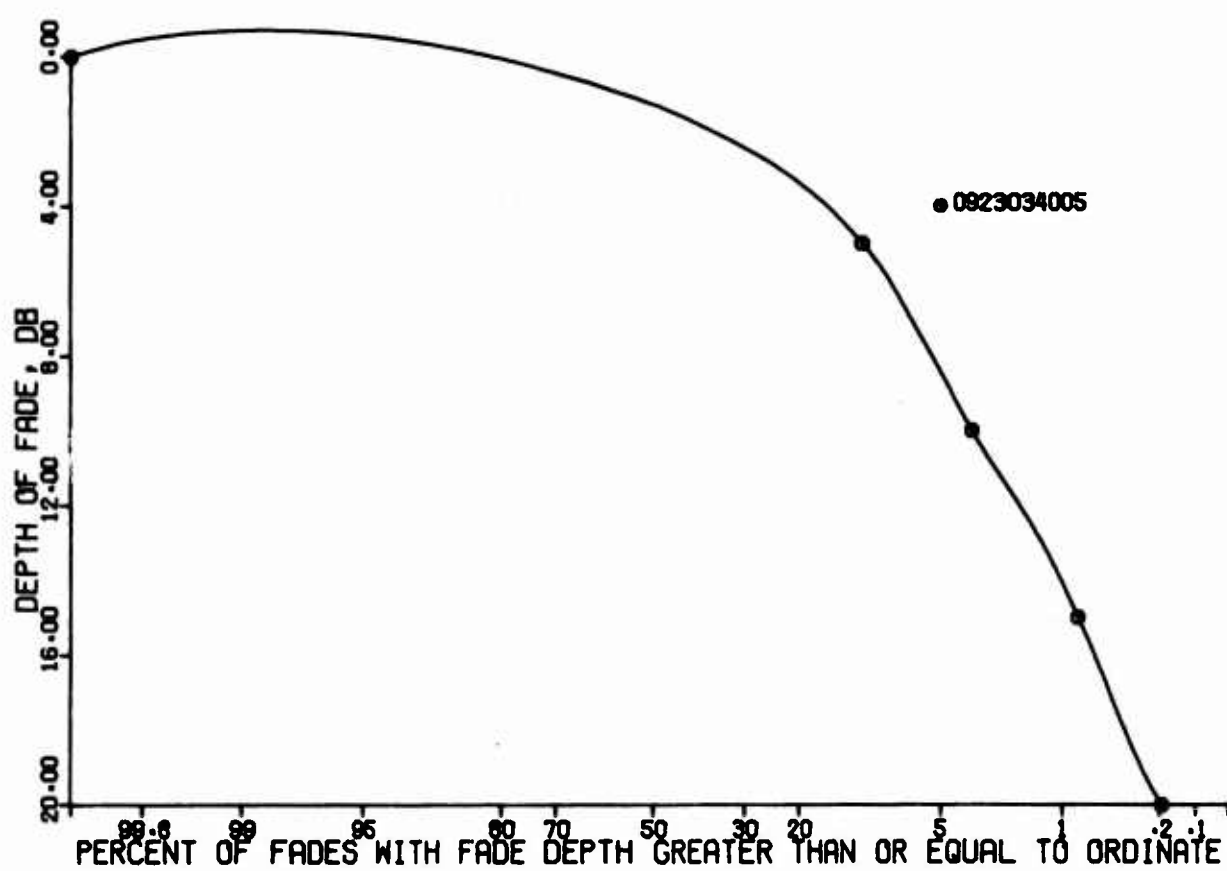


Figure 122. Distribution of Depth of Fades  
Point Petre, September; C-Band

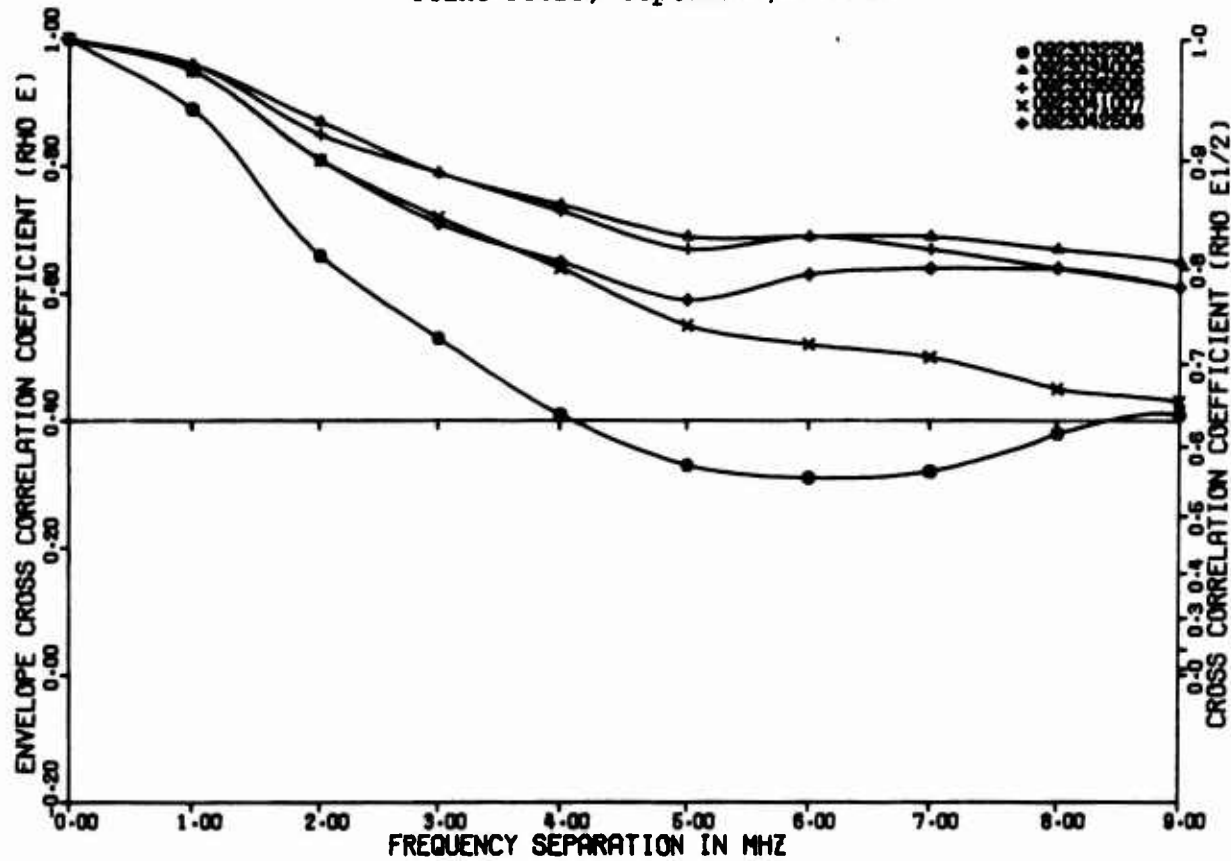


Figure 123. Envelope Cross Correlation Coefficients  
Point Petre, September; X-Band, Wide

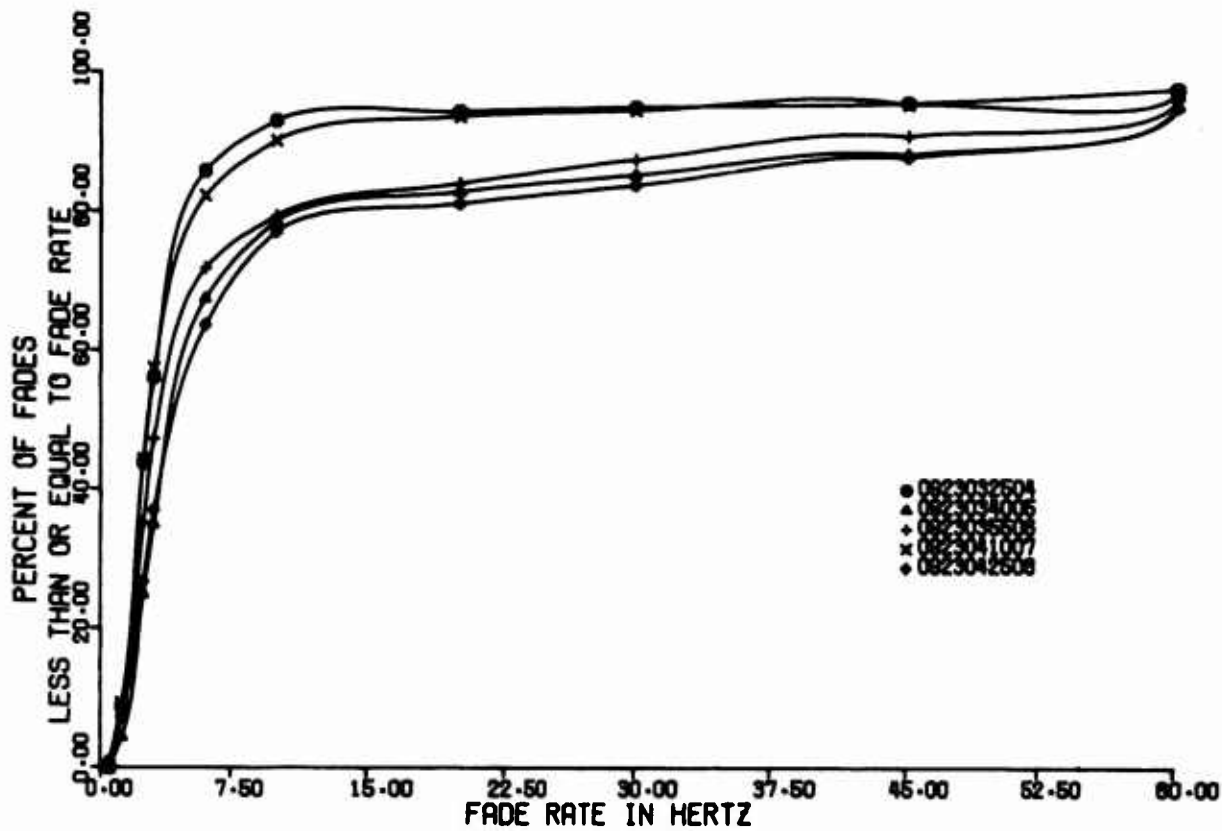


Figure 124. Fade Rate Distribution  
Point Petre, September; X-Band

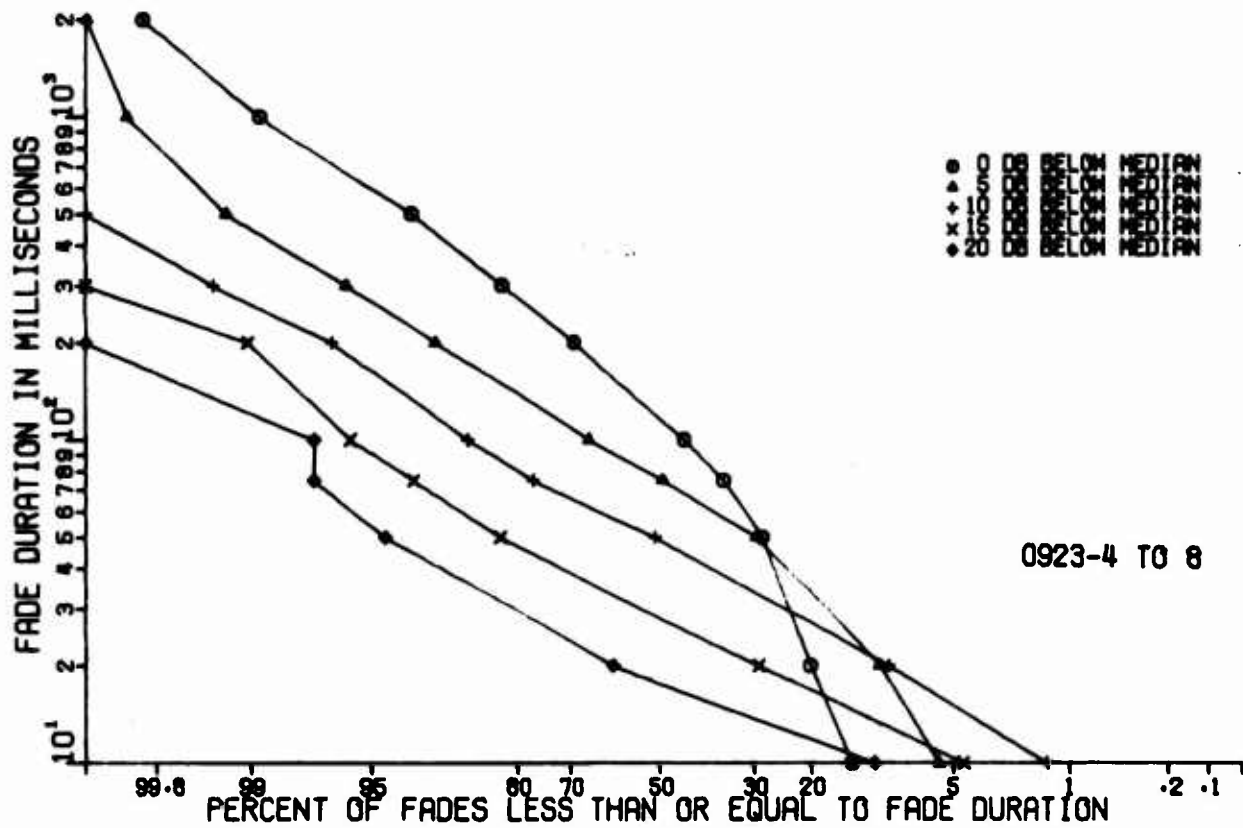


Figure 125. Distribution of Fade Duration  
Point Petre, September; X-Band

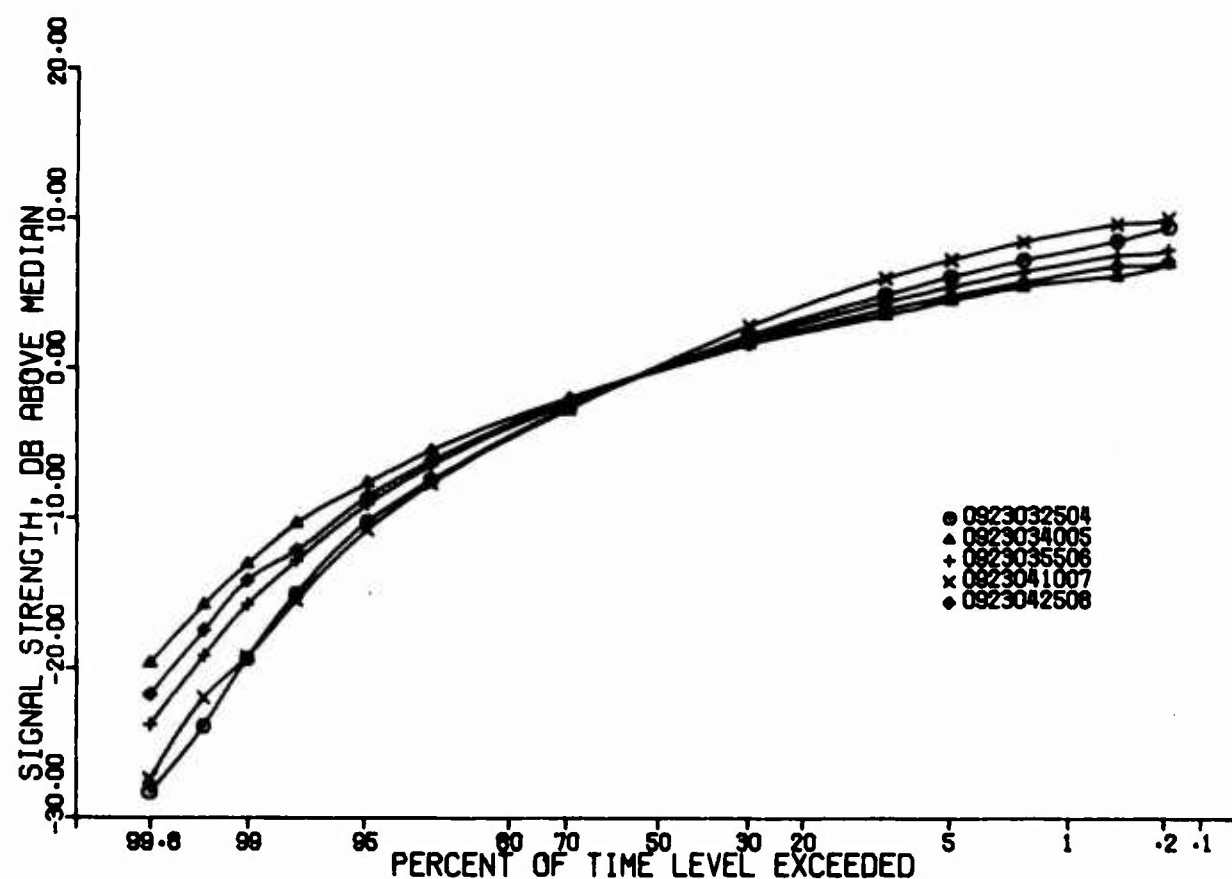


Figure 126. Signal Amplitude Level  
Point Petre, September; X-Band

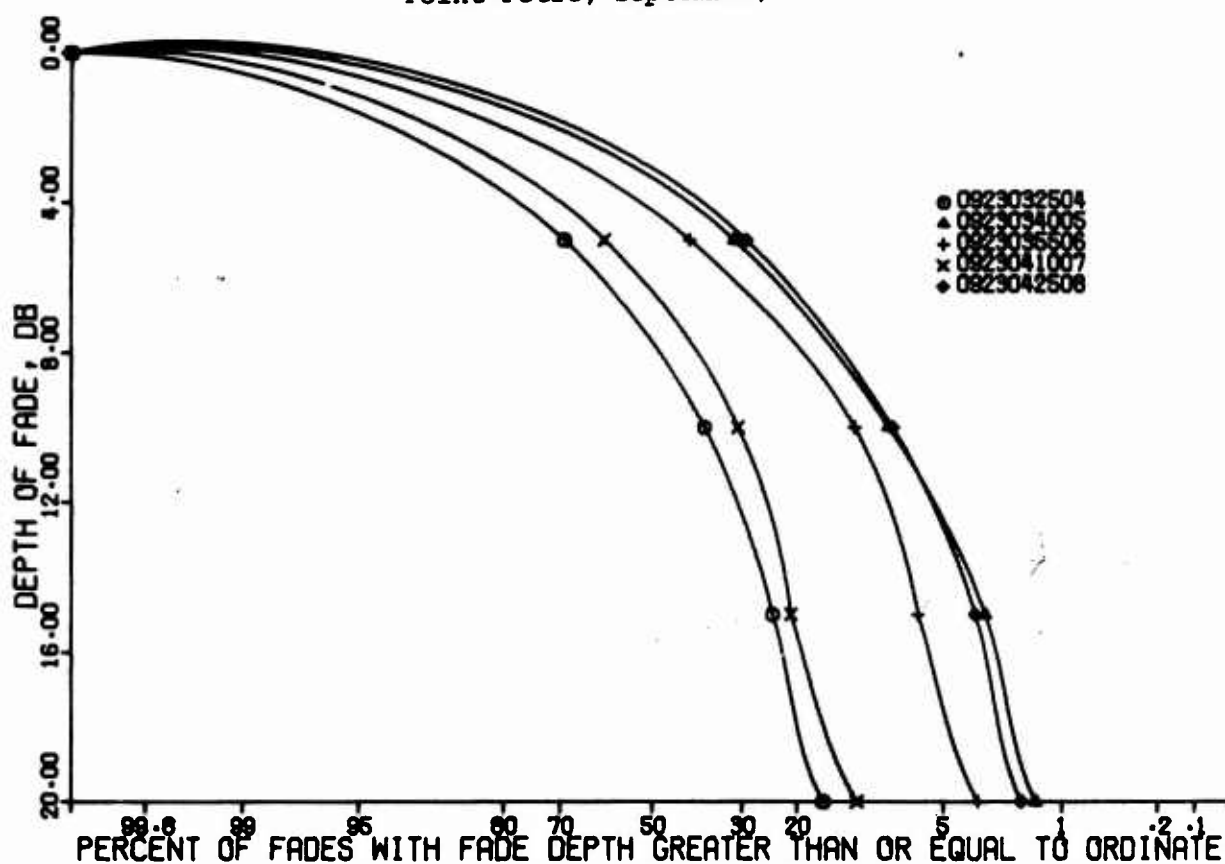


Figure 127. Distribution of Depth of Fades  
Point Petre, September; X-Band

## 2. Aircraft Effects

Aircraft effects should not be called an anomalous condition because it is a condition often present in both military and civilian environments. The presence of the aircraft for a short interval has very little effect on a statistical test of relatively long time duration. In fact, its effect is only noticeable for the short period that the aircraft is directly in the beam. Figures 128 and 129 show the presence of the aircraft by the rise in correlation coefficient, but has little effect on the overall test. The fade rates shown in Figures 130 and 131 are averaged over the entire test number 15 and 13 to indicate that the effect is noticeable over the entire test, but during the time that the aircraft were actually present in the beam the fade rates were much higher than shown on the curves.

The frequency-time modems can operate through this type of environment. The adaptive frequency modems were found to have difficulty due to the high fade rates in Reference 2.

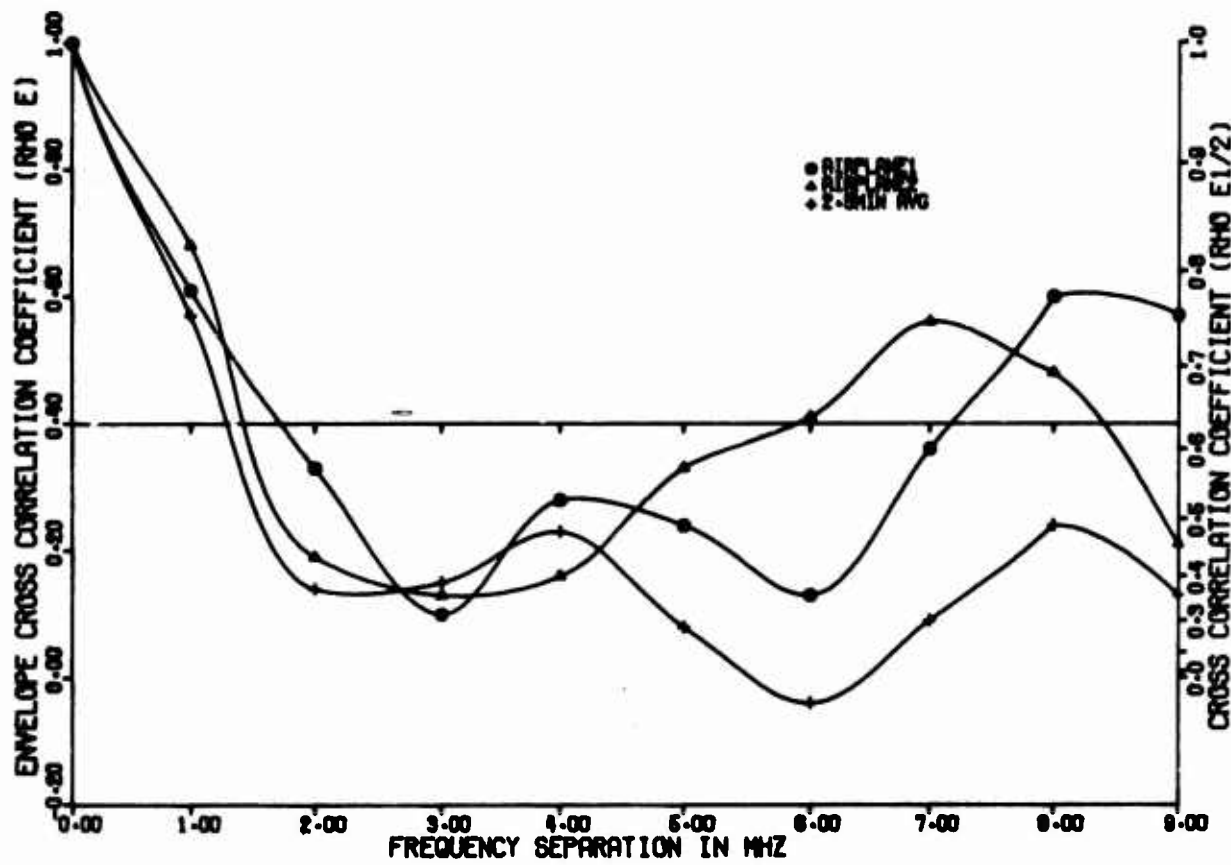


Figure 128. Envelope Cross Correlation Coefficients  
Ontario Center, Summer; X-Band, Wide; Airplane Effect 1

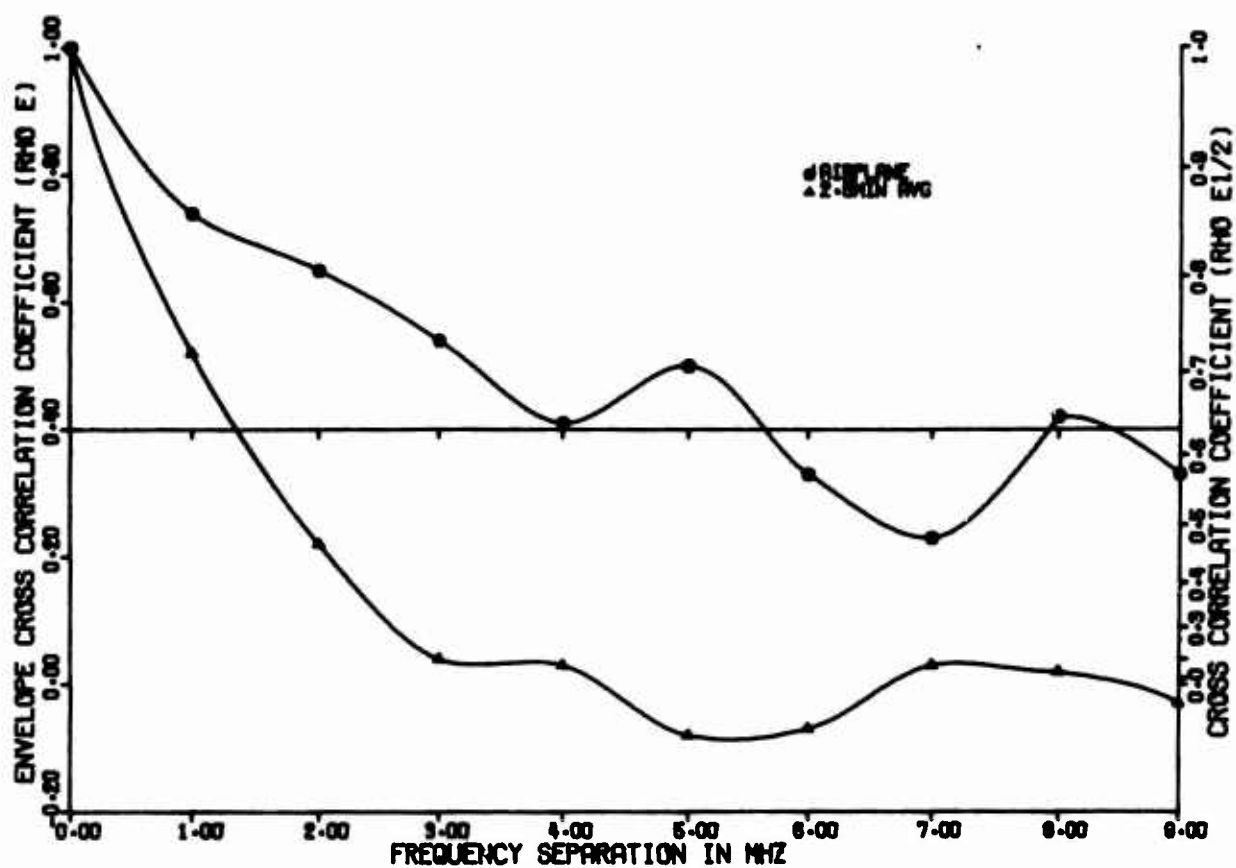


Figure 129. Envelope Cross Correlation Coefficients  
Ontario Center, Summer; X-Band, Wide; Airplane Effect 2

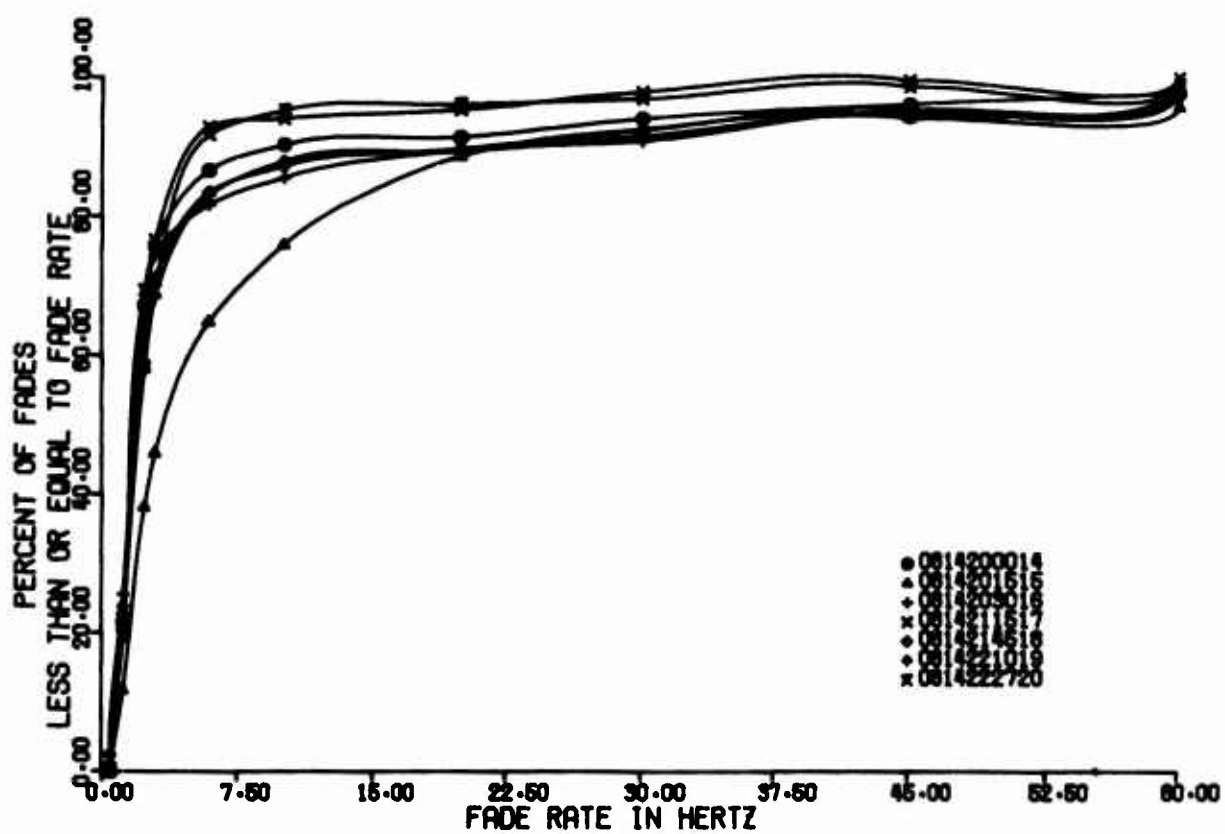


Figure 130. Fade Rate Distribution  
Ontario Center, Summer; X-Band

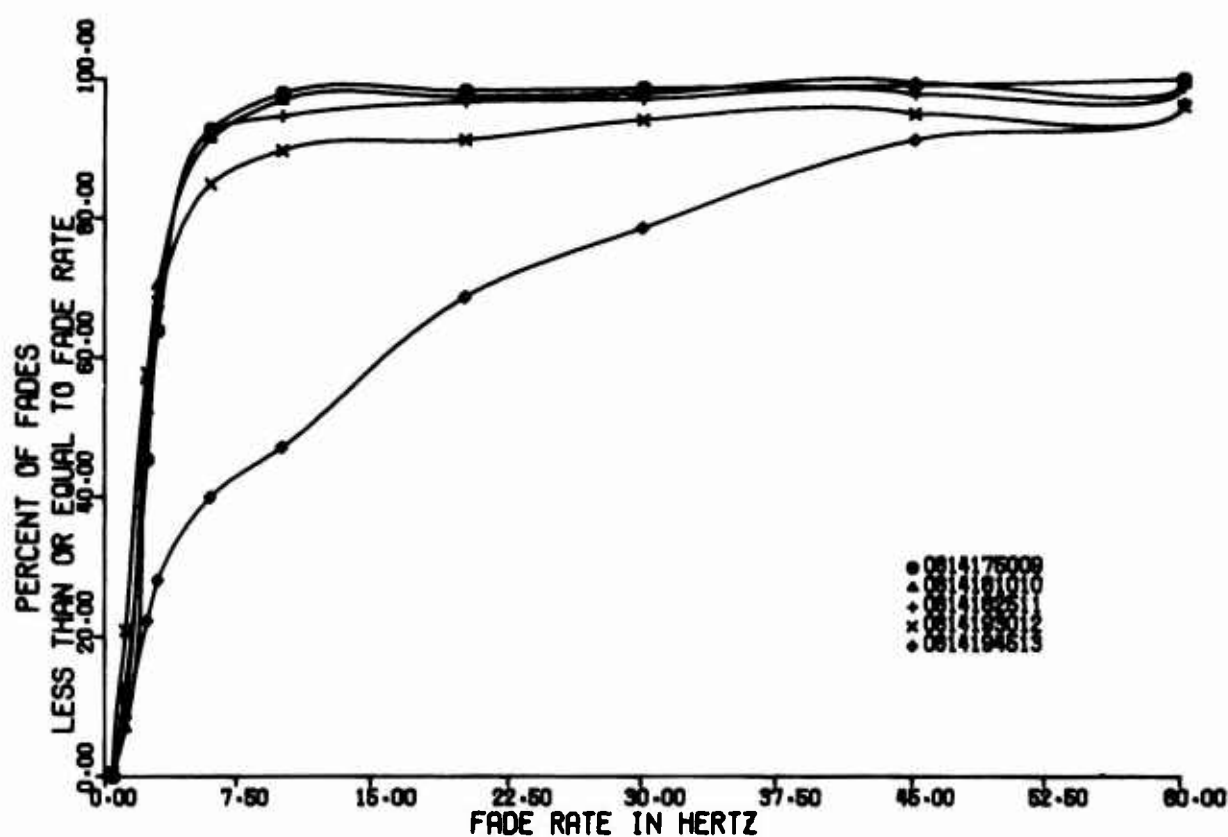


Figure 131. Fade Rate Distribution  
Ontario Center, Summer; X-Band; Temperature Over 85°F

### 3. Unusual Shape in the Correlation Coefficient Curves

Some unusual shapes in the correlation coefficient curves were noted often enough to consider them as perhaps a part of the fading and multipath mechanism occasionally present in the common volume. This phenomenon was not observed in the previous troposcatter propagation work in Reference 2. If it were present, it went undetected. The correlation bandwidth curves are presented in Figures 132 and 133 because they might give a clue to the behavior of the common volume. The curves appear as if they are following some sort of sine  $x/x$  function. In Figure 132 it appears suddenly in test 12 at 1930 hours and gradually diminishes, changing its periodicity, over the several hours. The phenomenon is repeated to a lesser degree in Figure 133.

This type of propagation should have no unusual effect to any of the frequency diversity modems. The results of the tests not shown were typically the same as the tests that are shown.

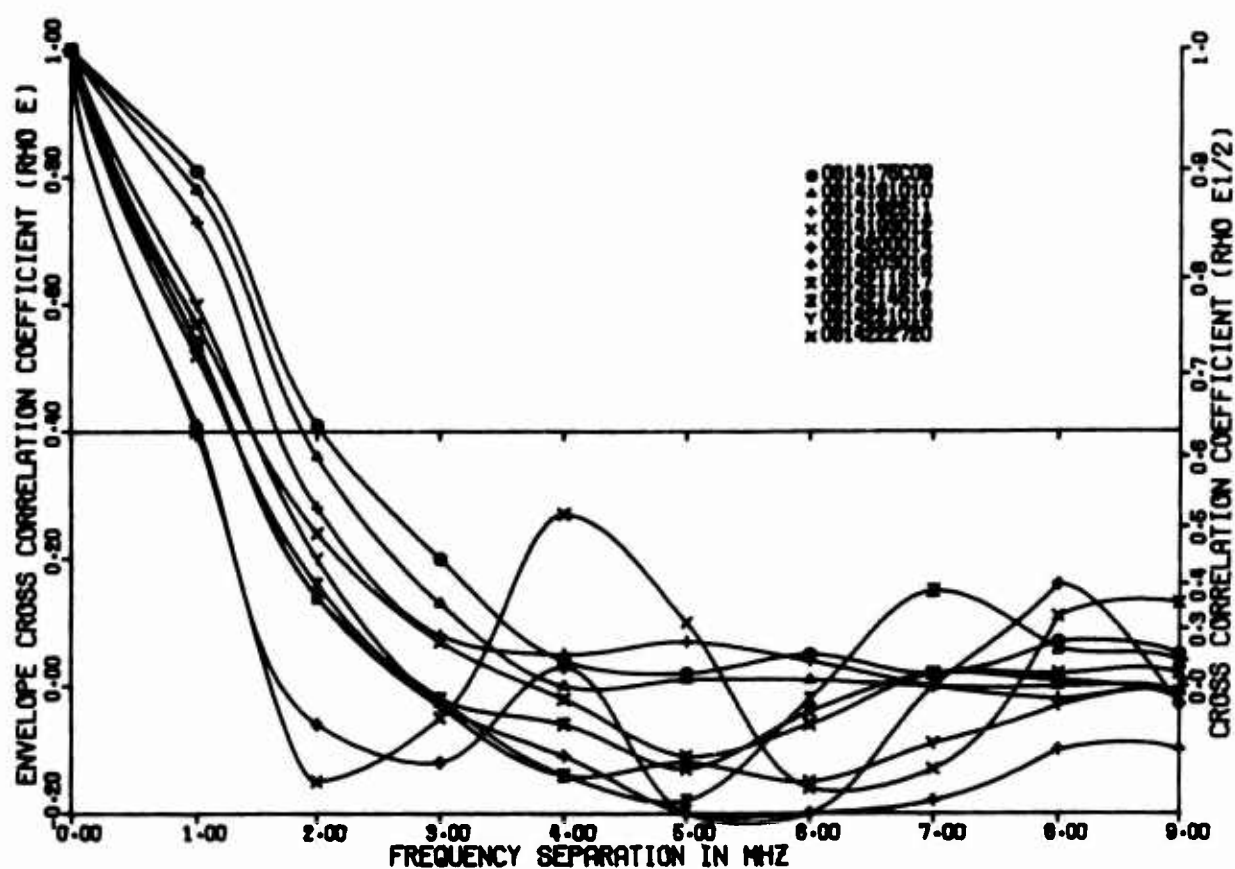


Figure 132. Envelope Cross Correlation Coefficients  
Ontario Center, Summer; X-Band, Wide; Temperature Over 85°F

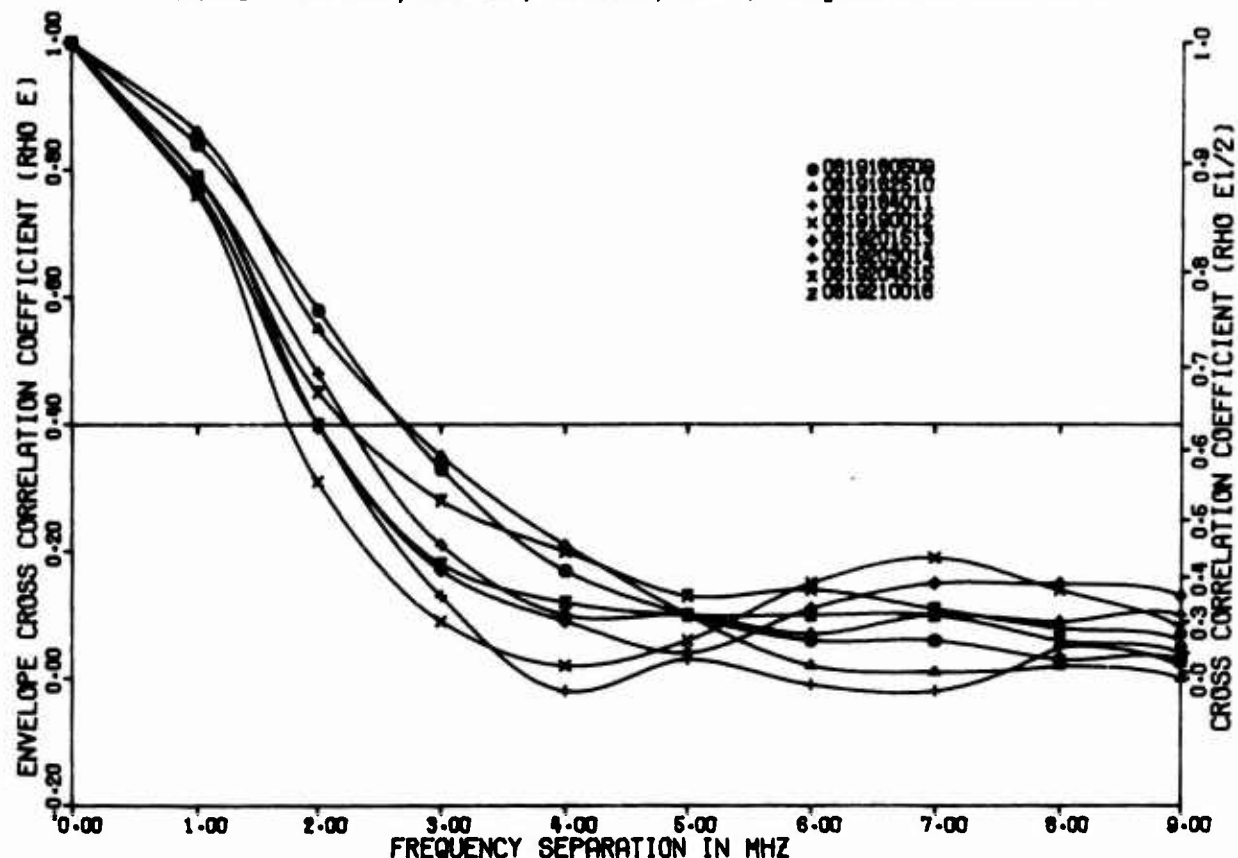


Figure 133. Envelope Cross Correlation Coefficients  
Ontario Center, Summer; C-Band, Wide

#### 4. High Fade Rates

Occasionally high fade rates are encountered that could have some effect on adaptive frequency modems. Figures 134 and 135 are examples of some of the very high fade rates. These high fade rates render the best frequency select circuits to be at times spoofed and cause the adaptive frequency modem to go to a less than best frequency. Sometimes this can cause an error in the received frequency commands and can cause the link to become broken. The frequency-time modems can operate in the high fade rates without difficulty.

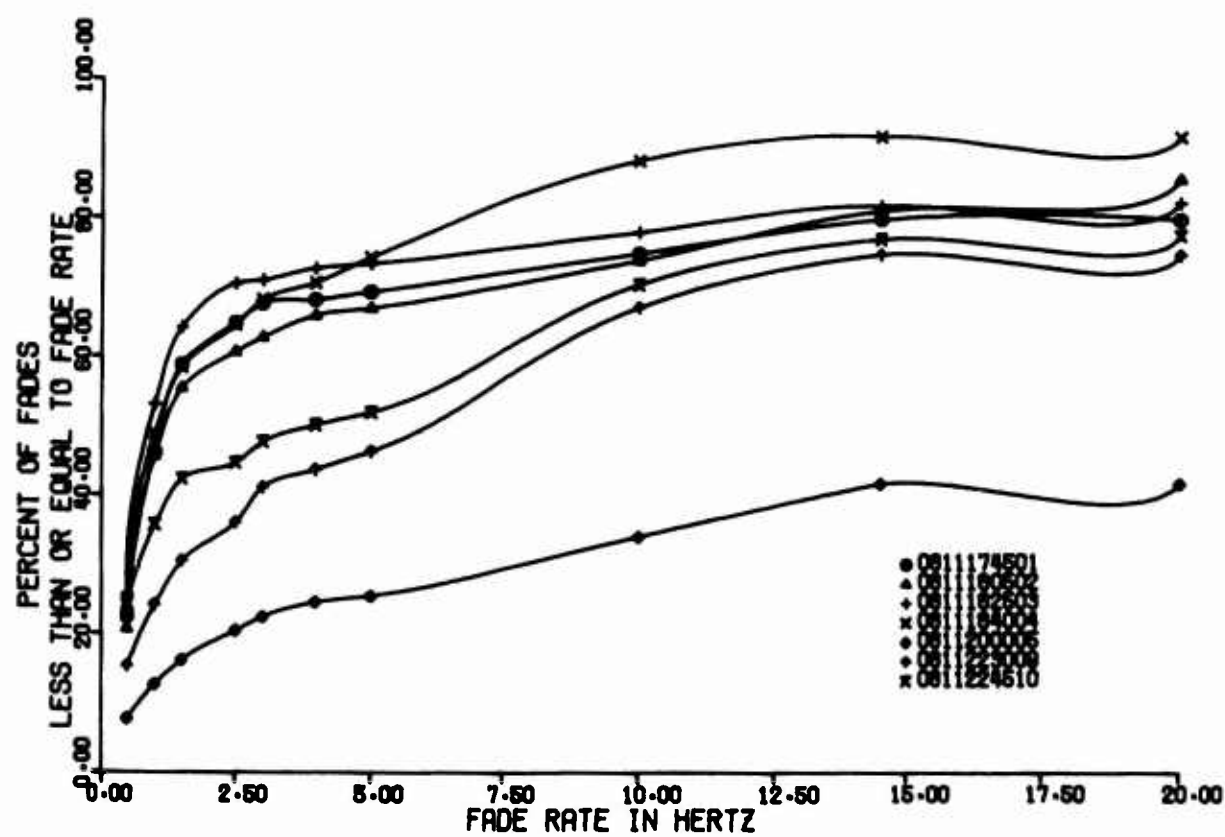


Figure 134. Fade Rate Distribution  
Ontario Center, Summer; C-Band

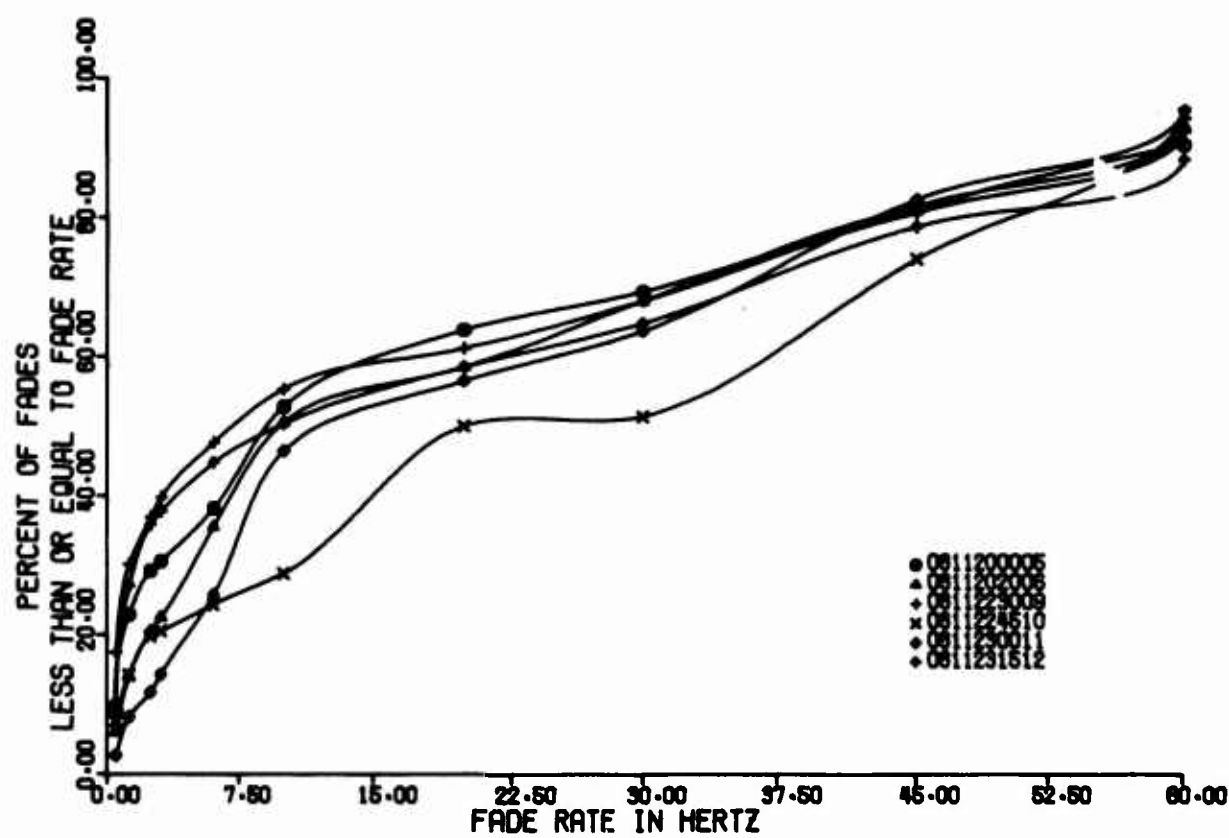


Figure 135. Fade Rate Distribution  
Ontario Center, Summer; X-Band

APPENDIX A  
CORRELATION BANDWIDTH COMPUTER PROGRAM

**PRECEDING PAGE BLANK-NOT FILMED.**

**APPENDIX A  
CORRELATION BANDWIDTH COMPUTER PROGRAM**

A computer program was developed which provides correlation bandwidth solutions for a troposcatter link as a function of antenna beamwidths, distance between sites and meteorological conditions in the vicinity of the common volume, i.e., temperature, humidity, and pressure. The geometry for the correlation bandwidth computer program is shown in Figure 136 for reference.

A program flow chart is shown in Figure 137. As can be seen in that figure, the meteorological conditions are used to solve for the surface refractive index constant,  $N_s$ . An exponential model for refractive index versus altitude is assumed for purposes of computing ray bending due to refraction. Based on path geometry, calculated  $N_s$ , and antenna beamwidth, ray trace solutions for the upper and lower antenna beam ray edges are then obtained such that the multipath spread  $\Delta$  in microseconds can be obtained. Although the present form of the computer program assumes equal transmitting and receiving antenna beamwidths and zero initial takeoff angle (lower edge of antenna beam on horizon), a more sophisticated version of this program is being developed which will treat the case of nonzero takeoff angles which may be different at the two sites. However, for purposes of analysis of the current experimental data, the form of the computer program as presented is adequate.

Once  $\Delta$ , the multipath spread is computed, the computer program employs the gaussian (Rice derived) model for the correlation bandwidth for computation of numerical values of the envelope correlation function versus frequency separation in MHz. As can be seen in the flow diagram, a scale factor SF is incorporated within the correlation bandwidth model to account for condition of the troposphere which may vary throughout a given day. That is, the air within the common volume may be turbulent or may exist in layers in which case SF must be altered in accordance.

A listing of the actual computer program is shown on the following pages for reference. Written in standard Fortran IV, the program was executed on the Martin Marietta CDC 6400 computer facility. Very minor modifications, mainly in formatting, will permit execution of the program on other machines such as the IBM 360 or IBM 1130. To demonstrate the operation of the computer code, several test conditions were programmed. The first is the X-band wide Whitford data taken on 29 August at 1450 and 1535 hours, respectively. The other is C-band wide Whitford data also taken on 29 August at 1450 and 1550 hours. These are both shown on the following pages.

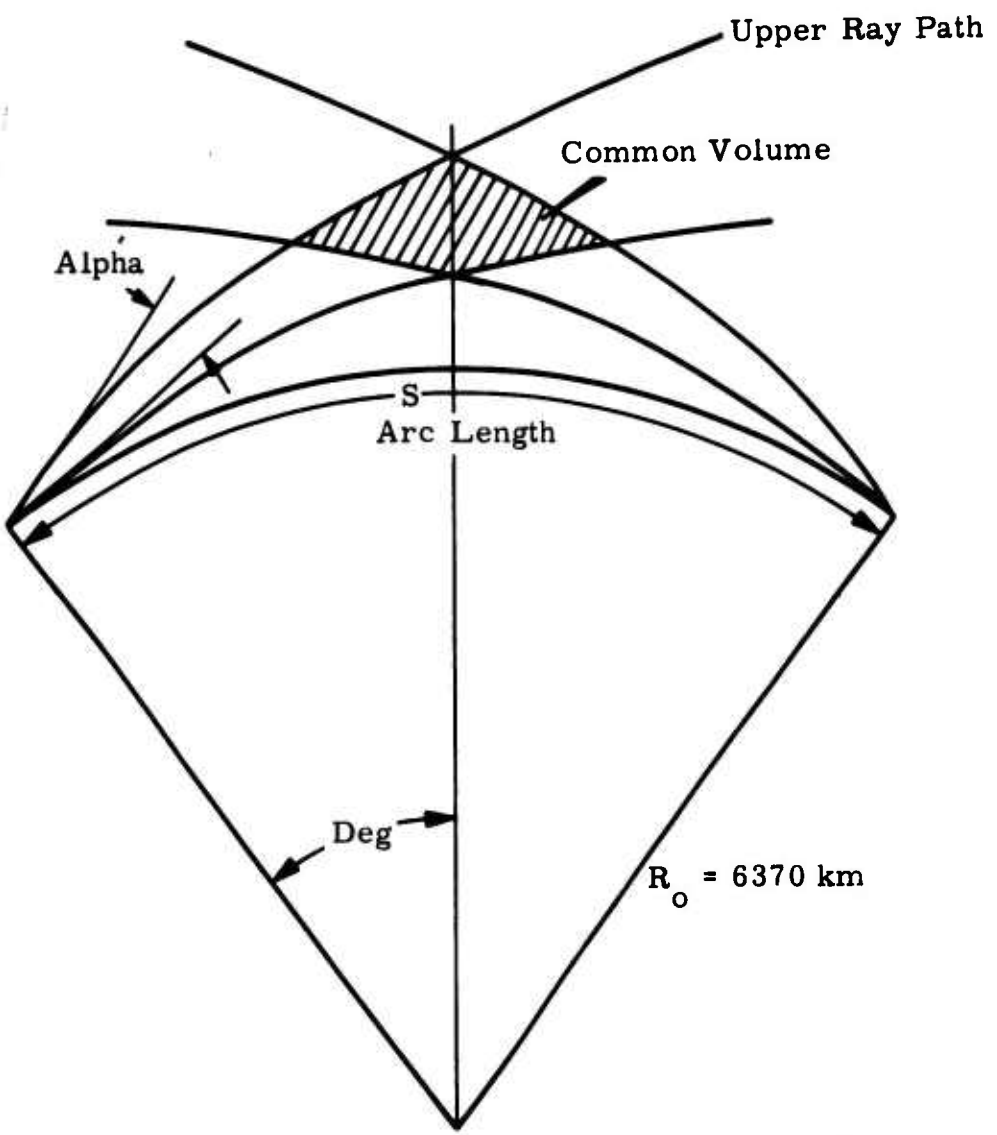
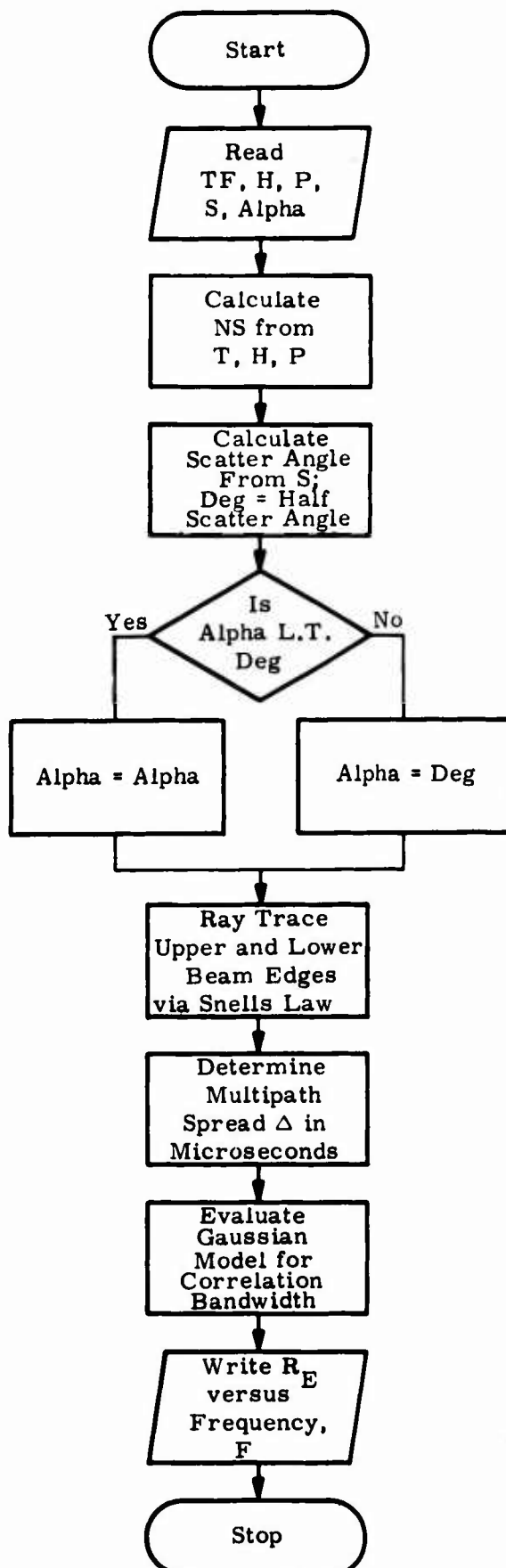


Figure 136. Geometry Applicable to Correlation Bandwidth Computer Program



#### Inputs

$T_F$  = Temperature in Degrees F  
 $H$  = Humidity in Percent  
 $P$  = Atmospheric Pressure in Inches Mercury  
 $S$  = Distance Between Sites in Kilometers  
 $\alpha$  = Antenna Half Power Beamwidth  
 $SF$  = Scale Factor Related to Condition of the Troposphere

#### Output

$R_E$  = Envelope Correlation Function  
 $F$  = Frequency Separation in MHz

Figure 137. Computer Flow Diagram for Correlation Bandwidth Computation

```

PROGRAMRAY(INPUT,TAPE 5=INPUT,OUTPUT,TAPE 6=OUTPUT)

000003 C DIMENSION RL(1010),RL(1010),RE(101),TEST(2)
C PRECISION OF CORRELATION BANDWIDTH BASED
C ON LINK PARAMETERS,WEATHER AND TROPOSPHERE CONDITION
      REAL K1,K2,K3,K4,P,PM,PN,NS
      READ(5,250) TEST,TF,H,P,S,SF
      FORMAT(A6,A6,3X,F10.2,3X,F10.3,3X,F8.3)
      AU(1)=6370.
      FL(1)=6370.

000023
000024 C S=DISTANCE BETWEEN SITES IN KILOMETERS
      C=S/2.
      CEQ=D/6370.
      C EFFECTIVE ANTENNA AN ACCORDING TO GORDON
      C ALPHABMW SCATTER ANGLE=DEG
      ALPHA=DEG

000031 C PROGRAM ASSUMES ANTENNA BW IS E.1. OR G.T. DEG
      C IF BW IS L.T. DEG THEN LET ALPHA=BW
      C TEMP=TEMPERATURE IN DEGREES FAHRENHEIT
      C CONVERT TO DEGREES CELSIUS(GRADE),TC
      C P=ATMOSPHERIC PRESSURE IN INCHES MERCURY
      C CONV=PI*3.14 MILLIBARS. PM

000032 C RELATIVE HUMIDITY IN PERCENTURE IN MILLIBARS
      C COMPUTATION OF RS(0391*TC)

000036
000040 C
000045
000047
000050
000056 C RAY TRACE LOWER EDGE OF ANTENNA BEAM ON HORIZON
      SL=0.
      K1=77.6
      K2=4R.1
      RATE=PM*((K2*H*PW)/(273.+TC))
      NS=(K1*RATE)/(273.+TC)
      H=NS*EXP((-0.1057*MM))
      CNDR=0.1057*AN
      K3=1.+(6370.*DNDR*1.E - 6)
      ARK
      ESG=(AK*DEG/1000.)**2
      AAA=0.5*K3*B20
      RL(K+1)=6370.*EXP(AAA)
      XRL(K+1)=RL(K)
      Y=(RL(K)*DEG)/1000.
      DS=SIGN(X**2)+(Y**2)
      SL=SL+DS
      CONTINUE

000101
000104
000106
000113
000114
000117
000124
000126

```

```

C RAY TRACE UPPER EFFECTIVE EDGE OF ANTENNA BEAM
0000131
0000132
0000133
0000134
0000135
0000142
0000143
0000146
0000150
0000153
0000156
0000160
0000166
0000167
0000172
0000177
0000201
0000210
0000212
0000215
0000224
0000226
0000231
0000231
0000241
0000243
0000253
0000265
0000267
0000270
0000273
0000302

DO 20 I=1,1000
PM=RU(1)-6370.
N=NS*EXP(-0.1057*MM)
CNDR=0.1057*MM
K3=1.+6370.*DNDR*1.E-6)
AI=1
BSQ=(AI*DEG/1000.)*#2
K4=ALPHASAI*DEG/1000.
BBBK4=(0.5*K3*BSQ)
RU(1)=6370.*EXP(BBBK4)
X=RU(1)-RU(1)
Y=(RU(1)*DEG)/1000.
CS=SQR((X*X)+(Y*Y))
SUN=SY*D5
20
C DETERMINE MULTIPATH SPREAD. DELTA IN SECONDS
C DELTA=(SU-SL)/(1.SE*SF)
C SF IS A SCALE FACTOR WHICH IS RELATED TO STABILITY OF THE TROPOSPHERE
C RICE MODEL FOR CORRELATION BANDWIDTH (GAUSSIAN MODEL)
RE(1)=1.
DO 30 J=2,11
Z=(J-1)*1.E+6
AE(J)=EXP(-(ISF*Z*DELTAF)**2)
CONTINUE
WRITE(6,40)
FORMAT(1H,10X,67MPREDICTION OF ENVELOPE CORRELATION FUNCTION FOR
1A TROPOSCATTER PATH//,
1A WRITE(6,10)PM,S
FORMAT(1H,10X,26MPRESSURE IN MILLIBARS.PM= ,F10.2,10X,32MDISTANCE
1 BETWEEN SITES IN KM,S= ,F12.5,/)
1A WRITE(6,90)TCP,H,SF
FORMAT(1H,10X,3HTC=,F6.2,10X,22MHUMIDITY IN PERCENT.H=,F6.2,10X,3
1MSF=,F8.3,/)
FORMAT(1H,10X,3HNS=,F7.1,10X,6HALPHA=,F10.6,10X,8MTST NO.,A6.A6/
1)
AA=2.*SU
AB=2.*SL
AC=DELTAF*E**6
FORMAT(1H,10X,24MUPEH RAY LENGTH IN KM.,,F10.4,,F10.4,/)
ILENGTH IN KM.,,F10.4,/
125

```

```
000302      WRITE(6,150)AC
000310      FORMAT(1H,10X,30HMULTIPATH SPREAD IN MICROSEC.,-F10.5//)
000310      WRITE(6,60)
000314      60      FORMAT(1H,10X,25MFREQUENCY SEPARATION MHz.,10X,42MENVELOPE FREQUE
1NCY CORRELATION FUNCTION,RE//)
000314      CO 70 I=1,1
000316      J=I-1
000320      WRITE(6,80)J,RE(I)
000320      FORMAT(1H,20X,I2,30X,F10.6//)
000327      80      CONTINUE
000327      70      GO TO 300
000331      END
000332
```

PREDICTION OF ENVELOPE CORRELATION FUNCTION FOR A TROPOSCATTER PATH

PRESSURE IN MILLIBARS.PM=	1010.04	DISTANCE BETWEEN SITES IN KM.S=	199.10000
TC= 29.58	HUMIDITY IN PERCENT.H= 49.50	SF= 3.336	
NS= 343.7	ALPHA= .015628	TEST NO.08291450XMMH	
UPPER RAY LENGTH IN KM.= 199.1804	LOWER RAY LENGTH IN KM.= 199.1113		
MULTIPATH SPREAD IN MICROSEC.= .23050			
FREQUENCY SEPARATION MHZ.	ENVELOPE FREQUENCY CORRELATION FUNCTION,WE		
0	.000000		
1	.553604		
2	.093928		
3	.004884		
4	.000078		
5	.000000		
6	.000000		
7	.000000		
8	.000000		
9	.000000		
10	.000000		

PREDICTION OF ENVELOPE CORRELATION FUNCTION FOR A TROPOSCATTER PATH

PRESSURE IN MILLIBARS.PK= 1010.04 DISTANCE BETWEEN SITES IN KM.S= 199.10000

T<sub>C</sub>= 28.47 HUMIDITY IN PERCENT.H= 49.50 SF= 1.0446

NS= 341.7 ALPHA= .015628 TEST NO.08291535XXXX

UPPER RAY LENGTH IN KM.= 199.1005 LOWER RAY LENGTH IN KM.= 199.1113

MULTIPATH SPREAD IN MICROSEC.= .23058

FREQUENCY SEPARATION MHz.

ENVELOPE FREQUENCY CORRELATION FUNCTION.RE

FREQUENCY SEPARATION MHz.	ENVELOPE FREQUENCY CORRELATION FUNCTION.RE
0	.000000
1	.894786
2	.641027
3	.367682
4	.168852
5	.062084
6	.016276
7	.004308
8	.000813
9	.000123
10	.000015

PREDICTION OF ENVELOPE CORRELATION FUNCTION FOR A TROPOSCATTER PATH

PRESSURE IN MILLIBARS.PMS 1010.00 DISTANCE BETWEEN SITES IN KM.S= 199.10000

TC= 29.58 HUMIDITY IN PERCENT.H= 49.50 SF= 3.615

NGS= 343.7 ALPHAS= .015628 TEST NO.00291450CMMH

UPPER RAY LENGTH IN KM.= 199.1804 LOWER RAY LENGTH IN KM.= 199.1113

MULTIPATH SPREAD IN MICROSECS.= .23050

FREQUENCY SEPARATION MHZ. ENVELOPE FREQUENCY CORRELATION FUNCTION.RE

0	1.000000
1	.499400
2	.062201
3	.001932
4	.000015
5	.000000
6	.000000
7	.000000
8	.000000
9	.000000
10	.000000

PREDICTION OF ENVELOPE CORRELATION FUNCTION FOR A TROPOSCATTER PATH

PRESSURE IN MILLIBARS.PMS =	1010.0	DISTANCE BETWEEN SITES IN KM.S =	199.10000
TC = 20.47	HUMIDITY IN PERCENT.H = 49.50	SF = 1.606	
NS = .341.7	ALPHAS = .0156228	TEST NO. 00291550CWWH	
UPPER RAY LENGTH IN KM.S = 199.1805	LOWER RAY LENGTH IN KM.S = 199.1113		
MULTIPATH SPREAD IN MICROSEC. = .23058			
FREQUENCY SEPARATION MHz.	ENVELOPE FREQUENCY CORRELATION FUNCTION.RE		
0	1.000000		
1	.871853		
2	.577795		
3	.291065		
4	.111454		
5	.032440		
6	.007177		
7	.001207		
8	.000154		
9	.000015		
10	.000001		

APPENDIX B  
TEST RECORDS

## ONTARIO CENTER SUMMER X-BAND

TEST	WEATHER	RECEIVED SITE TEMP	REL HUM	BAND PRES	WIND	TRANSMIT SITE TEMP	REL HUM	BAND PRES	WIND	SIGNAL STRG
0805102001wx FAZY	FAZY	78 TU 81	51	29.99	9	82 TU 85	51	29.99	10	76.3
0805110002wx FAZY	FAZY	78 TU 81	51	29.99	9	82 TU 85	51	29.99	10	76.4
0805141003wx FAZY	FAZY	78 TU 81	51	29.99	9	82 TU 85	51	29.99	10	84.0
0805150005wx FAZY	FAZY	78 TU 81	51	29.99	9	82 TU 85	51	29.99	10	86.5
0805153006wx FAZY	FAZY	78 TU 81	51	29.99	9	82 TU 85	51	29.99	10	91.5
0805171507wx FAZY	FAZY	78 TU 81	51	29.99	9	82 TU 85	51	29.99	10	87.3
0805174008wx FAZY	FAZY	78 TU 81	51	29.99	9	82 TU 85	51	29.99	10	86.6
0805181009wx FAZY	FAZY	78 TU 81	51	29.99	9	82 TU 85	51	29.99	10	88.7
0806123001wx FAZY	FAZY	78 TU 81	77	30.2	15	82 TU 85	51	29.99	10	73.5
0806130002wx FAZY	FAZY	78 TU 81	77	30.2	15	82 TU 85	51	29.99	10	76.9
0806135004wx FAZY	FAZY	78 TU 81	77	30.2	15	82 TU 85	51	29.99	10	79.7
0806160006wx FAZY	FAZY	82 TU 65	60	29.99	13	82 TU 85	51	29.99	10	82.8
0806162507wx FAZY	FAZY	82 TU 85	60	29.99	13	82 TU 85	51	29.99	10	81.6
0806165008wx FAZY	FAZY	82 TU 85	60	29.99	13	82 TU 85	51	29.99	10	81.0
0807093001wx FAZY	FAZY	74 TU 77	76	29.42	25	78 TU 81	56	29.36	13	90.6
0807095002wx FAZY	FAZY	74 TU 77	76	29.42	25	78 TU 81	56	29.36	13	89.1
0807101503wx FAZY	FAZY	74 TU 77	76	29.42	25	78 TU 81	56	29.36	13	84.1
0807104004wx FAZY	FAZY	74 TU 77	76	29.42	25	78 TU 81	56	29.36	13	81.7
0807153005wx FAZY	FAZY	86 TU 88	64	29.88	34	70 TU 73	77	29.34	17	87.0
0807160006wx FAZY	FAZY	86 TU 88	64	29.88	34	70 TU 73	77	29.34	17	81.3
0807163007wx FAZY	FAZY	80 TU 66	64	29.88	34	70 TU 73	77	29.34	17	78.5
0807184008wx FAZY	FAZY	82 TU 65	64	29.88	34	70 TU 73	77	29.34	17	79.4
0807185009wx FAZY	FAZY	82 TU 65	57	29.84	25	70 TU 73	77	29.34	17	80.4
0807191010wx FAZY	FAZY	82 TU 65	57	29.84	25	70 TU 73	77	29.34	17	87.6
0807192611wx FAZY	FAZY	82 TU 65	57	29.84	25	70 TU 73	77	29.34	17	83.3
0807203012wx FAZY	FAZY	82 TU 65	57	29.84	25	70 TU 73	77	29.34	17	83.0
0807205013wx FAZY	FAZY	82 TU 65	57	29.84	25	70 TU 73	77	29.34	17	55.4
0807211715wx FAZY	FAZY	82 TU 85	57	29.84	25	70 TU 73	77	29.34	17	77.8
0807215017wx FAZY	FAZY	82 TU 85	57	29.84	25	70 TU 73	77	29.34	17	74.9
0811200005wx RAIN.	CUM CLOUD	74 TU 77	47	29.44	7	76 TU 81	47	29.97	7	75.5
0811202006wx RAIN.	CUM CLOUD	74 TU 77	47	29.44	7	78 TU 81	47	29.97	7	69.3
0811203007wx RAIN.	CUM CLOUD	74 TU 77	47	29.44	7	78 TU 81	47	29.97	7	60.2
0811215017wx RAIN.	CUM CLOUD	74 TU 77	47	29.44	7	78 TU 81	47	29.97	7	61.0
0811223009wx RAIN.	CUM CLOUD	74 TU 77	47	29.44	7	78 TU 81	47	29.97	7	74.1
0811224510wx RAIN.	CUM CLOUD	74 TU 77	47	29.44	7	78 TU 81	47	29.97	7	73.6
081123011wx RAIN.	CUM CLOUD	74 TU 77	47	29.44	7	78 TU 81	47	29.97	7	71.9
0811231512wx RAIN.	CUM CLOUD	74 TU 77	47	29.44	7	78 TU 81	47	29.97	7	68.7
081213001wx RAIN.	CUM CLOUD	74 TU 77	47	29.44	7	78 TU 81	47	29.97	7	77.2
0812144502wx RAIN.	CUM CLOUD	74 TU 77	47	29.44	7	78 TU 81	47	29.97	7	103
0812120003wx RAIN.	CUM CLOUD	74 TU 77	47	29.44	7	78 TU 81	47	29.97	7	88.7
0812121504wx RAIN.	CUM CLOUD	74 TU 77	47	29.44	7	78 TU 81	47	29.97	7	77.2
081214005wx RAIN.	CUM CLOUD	74 TU 77	47	29.44	7	78 TU 81	47	29.97	7	77.2
0812142506wx RAIN.	CUM CLOUD	74 TU 77	47	29.44	7	78 TU 81	47	29.97	7	77.2

PRECEDING PAGE BLANK NOT FILMED.

0812144007wx	RAIN.	CUM	CLOUD	78.2
0812150608wx	RAIN.	CUM	CLOUD	78.2
0812152509wx	RAIN.	CUM	CLOUD	72.6
0812154010wx	RAIN.	CUM	CLOUD	74.2
0813095001wx	CLEAR	CUM	CLOUD	75.7
0813101002wx	CLEAR	CUM	CLOUD	72.2
0813103003wx	CLEAR	CUM	CLOUD	69.2
0813105004wx	CLEAR	CUM	CLOUD	68.3
0813111505wx	CLEAR	CUM	CLOUD	73.0
0813113006wx	CLEAR	CUM	CLOUD	75.6
0813114507wx	CLEAR	CUM	CLOUD	75.7
0813120008wx	CLEAR	CUM	CLOUD	75.4
0814150601wx	LIGHT HAZE	CUM	CLOUD	76.0
0814152002wx	LIGHT HAZE	CUM	CLOUD	77.6
0814154503wx	LIGHT HAZE	CUM	CLOUD	77.5
0814155904wx	LIGHT HAZE	CUM	CLOUD	79.3
0814155904wx	LIGHT HAZE	CUM	CLOUD	79.3
0814161505wx	LIGHT HAZE	CUM	CLOUD	79.3
0814164506wx	LIGHT HAZE	CUM	CLOUD	80.6
0814170007wx	LIGHT HAZE	CUM	CLOUD	81.9
0814171506wx	LIGHT HAZE	CUM	CLOUD	82.6
0814175009wx	LIGHT HAZE	CUM	CLOUD	82.4
0814181010wx	LIGHT HAZE	CUM	CLOUD	84.9
0814182511wx	LIGHT HAZE	CUM	CLOUD	83.9
0814193012wx	LIGHT HAZE	CUM	CLOUD	83.0
0814194513wx	LIGHT HAZE	CUM	CLOUD	78.8
0814200014wx	LIGHT HAZE	CUM	CLOUD	83.0
0814201515wx	LIGHT HAZE	CUM	CLOUD	84.2
0814203016wx	LIGHT HAZE	CUM	CLOUD	83.0
0814211517wx	LIGHT HAZE	CUM	CLOUD	86.8
0814214518wx	LIGHT HAZE	CUM	CLOUD	83.2
0814221019wx	LIGHT HAZE	CUM	CLOUD	84.3
0814222720wx	LIGHT HAZE	CUM	CLOUD	89.5
0819180509nx	CLEAR	CUM	CLOUD	87.6
0819182510nx	CLEAR	CUM	CLOUD	88.9
0819184011nx	CLEAR	CUM	CLOUD	89.3
0819190012nx	CLEAR	CUM	CLOUD	88.9
0819203014nx	CLEAR	CUM	CLOUD	90.5
0819204515nx	CLEAR	CUM	CLOUD	89.4
0819210016nx	CLEAR	CUM	CLOUD	88.7
0820100001wx	CLEAR	CUM	CLOUD	77.5
0820102502wx	CLEAR	CUM	CLOUD	72.0
0820104503wx	CLEAR	CUM	CLOUD	69.8
0820110004wx	CLEAR	CUM	CLOUD	70.5
0820120005wx	CLEAR	CUM	CLOUD	69.7
0820122006wx	CLEAR	CUM	CLOUD	70.5
0820123507wx	CLEAR	CUM	CLOUD	69.7
0820125508wx	CLEAR	CUM	CLOUD	69.9

TEST	WEATHER	ONTARIO CENTER, SUMMER			C-BAND	RECEIVE SITE	TEMP	REL HUM	BAHU PRES	WINU	WEATHER	TRANSMIT SITE	TEMP	REL HUM	BAHU PRES	PHES	WIND	SIGNAL STRG
		51	29.99	9														
0805144004WC	HAZY	78	70	81	51	29.99	9	STRATUS	CLOUDING	82	TU	85	51	29.99	10	77.2	77.2	77.2
0805150005WC	HAZY	78	70	81	51	29.99	9	STRATUS	CLOUDING	82	TU	85	51	29.99	10	77.4	77.4	77.4
0805153506WC	HAZY	78	70	81	51	29.99	9	STRATUS	CLOUDING	82	TU	85	51	29.99	10	75.9	75.9	75.9
08051630002WC	HAZY	78	70	81	51	29.99	9	STRATUS	CLOUDING	82	TU	85	51	29.99	10	77.0	77.0	77.0
0805171507WC	HAZY	78	70	81	51	29.99	9	STRATUS	CLOUDING	82	TU	85	51	29.99	10	77.1	77.1	77.1
0805174008WC	HAZY	78	70	81	51	29.99	9	STRATUS	CLOUDING	82	TU	85	51	29.99	10	77.6	77.6	77.6
0805181009WC	HAZY	78	70	81	51	29.99	9	STRATUS	CLOUDING	82	TU	85	51	29.99	10	79.8	79.8	79.8
0806123001WC	HAZY	78	70	81	51	29.99	9	STRATUS	CLOUDING	82	TU	85	51	29.99	10	72.9	72.9	72.9
0806130002WC	HAZY	78	70	81	51	29.99	9	STRATUS	CLOUDING	82	TU	85	51	29.99	10	74.0	74.0	74.0
0806132503WC	HAZY	78	70	81	51	29.99	9	STRATUS	CLOUDING	82	TU	85	51	29.99	10	75.2	75.2	75.2
0806135004WC	HAZY	78	70	81	51	29.99	9	STRATUS	CLOUDING	82	TU	85	51	29.99	10	75.2	75.2	75.2
08061602509WC	HAZY	78	70	81	51	29.99	9	STRATUS	CLOUDING	82	TU	85	51	29.99	10	78.1	78.1	78.1
0806162509WC	HAZY	78	70	81	51	29.99	9	STRATUS	CLOUDING	82	TU	85	51	29.99	10	78.1	78.1	78.1
0809165008WC	HAZY	82	75	85	60	29.99	13	HAZY	HAZY	78	TU	81	56	29.98	13	77.5	77.5	77.5
0809175005WC	HAZY	82	75	85	60	29.99	13	HAZY	HAZY	78	TU	81	56	29.98	13	77.5	77.5	77.5
0811174501WC	CUMULUS	74	70	86	64	29.88	13	HEAVY	HAZY	78	TU	81	56	29.97	13	76.3	76.3	76.3
0811180502WC	CUMULUS	74	70	87	67	29.44	7	CUMULUS	CLOUDING	74	TU	85	47	29.97	7	80.2	80.2	80.2
0811182503WC	CUMULUS	74	70	87	67	29.44	7	CUMULUS	CLOUDING	74	TU	85	47	29.97	7	81.9	81.9	81.9
0811184004WC	CUMULUS	74	70	87	67	29.44	7	CUMULUS	CLOUDING	74	TU	85	47	29.97	7	82.0	82.0	82.0
0811200005WC	CUMULUS	74	70	87	67	29.44	7	CUMULUS	CLOUDING	74	TU	85	47	29.97	7	79.4	79.4	79.4
0811223009WC	CUMULUS	74	70	87	67	29.44	7	CUMULUS	CLOUDING	78	TU	81	47	29.97	7	76.7	76.7	76.7
0811224510WC	CUMULUS	74	70	87	67	29.44	7	CUMULUS	CLOUDING	78	TU	81	47	29.97	7	75.6	75.6	75.6
0811230011WC	CUMULUS	74	70	87	67	29.44	7	CUMULUS	CLOUDING	78	TU	81	47	29.97	7	77.6	77.6	77.6
080812124503WC	CUMULUS	74	70	87	67	29.44	7	CUMULUS	CLOUDING	78	TU	81	47	29.97	7	76.6	76.6	76.6
0812154010WC	CUMULUS	74	70	87	67	29.44	7	CUMULUS	CLOUDING	78	TU	81	47	29.97	7	76.6	76.6	76.6
0813095001WC	CLEAR	70	70	73	76	29.48	10	LIGHT	FOG	70	TU	73	66	30.14	8	67.8	67.8	67.8
0813101002WC	CLEAR	70	70	73	76	29.48	10	LIGHT	FOG	70	TU	73	66	30.14	8	66.4	66.4	66.4
0813103003WC	CLEAR	70	70	73	76	29.48	10	LIGHT	FOG	70	TU	73	66	30.14	8	66.7	66.7	66.7
0813105004WC	CLEAR	70	70	73	76	29.48	10	LIGHT	FOG	70	TU	73	66	30.14	8	66.7	66.7	66.7
0813111505WC	CLEAR	74	70	77	76	29.48	10	LIGHT	FOG	70	TU	73	66	30.14	8	71.5	71.5	71.5
0813113006WC	CLEAR	74	70	77	76	29.48	10	LIGHT	FOG	70	TU	73	66	30.14	8	72.3	72.3	72.3
0813114507WC	CLEAR	74	70	77	76	29.48	10	LIGHT	FOG	70	TU	73	66	30.14	8	71.3	71.3	71.3
0813120008WC	CLEAR	74	70	77	76	29.48	10	LIGHT	FOG	70	TU	73	66	30.14	8	70.6	70.6	70.6
08131135503WC	CLEAR	74	70	77	76	29.48	10	LIGHT	FOG	70	TU	73	66	30.14	8	72.6	72.6	72.6
0819145505WC	CLEAR	74	70	77	76	29.48	10	LIGHT	FOG	70	TU	73	66	30.14	8	74.9	74.9	74.9
0819151506WC	CLEAR	74	70	77	76	29.48	10	LIGHT	FOG	70	TU	73	66	30.14	8	75.8	75.8	75.8
0819154007WC	CLEAR	74	70	77	76	29.48	10	LIGHT	FOG	70	TU	73	66	30.14	8	77.9	77.9	77.9
0819155508WC	CLEAR	74	70	77	76	29.48	10	LIGHT	FOG	70	TU	73	66	30.14	8	78.3	78.3	78.3
0819180509WC	CLEAR	74	70	77	76	29.48	10	LIGHT	FOG	70	TU	73	66	30.14	8	78.0	78.0	78.0
0819190012WC	CLEAR	74	70	77	76	29.48	10	LIGHT	FOG	70	TU	73	66	30.14	8	79.0	79.0	79.0
0819201513WC	CLEAR	70	70	73	79	29.85	16	CLEAR	CLEAR	70	TU	81	40	29.21	16	74.9	74.9	74.9
0819203014WC	CLEAR	74	70	77	77	29.85	16	CLEAR	CLEAR	70	TU	81	40	29.21	16	75.8	75.8	75.8
0819204515WC	CLEAR	70	70	73	75	29.85	16	CLEAR	CLEAR	70	TU	81	40	29.21	16	76.7	76.7	76.7
0819210016WC	CLEAR	70	70	73	75	29.85	16	CLEAR	CLEAR	70	TU	81	40	29.21	16	78.0	78.0	78.0

TEST	WEATHER	RECEIVE SITE			TRANSMIT SITE			X-BAND			SIGNAL STRG	
		TEMP	RFL	HUM	PRES	WIND	TEMP	RFL	HUM	BAKU	PHES	
0828165501wx	CLEAR	86	TU	88	36	30.21	10	CLEAR	86	10	88	29.52
0828172502wx	CLEAR	86	TU	88	36	30.21	10	CLEAR	86	10	88	29.52
0828174503wx	CLEAR	86	TU	88	36	30.21	10	CLEAR	86	10	88	29.52
0828182004wx	CLEAR	86	TU	88	36	30.21	10	CLEAR	86	10	88	29.52
0828184005wx	LIGHT HAZE	82	TU	85	42	30.17	27	LIGHT HAZE	82	10	85	30.12
0828194006nx	LIGHT HAZE	82	TU	85	42	30.17	27	LIGHT HAZE	82	10	85	30.12
0828195507nx	LIGHT HAZE	82	TU	85	42	30.17	27	LIGHT HAZE	82	10	85	30.12
0829063501nx	LIGHT HAZE	70	TU	73	68	30.19	15	LIGHT HAZE	74	10	77	29.52
0829085002nx	LIGHT HAZE	70	TU	73	68	30.19	15	LIGHT HAZE	74	10	77	29.52
0829090703nx	LIGHT HAZE	70	TU	73	68	30.19	15	LIGHT HAZE	74	10	77	29.52
0829092504nx	LIGHT HAZE	70	TU	73	68	30.19	15	LIGHT HAZE	74	10	77	29.52
0829094005nx	LIGHT HAZE	70	TU	73	68	30.19	15	LIGHT HAZE	74	10	77	29.52
0829102506nx	LIGHT HAZE	74	TU	77	57	30.18	15	LIGHT HAZE	78	10	81	29.52
0829111008nx	LIGHT HAZE	74	TU	77	57	30.18	15	LIGHT HAZE	78	10	81	29.52
0829120509wx	LIGHT HAZE	74	TU	77	57	30.18	15	LIGHT HAZE	78	10	81	29.52
0829123010wx	LIGHT HAZE	74	TU	77	57	30.18	15	LIGHT HAZE	78	10	81	29.52
0829125511wx	LIGHT HAZE	62	TU	85	57	30.18	15	LIGHT HAZE	74	10	77	29.52
0829131512wx	LIGHT HAZE	62	TU	85	53	30.18	14	LIGHT HAZE	62	10	85	29.52
0829133513wx	LIGHT HAZE	62	TU	85	43	30.18	14	LIGHT HAZE	62	10	85	29.52
0829145014wx	LIGHT HAZE	66	FU	88	64	30.18	10	LIGHT HAZE	62	10	88	29.49
0829150515wx	LIGHT HAZE	66	FU	88	64	30.17	10	LIGHT HAZE	62	10	88	29.49
0829152016wx	LIGHT HAZE	66	FU	88	64	30.17	10	LIGHT HAZE	62	10	88	29.49
0829153517wx	LIGHT HAZE	66	FU	88	64	30.17	10	LIGHT HAZE	62	10	88	29.49
0829155201nx	LIGHT HAZE	94	TU	97	62	30.17	10	LIGHT HAZE	82	10	85	29.49
0829158103nx	LIGHT HAZE	74	TU	77	62	30.17	10	LIGHT HAZE	82	10	85	29.49
0905134004nx	LIGHT HAZE	74	TU	77	62	30.17	10	LIGHT HAZE	82	10	85	29.49
0905135505nx	LIGHT HAZE	74	TU	77	57	30.14	21	LIGHT HAZE	82	10	85	29.49
0905141006nx	CUMULUS CLOUDING	78	TU	81	57	30.14	21	LIGHT HAZE	82	10	85	29.49
0905144508nx	CUMULUS CLOUDING	78	TU	81	57	30.14	21	LIGHT HAZE	82	10	85	29.49
0905153509nx	CUMULUS CLOUDING	78	TU	81	57	30.14	21	LIGHT HAZE	82	10	85	29.49
0905155510nx	CUMULUS CLOUDING	78	TU	81	57	30.14	21	LIGHT HAZE	82	10	85	29.49
0905161011nx	CUMULUS CLOUDING	78	TU	81	57	30.14	21	LIGHT HAZE	82	10	85	29.49
0905163012nx	CUMULUS CLOUDING	78	TU	81	57	30.14	21	LIGHT HAZE	82	10	85	29.49
0908112501wx	CUMULUS CLOUDING	66	TU	88	87	28.29	15	CLEAR	7	CLEAR	29.52	
0908112503wx	CUMULUS CLOUDING	66	TU	88	87	28.29	15	CLEAR	7	CLEAR	29.52	
0908131505wx	CUMULUS CLOUDING	66	TU	88	73	29.52	15	CLEAR	11	CLEAR	29.52	
0908141006wx	CUMULUS CLOUDING	66	TU	88	73	29.52	15	CLEAR	11	CLEAR	29.52	
0908171511wx	CUMULUS CLOUDING	74	TU	77	46	29.84	15	CLEAR	74	TU	77	30.00
0908175013wx	CUMULUS CLOUDING	74	TU	77	46	29.84	15	CLEAR	74	TU	77	30.00
0908194017wx	CUMULUS CLOUDING	74	TU	77	46	29.84	15	CLEAR	74	TU	77	30.00

TEST	RECEIVE SITE				SUMMER C-BAND				TRANSMIT SITE				WINTER C-BAND					
	TEMP	REL HUM	BARO PRES	WIND	WEATHER	TEMP	REL HUM	BARO PRES	WIND	WEATHER	TEMP	REL HUM	BARO PRES	WIND	WEATHER			
0828165501NC	CLEAR	36	30.021	10	CLEAR	86	10	88	53	29.54	47	49.6	47	49.54	47	49.6		
0828172502NC	CLEAR	86	36	30.021	10	CLEAR	86	10	88	53	29.52	47	49.2	47	49.52	47	49.2	
0828174503NC	CLEAR	86	36	30.021	10	CLEAR	86	10	88	53	29.52	47	49.6	47	49.52	47	49.6	
0828182004NC	CLEAR	86	36	30.021	10	CLEAR	86	10	88	53	29.52	47	49.7	47	49.52	47	49.7	
0828184005NC	LIGHT HAZE	82	42	30.017	27	LIGHT HAZE	82	10	85	41	30.12	27	97.1	27	116.3	27	97.1	
0828194006NC	LIGHT HAZE	82	42	30.017	27	LIGHT HAZE	82	10	85	41	30.12	27	96.6	27	117.7	27	96.6	
0828195507WC	LIGHT HAZE	82	42	30.017	27	LIGHT HAZE	82	10	85	41	30.12	27	96.6	27	117.7	27	96.6	
0829083501WC	LIGHT HAZE	70	73	36	30.019	15	LIGHT HAZE	74	10	77	77	29.52	44	96.9	44	96.9	44	96.9
0829083502WC	LIGHT HAZE	70	73	68	30.019	15	LIGHT HAZE	74	10	77	77	29.52	44	96.7	44	96.7	44	96.7
0829090703WC	LIGHT HAZE	70	73	68	30.019	15	LIGHT HAZE	74	10	77	77	29.52	44	94.7	44	94.7	44	94.7
0829092504WC	LIGHT HAZE	70	73	68	30.019	15	LIGHT HAZE	74	10	77	77	29.52	44	91.0	44	91.0	44	91.0
0829094005WC	LIGHT HAZE	70	73	68	30.019	15	LIGHT HAZE	74	10	77	77	29.52	44	90.4	44	90.4	44	90.4
0829102506WC	LIGHT HAZE	74	77	57	30.018	15	LIGHT HAZE	78	10	81	72	29.52	44	94.2	44	94.2	44	94.2
0829105007WC	LIGHT HAZE	74	77	57	30.018	15	LIGHT HAZE	78	10	81	72	29.52	44	93.4	44	93.4	44	93.4
0829110008WC	LIGHT HAZE	74	77	57	30.018	15	LIGHT HAZE	78	10	81	72	29.52	44	93.4	44	93.4	44	93.4
0829120509NC	LIGHT HAZE	74	77	57	30.018	15	LIGHT HAZE	78	10	81	72	29.52	44	115.3	44	115.3	44	115.3
0829123010NC	LIGHT HAZE	74	77	57	30.018	15	LIGHT HAZE	78	10	81	72	29.52	44	114.5	44	114.5	44	114.5
0829123511NC	LIGHT HAZE	82	85	43	30.018	14	LIGHT HAZE	82	10	85	61	29.52	44	85.4	44	85.4	44	85.4
0829123512NC	LIGHT HAZE	82	85	43	30.018	14	LIGHT HAZE	82	10	85	61	29.52	44	84.6	44	84.6	44	84.6
0829123513NC	LIGHT HAZE	82	85	43	30.018	14	LIGHT HAZE	82	10	85	61	29.52	44	82.2	44	82.2	44	82.2
0829123514WC	LIGHT HAZE	86	85	44	30.017	10	LIGHT HAZE	86	10	85	55	29.49	44	85.0	44	85.0	44	85.0
0829150515WC	LIGHT HAZE	86	85	44	30.017	10	LIGHT HAZE	82	10	85	55	29.49	44	85.4	44	85.4	44	85.4
0829152016WC	LIGHT HAZE	86	85	44	30.017	10	LIGHT HAZE	82	10	85	55	29.49	44	84.6	44	84.6	44	84.6
0829153517WC	LIGHT HAZE	86	85	44	30.017	10	LIGHT HAZE	78	10	81	55	29.49	44	85.7	44	85.7	44	85.7
0829155018WC	LIGHT HAZE	86	85	44	30.017	10	LIGHT HAZE	78	10	81	55	29.49	44	85.0	44	85.0	44	85.0
0902103002WC	STRATUS CLOUDING	70	73	16	30.019	5	STRATUS CLOUDING	70	10	73	82	29.50	5	91.2	5	91.2	5	91.2
0902104003WC	STRATUS CLOUDING	70	73	16	30.019	5	STRATUS CLOUDING	70	10	73	82	29.50	5	92.4	5	92.4	5	92.4
0902105504WC	STRATUS CLOUDING	70	73	16	30.019	5	STRATUS CLOUDING	70	10	73	82	29.50	5	92.4	5	92.4	5	92.4
090211005WC	STRATUS CLOUDING	70	73	16	30.019	5	STRATUS CLOUDING	70	10	73	82	29.50	5	95.3	5	95.3	5	95.3
0902112506WC	STRATUS CLOUDING	70	73	16	30.019	5	STRATUS CLOUDING	70	10	73	82	29.50	5	94.6	5	94.6	5	94.6
0902122007WC	STRATUS CLOUDING	70	73	16	30.019	5	STRATUS CLOUDING	70	10	73	82	29.50	5	95.2	5	95.2	5	95.2
0902131008WC	STRATUS CLOUDING	70	73	71	30.020	5	STRATUS CLOUDING	70	10	73	76	29.51	5	92.2	5	92.2	5	92.2
0902131009WC	STRATUS CLOUDING	70	73	71	30.020	5	STRATUS CLOUDING	70	10	73	76	29.51	5	89.6	5	89.6	5	89.6
0902140011WC	STRATUS CLOUDING	70	73	71	30.020	5	STRATUS CLOUDING	70	10	73	76	29.51	5	90.0	5	90.0	5	90.0
0902141512WC	STRATUS CLOUDING	70	73	71	30.020	5	STRATUS CLOUDING	70	10	73	76	29.51	5	94.8	5	94.8	5	94.8
0902143513WC	STRATUS CLOUDING	70	73	71	30.020	5	STRATUS CLOUDING	70	10	73	76	29.51	5	95.0	5	95.0	5	95.0
0902151014WC	STRATUS CLOUDING	70	73	71	30.020	5	STRATUS CLOUDING	70	10	73	76	29.51	5	89.3	5	89.3	5	89.3
0902152515WC	STRATUS CLOUDING	70	73	71	30.020	5	STRATUS CLOUDING	70	10	73	76	29.51	5	92.5	5	92.5	5	92.5
0902154516WC	STRATUS CLOUDING	78	73	71	30.020	5	STRATUS CLOUDING	78	10	73	76	29.51	5	93.6	5	93.6	5	93.6
0902160117WC	STRATUS CLOUDING	78	73	71	30.020	5	STRATUS CLOUDING	78	10	73	76	29.51	5	93.0	5	93.0	5	93.0
0903133009NC	CLEAR	78	70	50	30.019	3	CLEAR	78	10	61	53	29.52	5	112.9	5	112.9	5	112.9
0903142009NC	CLEAR	78	70	50	30.019	3	CLEAR	78	10	61	53	29.52	5	112.9	5	112.9	5	112.9

0903143510NC	CLEAR	58	30:19	3	CLEAR	78	10:53	5	107:4
0903151010NC	CLEAR	78	50	5	CLEAR	78	10:53	5	109:8
0904151503NC	STRATUS CLOUDING	78	54	5	STRATUS CLOUDING	78	10:53	7	111:6
0904153004NC	STRATUS CLOUDING	78	54	5	STRATUS CLOUDING	78	10:53	7	113:0
0904155005NC	STRATUS CLOUDING	78	54	5	STRATUS CLOUDING	78	10:53	7	116:8
0904160006NC	STRATUS CLOUDING	78	54	5	STRATUS CLOUDING	78	10:53	7	116:4
0904161707NC	STRATUS CLOUDING	78	54	5	STRATUS CLOUDING	78	10:53	7	116:4
0905114501WC	LIGHT MAZE	74	10:77	62	30:19	10	10:53	63	97:6
09051210102WC	LIGHT MAZE	74	10:77	62	30:19	10	10:53	63	99:3
0905121703WC	LIGHT MAZE	74	10:77	62	30:19	10	10:53	63	99:5
090513004WC	LIGHT MAZE	74	10:77	62	30:19	10	10:53	63	99:6
0905133505WC	LIGHT MAZE	74	10:77	62	30:19	10	10:53	63	99:9
0905141006WC	CUMULUS CLOUDING	78	10:81	57	30:14	21	10:53	63	99:9
0905142507WC	CUMULUS CLOUDING	78	10:81	57	30:14	21	10:53	63	99:9
0905144508WC	CUMULUS CLOUDING	78	10:81	57	30:14	21	10:53	63	99:9
0905153509WC	CUMULUS CLOUDING	78	10:81	57	30:14	21	10:53	63	99:9
0905155510WC	CUMULUS CLOUDING	78	10:81	57	30:14	21	10:53	63	99:9
0905163012WC	CUMULUS CLOUDING	78	10:81	57	30:14	21	10:53	63	99:9
0908110020WC	CUMULUS CLOUDING	66	10:69	67	29:29	15	10:53	63	99:9
0908112503WC	CUMULUS CLOUDING	66	10:69	67	29:29	15	10:53	63	99:9
0908114004WC	CUMULUS CLOUDING	66	10:69	67	29:29	15	10:53	63	99:9
0908131505WC	CUMULUS CLOUDING	66	10:69	67	29:29	15	10:53	63	99:9
0908133507WC	CUMULUS CLOUDING	66	10:69	67	29:29	15	10:53	63	99:9
0908141008WC	CUMULUS CLOUDING	66	10:69	67	29:29	15	10:53	63	99:9
0908150009WC	CUMULUS CLOUDING	66	10:69	67	29:29	15	10:53	63	99:9
0908171511NC	CUMULUS CLOUDING	74	10:71	53	29:29	15	10:53	63	99:9
0908173012NC	CUMULUS CLOUDING	74	10:71	53	29:29	15	10:53	63	99:9
090818014WC	CUMULUS CLOUDING	74	10:71	53	29:29	15	10:53	63	99:9
0908183216WC	CUMULUS CLOUDING	74	10:71	53	29:29	15	10:53	63	99:9
090820018WC	CUMULUS CLOUDING	74	10:71	53	29:29	15	10:53	63	99:9
0908201519NC	CUMULUS CLOUDING	74	10:71	53	29:29	15	10:53	63	99:9
0909045001NC	CLEAR	62	10:65	63	CLEAR	74	10:71	53	118:2
0909100802WC	CLEAR	62	10:65	63	CLEAR	74	10:71	53	119:7
0909103003NC	CLEAR	62	10:65	63	CLEAR	74	10:71	53	119:7
0909105004WC	CLEAR	62	10:65	63	CLEAR	74	10:71	53	119:7

## POINT PEGUE, SEPT

X-BAND

TEST	WEATHER	RECEIVE SITE	TEMP	KTL HUM BAKU PRES	WIND	WEATHER	TEMP	KTL HUM BAKU PRES	WIND	WEATHER	TEMP	KTL HUM BAKU PRES	WIND	SIGNAL
0915203001wx	CARK	66 TU 69	16	29.92	30	DARK	66 TU 69	14	29.92	30	89.0	2		
0915211003wx	CARK	66 TU 69	76	29.92	30	DARK	66 TU 69	19	29.92	30	87.0	3		
0915212604wx	CARK	66 TU 69	76	29.92	30	DARK	66 TU 69	79	29.92	30	87.0	3		
0916110001wx	STATUS CLOUDING	66 TU 69	85	29.91	25	RAIN. STATUS CLOUDING	70 TU 73	54	29.95	20	88.0	3		
0916151509wx	STATUS CLOUDING	66 TU 69	85	29.91	25	STATUS CLOUDING	78 TU 81	65	29.96	20	87.0	7		
0916153510wx	STATUS CLOUDING	70 TU 73	73	29.86	30	STATUS CLOUDING	74 TU 81	65	29.92	20	86.7	7		
0916155511wx	STATUS CLOUDING	70 TU 73	73	29.86	30	STATUS CLOUDING	76 TU 81	65	29.92	20	84.9	7		
0916161012wx	STATUS CLOUDING	70 TU 73	73	29.86	30	STATUS CLOUDING	78 TU 81	65	29.92	20	84.9	7		
0917094501wx	RAIN. STAT CLOUD	54 TU 57	94	29.93	15	STATUS CLOUDING	54 TU 57	54	29.93	15	88.0	3		
0917100502wx	RAIN. STAT CLOUD	54 TU 57	94	29.93	15	STATUS CLOUDING	54 TU 57	54	29.93	15	88.0	3		
0917110203nx	STATUS CLOUDING	54 TU 57	94	30.01	15	STATUS CLOUDING	54 TU 57	54	29.93	15	87.0	0		
0917112004nx	STATUS CLOUDING	50 TU 53	94	30.01	15	STATUS CLOUDING	54 TU 57	54	29.93	15	87.0	4		
0917113505nx	STATUS CLOUDING	50 TU 53	94	30.01	15	STATUS CLOUDING	54 TU 57	54	29.93	15	86.2	3		
0917115606nx	STATUS CLOUDING	50 TU 53	94	30.01	15	STATUS CLOUDING	54 TU 57	54	29.93	15	86.2	3		
0917140407wx	STATUS CLOUDING	54 TU 57	73	30.01	15	STATUS CLOUDING	54 TU 57	54	29.93	15	86.2	3		
0917151009wx	STATUS CLOUDING	54 TU 57	73	30.01	15	STATUS CLOUDING	54 TU 57	54	29.93	15	86.2	3		
0917172510wx	STATUS CLOUDING	54 TU 57	73	30.01	15	STATUS CLOUDING	54 TU 57	54	29.93	15	86.2	3		
0917160012wx	STATUS CLOUDING	54 TU 57	76	30.01	15	STATUS CLOUDING	54 TU 57	54	29.93	15	86.2	3		
0918091501wx	CLEAR	50 TU 53	51	30.01	15	CUMULUS CLOUDING	50 TU 53	50	29.67	17	86.7	0		
0918093502wx	CLEAR	50 TU 53	51	30.01	15	CUMULUS CLOUDING	50 TU 53	50	29.67	17	86.7	0		
0918095003wx	CLEAR	50 TU 53	51	30.01	15	CUMULUS CLOUDING	50 TU 53	50	29.67	17	86.7	0		
0918100504wx	CLEAR	50 TU 53	51	30.01	15	CUMULUS CLOUDING	50 TU 53	50	29.67	17	86.7	0		
0918110005wx	CLEAR	50 TU 53	51	30.01	15	CUMULUS CLOUDING	50 TU 53	50	29.67	17	86.7	0		
0918111606wx	CLEAR	50 TU 53	51	30.01	15	CUMULUS CLOUDING	50 TU 53	50	29.67	17	86.7	0		
2918113507wx	CUMULUS CLOUDING	54 TU 57	69	30.01	15	CUMULUS CLOUDING	54 TU 57	53	29.70	17	84.2	2		
0918154006wx	CUMULUS CLOUDING	54 TU 57	69	30.01	15	CUMULUS CLOUDING	54 TU 57	53	29.70	17	83.6	6		
0918133205wx	CLEAR	58 TU 61	55	30.01	13	CLEAR	56 TU 64	48	29.71	17	80.7	7		
0918135010wx	CLEAR	58 TU 61	55	30.01	13	CLEAR	66 TU 69	48	29.71	17	80.7	7		
0918140611wx	CLEAR	58 TU 61	55	30.01	13	CLEAR	66 TU 69	48	29.71	17	80.7	7		
0918142512wx	CLEAR	58 TU 61	55	30.01	13	CLEAR	66 TU 69	48	29.71	17	83.5	0		
0918153013wx	CUMULUS CLOUDING	58 TU 61	52	30.01	13	CLEAR	66 TU 69	48	29.71	17	83.5	0		
0918155014wx	CUMULUS CLOUDING	58 TU 61	52	30.01	13	CLEAR	66 TU 69	48	29.71	17	83.5	0		
0918165015nx	CUMULUS CLOUDING	58 TU 61	52	30.01	13	CLEAR	66 TU 69	48	29.71	17	82.7	1		
0918170516nx	CUMULUS CLOUDING	58 TU 61	52	30.01	13	CLEAR	66 TU 69	48	29.71	17	82.3	1		
0918172017nx	CUMULUS CLOUDING	58 TU 61	52	30.01	13	CLEAR	66 TU 69	48	29.71	17	82.3	1		
0918173518nx	CUMULUS CLOUDING	58 TU 61	52	30.01	13	CLEAR	66 TU 69	48	29.71	17	81.9	1		
0918193021wx	CUMULUS CLOUDING	58 TU 61	49	30.01	20	CLEAR	62 TU 65	41	29.73	15	92.6	8		





TEST	RECEIVE SITE			POINT-PETRE. SEPT C-BAND			TRANSMIT SITE			SIGNAL STRG					
	WEATHER	TEMP	REL HUM	BARO PRES	WIND	WEATHER	TEMP	REL HUM	BARO PRES	WIND	WEATHER	TEMP			
0915203001WC	DARK	76	29.92	30	DARK	66	10.62	19	82.3	30	82.3	79.9			
0915204602WC	CARK	76	29.92	30	DARK	66	10.62	19	79.9	30	79.9	80.4			
0915211003WC	CARK	66	76	29.92	30	DARK	66	10.62	19	76.6	30	76.6	84.3		
0915212604WC	CARK	66	76	29.92	30	DARK	66	10.62	19	29.92	30	29.92	83.0		
0916110001WC	STATUS CLOUDING	66	76	29.91	25	RAIN.	70	10.73	59	29.95	20	29.95	82.2		
0916111602WC	STATUS CLOUDING	66	76	29.91	25	RAIN.	70	10.73	59	29.95	20	29.95	83.3		
0916113003WC	STATUS CLOUDING	66	76	29.91	25	HAIN.	70	10.73	59	29.95	20	29.95	76.6		
0916115404WC	STATUS CLOUDING	66	76	29.91	25	HAIN.	70	10.73	59	29.95	20	29.95	77.3		
09161123505WC	STATUS CLOUDING	66	76	29.91	25	HAIN.	70	10.73	59	29.95	20	29.95	79.2		
0916133006WC	STATUS CLOUDING	66	76	29.91	25	STRATUS	78	10.81	65	29.96	23	29.96	82.3		
0916134507WC	STATUS CLOUDING	66	76	29.91	25	STRATUS	78	10.81	65	29.96	23	29.96	83.3		
0916140008WC	STATUS CLOUDING	66	76	29.91	25	STRATUS	78	10.81	65	29.96	23	29.96	79.2		
0916151509NC	STATUS CLOUDING	66	76	29.91	25	STRATUS	78	10.81	65	29.96	23	29.96	79.2		
0916153510NC	STATUS CLOUDING	70	73	29.86	30	STRATUS	76	10.81	65	29.96	20	29.96	95.0		
0916155511NC	STATUS CLOUDING	70	73	29.86	30	STRATUS	76	10.81	65	29.96	20	29.96	95.3		
0916161012NC	STATUS CLOUDING	70	73	29.86	30	STRATUS	76	10.81	65	29.96	20	29.96	97.3		
0917094501NC	RAIN. STAT CLOUD	54	70	94	29.93	15	STRATUS	76	10.81	65	29.96	23	29.96	102.5	
0917100502NC	RAIN. STAT CLOUD	54	70	94	29.93	15	STRATUS	76	10.81	65	29.96	23	29.96	98.6	
09171110203WC	STATUS CLOUDING	54	70	94	30.01	1	STRATUS	76	10.81	65	29.96	23	29.96	79.0	
0917113505WC	STATUS CLOUDING	54	70	94	30.01	1	STRATUS	76	10.81	65	29.96	23	29.96	75.5	
0917115606WC	STATUS CLOUDING	54	70	94	30.01	1	STRATUS	76	10.81	65	29.96	23	29.96	77.5	
0917140407WC	STATUS CLOUDING	54	70	73	30.03	3	STRATUS	76	10.81	65	29.96	23	29.96	82.9	
0917142008WC	STATUS CLOUDING	54	70	73	30.03	3	STRATUS	76	10.81	65	29.96	23	29.96	82.5	
0917151009WC	STATUS CLOUDING	54	70	73	30.03	3	STRATUS	76	10.81	65	29.96	23	29.96	84.8	
0917152510WC	STATUS CLOUDING	54	70	73	30.03	3	STRATUS	76	10.81	65	29.96	23	29.96	85.2	
0917160012WC	STATUS CLOUDING	54	70	73	30.03	3	STRATUS	76	10.81	65	29.96	23	29.96	83.3	
0918091501WC	CLEAR	50	73	81	30.34	10	CUMULUS	70	10.57	63	29.07	17	29.07	82.7	
0918093502WC	CLEAR	50	73	81	30.34	10	CUMULUS	70	10.57	63	29.07	17	29.07	81.6	
0918095003WC	CLEAR	50	73	81	30.34	10	CUMULUS	70	10.57	63	29.07	17	29.07	83.0	
0918100504WC	CLEAR	50	73	81	30.34	10	CUMULUS	70	10.57	63	29.07	17	29.07	83.0	
0918110005WC	CLEAR	50	73	81	30.34	10	CUMULUS	70	10.57	63	29.07	17	29.07	87.6	
0918111606WC	CLEAR	50	73	81	30.34	10	CUMULUS	70	10.57	63	29.07	17	29.07	86.2	
0918113507WC	CUMULUS CLOUDING	54	70	57	69	30.36	15	CUMULUS	62	10.65	53	29.70	17	29.70	89.1
0918115408WC	CUMULUS CLOUDING	54	70	57	69	30.36	15	CUMULUS	62	10.65	53	29.70	17	29.70	89.0
0918133209WC	CLEAR	58	70	61	55	30.36	13	CLEAR	66	10.69	48	29.71	17	29.71	87.6
0918135010WC	CLEAR	58	70	61	55	30.36	13	CLEAR	66	10.69	48	29.71	17	29.71	86.2
0918140611WC	CLEAR	58	70	61	55	30.36	13	CLEAR	66	10.69	48	29.71	17	29.71	89.9
0918142512WC	CLEAR	58	70	61	55	30.36	13	CLEAR	66	10.69	48	29.71	17	29.71	89.9

091815Z013WC	CUMULUS CLOUDING	58	10 61	52	30° 7	10	CLEAR
0918155014WC	CUMULUS CLOUDING	58	10 61	52	30° 7	10	CLEAR
0918165015WC	CUMULUS CLOUDING	58	10 61	52	30° 7	10	CLEAR
0918170516WC	CUMULUS CLOUDING	58	10 61	52	30° 7	10	CLEAR
0918172017WC	CUMULUS CLOUDING	58	10 61	52	30° 7	10	CLEAR
0918173518WC	CUMULUS CLOUDING	58	10 61	52	30° 7	10	CLEAR
0918175519WC	CUMULUS CLOUDING	58	10 61	52	30° 7	10	CLEAR
0918190520NC	CUMULUS CLOUDING	58	10 57	52	30° 7	10	CLEAR
0918193021NC	CUMULUS CLOUDING	58	10 57	52	30° 1	20	CLEAR
0918194522NC	CUMULUS CLOUDING	58	10 57	52	30° 1	20	CLEAR
0918205023WC	CUMULUS CLOUDING	54	10 57	54	30° 1	20	CLEAR
0918210524WC	CUMULUS CLOUDING	54	10 57	54	30° 1	20	CLEAR
0918212816WC	CUMULUS CLOUDING	54	10 57	54	30° 1	20	CLEAR
0918214026WC	CUMULUS CLOUDING	54	10 57	54	30° 1	20	CLEAR
0923032504WC	CLEAR	46	10 49	46	30° 7	20	LIGHT FOG
0923034005WC	LIGHT FOG	46	10 49	46	29° 9	25	LIGHT FOG
0923035006WC	LIGHT FOG	46	10 49	46	29° 9	25	LIGHT FOG
0923041007WC	LIGHT FOG	46	10 49	46	29° 9	25	LIGHT FOG
0923042508WC	LIGHT FOG	46	10 49	46	29° 9	25	LIGHT FOG
0923051009WC	CLEAR	46	10 49	46	29° 9	25	CLEAR
0923052510WC	CLEAR	46	10 49	46	29° 9	25	CLEAR
0923054511WC	CLEAR	46	10 49	46	29° 9	25	CLEAR
0923060112WC	CLEAR	46	10 49	46	29° 9	25	CLEAR
0923061513WC	CLEAR	46	10 49	46	29° 9	25	CLEAR
0923065514WC	CLEAR	42	10 49	42	29° 9	20	CLEAR
0923071515WC	CLEAR	42	10 49	42	29° 9	20	CLEAR
0923073016WC	CLEAR	42	10 49	42	29° 9	20	CLEAR
0923075017WC	CLEAR	42	10 49	42	29° 9	20	CLEAR
0923080518WC	CLEAR	42	10 49	42	29° 9	20	CLEAR
0923093019WC	CLEAR	50	10 53	50	29° 9	20	HAZY
0923094520WC	CLEAR	50	10 53	50	29° 9	20	HAZY
0924101801WC	RAIN.	STAT CLUUD	56	10 01	56	15	RAIN.
0924103502WC	RAIN.	STAT CLUUD	56	10 01	56	15	RAIN.
0924105003WC	RAIN.	STAT CLUUD	56	10 01	56	15	RAIN.
0924110504NC	RAIN.	STAT CLUUD	56	10 01	56	15	RAIN.
0924112005NC	RAIN.	STAT CLUUD	56	10 01	56	15	RAIN.
0924132506WC	RAIN.	STAT CLUUD	56	10 01	56	15	RAIN.
0924134507WC	RAIN.	STAT CLUUD	56	10 01	56	15	RAIN.
0924140208WC	CUMULUS CLOUDING	54	10 57	56	29° 7	15	RAIN.
0924142009WC	CUMULUS CLOUDING	54	10 57	56	29° 7	15	RAIN.
0924144010WC	CUMULUS CLOUDING	54	10 57	56	29° 7	15	RAIN.



APPENDIX C  
ROCHESTER WEATHER DATA

PRECEDING PAGE BLANK NOT FILMED.



LOCAL CLIMATOLOGICAL DATA  
U S DEPARTMENT OF COMMERCE - MAURICE H. STANS, Secretary

ROCHESTER, NEW YORK  
ROCHESTER-MONROE COUNTY AP  
AUGUST 1969

Latitude	43° 07' N	Longitude	77° 40' W	Elevation (ground)	547 ft	Standard time used	ENVIRONMENTAL DATA SERVICE		Wind	Sunshine	Sky cover (Tenths)
							Temperature (° F)	Weather types shown by code	Snow, Sleet, or Rain	Avg. pressure station	Fastest mile
1	2	3	4	5	6	7A	7B	8	9	10	11
1	68	65	77	5	5	55	0	12	3	6.4	7.9
2	81	65	73	1	1	66	0	8	1 3 5	0.92	0.29.38
3	82	61	72	-1	0	64	0	7	1	0	0.29.47
4	77	65	71	-1	1	64	0	6	0	0	0.29.44
5	83	63	73	2	2	64	0	8	1	.03	0.29.41
6	85	61	73	2	2	64	0	8	0	0	0.29.42
7	88	66	77	6	6	64	0	12	0	0	0.29.35
8	83	71	77	6	6	62	0	12	0	0	0.29.12
9	82	66	74	3	3	63	0	9	0	0	0.29.14
10	75	58	67	-4	4	62	0	2	0	.18	0.29.19
11	77	55	66	-5	5	55	0	1	0	.18	0.29.39
12	61	57	69	-2	2	57	0	4	0	0	0.29.47
13	84	59	70	-1	1	56	0	5	0	0	0.29.52
14	89	62	76	5	5	60	0	11	0	0	0.29.50
15	88	64	76	6	6	63	0	11	0	0	0.29.35
16	87	70	79	9	9	69	0	14	0	.10	0.29.26
17	83	69	76	6	6	68	0	11	1	.20	0.29.29
18	85	68	77	7	7	67	0	12	0	0	0.29.25
19	79	61	70	0	0	59	0	5	0	.14	0.29.44
20	70	51	61	-9	4	46	0	0	0	0	0.29.49
21	74	49	62	-8	47	3	0	0	0	0	0.29.54
22	80	49	65	-4	52	0	0	0	0	0	0.29.56
23	85	55	70	1	1	59	0	5	0	0	0.29.50
24	91	60	76	7	6	63	0	11	1	0	0.29.37
25	89	61	75	6	6	60	0	10	1	0	0.29.51
26	72	57	65	-4	50	0	0	0	0	0	0.29.63
27	77	46	62	-6	48	3	0	0	0	0	0.29.61
28	88	60	74	6	5	55	0	9	0	0	0.29.58
29	88	64	76	8	6	61	0	11	0	.07	0.29.61
30	90	66	78	11	11	65	0	13	1	0	0
31	92	70	81	14	14	65	0	16	1	0	0
							Total	Total	Total	Total	Total
							Number of days	Number of days	Number of days	Number of days	Number of days
							Total	Total	Total	Total	Total
							Avg.	Avg.	Avg.	Avg.	Avg.
							Dep.	Dep.	Dep.	Dep.	Dep.
							Dep.	Dep.	Dep.	Dep.	Dep.
							Total	Total	Total	Total	Total
							Maximum Temp	Minimum Temp	Heating	Cooling	Season to date
							-32°	-90°	-32°	-0°	-12°
							0	3	0	0	0

HOURLY PRECIPITATION (Water equivalent in inches)

Date	A.M. Hour ending at							P.M. Hour ending at																
	1	2	3	4	5	6	7	8	9	10	11	12	1	2	3	4	5	6	7	8	9	10	11	12
1																								
2		.43	T																					
3																								
4																								
5																								
6																								
7																								
8																								
9																								
10	.17	T	T	T	T	T																		
11																								
12																								
13																								
14																								
15																								
16																								
17	.02	.01	.04	.03	.02	.02	T																	
18																								
19																								
20																								
21																								
22																								
23																								
24																								
25																								
26																								
27																								
28																								
29																								
30																								
31																								

Any errors detected will be corrected and changes in summary data will be annotated in the annual summary.

Subscription Price: Local Climatological Data \$1.00 per year including annual Summary if published. Single copy: 10 cents for monthly Summary; 15 cents for annual Summary. Checks or money orders should be made payable and remittances and correspondence should be sent to the Superintendent of Documents, U. S. Government Printing Office, Washington, D. C. 20402.

I certify that this is an official publication of the Environmental Science Services Administration, and is compiled from records on file at the National Weather Records Center, Asheville, North Carolina 28801.

William J. Hagard

Director, National Weather Records Center

SUMMARY BY HOURS

AVERAGES

Hour (Local time)	Sky cover (in tenths)	Station pressure (in millibars)	Dry bulb (°F)	Wet bulb (°F)	Rel. hum. (%)	Dew point (°F)	Wind speed (in mph)	Resultant wind direction
01	4	29.42	65	62	84	60	5.9	23 4.3
04	4	29.42	63	61	88	59	6.3	23 5.1
07	4	29.45	66	63	84	61	7.1	22 5.0
10	4	29.46	76	67	63	62	9.7	23 6.7
13	5	29.43	81	67	48	59	10.9	27 8.3
16	5	29.40	81	67	47	58	10.5	28 7.2
19	5	29.41	74	65	64	60	7.0	25 4.0
22								

## OBSERVATIONS AT 3-HOUR INTERVALS

**6 ADDITIONAL DATA**  
Other observational data contained in records on file can be furnished at cost via microfilm or microfiche  
copy of the original record. Requests should be addressed to:  
**12 Director, National Weather Records Center, Federal Building, Asheville, NC 28801**



## LOCAL CLIMATOLOGICAL DATA

U S DEPARTMENT OF COMMERCE - MAURICE H. STANS, Secretary  
ENVIRONMENTAL SCIENCE SERVICES ADMINISTRATION  
ENVIRONMENTAL DATA SERVICE

ROCHESTER, NEW YORK  
ROCHESTER-MONROE COUNTY AM  
SEPTEMBER 1969

Latitude	N	Longitude		77° 40' W		Elevation ground	547 ft		Standard time used		EASTERN		Sunshine	Sky cover (Tenths)								
		Temperature	F	Temperature	F		Weather types	shown by code	Precipitation	Avg station pressure	Wind	Fastest mile										
Date		Maximum	Minimum	Average	Departure from prev. day	Degree days Base 65°	1-9 on dates of occurrence	Water elevation feet in	Snow depth feet in	Wind direction	Speed m.p.h.	Hours and tenths	Percent of possible	rise to set	Midnight to midnight							
1	90°	67	79	72	-6	7A	7B	8	9	10	11	12	13	14	15	16	17	18	19	20	21	
2	74	63	69	62	-2	62	6	1	0	0	0	0	0	0	0	0	0	0	7.2	55	4	5
3	80	55	68	59	-2	59	0	0	0	0	0	0	0	0	0	0	0	0	0.0	92	10	5
4	83	59	71	52	-5	52	0	0	0	0	0	0	0	0	0	0	0	0	12.1	52	9	7
5	88	63	76	10	-6	64	0	0	0	0	0	0	0	0	0	0	0	0	7.5	57	9	8
6	86	71	79	14	-6	68	0	0	0	0	0	0	0	0	0	0	0	0	6.4	49	9	8
7	81	65	73	8	-6	66	0	0	0	0	0	0	0	0	0	0	0	0	7.5	58	8	7
8	77	55	66	1	-6	56	0	0	0	0	0	0	0	0	0	0	0	0	2.3	18	10	6
9	68	49	59	-6	-50	50	0	0	0	0	0	0	0	0	0	0	0	0	8.4	65	6	6
10	70	49	60	-4	-4	42	5	0	0	0	0	0	0	0	0	0	0	0	4.9	38	6	6
11	70	47	59	-5	-4	47	6	0	0	0	0	0	0	0	0	0	0	0	10.4	81	3	4
12	79	50	65	1	-1	49	0	0	0	0	0	0	0	0	0	0	0	0	1.6	13	10	7
13	84	62	73	9	-5	57	0	0	0	0	0	0	0	0	0	0	0	0	10.7	84	3	1
14	86	56	71	8	-5	57	0	0	0	0	0	0	0	0	0	0	0	0	11.7	92	2	2
15	84	63	74	11	-5	56	0	0	0	0	0	0	0	0	0	0	0	0	12.6	100	5	1
16	81	65	73	10	-5	58	0	0	0	0	0	0	0	0	0	0	0	0	7.3	58	7	7
17	66	51	59	-3	-3	55	6	0	0	0	0	0	0	0	0	0	0	0	0.3	2	10	10
18	63	44	54	-8	-8	44	11	0	0	0	0	0	0	0	0	0	0	0	0.0	65	6	5
19	63	39°	51	-10	-10	42	14	0	0	0	0	0	0	0	0	0	0	0	10.9	89	8	1
20	69	45	57	-4	-4	44	8	0	0	0	0	0	0	0	0	0	0	0	8.1	66	5	3
21	74	46	60	-1	-1	48	5	0	0	0	0	0	0	0	0	0	0	0	11.3	93	2	2
22	77	46	62	1	-1	49	3	0	0	0	0	0	0	0	0	0	0	0	12.2	100	0	0
23	79	47	63	3	-3	50	2	0	0	0	0	0	0	0	0	0	0	0	8.6	71	6	5
24	66	53	60	0	-5	55	5	0	1	0	0	0	0	0	0	0	0	0	0.0	0	10	10
25	55	51	53	-6	-6	46	14	0	0	0	0	0	0	0	0	0	0	0	0.0	0	10	2
26	66	51	59	0	-6	48	6	0	0	0	0	0	0	0	0	0	0	0	7.3	61	6	6
27	64	47	56	-3	-3	49	9	0	0	0	0	0	0	0	0	0	0	0	0.7	6	9	6
28	62	44	53	-6	-6	45	12	0	0	0	0	0	0	0	0	0	0	0	6.1	34	6	6
29	63	42	53	-3	-3	42	12	0	0	0	0	0	0	0	0	0	0	0	6.8	40	8	9
30	72	49	61	3	-6	46	4	0	0	0	0	0	0	0	0	0	0	2.9	23	8	8	
Sum	Sum	Total	Total	Total	Total	Total	Number of days	Total	Total	For the month	Total	Total	Total	Total	Total	Total	Total	Sum	Sum	Sum	Sum	
2220	1596	126	92	126	92	126	Precipitation	1.77	0.2950	24	3.9	7.9	32	5W	189.8	for	201	185				
Avg	Avg	Avg	Avg	Dep	Dep	Dep	Precipitation	Dep	Dep	Date	12	Possible	month	Avg	Possible	month	Avg					
74.0	52.1	63.6	1.2	53	0	0	0.01 inch	0.76	0.76						374.9	31	6.7	6.2				
Season to date		Snow, sleet		Greatest in 24 hours and dates		Greatest depth on ground of		Maximum Temp		Thunderstorms		Snow, Sleet		snow, sleet or ice and date		Minimum Temp		Heavy fog		0.23		
Number of days		Total		0		1-10 inch		0		1		0		0		0		0		0		
Maximum Temp		-32°		> 90°		-32°		0		Dep		Dep		0		0		0		0		

- Extreme temperatures for the month. May be the last of more than one occurrence.
  - Below zero temperature or negative departure from normal.
  - $\pm$   $\leq 70^{\circ}$  at Alaskan stations.
  - $\pm$  Also on an earlier date, or dates.
  - X Heavy fog restricts visibility to  $\frac{1}{4}$  mile or less.
  - T In the Hourly Precipitation table and in columns 9, 10, and 11 indicates an amount too small to measure.

The season for degree days begins with July for heating and with January for cooling.

Data in columns 6, 12, 13, 14, and 15 are based on 8 observations per day at 3-hour intervals.

Wind directions are those from which the wind blows. Resultant wind is the vector sum of wind directions and speeds divided by the number of observations. Figures for directions are tens of degrees from true North; i.e., 09 = East, 18 = South, 27 = West, 36 = North and 00 = Calm. When directions are in tens of degrees in Col. 17, entries in Col. 16 are fastest observed 1-minute speeds. If the / appears in Col. 17, speeds are gusts.

Any errors detected will be corrected and changes in summary data will be annotated in the annual summary

Subscription Price Local Climatological Data \$1.00 per year including annual Summary if published. Single copy 10 cents for monthly Summary, 15 cents for annual Summary. Checks or money orders should be made payable and remittances and correspondence should be sent to the Superintendent of Documents, U. S. Government Printing Office, Washington, D. C. 20402.

I certify that this is an official publication of the Environmental Science Services Administration, and is compiled from records on file at the National Weather Records Center, Asheville, North Carolina 28801.

SUMMARY BY HOURS AVERAGES										Resistant wind
Hour of day	Wind direction in tenths	Station pressure	Dry bulb °F	Wet bulb °F	R.H. %	Dew point °F	Wind speed m.p.h.	(Dir.)	Spiral wind	
01	4	29.50	58	55	83	52	5.7	22	9.3	
04	5	29.50	57	54	85	52	6.1	21	5.9	
07	7	29.52	58	55	83	53	6.4	22	4.2	
10	7	29.53	67	59	63	53	9.9	25	6.7	
13	8	29.50	71	60	54	52	11.0	27	9.1	
16	6	29.48	71	60	54	52	10.6	20	4.7	
19	6	29.69	64	58	69	53	7.2	23	1.6	
22	5	29.51	60	56	70	53	6.4	22	2.7	

William J. Haggard

Director, National Weather Records Center

## OBSERVATIONS AT 3-HOUR INTERVALS

**ADDITIONAL DATA**  
Other observational data contained in records on file can be furnished at cost via microfilm or microfiche copies of the original records. Inquiries as to availability and costs should be addressed to Director, National Weather Records Center, Federal Building, Asheville, N.C. 28801.

STATION: ROCHESTER N Y                            YEAR & MONTH: 69-09

## References

1. Branham, Manders, Kozakoff, CORRELATION BANDWIDTH MEASUREMENTS OVER TROPOSCATTER PATHS, First Interim Report ECOM-0251-1, Martin Marietta Corporation, August 1969.
2. Branham, Manders, Reinstatler, TROPOSCATTER TRANSMISSION OF HIGH SPEED DIGITAL SIGNALS, ECOM Technical Report 0042-F, Martin Marietta Corporation, December 1968.
3. Birkemeier, W. P., Merrill, H. S., Sargeane, Jr., D. H., Thomson, D. W., Beamer, C. M., and Bergeman, G. T., "Observation of Wind-Produced Doppler Shifts in Tropospheric Scatter Propagation. Radio Science, Vol 3, No. 4, pp 309-317, April 1968.